

Mathematical Modelling
and
Computer Simulation
of
Biomechanical Systems

This page is intentionally left blank

Mathematical Modelling
and
Computer Simulation
of
Biomechanical Systems

A V Zinkovsky
V A Sholuha
A A Ivanov

*State Technical University of
St. Petersburg, Russia*



World Scientific

Singapore • New Jersey • London • Hong Kong

Published by

World Scientific Publishing Co. Pte. Ltd.

P O Box 128, Farrer Road, Singapore 912805

USA office: Suite 1B, 1060 Main Street, River Edge, NJ 07661

UK office: 57 Shelton Street, Covent Garden, London WC2H 9HE

British Library Cataloguing-in-Publication Data

A catalogue record for this book is available from the British Library.

**MATHEMATICAL MODELLING AND COMPUTER SIMULATION OF
BIOMECHANICAL SYSTEMS**

Copyright © 1996 by World Scientific Publishing Co. Pte. Ltd.

All rights reserved. This book, or parts thereof, may not be reproduced in any form or by any means, electronic or mechanical, including photocopying, recording or any information storage and retrieval system now known or to be invented, without written permission from the Publisher.

For photocopying of material in this volume, please pay a copying fee through the Copyright Clearance Center, Inc., 222 Rosewood Drive, Danvers, MA 01923, USA. In this case permission to photocopy is not required from the publisher.

ISBN 981-02-2395-1

Printed in Singapore.

Preface

Attempts to understand motion control mechanism in living organisms have for a long time occupied minds of specialists in biomechanics. However, up to now this problem remains to be more of a riddle rather than an unravelled tangle. Experimental analysis and mathematical modelling encounter serious difficulties in resolving this problem. That is why up to now no sufficiently general exhausting theory of biomechanical systems motion has been developed. No exact control laws of complete motion act have been formulated nor anthropomorphic mechanism (AM) motions which kinematic and dynamic characteristics would satisfactorily resemble that ones natural for human beings with satisfactory quality have been formulated.

The feeling of euphoria aroused among scientists in the 80–90s by fast development of computer technology, which gave grounds for hopes for a serious breakthrough in the field of biomechanical systems modelling, seems to have been premature.

Limited results obtained through attempts of simulation of biomechanical systems are mainly due to the following reasons: 1) human skeletal-muscular apparatus (SMA) complexity; 2) insufficient development of mathematical methods intended for biological systems modelling and 3) limited opportunities of mathematical modelling methodology. The last reason is obviously the most important one because direct transfer of modelling methods and approaches traditional in technical sciences to more complex, intricate systems studied in biomechanics is hardly promising. Therefore, despite important achievements in the field of mathematical modelling (Wittenburg, Vukobratovich, Beletsky, etc.) and development of corresponding software (e.g. ADAMS software packages), no essential progress in human motion analysis and synthesis has been made.

Presently we witness successful development of applied systems analysis methods, in particular, imitational modelling — a powerful tool of complex systems investigation. Imitational dynamic modelling allowed to make significant progress in research done by, for example, D. Forester, R. Shennon and N. Moiseev in studies of different large and complex economical, technical, ecological and manufacturing systems.

Imitational dynamic modelling was for the first time employed for biomechanical systems motion analysis in the research done by the authors of this monograph. Results yielded by that research have been presented in our papers in the following scientific journals: “Biophysics” [105], “Cybernetics and computer technology” [104] and in reports at international conferences on biomechanics in Rome (1992), Paris

(1993), Amsterdam (1994) and Jyväskylä (1995).

In contradistinction to traditional simulation where a model worked out beforehand is employed in investigation of the object properties, in imitational modelling the process of model formation is evolutionary, i.e. development of the starting base model is just the first step of modelling. As research progresses — certain tasks are solved and new ones are formulated or/and it becomes an obvious necessity for a better reflection of the object behaviour by its model — the model is structurally and parametrically modified. Thus, imitational model is continuously corrected and adjusted in research so that it would meet requirements of the investigation being undertaken.

Thus, imitational modelling is a special method of systems simulation based on “step-by-step”, iteration-like adjustment of the model with an eye to reflect better real system behaviour. Hereafter we will be mainly employing the term “imitational modelling” instead of a more general term “simulation”, because we have employed imitational dynamic modelling methodology of biomechanical systems motion simulation throughout our investigations.

Development of imitational models of biomechanical systems is to a great extent not “once and for all” defined procedure but an informal process which always draws on experimental data. The main goal of biomechanical system analysis is to single out from the whole system a subsystem which actually performs the motion which will interest researchers, to formulate subsystem selection principles. Since we are dealing with an open subsystem we have to define the influence of the discarded part on the chosen subsystem. Principles of models choice should take into account estimation of this influence in order to find a model of a certain complexity level and providing for maximum accuracy. The only way of imitational modelling realization is the creation of universal anthropomorphic models.

Possibility of operation with a variety of models is a principal element of motion imitation. One gets this variety by variation of model parameters. The basis of imitational modelling method consists in realization of iterational procedures providing for adjustment of the model so that its behaviour resembles more and more the behaviour of a real biomechanical system. We introduce adequacy criteria which serve as formal check of this resemblance.

The adequacy of the model is the main problem of any modelling and its solution is possible only by utilization of experimental, mathematical and numerical methods.

Human SMA modelling requires such initial data as mass-inertia characteristics of different parts of the body, characteristics of model element junctions, and the number of degrees of freedom. Most of the model parameter values are assessed by regression analysis with quite large error margins. These errors are passed on and practically devaluate modelling results because we use registered motion data for calculating dynamic variables from model equations. For simulation adequacy criterion we can take, for example, sum of norms of differences of corresponding calculated and measured values. This criterion is formulated in the most simple way

for a free fall phase of motion. In this case values of the ground reaction and external moment should be equal to zero, which is used for evaluation of number of degrees of freedom and links parameters.

Already at the beginning of our research work employing imitational dynamic modelling allowed us to find out that for simple motions performed at the speed convenient for the individual, the central nervous system forms optimal control interelement moments. These moments are, in fact, solution of a complex variation problem — the problem of definition of minimum energy loss when repositioning SMA elements under constraints on velocities, maximum moment values, requirement of minimal oscillations of elements about the new position, etc. Thus, it was shown that elementary motions control moments are close to the optimal ones received by solving the corresponding automatic control theory problem.

Complex motions are characterized by presence of the so-called leading (controlling) and compensating (stabilizing) interelement moments. During motion the peak of the leading moment passes in a wave-like manner along the kinematic chain starting from the element closest to the ground and successively to other elements. Results received by imitational modelling method and characterizing behaviour of control functions both for simple and complex motions agree with experimental data available.

In our further research we concentrated on development of technology of imitational modelling. The methodology of imitational modelling allows one to synthesize various "goal oriented" motions, i.e. determine control moments and forces behaviour necessary for realization of motion with certain goals.

If under certain control, motion goal is achieved then it can be formalized, i.e. presented in the form of equations with respect to controlled object co-ordinates. The set of equations which express motion goal is called motion program. These program equations can be algebraic, differential or integro-differential. Developed by the authors software it provides for different ways of control formation. Three main factors are distinguished: interelement moments; external forces and moments; reactions of external and internal constraints. Real motions are performed as a rule under influence of two or all three from these factors. However, from interelement control moments synthesis point of view, realization of desired kinematics due to external forces and constraints only is possible. In this case interelement moments are determined from solution of the direct problem of dynamics.

The monograph contains five chapters. In the first chapter a thorough review of the current state of human and anthropomorphic mechanisms motion control problem is given. On the basis of contemporary literature analysis (over 100 references) the importance of the problem solution for sciences such as biomechanics, robotics and medicine is shown. Methodological obstacles creating difficulties on the way to successive solution of some theoretical and applied problems in these fields are described. It is also discussed that biomechanical problems can be treated only on the basis of system approach.

The second chapter is devoted to mathematical models of anthropomorphic mechanisms. Some necessary pieces of information from dynamics of solid and visco-elastic bodies are given. Main principles of modelling are reviewed in detail. The procedures of plane and 3-D human motion models development are described. We also address here the issue of various possible constraints which can be imposed on the model and write them in mathematical form.

In the third chapter we first discuss experimental data processing and smoothing. Human SMA modelling requires such initial data as mass-inertia characteristics of different parts of the body, characteristics of model elements junctions, the number of degrees of freedom and one of the paragraphs from this chapter is devoted to model parameters' estimation and to processing of kinematic picture of motion by means of iterational parametric adjustment. Then we address the issues of control structure and integration of motion equations with constraints (holonomic and non-holonomic).

The fourth chapter contains basic principles and results of analysis of different human and anthropomorphic motions.

The fifth chapter is completely devoted to motions synthesis and optimisation. Typical problems of synthesis of SMA motion with desired kinematics are considered (walking, gymnast and track-and-field sportsman motions, human motion in weightlessness and under overloads). Synthesis methodology essentially draws on usage of non-stationary constraint equations. Such an approach allows one to assess needed energy expenditures for performance of "record beating" locomotions. Therefore we also give description of typical non-stationary constraints.

This monograph summarizes the results of the scientific research of the authors during the last ten years in the Laboratory of the Biocybernetics of the St. Petersburg State Technical University (SPSTU) which is headed by Prof. A. Zinkovsky. The experience of the authors in the fields of Applied Mathematics (Dr. V. Sholuha) and Theoretical Mechanics (Dr. A. Ivanov) led them to develop the main principles of analysis, synthesis and optimization of the human SMA motions and to implement it in the computer software.

The results of these authors have been discussed in scientific seminars. The authors would like to thank all their colleagues, who took part in these seminars, especially Prof. V. Palmov (SPSTU, Russia), Prof. F. Kulakov (SPIIRAS, Russia), Prof. W. Gutewort (University of Jena, Germany), Prof. K.J. van Zwieten and Prof. P.L. Lippens (LUC, Belgium), Prof. R.M. Bartlett (MMU, England), and Prof. A. Voloshin (Lehigh University, USA).

The main part of all the calculations and the computer design with \TeX software of our monograph were made with assistance of the collaborators of Open System Laboratory (SPSTU). Using this opportunity, the authors would also like to thank their patient wives and children, who understand that the work is very important. The authors would especially like to thank Dr. Stanislav Zinkovsky and Dr. Evgene Zinkovsky who have made a number of valuable remarks on the text while preparing it for publishing in English.

CONTENTS

| | |
|--|-----------|
| Preface | v |
| 1 Human Motion Modelling | 1 |
| 1.1 Some History | 1 |
| 1.2 Contemporary State of the Problem | 3 |
| 1.3 System Approach to Biomechanical Investigations | 8 |
| 2 Mathematical Anthropomorphic Models | 13 |
| 2.1 Extracts from Solid Body Dynamics | 13 |
| 2.2 Description of a System of Solid Bodies Structure | 15 |
| 2.3 Spatial Model with Spherical Joints | 19 |
| 2.3.1 Structure Description | 19 |
| 2.3.2 Expressions for Fundamental Dynamic Quantities | 24 |
| 2.3.3 Equations of Motion | 26 |
| 2.3.4 Quantitative Characteristics of AM Dynamics | 28 |
| 2.4 Planar Motion | 31 |
| 2.5 System of Arbitrary Connected Bodies in 3-D Space | 35 |
| 2.6 Additional Restrictions on the Base Model | 40 |
| 2.6.1 Linear Constraints | 41 |
| 2.6.2 Preset Distance between Certain Points of Two Bodies | 41 |
| 2.6.3 Preset Behaviour of Certain Point Radius Vector Projection onto Fixed Direction in Selected Basis | 41 |
| 2.6.4 Preset Behaviour of Two Bodies Relative Angular Velocity Projection onto Fixed Direction in Selected Basis | 42 |
| 2.6.5 Preset Surface Shapes of Two Adjoined Bodies | 42 |
| 2.6.6 Preset "Force" Constraint | 43 |
| 2.6.7 Generalised Form of Constraint Equations | 43 |
| 2.7 AM Equations in Generalized Coordinates | 44 |

| | | |
|----------|--|------------|
| 3 | The Imitational Modelling Attributes | 45 |
| 3.1 | Experimental Data Processing | 45 |
| 3.1.1 | Filmed or Video-taped Motion Processing | 45 |
| 3.1.2 | GMIC and Reduction of AM Degrees of Freedom | 48 |
| 3.1.3 | Trajectories Smoothing | 52 |
| 3.2 | Choice of the Optimal Model Parameters | 54 |
| 3.3 | Control Structure | 62 |
| 3.3.1 | Stationary Control | 62 |
| 3.4 | Integration of Motion Equations for Mechanical System with Constraints | 67 |
| 3.4.1 | Implicit Form of Equations for Mechanical System with Constraints | 68 |
| 3.4.2 | Corrections Calculation for Arbitrary Constraints | 69 |
| 3.4.3 | Holonomic Constraints | 71 |
| 3.4.4 | Nonholonomic Constraints of the First Order | 73 |
| 3.4.5 | Regularization According to Baumgarte | 75 |
| 4 | Analysis | 77 |
| 4.1 | Basic Principles | 77 |
| 4.2 | Analysis of the Synthesized Motion | 80 |
| 4.3 | Analysis of a Real Experiment | 93 |
| 4.4 | Analysis of Grand Circles on the Horizontal Bar | 97 |
| 4.5 | Some Conclusions | 108 |
| 5 | Synthesis | 111 |
| 5.1 | General Points (Fundamentals) | 111 |
| 5.2 | Typical Non-Stationary Constraints | 115 |
| 5.3 | Synthesis of Grand Circles on the Horizontal Bar (3-element model) | 123 |
| 5.4 | Single-Support Motion (7-element model) | 128 |
| 5.5 | Walking | 143 |
| 5.6 | Gymnastic Exercises | 157 |
| 5.7 | Running Long Jump | 169 |
| 5.8 | Human Motion in Weightlessness and under Overloads | 180 |
| 5.9 | Some Notes and Conclusions | 192 |
| | Conclusion | 195 |
| | Bibliography | 197 |
| | Index | 203 |

CHAPTER 1

HUMAN MOTION MODELLING

1.1 Some History

Interest on motions of animals and humans started long ago. In IV-th age B.C. Aristotel wrote a work on this subject [2]. Later Galen K. (131–201 A.D.) detected connection of muscles work with motions in joints [67].

In 1679 Borelli D. wrote a book entitled “De motu animal” [12], in which he summarised all the little information on animal motion that was known by that time. On the basis of achievements in mechanics Borelli considered conditions of equilibrium of animals bodies, defined and calculated position of the center of mass of human body.

Human motions interested many scientists in the 17th and 18th centuries. Issac Newton was no exception. He was interested in how human motions follow human will [68]. Systematic investigation of human and animal motion took place much later. In 1836 a fundamental work by Weber brothers [98] was published, which presented experimental material on human walking kinematics. Interest on investigating human motion increased upon discovery of photography. Much work done at that period was on photorecords of successive phases of human and animal motion and its kinematic characteristics analysis [57, 58].

First investigators of human motion dynamics were German scientists Braune B. and Fisher O. [14, 15, 29]. Their main achievement was that they did not restrict themselves to considering of kinematic picture of motion. These researchers modelled human body by a system of 14 rigid segments, connected by joints. In order to have their model as close to the real object as possible, Braune and Fisher conducted experimental measurements to find positions of centres of mass and moments of inertia of separate body parts and kinematic chains. Finally, they wrote down Newton-Euler motion equations of the model. Thus, Braune and Fisher for the first time, formulated a mathematical problem the solution of which would fully describe motion of the chosen model of human body.

In the beginning of the 20th century there were no real possibilities to carry out investigation on Braune and Fisher’s model behaviour. This was due to absence of adequate motion registration devices, computers and methodology of experimental data processing. However, general ideas of the suggested approach are widely used in modern practice. As a new important stage in biomechanics development we should acknowledge work by Bernstein N. [7]–[9]. He formulated and investigated motion

equation of one element as a result of action of one muscle and of the gravity field

$$J\ddot{\alpha} = F(E, \alpha, \dot{\alpha}) + G(\alpha),$$

where F — moment of the muscle force; α — interelement angle; J — moment of inertia of the element; G — gravity force moment; E — function of innervation state of the muscle. This fundamental equation is a differential equation of the second order, which can be integrated if functions F and G are known. Solution of this equation, that is corresponding motion, will depend on initial conditions, that is initial position of the element (angle α_0) and its initial angular velocity $d\alpha_0/dt$. First of all, it should be noted that this motion equation points out cyclic character of link between muscle moment F and element position α . Element position is changed due to action of muscle force moment F , but the moment in its turn is changed due to changes in element position α . Therefore, we have a closed loop of causes and consequences. This loop would be ideal if the moment depended only on α and $d\alpha/dt$, that is if motion was absolutely passive (for example, hand dropping). But, in general, the muscle force also depends on value of muscle activation E . Muscle tension is function of, first, its tonic condition E , and, second, its length and velocity of muscle length change at a given point of time. In humans muscle length is in its turn function of interelement angle α . Thus, we see in the main motion equation superposition of two cycle links. The first cycle link is a mutual influence of position angle α and moment F , which is of a mechanic nature. The second link, link of a higher order, is a similar mutual influence of the angle α (and angular velocity as well) and muscle activation E . This link is closely connected with central neural system activity. It is easy to understand the principal meaning of these facts. An old, preserved (by many physiologists and clinicians), point of view considers skeletal elements as absolutely obedient to central neural system. According to this point of view central impulse a always causes motion A , and impulse b causes motion B . Such a view helps to create an image of cortex motion zone as a control desk. However, one and the same impulse $E(t)$ (ignoring periphery) can lead to different effects due to various combinations of external forces and initial conditions. On the contrary certain motion effect achievement is possible only if impulse E is adjustable to various initial conditions and position of the body element. Experimental investigations, which followed later, confirmed conclusions made by Bernstein via analytical investigation. N. Bernstein for the first time formulated the problem of calculation of forces moments at leg joints during locomotion.

After Bernstein's work was published N. Elfman made an attempt [24, 25] to calculate values of moments acting on the foot, shin, hip and body trunk during the support phase of walking. It was assumed that motion takes place only in the sagittal plane.

In investigations made by Bresler and Frankler [16], internal forces and moments at the hip, knee and ankle joints were determined. Kinetostatics equations were used for motion equations. Kinematic characteristics of motions were obtained via

double side chronophotography. Dynamographic platform allowed to measure the reaction force. However, calculated joint moments and forces were apparently incorrect because researchers employed double graphic differentiation method.

1.2 Contemporary State of the Problem

Most active research in biomechanics started in the late 70s. This boom was due to intensive development of robotics, achievements in space flights, getting into fashion of healthy way of life, as well as by demands of medicine and sport.

Many different types of works were carried out considering dynamics of systems of connected bodies. The number of bodies can be rather high and usually the problem is more complex than ones of classical literature which allow for solution in a closed form. Different parts of the body can be both rigid and elastic. The system can have the "tree" type topology or contain closed loops. Relative motion of body parts can be due to control forces and moments or simply inertial forces. When modelling human motions we have to deal with solving of one of the following problems:

1. Direct problem of dynamics. In this problem moments and forces are found as functions of time (i.e. control pattern) based on given system motion character.
2. Inverse problem of dynamics. In this case biomechanical system motion is synthesized based on given control forces and moments functions and initial conditions.
3. Mixed problem. In this problem direct and inverse problems of dynamics are solved in combination. One of the most frequently considered problems from this class is determination kinematic characteristics of a body motion in an inertial space under given relative motion of other system bodies and under given forces and initial conditions.
4. Optimization problem. According to selected optimization criterion optimal solution out of a set of possible solutions (on the basis of variational calculus) is found.

Thus, modelling allows to solve motion analysis, synthesis and optimization problems.

Along with modelling research development, studies on continuous development and design of various measurement devices intended for experimental studies of biological systems kinematics and dynamics: optical devices for kinematics registration (ELITE motion analyser, VICON system, EMED system), dynamometric platforms, accelerometers and passive measurement exoskeletons has also been carried out [11, 22, 23, 52, 96].

All these measurement devices allow to increase data accuracy and simplify biomechanical investigation process automatization. Usually, measurement devices can be hooked up to a computer, which allows to process information in "on-line" regime and present experimental data on motion screen. Then, this data can be approximated by special functions. Several investigators have recently made attempts to develop a more accurate methodology of body mass-inertia characteristics estimation [37, 76, 102, 103]. The most reliable method is considered to be the radioisotopic one [102]. On the basis of this method lies the physical law which states that monoenergetic gamma-radiation beam is weakened by a known degree after passing through a layer of material of certain thickness. The studied object is scanned by gamma-radiation. Special measurements allow to determine the object's mass, center of mass coordinates and moments of inertia. It became possible to use this technique for living organisms and especially for body analysis after detector sensitivity was increased and a wide beam of gamma-radiation was proposed to be used.

Investigations on phantoms have shown that mass estimation error for this method does not exceed 2% and moments of inertia estimation error is bounded by the level of 3–5%. Investigations on humans have shown high reliability of mass-inertia data obtained via radioisotopy method application.

Recently, computer software packages intended to make easier investigation of biomechanical systems have been invented. These programme packages [65] are designed for solution of concrete practical problems.

It should be stated that despite vigorous attempts of various scientists-experts in mathematics, cybernetics, biomechanics, engineering and medical sciences, and despite employment of contemporary scientific equipment, including supercomputers, problems of analysis, synthesis and optimization of biomechanical systems motion remain to a great extent unsolved.

There is a whole set of difficulties which present serious obstacles for researchers in biomechanics. Biomechanical system motion is described by nonlinear differential equations. Analytical mechanics proposes many forms of motion equations for discrete systems of solid bodies [46, 56, 94, 101]. However, as Lilov [54] justly notes, detailed consideration shows that classical motion equations often prove to be not the best to describe dynamics of a system of linked bodies. In particular, the well-developed Lagrange approach brings us to a complex expression for system kinetic energy, requiring double differentiation — first, with respect to generalized velocities, second, with respect to time variable. This is not a simple technical problem even for a simple system. Next important aspect is that all various forms of motion equations are written for generalized variables, i.e. for a system of independent parameters which uniquely define biomechanical system state. It is easy to point out such generalized coordinates for a system of solid bodies with "tree-like" structure. For example, it could be the system of independent coordinates describing relative motion of connected bodies of the model. However, these parameters are not independent for a system of bodies possessing closed loops in the kinematic chain (as, for example, in

classical biomechanics problem of two-support phase of walking). Therefore, the first question is which system of independent generalized coordinates to choose. In order to do so, one has to write down analytical constraint equations. Analytical mechanics does not suggest any general method of constraint equations derivation and they are usually considered to be given a priori. Holonomic system constraint equations are supposed to be satisfied simply via employment of generalized coordinates, while for nonholonomic systems an important suggestion that constraint equations are independent is usually made.

The third essential aspect concerning employment of certain form of motion equations for biomechanical systems motion modelling is that they should be adapted for computer modelling. Usually, biomechanical system motion equations are so complex that their analysis is impossible without computer employment.

The most general approach to investigation of kinematics and dynamics of systems with tree-like structure was proposed by Vereshagin [94], Lilov [54] and Wittenburg [101]. Analytical mechanics methods combined with graphs employed for model structure description allowed one to study most general systems of connected solid bodies with "tree-like" structures with arbitrary number of bodies and junction types. Connections between bodies can be stationary, nonstationary, holonomic or nonholonomic. Much more difficult is to study motion of connected bodies systems with loops in the kinematic chain. One of the first and quite general investigations concerning this topic was one by Uicker [92, 93]. In his work on the basis of Lagrange equations of the 2-d kind he proposed an approach to investigation of dynamics of spatial mechanisms with closed kinematic loops.

In Wittenburg and Lilov's works it has been shown that decisive difficulties in this problem are connected with constraint equations.

One of the possible approaches to constraint equations formulation for a system with closed kinematic chain is proposed in Refs. [54] and [101]. Correct formulation of constraint equations is important for kinematic and dynamic modelling of systems of connected bodies, but these equations can also serve as a means of formal expression of motion goal. Motion equations together with constraint equations form a system of equations of goal-oriented human motions.

The possibility of such use of constraint equations in biomechanics was for the first time suggested by Korenev V.G. [47, 48] and then successfully used in our own research.

Considerable difficulties in investigation appear on switching from continual, with respect to time, mathematical model to a discrete one. And this is always done when researchers want to use numerical methods of investigation. The integral in this case is substituted by a finite sum of terms and the derivation by certain approximation formula including function values at different node points. The main problem appearing in this case is stability of the calculation process. It is necessary to analyse behaviour of the integral error made from approximation and rounding off errors.

One of the most widely used methods of approximations of functions given in a

table form is the method of smoothing spline-functions [81]. This method is used in biomechanics for processing of experimental data. The most difficult part of this method is sensible choosing of smoothing parameters, so as to provide for good approximation of the experimental table data and of the function derivation (which are needed for solution of dynamics problem).

For biomechanical systems with large number of freedom degrees the complexity of the problem is increased proportionally to the number of approximated displacements. In this case choice of smoothing parameters for different curves should be made in coordination with their contribution to the movement of the whole SMA. Here we should agree with Shennon [83] who noted that for overcoming of such difficulties good scientific knowledge, and, excellent skill and mastery of the researcher are essential.

Therefore, it is helpful to have additional experimental data received by different methods (for example, accelerations of different points, registered by special devices). Smoothing of the trajectory received by some optical method (using say "ELITE" or "ARIEL" devices) and its further differentiation can then give experimental accelerations, which can be compared with model ones for correction of smoothing parameters.

However, it should be noted that the integral error, appearing as a result of numerical modelling of biomechanical systems, cannot be found analytically due to complexity of the modelling object and to necessity of approximations made when presenting skeletal-muscular apparatus by a system of anthropomorphic segments. Significant part of the integral error of numerical modelling is due to error of the optical devices, error of coordinates calculation, rounding off and approximation errors.

Therefore the error introduced by the whole information channel can be estimated only on the basis of a real experiment, when the whole system is checked on a test problem. Examples of such approach will be considered in Chapter 4.

One of the most important problems to be solved in the process of systems of bodies motion modelling is the problem of system of differential algebraic equations integration. Presently for solving this problem various methods can be employed, implemented in software packages (e.g. LINPACK) or those described in appropriate literature (e.g. [38, 61, 66]). Software packages allow to choose between quite a wide variety of methods. Quite frequently the final decision on which method to choose depends on the structure of system of motion equations. This depends on number of bodies in the system model, inertia, rigidity-elasticity, viscosity and other system parameters, type of motion being modelled, and the character of constraints. Therefore, even some comparatively simple and wide-spread method can sometimes satisfy the investigator. It should be noted, that problem of adequate choice of the most universal and "quick" (in the sense of computation time required) method is not solved even in the biggest and well-advertised packages. In the reports of leading investigators in the field of numerical integration of system of differential equation (published by NATO [66]) authors describe current state of the problem and suggest

possible ways of its solution. Analysis of these reports show that, despite considerable achievements, the problem remains open and modelling of any concrete biomechanical system may be seriously impeded due to known obstacles.

Analysis of general aspects and current state of the problem of human motion modelling and optimization allows one to make the following conclusions.

- (i) Human motion modelling proves to be an important, topical problem which is studied by specialists in biomechanics [1, 39, 40, 75, 109], robotics [17, 32, 53, 82], astronautics [5, 108], orthopaedics and prosthetics [28, 36, 79, 100], sport [43, 59, 69, 70, 80].
- (ii) In order to model human skeletal-muscular apparatus motion, usually simple open ramified kinematic chains, comprised of rigid rods of various mass and moment of inertia, which correspond to different body elements are used. Joints linking kinematic chain elements together are considered to be spherical or cylindrical hinges. Links between model elements are considered to be stationary. Constraints are holonomic. Mass-inertia and dimension characteristics are determined on the basis of averaged anthropomorphic data and model experiments.
- (iii) In order to determine dynamic characteristics of modelled body elements, they are sometimes approximated by various geometric figures [36, 76]. In other cases moments of inertia are determined experimentally by employing of mechanical [37, 91] or radioisotope method [102, 103]. In the majority of investigations optical motion registration data is used to determine control moments at joints (appearing during certain goal-oriented locomotion) via mathematical modelling.
- (iv) Mathematical apparatus of analytical mechanics is employed for the modelling. Differential equations of human motion are often written in the Lagrange form of the second order or in the kinetostatics form. Besides, general dynamics equations (Appel's equations system, center of mass motion equations and theorem of moment of momentum increment) are also used. However, expediency of employment of any of these equations depends on problem formulation and introduced motion constraints.
- (v) In human motion modelling it is important to obtain concrete numeric characteristics of real forces causing motion. Therefore coordinate systems which allow to obtain control moments with respect to main joints of human skeletal-muscular apparatus can be called most "anthropomorphic". In case if such an approach makes mathematical analysis too complex, some convenient (from mathematical point of view) coordinate system with following variables substitution aimed at determination of the control moments at human joints (i.e. of such generalised forces which corresponding generalized coordinates are intrument joint angles and which dimension is that of moments) should be employed.

- (vi) The problem of motion synthesis is most effectively solved in robotics and prosthetics. In the basis of robots and manipulators creation lies the idea that motion control can be organised in the form typical for living organisms. Algorithms of autonomous control system in such artificial mechanisms are constructed as in human organism on the principle of closed loop of afferent and efferent impulses interaction. The control system itself is multilevel [71, 72].
- (vii) Model investigations in the field of human motion analysis and synthesis so far have shown limited results. There are several reasons for it. First is human skeletal-muscular apparatus complexity; second — insufficient development of mathematical apparatus and third — deficiencies of the methodology which has been employed in most of these investigations. The last reason is obviously the most substantial because simple transference of modelling methods of technical sciences into such complex systems as biomechanical ones proves to be not efficient.
- (viii) One of the most important and complex problems is the problem of human motion optimization. Some theoretical and experimental data which can be derived from contemporary literature on this topic allow one to make a hypothesis that human motion is governed by optimality principle [60, 70, 105]. However, this data is available for instinctive motions, performed frequently by humans. It remains to be proven that this principle also holds for motions skills developed by humans in their professional and sports activities.

1.3 System Approach to Biomechanical Investigations

Summary of the available theoretical and experimental investigations on the biomechanical systems motion analysis and synthesis convinces one that the study of human motion should be viewed as complex systems investigation. The only methodology which can be successfully employed for such systems analysis (exempting experimental methodology) is the systems theory methodology. Let us therefore consider the most significant features which put biomechanical systems in the range of complex ones. Biomechanical systems are characterized by the high number of interconnected and interacting elements. Human skeletal-muscular apparatus includes about 150 mobile bones and over 800 muscles. Number of freedom degrees for the whole system lies according to various researchers in the range from 244 to 500 [21, 29, 86, 102].

For biomechanical systems there is typical multilevel and multi-loop control. According to contemporary understanding human motion control consists of at least 4–5 levels and incorporates multiple information loops [8, 35, 49, 50]. Moreover, diversity of elements junctions types and link patterns (“tree-like”, hierarchical) is observed, which causes much difficulties in structuring and analysing such systems.

In biomechanical systems positive and negative feedback loops are present. Negative feedback loops serve for motion goal search and regulate biomechanical system

trajectory with respect to motion goal. Positive feedback loops serve for exponential deviation of biomechanical system from certain point of unstable equilibrium.

For biomechanical systems there is characteristic high functioning adaptation, i.e. motion remains goal-oriented in changing environment and under influence of some random disturbances.

Biomechanical systems are nonlinear systems: existence of nonlinear functional dependencies makes the system highly sensitive to values of number of its own characteristics and parameters and at the same time resistant to disturbing impulses. As a result, biomechanical systems are very adaptive, reliable and energy-saving.

Biomechanical systems functioning can be assessed via various criteria employment [60, 73] as is usually done for complex systems. In fact, adjustment of such systems will lead to adequate results only when various criteria of such work is used. For example, maximal output muscles power growth leads to an increase in human activity capabilities under various extreme conditions and therefore this characteristic is an important biomechanical system functioning criterion. However, need in developing this maximal output power arises relatively seldom; usually it is more desirable to have average output power but with maximal value of performance. Thus, it appears clear that biomechanical systems functioning quality criterion should take into account both of these requirements: output power and performances value maximization.

Biomechanical systems, as all complex systems, possess certain characteristics which are, in general, unknown and also a set of inertial inter-element connections which principally cannot be taken into account. This leads to uncertainty in biomechanical system behaviour. One can say that these connections which are excluded from the model, serve as a source of random process influencing biomechanical system motion. Deviation from expected trajectory caused by this random process can be in some cases so significant that it will completely change motion pattern.

All these features which characterize biomechanical systems as complex ones, along with insufficient development of analytical and numerical methods for analysis of such large-dimension systems makes it necessary to apply systems theory.

Systems theory methodology implies integral analysis of the working system instead of studying of separate inter-element connections and phenomena [10, 30, 62, 64]. One of the features of systems theory is that it always considers any system as a subsystem of some larger system. The studied system is considered to be open with respect to the larger one [62, 83].

Another important aspect of systems theory is that any system is not simply a union of several subsystems but, in fact, a qualitatively new formation. In literature devoted to investigation of complex systems and systems theory numerous different definitions of the term "system" can be found. This variety of approaches to description of this term only proves that a complex system is characterised by many specific features.

We believe that one of the best definitions of a complex system is given by Forster

[30]. According to him the term “complex system” implies a multi-element structure of high dimension (with respect to unknown variables) with nonlinear feedback. The system dimension is determined by number of equations describing dynamic behaviour of the system. Application of the methodology of complex systems analysis to human locomotions investigation presents an integrated approach allowing to determine intrinsic laws controlling the motion.

System analysis is, in fact, a discipline combining different methods, based on the use of formalised models and informal procedures using verbal, qualitative description. System analysis implies building of imitational model of the object under consideration.

In contradistinction, analytical models developed by means of imitational methodology do not provide a ready solution but serve as a means for analysis of the system behaviour in conditions chosen by the experimenter. Therefore, as it can be clearly seen, imitational modelling is not a theory, but a methodology for problems solution [83]. In spite of insufficient mathematical elegance imitational modelling is one of the widely used qualitative methods used for control of problems solution.

Distinct from traditional modelling which is widely used in biomechanics and is based on use of one concrete model, imitational modelling implies evolution of the model. Traditionally, one particular model is used throughout all investigations. Imitational modelling deals with a whole series of models. As soon as set problems have been solved new ones can be formulated. In case there is a need to increase the solution accuracy, the model is corrected and the problem is solved anew. Thus, during investigation, the model can be modified many times according to requirements of the investigation. The process of imitational dynamics model creation includes the following steps [30]:

- 1). determination of the model purpose;
- 2). determination as to which components of the object under investigation should be included into the model;
- 3). determination of model parameters;
- 4). determination of the type of functional relations between model components, parameters and variables.

Deciding as to which object components should be included in the model depends on the number of variables that are to be taken into account. The number of output variables is usually easily determined according to investigation goals. Problems appear when choosing which input and state variables are of importance in the effects under investigation. On one hand it is convenient to have the model as simple as possible and thus simplify problem solution. On the other hand, the investigator is interested to have an accurate solution. The problem is to choose the model so as to satisfy both the model level of accuracy and make the solution possibly simpler.

This general problem of imitational modelling is also to be solved when modelling human skeletal-muscular apparatus motions. Most scientific works have a tendency to consider very simple models. Thus, they have a small number of model elements, the elements are considered as rigid, etc. As a result of this the following apprehension appears — all these simplifications can essentially distort the model behaviour in comparison with motion of the real object. However, increase of the model dimension leads to increase of computer time needed. Moreover, as a rule “the level of phenomenon understanding is inversely proportional to the number of variables used for its description” [30]. One has to agree with Beletski that “problem formulation has to be quite sensible, as to describe main effects and properties of the investigated process and, at the same time, as to allow for effective analysis” [4].

A rational compromise can be achieved only as a result of investigation of the model adequacy to the real biomechanical system. Estimation of the model adequacy is usually carried out in three steps:

- 1). verification of correspondence of the model behaviour to principles put on it by the investigator;
- 2). verification of the correspondence of the model behaviour to that of the real system;
- 3). problem analysis, i.e. formulating of statistically significant conclusions on the basis of the data received by computer experiment.

One of the advantages of imitational modelling is simplicity of the model sensitivity analysis. Sensitivity analysis implies investigation of influence of small variations of different model parameters or input variables on the output variables. Investigation of the sensitivity of the model can sufficiently help in determination of its adequacy.

Since most of the data used for model creation are known to have certain levels of error, it is very important to find out the error margin, at which data received by modelling is not yet significantly distorted, and can be considered valid for further investigation. If the model is robust, i.e. its output variables do not change significantly as a result of variation of some of the input parameters, then, there is no need to worry much about this input data accuracy. Otherwise, special attention should be paid to get accurate enough estimations of these parameters [30, 63, 83].

It is quite clear that the imitational model should suffice the following requirements. It must be:

- simple enough and convenient for user;
- goal oriented;
- reliable (i.e. protected from absurd results);
- complete (in respect to possibility of main problems solution);

— adaptive, allowing for easy transformations to new modifications.

Imitational modelling allows one to control the speed of the process under investigation by its accelerating (or decelerating). In application to biomechanics this option makes possible analysis of motions evolution. The main advantage of the imitational modelling methodology is the possibility of solving problems of extreme complexity: the system under investigation can be described by cumbersome equations, exposed to influence of many stochastic factors of complex nature, comprised of both rigid and elastic elements, elastic-plastic bodies, etc.

The basis of imitational modelling is a complex of mathematical models, describing the processes in real biomechanical system under investigation. The user software package should be organised such that each model is be easy to be employed for investigations; results of modelling can be visualised. Much attention should also be paid to creation of convenient information input and editing facilities.

So, as it can be seen, imitation process implies creation of problem-oriented complex mathematical models reflecting the investigated system behaviour. It is also necessary to work out a package of auxiliary programmes which together with special data base allow for fast and convenient realization of computer experiments. Due to the complexity of problems of analysis and synthesis of human locomotions, methodology of imitational modelling, employing general system theory techniques is the most promising approach to their solution.

CHAPTER 2

MATHEMATICAL ANTHROPOMORPHIC MODELS

The approach to description of human SMA as a system of interconnected solid bodies has been developed for over several decades. In the monograph of Wittenburg which has become classical motion equations are derived for a system of solid bodies mathematical model via skilful transformations accompanied by detailed discussion. The author notes that the results obtained independently repeat results of Fisher [29] published in 1906. Since Wittenburg's work was published (over 30 years ago), new studies on this topic have been carried out. Among them there are studies concerning development of universal software on modelling systems of solid bodies dynamics.

The diversity of existing mathematical models of AM has been brought about by their applications demand and this reflects structurally the methodology of mathematical modelling. New programs development and system design problems require mathematical models of the most general type which allow for variation of elements and joints characteristics, external forces and their nature, in particular, impact loads, thermal, chemical and other factors influence on AM mechanical characteristics. In the next sections we will describe some special and universal solid body mathematical models of AM. The first section contains some basics of solid dynamics.

2.1 Extracts from Solid Body Dynamics

A solid body is the main element of all modern models of AM. Therefore, we begin our discussion from a simple solid body motion. Essential difference of a solid body dynamics from particle mechanics shows itself when we study body rotation.

For a particle of mass m , momentum is defined as

$$\underline{q} = m \underline{\dot{z}}, \quad (2.1)$$

moment of momentum with respect to point O

$$\underline{k}_O = \underline{z} \times m \underline{\dot{z}}, \quad (2.2)$$

and kinetic energy

$$T = \frac{1}{2} m |\underline{\dot{z}}|^2. \quad (2.3)$$

Here $\underline{\dot{z}}$ — is the absolute velocity vector (the sign of line under a letter appears when corresponding variable is a vector, a point over letter assigns a derivative with respect to time variable).

If we consider a solid body to be an aggregate of particles of mass dm (mass differential), then its momentum, moment of momentum, and kinetic energy can be obtained by integration

$$\underline{Q} = \int_m \dot{\underline{z}} dm, \quad \underline{K}_O = \int_m \underline{z} \times \dot{\underline{z}} dm, \quad T = \frac{1}{2} \int_m |\dot{\underline{z}}|^2 dm. \quad (2.4)$$

According to the solid body kinematics [55]

$$\dot{\underline{z}} = \dot{\underline{z}}_c + \underline{\omega} \times \underline{r},$$

where \underline{z}_c — is the center of mass C radius vector, $\underline{\omega}$ — vector of absolute angular velocity, \underline{r} — particle radius vector with respect to the body center of mass. This nomenclature is illustrated in Fig. 2.1.

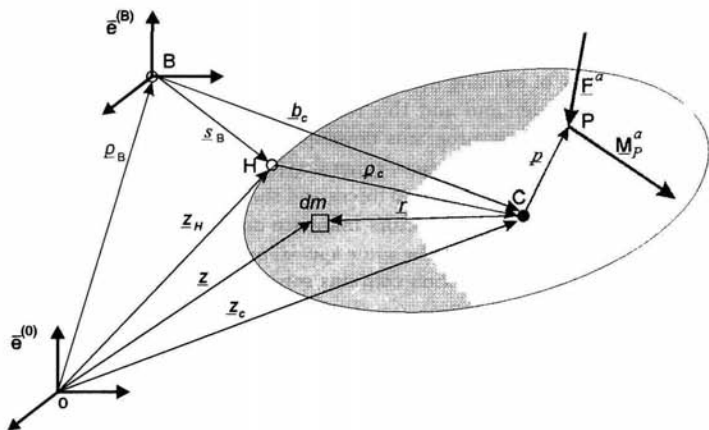


Fig. 2.1. A solid body with some characteristic points (H — joint, B — another body point, P — active forces application point).

Substituting expression for $\dot{\underline{z}}$ into Eq. (2.4) we will have

$$\underline{Q} = m \dot{\underline{z}}_c, \quad \underline{K}_O = m \underline{z}_c \times \dot{\underline{z}}_c + \int_m \underline{r} \times (\underline{\omega} \times \underline{r}) dm, \quad T = \frac{1}{2} (m |\dot{\underline{z}}_c|^2 + \int_m |\underline{\omega} \times \underline{r}|^2 dm). \quad (2.5)$$

Taking advantage of the following vector and mixed product properties:

$$\begin{aligned} (\underline{\omega} \times \underline{r}) \cdot (\underline{\omega} \times \underline{r}) &= \underline{\omega} \cdot (\underline{r} \times (\underline{\omega} \times \underline{r})), \\ \underline{r} \times (\underline{\omega} \times \underline{r}) &= \underline{\omega} \underline{r} \cdot \underline{r} - \underline{r} \underline{r} \cdot \underline{\omega} = (\underline{E} \underline{r}^2 - \underline{r} \underline{r}) \cdot \underline{\omega}, \end{aligned} \quad (2.6)$$

(where \underline{E} — is a unit tensor; $\underline{r} \underline{r}$ — vector diad; and point stands for scalar product), one can obtain the final expression

$$T = \frac{1}{2}(m\dot{z}_c^2 + \underline{\omega} \cdot \underline{J}^c \cdot \underline{\omega}), \quad \underline{K}_O = m \underline{z}_c \times \dot{\underline{z}}_c + \underline{J}^c \cdot \underline{\omega}, \quad (2.7)$$

where $\underline{J}^c = \int (\underline{E} r^2 - \underline{r} \underline{r}) dm$ — is a characteristic of the solid body inertia properties with respect to point C (center of mass). It is called tensor of inertia with respect to point C . A solid body is represented by a system of fixed parameters: center of mass radius vector $\underline{\rho}_c$, inertia characteristics m , \underline{J}^c and location of joints on the body surface. Center of mass motion theorem for a solid body is analogous to particle motion theorem

$$m \ddot{\underline{z}}_c = \underline{F}, \quad (2.8)$$

where \underline{F} — resultant vector of external forces exerted to the body. Analogously rotational motion is governed by the theorem of moment of momentum variation

$$\dot{\underline{K}}_O = \underline{M}_O. \quad (2.9)$$

Here \underline{M}_O — is resultant moment of external forces moments with respect to the point O . It will be of use further on to consider now a specific case when a body is exposed to gravity force $m\underline{g}$, external force \underline{F}^a applied at a given point (with radius vector \underline{p}) and \underline{M}_P^a — moment of system of external forces with respect to point P . Differentiating \underline{K}_O in Eq. (2.7) and substituting \underline{M}_O and \underline{F} in Eq. (2.8), Eq. (2.9) with corresponding components we obtain

$$m \ddot{\underline{z}}_c = m \underline{g} + \underline{F}^a, \quad (2.10)$$

$$m \underline{z}_c \times \ddot{\underline{z}}_c + \underline{\omega} \times \underline{J}^c \cdot \underline{\omega} + \underline{J}^c \cdot \dot{\underline{\omega}} = m \underline{z}_c \times \underline{g} + (\underline{z}_c + \underline{p}) \times \underline{F}^a + \underline{M}_P^a \quad (2.11)$$

Substituting $m \ddot{\underline{z}}_c$ in the second equation with the right part of the first one we get

$$\underline{J}^c \cdot \dot{\underline{\omega}} + \underline{\omega} \times \underline{J}^c \cdot \underline{\omega} = \underline{p} \times \underline{F}^a + \underline{M}_P^a. \quad (2.12)$$

Eq. (2.12) is a restatement of Eq. (2.9) where moment of momentum is calculated with respect to body center of mass C . By now we have addressed major solid body dynamics topics without paying attention to concrete representations of given equations in Cartesian or generalized coordinates (Euler, Cardan angles; Eulerian parameters). In applications, especially in case of small parameters, symmetry or other simplifying factors, some analytical solutions or solution estimates can be obtained [56, 101].

2.2 Description of a System of Solid Bodies Structure

As soon as we assume that an anthropomorphic object dynamics can be modelled by a system of n solid bodies (which are usually connected) we should describe this system structure. The first stage of the description consists of identification and

ranging of the anthropomorphic model elements. Let each of the AM elements have a label (number). With no harm to generality, we can number all solid bodies from 1 to n . For example, we numbered the body elements of a runner (see Fig. 2.1). Let the numbering be successive and such that for each element (solid body) vector \underline{b}_j is introduced, the beginning of which is located in arbitrary point B_i on a body number $i < j$ and the end is marked by point B_j of body number j . As for the vector \underline{b}_1 , its beginning corresponds to point B_0 belonging to the first element. It is clear (for example from Fig. 2.3) that such identification result is not unambiguous (i.e. there are many solutions of identification task), however it always leads to a structure which can be described by a "tree-like" unidirectional graph [26, 54]. Structure matrix μ , which determines the order of graph nodes (i.e. points B_j of elements j), contains a unit (1) in line i and column j if point B_j is located on the way from point B_0 to B_i and zero (0) if this is not so. On the left part of Table 2.1 (page 20), structure matrix for AM is given which consists of 11 elements (see Fig. 2.3).

The structure matrix μ makes it possible to determine the position of any point of element number i according to the formula

$$\underline{P}_i = \sum_{j=1}^i \mu_{ij} \underline{b}_j + \underline{z}_i. \quad (2.13)$$

It should be noted that there is no need in multiplication by 1 or 0 in the process of summing. It is enough to use matrix μ as a binary indication of participation of vector \underline{b}_j in the chain linking points B_0 and B_i .

If spatial system of disconnected solid bodies possesses n freedom degrees, then the number of freedom degrees of AM comprising these bodies is less than that and is determined, as follows from general theory of systems with internal links, by the number of geometric restrictions imposed on the system elements. Description of the elements links structure can be obtained via graph theory. Considering system elements (solid bodies of the AM) as graph nodes and links between them as graph arcs, we can introduce for each arc value $\gamma_{ij} = \overline{0, 7}$ which will determine mobility of the links. (It is convenient to use numbers from 0 to 7 to enable to point out any of the possible links — from rigid link to absence of link between two solid bodies even by force interaction).

As soon as we have introduced such characteristics the graph is called "weighted". It can describe an arbitrary structure which is not necessarily a "tree-like" one. Moreover, it can contain such subsets of arcs which form closed loops. It is not always a solvable task to choose independent characteristics for description of dynamics of such systems. Therefore, for modelling of systems with complex graph presentation, the approach used is some graph arcs are severed in order to obtain a subgraph with a "tree-like" structure.

Construction of such subgraphs can be performed by means of successive numbering of AM elements as was described above. However, it is very likely that the number of freedom degrees for such arbitrary graph will be higher than it would be

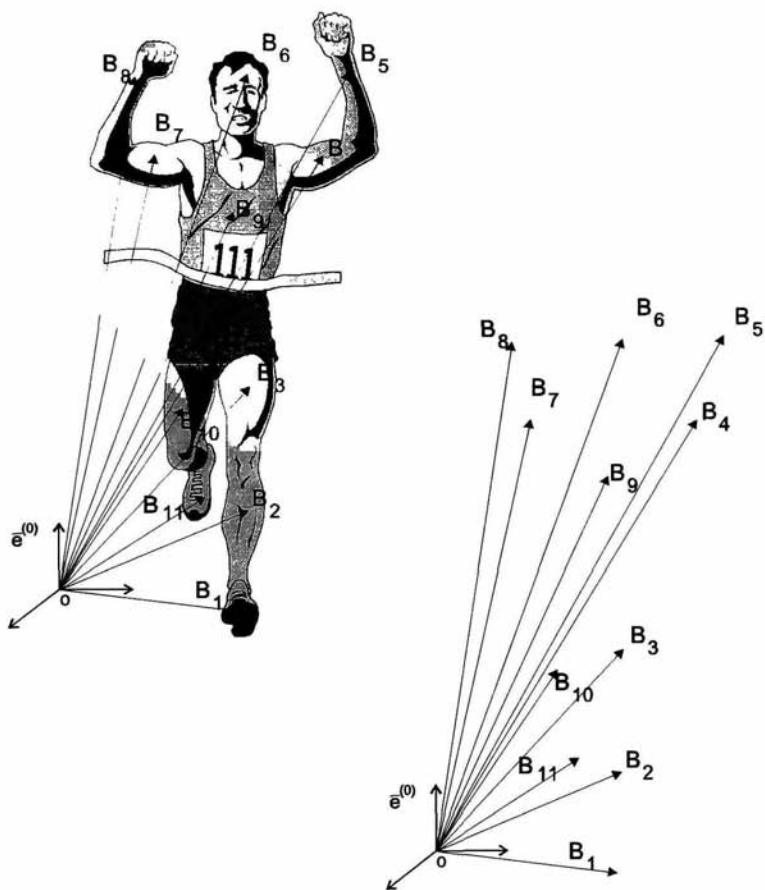


Fig. 2.2. Bush-like graph of Microsoft Power Point "winner".

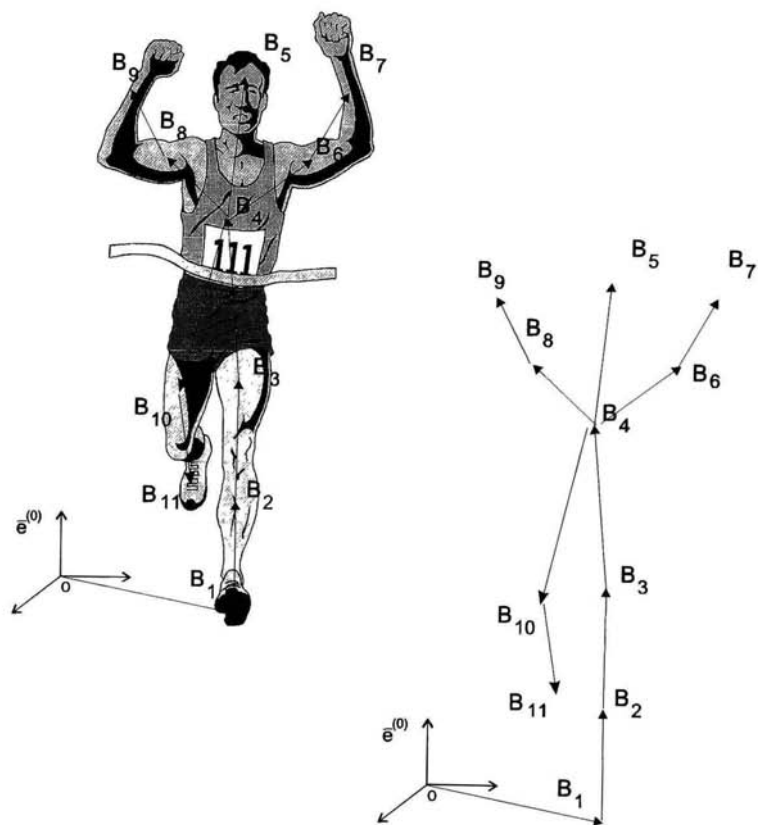


Fig. 2.3. Tree-like framework graph of Microsoft Power Point “winner”

for some other order of numeration.

Let us define “weight” of the sectional arc joining two points as sum of weights which correspond to the arcs composing the sectional arc. Then the subgraph of minimal “weight” which incorporates all of such sectional arcs for different elements of AM is called optimal. This optimal subgraph is also called “framework” in graph theory. There exist effective algorithms allowing one to determine the framework of an arbitrary graph (e.g. algorithm of Kruskal [26, 51]). Thus we can partly describe an arbitrary system of solid bodies structure by “optimal tree-like graph”. Other links among bodies must be defined additionally by link equations. System graph forming can be done differently. We will see that later.

2.3 Spatial Model with Spherical Joints

2.3.1 Structure Description

Let us model the AM as a system of solid bodies linked up by spherical joints. Each body in the system corresponds to a segment of the AM. Hereafter we will assume that any segment has two or less joints which location fixed in respect to the body coordinate system. This limitation, however, allows for coaxial cylindrical joints. To model a segment with more than two joints stationary confining constraints can be used in this model.

Let us introduce a fixed coordinate system orthogonal basis $\bar{e}^{(0)}$, consisting of a set of three vectors $\underline{e}_k^{(0)}$, $k = \overline{1, 3}$. Herebelow the sign of a line over a letter stands for a vector array and over two figures separated by a comma stands for a range of an integer variable.

Let us also introduce orthogonal bases $\bar{e}^{(i)}$ each fixed in respect to corresponding AM segment i with basis vectors $\underline{e}_k^{(i)}$, $k = \overline{1, 3}$, $i = \overline{1, n}$. So we have $3(n+1)$ basis vectors \underline{e}_k^i , characterizing mutual orientation of our model segments (elements).

Let us orient basis $\bar{e}^{(i)}$ so that unit vector $\underline{e}_1^{(i)}$ would be directed along the line joining joints of the element i and towards the joint furthest from support with radius-vector r_0 (towards the joint with greater cardinal number). Let unit vector $\underline{e}_2^{(i)}$ lie in the plane containing $\underline{e}_1^{(i)}$ and the center of mass (CM), unless the CM lies on the line containing $\underline{e}_1^{(i)}$. Then orientation is determined by corresponding element geometry. Hereafter we will assume that all bases are right-hand.

For each segment i we shall assign vector r_i joining joint points. Then

$$r_i = l_i \underline{e}_1^{(i)}, i = \overline{1, n}, \quad (2.14)$$

where $l_i = |r_i|$ — so called “length” of segment i .

Structure matrix μ of $(n \times n)$ dimension will help us to describe ramified kinematic chain, i.e. how model elements are joined together. Each matrix element μ_{ij} can be either 0 or 1. If absolute displacement of the kinematic chain element i depends on coordinates of element j , $\mu_{ij} = 1$, otherwise $\mu_{ij} = 0$. With no harm to generality of

analysis we will assume that elements are numerated in increasing order starting from r_0 and along the kinematic chain branches. As a result of this, matrix μ becomes triangular with units on its diagonal. An arbitrary AM point belonging to element i has radius vector \underline{P}_i

$$\underline{P}_i = r_0 + \sum_{j=1}^{i-1} \mu_{ij} r_j + z_i, \quad (2.15)$$

where vector z_i belongs to basis $\bar{e}^{(i)}$. It is clear, that matrix μ is the same as in Sec. 2.2.

In Fig. 2.4 we give an example of an 11-element AM with spherical joints and the corresponding μ and μ^{-1} matrices are given in Table 2.1.

Table 2.1. Structure matrix μ and matrix of incidence (inverse matrix of μ)
 $\mu^{(inc)} \equiv \mu^{-1}$

| | 1 | 2 | 3 | 4 | 5 | 6 | 7 | 8 | 9 | 0 | 1 | 1 | 2 | 3 | 4 | 5 | 6 | 7 | 8 | 9 | 0 | 1 |
|----|-------|---|---|---|---|---|---|---|---|---|---|------------|----|----|----|---|---|----|---|---|---|----|
| 1 | 1 | 0 | 0 | 0 | 0 | 0 | 0 | 0 | 0 | 0 | 0 | 1 | 0 | 0 | 0 | 0 | 0 | 0 | 0 | 0 | 0 | 0 |
| 2 | 1 | 1 | 0 | 0 | 0 | 0 | 0 | 0 | 0 | 0 | 0 | -1 | 1 | 0 | 0 | 0 | 0 | 0 | 0 | 0 | 0 | 0 |
| 3 | 1 | 1 | 1 | 0 | 0 | 0 | 0 | 0 | 0 | 0 | 0 | 0 | -1 | 1 | 0 | 0 | 0 | 0 | 0 | 0 | 0 | 0 |
| 4 | 1 | 1 | 1 | 1 | 0 | 0 | 0 | 0 | 0 | 0 | 0 | 0 | 0 | -1 | 1 | 0 | 0 | 0 | 0 | 0 | 0 | 0 |
| 5 | 1 | 1 | 1 | 1 | 1 | 0 | 0 | 0 | 0 | 0 | 0 | 0 | 0 | -1 | 1 | 0 | 0 | 0 | 0 | 0 | 0 | 0 |
| 6 | 1 | 1 | 1 | 1 | 0 | 1 | 0 | 0 | 0 | 0 | 0 | 0 | 0 | -1 | 0 | 1 | 0 | 0 | 0 | 0 | 0 | 0 |
| 7 | 1 | 1 | 1 | 1 | 0 | 1 | 1 | 0 | 0 | 0 | 0 | 0 | 0 | 0 | -1 | 1 | 0 | 0 | 0 | 0 | 0 | 0 |
| 8 | 1 | 1 | 1 | 1 | 0 | 0 | 0 | 1 | 0 | 0 | 0 | 0 | 0 | -1 | 0 | 0 | 0 | 1 | 0 | 0 | 0 | 0 |
| 9 | 1 | 1 | 1 | 1 | 0 | 0 | 0 | 1 | 1 | 0 | 0 | 0 | 0 | 0 | 0 | 0 | 0 | -1 | 1 | 0 | 0 | 0 |
| 10 | 1 | 1 | 1 | 0 | 0 | 0 | 0 | 0 | 0 | 1 | 0 | 0 | 0 | -1 | 0 | 0 | 0 | 0 | 0 | 0 | 1 | 0 |
| 11 | 1 | 1 | 1 | 0 | 0 | 0 | 0 | 0 | 0 | 1 | 1 | 0 | 0 | 0 | 0 | 0 | 0 | 0 | 0 | 0 | 0 | -1 |
| | μ | | | | | | | | | | | μ^{-1} | | | | | | | | | | |

Components of matrix μ^{-1} can be easily calculated either directly (according to definition of inverse matrix, taking into account the triangular form of the matrix μ) or with help of the following equations

$$\underline{R}_i = r_0 + \sum_{j=1}^i \mu_{ij} r_j - r_i, \quad \underline{R}'_i = \underline{R}_i - r_0 + r_i, \quad \underline{R}'_i = \sum_{j=1}^n \mu_{ij} r_j,$$

where \underline{R}'_i — radius-vector of element i end with respect to point H_1

Let us introduce the following nomenclature $\bar{R}' = (\underline{R}'_1, \dots, \underline{R}'_n)^T$, $\bar{r} = (r_1, \dots, r_n)^T$. Then, on one hand

$$\bar{r} = \mu^{-1} \bar{R}', \quad (2.16)$$

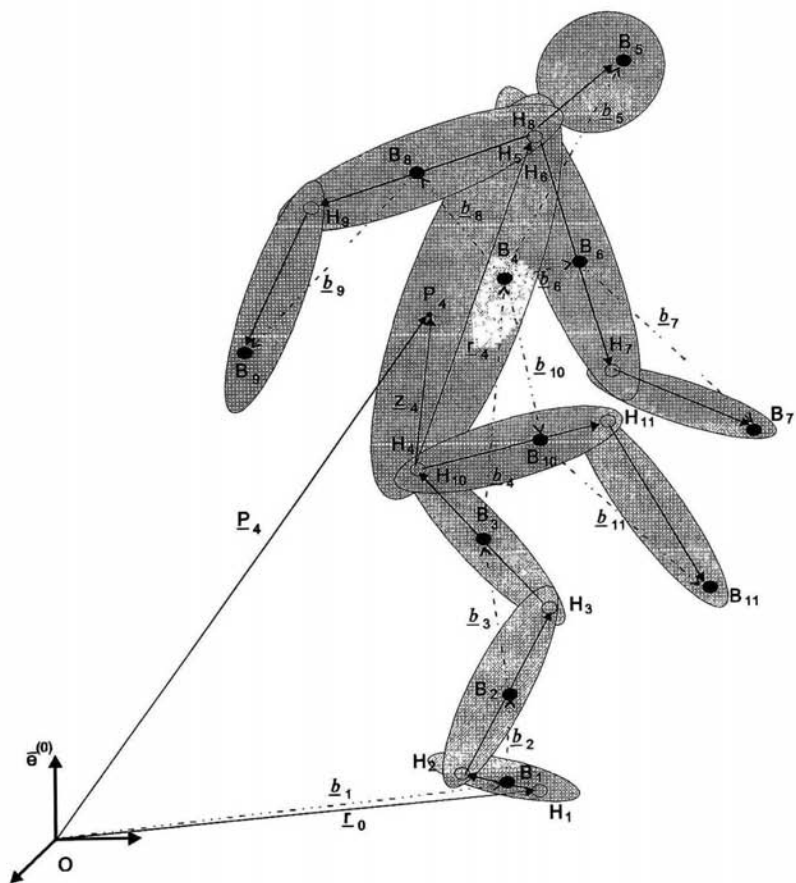


Fig. 2.4. 11-element AM kinematic chain with spherical joints.

and on the other hand, for example, $r_4 = \underline{R}'_4 - \underline{R}'_3$ which is obvious from Fig. 2.4. Such ordered elements numeration and triangular form of matrix μ allows one to somewhat reduce the volume of calculations for kinetic energy matrix assessment.

Let us now introduce geometrical and mass-inertia characteristics of AM elements: l_i — length, $\underline{\rho}_{ci}$ — center of mass radius vector with respect to point H_i ; m_i — element's mass; \underline{J}_i^c — central tensor of inertia. Expressions for $\underline{\rho}_{ci}$ and \underline{J}_i^c are defined as follows (Fig. 2.5)

$$m_i \underline{\rho}_{ci} = \int_{m_i} \underline{\rho}' dm, \quad \underline{J}_i^c = \int_{m_i} (\underline{E} \rho^2 - \underline{\rho} \rho) dm, \quad (2.17)$$

where $\underline{\rho}$, $\underline{\rho}'$ — radius vectors of mass dm , belonging to element i . They characterize

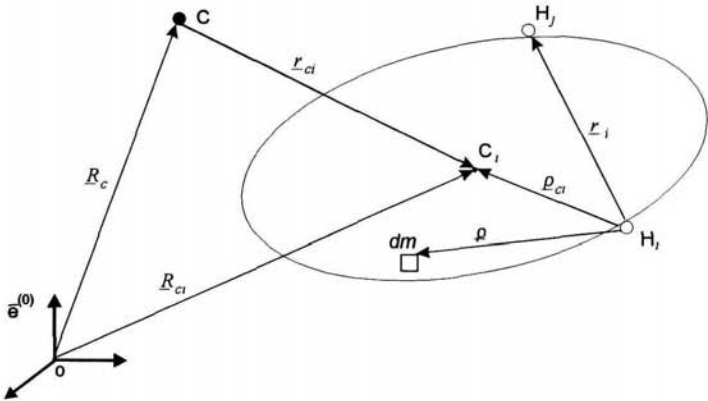


Fig. 2.5. AM element basic nomenclature.

the dm position with respect to the element's center of mass and joint H_i correspondingly. Center of mass C_i radius vector with respect to point O is \underline{R}_{ci} and

$$\underline{R}_{ci} = \underline{r}_0 + \sum_{k=1}^{i-1} \mu_{ik} \underline{r}_k + \underline{\rho}_{ci}. \quad (2.18)$$

Let $M^c = \sum_{i=1}^n m_i$ — be the total mass of AM. AM center of mass radius vector and its derivatives can be obtained from the following equality

$$M^c \underline{R}_c = \sum_{i=1}^n m_i \underline{R}_{ci} = M^c \underline{r}_0 + \sum_{i=1}^n \underline{\rho}_{ci} + \sum_{i=1}^n \sum_{k=1}^{i-1} m_i \mu_{ik} \underline{r}_k. \quad (2.19)$$

Hereafter we will need the following identities in order to be able to change the sum order (we give these identities without proof):

$$\sum_{i=1}^n \sum_{k=1}^{i-1} \alpha_{ik} = \sum_{k=1}^n \sum_{i=k+1}^n \alpha_{ik} = \sum_{i=1}^n \sum_{k=i+1}^n \alpha_{ki} \quad (2.20)$$

$$\begin{aligned} \sum_{i=1}^n \sum_{j=1}^{i-1} \sum_{k=1}^{i-1} \alpha_{ijk} &= \sum_{k=1}^n \sum_{j=1}^n \left(\sum_{\substack{i=k+1 \\ j < k}}^n \alpha_{ijk} + \sum_{\substack{i=k+1 \\ j=k}}^n \alpha_{ikk} + \sum_{\substack{i=j+1 \\ j > k}}^n \alpha_{ijk} \right) = \\ &= \sum_{i=1}^n \sum_{j=1}^n \left(\sum_{\substack{k=i+1 \\ j < i}}^n \alpha_{kji} + \sum_{\substack{k=i+1 \\ j=i}}^n \alpha_{kii} + \sum_{\substack{k=j+1 \\ j > i}}^n \alpha_{kji} \right) = \\ &= \sum_{k=1}^n \sum_{i=k+1}^n \sum_{j=1}^{i-1} \alpha_{ijk} = \sum_{i=1}^n \sum_{k=i+1}^n \sum_{j=1}^{k-1} \alpha_{kji} = \sum_{i=1}^n \sum_{j=i+1}^n \sum_{k=1}^{j-1} \alpha_{jki}. \end{aligned} \quad (2.21)$$

Using Eq. (2.20) we can reformulate Eq. (2.19) and also derive identities for derivatives of \underline{R}_c :

$$\begin{aligned} M^c(\underline{\dot{R}}_c - \dot{\underline{r}}_0) &= \sum_{i=1}^n \underline{C}_i, \quad M^c(\underline{\ddot{R}}_c - \ddot{\underline{r}}_0) = \sum_{i=1}^n \underline{\omega}_i \times \underline{C}_i, \\ M^c(\underline{\ddot{R}}_c - \ddot{\underline{r}}_0) &= \sum_{i=1}^n [\underline{\dot{\omega}}_i \times \underline{C}_i + \underline{\omega}_i \times (\underline{\omega}_i \times \underline{C}_i)], \end{aligned} \quad (2.22)$$

where

$$\underline{C}_i = m_i \underline{\rho}_{ci} + \left(\sum_{k=i+1}^n m_k \mu_{ki} \right) \underline{r}_i \quad (2.23)$$

— vector which belongs to element i and defines new center of mass position with respect to point H_i on the basis $\bar{e}^{(i)}$ taking into account added mass of bodies whose motion is influenced by the element i . We can define \underline{C}_i as static moment with respect to point H_i of influenced by body i bodies. This expression for vector \underline{C}_i is of use when studying mutual influence of external forces applied to AM. Gravity force applied to every AM element at point C_i is an example of such external force. Let us note that gravity force potential energy of the system can be expressed as follows (using the adopted nomenclature)

$$\Pi = -M^c \underline{R}_c \cdot \underline{g} = - \left(M^c \underline{r}_0 + \sum_{i=1}^n \underline{C}_i \right) \cdot \underline{g}. \quad (2.24)$$

2.3.2 Expressions for Fundamental Dynamic Quantities

Let us now derive system moment of momentum with respect to points O , H_1 , C and kinetic energy in fixed basis $\bar{e}^{(0)}$ and in bases $\bar{e}^{(H_1)}$ and $\bar{e}^{(c)}$ (center of mass basis). From the general definition of moment of momentum of a solid body we can write its expression for element i with respect to point O as

$$\underline{K}_{O_i} = m_i \underline{R}_c \times \dot{\underline{R}}_c + m_i (\underline{R}_c \times \dot{\underline{r}}_{ci} + \underline{r}_{ci} \times \dot{\underline{R}}_c) + \underline{k}_i, \quad (2.25)$$

where $\underline{k}_i = m_i \underline{r}_{ci} \times \dot{\underline{r}}_{ci} + \underline{J}_i^c \cdot \underline{\omega}_i$ — moment of momentum of element i with respect to system mass center C . Summing all the elements of AM we obtain the total AM moment of momentum

$$\underline{K}_O = \sum_{i=1}^n \underline{K}_{O_i} = M^c \underline{R}_c \times \dot{\underline{R}}_c + \underline{k}, \quad (2.26)$$

where \underline{k} — is total AM moment of momentum with respect to system mass center C .

Due to ordered numeration of AM elements and the way we have introduced coordinate systems, expression for moment of momentum of system with respect to point H_1 (\underline{K}'') takes the most clear and simple form in $\bar{e}^{(H_1)}$ basis

$$\begin{aligned} \underline{K}'' &= \underline{k} + M^c (\underline{R}_c - \underline{r}_0) \times (\dot{\underline{R}}_c - \dot{\underline{r}}_0) = \\ &= \underline{k} + \sum_{i=1}^n \sum_{j=1}^n \underline{C}_i \times (\underline{\omega}_j \times \underline{C}_j) / M^c = \\ &= \underline{k} + \sum_{i=1}^n \sum_{j=1}^n \{ [\underline{E}(\underline{C}_i \cdot \underline{C}_j) - \underline{C}_i \underline{C}_j] \cdot \underline{\omega}_j \} / M^c = \\ &= \sum_{i=1}^n \sum_{j=1}^n \underline{A}_{ij} \cdot \underline{\omega}_j. \end{aligned} \quad (2.27)$$

Where components of tensor matrix $\underline{\underline{A}}_{ij} = \{ \underline{A}_{ij} \}$ are defined as follows

$$\underline{A}_{ij} = \begin{cases} \underline{E}(\underline{a}_{ij} \cdot \underline{r}_j) - \underline{r}_j \underline{a}_{ij}, & j < i; \\ \underline{J}_i, & j = i; \\ \underline{E}(\underline{a}_{ji} \cdot \underline{r}_i) - \underline{a}_{ji} \underline{r}_i, & j > i, \quad i, j = \overline{1, n}, \end{cases} \quad (2.28)$$

and

$$\begin{aligned} \underline{a}_{ij} &= m_i \mu_{ij} \underline{\rho}_{ci} + \underline{r}_i \sum_{\substack{k=i+1 \\ j < k}}^n m_k \mu_{ki} \mu_{kj}; \\ \underline{J}_i &= \underline{J}_i^c + m_i (\underline{E} \underline{\rho}_{ci}^2 - \underline{\rho}_{ci} \underline{\rho}_{ci}) + (\underline{E} \underline{r}_i^2 - \underline{r}_i \underline{r}_i) \sum_{k=i+1}^n m_k \mu_{ki} \end{aligned}$$

The coefficient by which r_i is multiplied in expression for g_{ij} is a sum of masses of those AM elements whose motion is influenced by element i and j simultaneously. First three expressions in Eq. (2.27) can be easily derived from the set above identities. Last equality is obtained by direct substitution of all variables with their expressions through AM elements characteristics and further implementation of identities of Eq. (2.21) type. In particular, we can denote $\alpha_{kji} = m_k \mu_{kj} \mu_{ki} r_i \times (\omega_j r_j)$. The asterisk in Eq. (2.28) indicates tensor conjugation, i.e. change of diad product order. Kinetic energy of AM in bases $\bar{e}^{(0)}$, $\bar{e}^{(H_i)}$, $\bar{e}^{(c)}$ denoted hereafter T , T'' , T' correspondingly can be obtained from kinetic energy definition according to which

$$T_i = \frac{1}{2} m_i \dot{R}_{ci}^2 + \frac{1}{2} \underline{\omega}_i \cdot \underline{J}_i^c \cdot \underline{\omega}_i,$$

and therefore

$$\begin{aligned} T &= \sum_{i=1}^n T_i = \frac{1}{2} M^c \dot{R}_c^2 + \sum_{i=1}^n T_i' = \frac{1}{2} M^c \dot{R}_c^2 + T', \\ T'' &= T' + \frac{1}{2} M^c |\dot{R}_c - \dot{r}_0|^2 = \frac{1}{2} \sum_{i=1}^n \sum_{j=1}^n \omega_i \cdot \underline{A}_{ij} \cdot \omega_j. \end{aligned} \quad (2.29)$$

To understand how the last equality is derived one needs to follow transformation procedure analogous to one described above when explaining the last equality in Eq. (2.27). The most compact way to state Eq. (2.27), Eq. (2.29) is to write them in the matrix-tensor form

$$\begin{aligned} \underline{K}'' &= I \bar{\bar{A}} \cdot \bar{\omega}, & \underline{k} &= I \bar{\bar{G}} \cdot \bar{\omega}, \\ T'' &= \frac{1}{2} \bar{\omega}^T \cdot \bar{\bar{A}} \cdot \bar{\omega}, & T' &= \frac{1}{2} \bar{\omega}^T \cdot \bar{\bar{G}} \cdot \bar{\omega}, \end{aligned} \quad (2.30)$$

where $\bar{\omega} = (\omega_1, \dots, \omega_n)^T$ — column composed of absolute angular velocities vectors, $I = (1, \dots, 1)$ — unit line; multiplication of I and a tensor makes for convolution with respect to one of the indices (sum across one of the indices); $\bar{\bar{G}}$ — tensor matrix which components are defined as follows

$$\underline{\underline{G}}_{ij} = \underline{A}_{ij} - (\underline{E}(\underline{C}_i \cdot \underline{C}_j) - \underline{C}_i \underline{C}_j) / M^c, \quad i, j = \overline{1, n} \quad (2.31)$$

In Eq. (2.30) we imply matrices product to be scalar product (such approach is heavily employed in Ref. [101]). These identities are analogous in their form to the classical expressions for moment of momentum and kinetic energy of a solid body. It is quite obvious that $\bar{\bar{A}}$ — is system kinetic energy matrix, expressed in the form which is invariant to the coordinate system. From Eq. (2.31) one can see that imaginary translation of the support point to the system center of mass C leads to transformation of kinetic energy matrix components according to the following rule

$$\underline{A}_{ij} = \underline{\underline{G}}_{ij} + (\underline{E}(\underline{C}_i \cdot \underline{C}_j) - \underline{C}_i \underline{C}_j) / M^c, \quad (2.32)$$

where $\underline{C}_{i,j}$ vectors play the role of displacements (though, of course, they differ in their dimension) in Huggens-Steiner theorem of tensor of inertia transformation [56]. By now we have considered aspects and general identities which shed some light on analysis of motion of systems of solid bodies. Let us turn at this point to derivation of motion equations.

2.3.3 Equations of Motion

A thorough comparison of various approaches to derivation of motion equations [6, 17, 31, 32, 53, 56, 65, 82, 87, 94, 97, 101] allows one to combine several general techniques employed by different authors. The most widely used variant has to do with the Lagrange equations of the 2nd kind, however it requires selection of one concrete system of generalized coordinates for derivation and further differentiation of the expression for kinetic potential. Analogous restraints are introduced when employing Hamilton, Gaussian and other variation principles of mechanics [95]. The most general approach was proposed by Wittenburg J. [101]. Application of D'Alambert-Lagrange principle has allowed to write in vector form equations of motion of closed loop kinematic chains for arbitrary element joints and non-confining constraints.

In this subsection we will give derivation of motion equation for open loop kinematic chains with spherical joints as this will allow to obtain expressions which have clear comfortable form and can be used for creation of computer software. The model we consider serves as a basis for creation of software aimed at adequate mathematical modelling of professional, industrial and sports movements of human SMA. The direct derivation of motion equations gives a chance to understand deeper the mechanics of model's elements interaction, provide for different variants of element configuration, external forces and moments applied to AM during motion performance.

Let us start from writing down the center of mass motion theorem and moment of momentum variation theorem for each body of the system. Then, excluding internal forces and reaction forces we will obtain n equations in the Newton-Euler form. From the first theorem for the center of mass of element i we get

$$m_i \ddot{\underline{R}}_{ci} = m_i \underline{g} + \underline{N}_i^* + \underline{F}_i, \quad (2.33)$$

where $\ddot{\underline{R}}_{ci}$ — center of mass absolute acceleration for element i , \underline{N}_i^* — joint reaction forces resultant, \underline{F}_i — external forces resultant.

Such separation between forces applied to element i has to do with nature of their influence on this element. Vectors \underline{N}_i^* satisfy the following equality $\underline{N}_1 = \sum_{i=1}^n \mu_{i1} \underline{N}_i^*$, i.e. in single-support phase these forces influence AM motion only by means of support reaction force \underline{N}_1 , whereas each of forces \underline{F}_i is external with respect to the AM. Let us consider matrices-columns

$$\overline{N} = (\underline{N}_1, \dots, \underline{N}_n)^T, \quad \overline{N}^* = (\underline{N}_1^*, \dots, \underline{N}_n^*)^T, \quad (2.34)$$

where \underline{N}_i — joint i reaction force. Let us note that force $-\underline{N}_i$ is applied to previous element and, using structure matrix μ , we can write

$$\underline{N} = \mu^T \underline{N}^*, \quad \underline{N}^* = \mu^{-T} \underline{N}, \quad \underline{M} = \mu^T \underline{U}, \quad \underline{U} = \mu^{-T} \underline{M}, \quad (2.35)$$

where $\underline{M} = (\underline{M}_1, \dots, \underline{M}_n)^T$, $\underline{U} = (\underline{U}_1, \dots, \underline{U}_n)^T$ — matrices-columns comprised of interelement moments \underline{M}_i and resultant moments \underline{U}_i applied to element i . Main nomenclature is presented in Fig. 2.6.

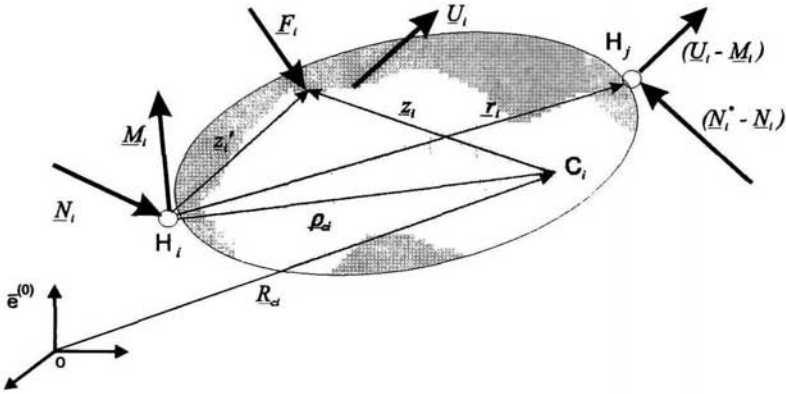


Fig. 2.6. Element i (main nomenclature).

Analogously to equality Eq. (2.12) theorem on moment of momentum increment in basis bound to point C_i yields

$$\underline{J}_i^c \cdot \dot{\underline{\omega}}_i + \underline{\omega}_i \times \underline{J}_i^c \cdot \underline{\omega}_i = -\underline{\rho}_{ci} \times \underline{N}_i + (\underline{r}_i - \underline{\rho}_{ci}) \times (\underline{N}_i^* - \underline{N}_i) + \underline{z}_i \times \underline{F}_i + \underline{U}_i. \quad (2.36)$$

Employing Eq. (2.33) and Eq. (2.35) we get

$$(\underline{N}_i^* - \underline{N}_i) = - \sum_{j=i+1}^n m_j \mu_{ji} \ddot{\underline{R}}_{cj} + \sum_{j=i+1}^n \mu_{ji} (m_j \underline{g} + \underline{F}_j),$$

and then expression Eq. (2.36) can be rewritten in the following detailed form

$$\begin{aligned} \underline{J}_{ci} \cdot \dot{\underline{\omega}}_i + \underline{\omega}_i \times \underline{J}_i^c \cdot \underline{\omega}_i + \underline{r}_i \times \sum_{j=i+1}^n m_j \mu_{ji} \ddot{\underline{R}}_{cj} + \underline{\rho}_{ci} \times m_i \ddot{\underline{R}}_{ci} = \\ = \left(\sum_{j=i+1}^n m_j \mu_{ji} \underline{r}_i + m_i \underline{\rho}_{ci} \right) \times \underline{g} + \\ + \underline{r}_i \times \sum_{j=i+1}^n \underline{F}_j \mu_{ji} + (\underline{\rho}_{ci} + \underline{z}_i) \times \underline{F}_i + \underline{U}_i \end{aligned} \quad (2.37)$$

Let us note that in the right-hand side of Eq. (2.37), the first item is the vector product of \underline{g} and \underline{C}_i which allows to get rid of gravity force moment given certain position of joints on element i (passive unloading under condition $\underline{C}_i = 0$). Substituting into Eq. (2.37) absolute accelerations expressed in AM elements characteristics and absolute angular velocities and omitting several derivation steps we can obtain the following $(n + 1)$ vector equations of motion

$$\begin{aligned} M^c \ddot{\underline{r}}_0 + \sum_{j=1}^n \dot{\underline{\omega}}_j \times \underline{C}_j &= \sum_{j=1}^n [\underline{C}_j \omega_j^2 - \underline{\omega}_j (\underline{\omega}_j \cdot \underline{C}_j)] + \underline{N}_1 + M^c \underline{g} + \sum_{j=1}^n \underline{F}_j, \\ \underline{C}_i \times \ddot{\underline{r}}_0 + \sum_{j=1}^n \underline{A}_{ij} \cdot \dot{\underline{\omega}}_j &= \\ = \sum_{j=1}^n (\underline{\omega}_j \underline{B}_{ij} - \underline{\omega}_j \times \underline{A}_{ij}) \cdot \underline{\omega}_j + \underline{C}_i \times \underline{g} + \underline{U}_i^* , \end{aligned} \quad (2.38)$$

where

$$\underline{U}_i^* = \underline{U}_i + (\underline{\rho}_{ci} + \underline{z}_i) \times \underline{F}_i + \underline{r}_i \times \sum_{j=i+1}^n \mu_{ji} \underline{F}_j, \quad i = \overline{1, n}.$$

Components of skew-symmetric matrix $\underline{B} = \{\underline{B}_{ij}\}$ are given below

$$\underline{B}_{ij} = \begin{cases} \underline{a}_{ij} \times \underline{r}_j, & j < i \\ 0, & j = i \\ -\underline{B}_{ji}, & j > i, \quad i, j = \overline{1, n}. \end{cases} \quad (2.39)$$

The first equation in Eq. (2.38) follows from the AM center of mass motion theorem: $M^c \ddot{\underline{R}}_c = M^c \underline{g} + \underline{N}_1 + \sum_{j=1}^n \underline{F}_j$. The others are theorem of moment of momentum with respect to joint i increment for subsystem influenced by body i .

Equations (2.38) are of general form and further simplification will require introduction of generalized coordinates. Presence of external forces in Eq. (2.38) allows one to describe multisupport phases of motion by giving concrete expression of \underline{F}_i dependence from absolute or relative velocities deviations, for example, by negative feedback principle implementation. Let us now focus our attention on some general equalities, characteristic for AM model.

2.3.4 Quantitative Characteristics of AM Dynamics

We will need several identities which will be given here without proof. Let

$$\underline{\dot{a}} = \underline{\omega}_a \times \underline{a}, \quad \underline{\dot{b}} = \underline{\omega}_b \times \underline{b}, \quad \underline{P} = \underline{E}(\underline{a} \cdot \underline{b}) - \underline{b} \underline{a},$$

then it can be shown that

$$\begin{aligned} d(\underline{P} \cdot \underline{\omega}_b) / dt &= (\underline{\omega}_a \times \underline{a}) \times (\underline{\omega}_b \times \underline{b}) + \underline{P} \cdot \dot{\underline{\omega}}_b + \underline{\omega}_b \times \underline{P} \cdot \underline{\omega}_b - \\ &\quad - \underline{\omega}_b (\underline{a} \times \underline{b}) \cdot \underline{\omega}_b, \\ d(\underline{\omega}_a \underline{P} \cdot \underline{\omega}_b) / dt &= \dot{\underline{\omega}}_a \cdot \underline{P} \cdot \underline{\omega}_b + \underline{\omega}_a \cdot \underline{P} \cdot \dot{\underline{\omega}}_b + \underline{\omega}_a \cdot \underline{P} \cdot \underline{\omega}_b, \\ \underline{\omega}_a \cdot \underline{P} \cdot \underline{\omega}_b &= \underline{\omega}_a \cdot (\underline{\omega}_b \times \underline{P} - \underline{P} \times \underline{\omega}_a - \underline{\omega}_b (\underline{a} \times \underline{b}) + (\underline{a} \times \underline{b}) \underline{\omega}_a) \cdot \underline{\omega}_b. \end{aligned} \quad (2.40)$$

First, let us consider the theorem on moment of momentum increment. Summing Euler equation terms in Eq. (2.38) and omitting intermediate transformations we get

$$\sum_{i=1}^n \sum_{j=1}^n (\underline{A}_{ij} \cdot \dot{\underline{\omega}}_j + \underline{\omega}_j \times \underline{A}_{ij} \cdot \underline{\omega}_j - \underline{\omega}_j \underline{B}_{ij} \cdot \underline{\omega}_j) = \sum_{i=1}^n \sum_{j=1}^n d(\underline{A}_{ij} \cdot \underline{\omega}_j)/dt = \dot{\underline{K}}''$$

and thus

$$\dot{\underline{K}}'' = M^c(\underline{R}_c - \underline{r}_0) \times (\underline{g} - \dot{\underline{r}}_0) + \underline{M}_1 + \underline{M}^*. \quad (2.41)$$

Here $\underline{M}^* = \sum_{i=1}^n (\underline{R}_{ci} + \underline{z}_i - \underline{r}_0) \times \underline{F}_i$ — sum of external forces moments with respect to the support point. For other bases analogous equalities take the following form

$$\begin{aligned} \dot{\underline{k}} &= (\underline{r}_0 - \underline{R}_c) \times \underline{N}_1 + \underline{M}_1 + \sum_{i=1}^n (\underline{r}_{ci} + \underline{z}_i) \times \underline{F}_i, \\ \dot{\underline{K}}_O &= \underline{r}_0 \times \underline{N}_1 + \underline{R}_c \times M^c \underline{g} + \underline{M}_1 + \sum_{i=1}^n (\underline{R}_c + \underline{r}_{ci} + \underline{z}_i) \times \underline{F}_i. \end{aligned} \quad (2.42)$$

Let us be reminded here that \underline{M}_1 — is an external moment with respect to AM in contradistinction from other interelement moments. Further, let us consider the full energy increment theorem. Absolute derivative of potential energy is

$$\dot{\Pi} = -M^c \dot{\underline{R}}_c \cdot \underline{g}. \quad (2.43)$$

Scalar multiplication of each of the equations in Eq. (2.38) by $\dot{\underline{r}}_0$ and $\underline{\omega}_i$ from the left-hand side and successive summing up yields for terms containing \underline{g}

$$\sum_{i=1}^n \underline{\omega}_i \cdot (\underline{C}_i \times \underline{g}) + M^c \dot{\underline{r}}_0 \cdot \underline{g} = M^c \dot{\underline{R}}_c \cdot \underline{g} = -\dot{\Pi},$$

and further

$$\sum_{i=1}^n (\underline{\omega}_i \times \underline{C}_i) \cdot \dot{\underline{r}}_0 + M^c \dot{\underline{r}}_0 \cdot \dot{\underline{R}}_c = M^c \frac{d}{dt} \left[(\dot{\underline{r}}_0 \cdot \dot{\underline{R}}_c) - \frac{1}{2} \dot{\underline{r}}_0^2 \right],$$

and taking into account Eq. (2.40) one can prove that

$$\begin{aligned} \sum_{i=1}^n \sum_{j=1}^n \underline{\omega}_i \cdot (\underline{A}_{ij} \cdot \dot{\underline{\omega}}_j + \underline{\omega}_j \times \underline{A}_{ij} \cdot \underline{\omega}_j - \underline{\omega}_j \underline{B}_{ij} \cdot \underline{\omega}_j) = \\ = \frac{1}{2} \sum_{i=1}^n \sum_{j=1}^n \frac{d}{dt} (\underline{\omega}_i \cdot \underline{A}_{ij} \cdot \underline{\omega}_j). \end{aligned}$$

Thus, taking into account given above equalities we get

$$dE/dt = d(T + \Pi)/dt = \sum_{i=1}^n \underline{\omega}_i \cdot \underline{U}_i^* + \dot{\underline{r}}_0 \cdot \left(\underline{N}_1 + \sum_{i=1}^n \underline{F}_i \right),$$

or substituting \underline{U}_i^* with its expression in bases $\bar{e}^{(0)}$, $\bar{e}^{(H_1)}$, $\bar{e}^{(c)}$ we obtain correspondingly

$$\begin{aligned}\dot{E} &= \sum_{i=1}^n \omega_i \cdot \underline{U}_i + \dot{r}_0 \cdot \underline{N}_1 + \sum_{i=1}^n (\dot{R}_{ci} + \dot{z}_i) \cdot \underline{E}_i, \\ \dot{E}'' &= \sum_{i=1}^n \omega_i \cdot \underline{U}_i + M^c \dot{r}_0 \cdot (\dot{r}_0 - \dot{R}_c) + \sum_{i=1}^n (\dot{R}_{ci} + \dot{z}_i - \dot{r}_0) \cdot \underline{E}_i, \\ \dot{T}' &= \sum_{i=1}^n \omega_i \cdot \underline{U}_i + (\dot{r}_0 - \dot{R}_c) \cdot \underline{N}_1 + \sum_{i=1}^n (\dot{r}_{ci} + \dot{z}_i) \cdot \underline{E}_i.\end{aligned}\quad (2.44)$$

In the last equality we imply that $\Pi' = 0$ (AM center of mass). Let us introduce now vectors-columns of relative angular velocities $\bar{\Omega} = (\Omega_1, \dots, \Omega_n)^T$, defined by relationships analogous to Eq. (2.35)

$$\bar{\Omega} = \mu^{-1} \bar{\omega}, \quad \bar{\omega} = \mu \bar{\Omega}. \quad (2.45)$$

Then from expressions for power we get

$$W = \bar{\omega}^T \cdot \bar{U} = (\mu \bar{\Omega})^T \cdot \mu^T \bar{M} = \bar{\Omega}^T \cdot \bar{M}. \quad (2.46)$$

The energy relationships Eq. (2.44) in combination with motion equations (Eq. (2.38)) and general theorems Eq. (2.41), Eq. (2.42) allow to carry out comprehensive analysis of AM behaviour during performance of given real or synthesized motions. Energy relationships reflecting integral properties of the model can at least serve for checking of numerical methods employed for experimental data processing and motion equations integration. Directly from relationships Eq. (2.42) and Eq. (2.44), it follows that moment of momentum conservation theorem holds in supportless phase of motion under absence of external forces and moments. As for kinetic energy T' in basis $\bar{e}^{(c)}$, it satisfies under these conditions the following equation

$$\dot{T}' = \sum_{i=2}^n \Omega_i \cdot \underline{M}_i, \quad (2.47)$$

which can be used in AM motion synthesis in supportless phase.

System of Eq. (2.38) as equations for a general type link can be written in appropriate generalized coordinates taking into account the type of each concrete link (junction) and convenience considerations of the researcher. If links between solid bodies of the model are of a general type (i.e. when not only rotation of one body with respect to another is possible but also translational motion), then identities $\underline{s}_j^{(i)} = \text{const}$ and $\rho_{ci} = \text{const}$ in their own basis $\bar{e}^{(i)}$ (see nomenclatures in Fig. 2.9 on page 35) are eliminated from geometrical properties of system admissions and corresponding model relations are obtained. In Sec. 2.6 we have considered a model that structures and receives system of equations for generalized type constraints. But before the general case description we will consider application of Eq. (2.38) to a more simple model.

2.4 Planar Motion

Human SMA planar model with cylindrical junctions (links) remains till now useful and effective for modelling and results interpreting. In fact it proves to be an optimal model according to many optimality criteria for investigation of numerous locomotions. If the researcher uses a planar model he should of course make sure that he employs appropriate equations free from general suppositions which do not hold for plane parallel motion of a solid bodies system.

Let us write equations for a planar model using results of Sec. 2.3. Motion equations and attendant relationships will be written in scalar form in $\bar{e}^{(0)}$ basis. Along with nomenclature we have been using to denote a vector basis $\bar{e}_i^{(0)}$, $i = \overline{1, n}$, in this section we will employ standard designation of unit vectors in 3-D basis $\underline{i}, \underline{j}, \underline{k}$. Let us assume that the plane of motion is defined by a pair of unit vectors $\underline{i}, \underline{j}$, belonging to the fixed coordinate system. Then, for all variables-vectors and tensors considered in previous sections the following relationships hold true

$$\begin{aligned} \underline{a} &= a_1 \underline{i} + a_2 \underline{j} + a_3 \underline{k}, & \underline{b} &= b_1 \underline{i} + b_2 \underline{j} + b_3 \underline{k}; \\ \underline{\omega} &= \omega_1 \underline{i} + \omega_2 \underline{j} + \omega_3 \underline{k}, & \underline{Q} &= \underline{b} \underline{a}, & \underline{P} &= \underline{E}(\underline{a} \cdot \underline{b}) - \underline{b} \underline{a}; \\ a_3 &= b_3 = 0, & \omega_1 &= \omega_2 = 0, \end{aligned}$$

$$P = \begin{pmatrix} b_2 a_2, & -b_1 a_2, & 0 \\ -b_2 a_1, & a_1 b_1, & 0 \\ 0, & 0, & a_1 b_1 + a_2 b_2 \end{pmatrix}, \quad Q = \begin{pmatrix} b_1 a_1, & b_1 a_2, & 0 \\ b_2 a_1, & a_2 b_2, & 0 \\ 0, & 0, & 0 \end{pmatrix}$$

and, therefore,

$$\begin{aligned} \underline{P} \cdot \underline{\omega} &= (a_1 b_1 + a_2 b_2) \omega_3 \underline{k} = \underline{a} \cdot \underline{b} \underline{\omega}, & \underline{\omega} \times \underline{P} \cdot \underline{\omega} &= 0, \\ \underline{c} &= (\underline{a} \times \underline{b}) = (a_1 b_2 - a_2 b_1) \underline{k}, & \underline{\omega} \underline{c} &= (a_1 b_2 - a_2 b_1) \omega_3 \underline{k} \underline{k}, \\ \underline{\omega} \underline{c} \cdot \underline{\omega} &= (a_1 b_2 - a_2 b_1) \omega_3^2 \underline{k} = (\underline{a} \times \underline{b}) \omega_3^2 \end{aligned}$$

In Fig. 2.7 we give depiction of arbitrary AM element i with attendant generalized coordinates nomenclature which will be used hereafter.

Let us determine the center of mass radius vector ρ_{ci} and radius vector r_i (which links joint points) projections onto basis unit vectors and express these projections in generalized coordinates φ_i . Let φ_i be equal to zero when r_i and $(-\underline{e}_2^0) = -\underline{j}$ are oriented in the same direction, then

$$\begin{aligned} r_i &= l_i (\sin \varphi_i \underline{i} - \cos \varphi_i \underline{j}), & \underline{e}_1^{(i)} &= r_i / l_i, & \underline{e}_2^{(i)} &= \underline{k} \times \underline{e}_1^{(i)}; \\ \rho_{ci} &= a_{1i} \underline{e}_1^{(i)} + a_{2i} \underline{e}_2^{(i)} = \rho_{ci} (\sin(\varphi_i + \alpha_i) \underline{i} - \cos(\varphi_i + \alpha_i) \underline{j}), \end{aligned}$$

where

$$\rho_{ci}^2 = a_{1i}^2 + a_{2i}^2, \quad \alpha_i = \arctan(a_{2i}/a_{1i}).$$

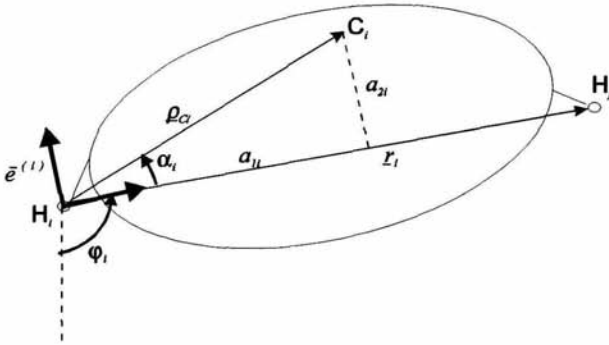


Fig. 2.7. Planar model.

Components of tensor matrix \underline{A}_{ij} can be written as follows

$$\underline{A}_{ij} = \underline{a}_{ij} \cdot \underline{r}_j = (A_{ij}^3 \underline{e}_1^{(i)} + A_{ij}^4 \underline{e}_2^{(i)}) \cdot l_j \underline{e}_2^{(j)}.$$

Here we have introduced designations with superscripts (see Fig. 2.8)

$$A_{ij}^3 = a_{1j} \mu_{ij} m_i + l_i \sum_{k=i+1}^n m_k \mu_{ki} \mu_{kj}, \quad A_{ij}^4 = a_{2i} \mu_{ij} m_i;$$

$$A_{ij}^1 = \arctan(A_{ij}^4/A_{ij}^3), \quad A_{ij}^0 = l_j [(A_{ij}^3)^2 + (A_{ij}^4)^2]^{\frac{1}{2}}; \quad (2.48)$$

$$A_i^2 = J_{ci} + m_i \rho_{ci}^2 + l_i^2 \sum_{k=i+1}^n m_k \mu_{ki}$$

Taking into account that $B_{ij} = (\underline{a}_{ij} \times \underline{r}_j) \cdot \underline{k}$, we get

$$A_{ij} = \begin{cases} A_{ij}^0 \cos(\varphi_i - \varphi_j + A_{ij}^1), & j < i \\ A_i^2, & j = i \\ A_{ji}^1, & j > i \end{cases} \quad (2.49)$$

$$B_{ij} = \begin{cases} A_{ij}^0 \sin(\varphi_i - \varphi_j + A_{ij}^1), & j < i \\ 0, & j = i \\ -B_{ji}^1, & j > i \end{cases}$$

$$i, j = \overline{1, n}.$$

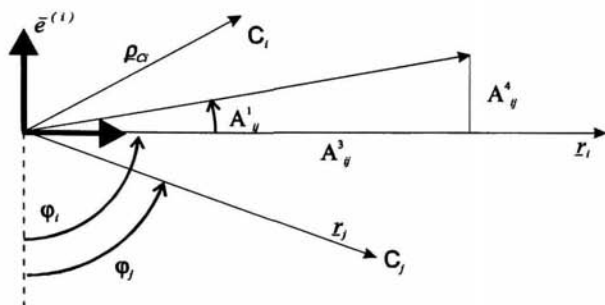


Fig. 2.8. Generalized coordinates and positions of reduced masses.

Let us write vector \underline{C}_i components projections

$$\underline{C}_i = m_i \underline{\rho}_c + r_i \sum_{k=i+1}^n m_k \mu_{ki} = C_i^3 \underline{e}_1^{(i)} + C_i^4 \underline{e}_2^{(i)} = D_i \underline{i} - C_i \underline{j},$$

where

$$D_i = C_i^0 \sin(\varphi_i + C_i^1); \quad C_i = C_i^0 \cos(\varphi_i + C_i^1);$$

$$C_i^3 = a_{1i} m_i + l_i \sum_{k=i+1}^n m_k \mu_{ki}; \quad C_i^4 = a_{2i} m_i;$$

$$C_i^0 = [(C_i^3)^2 + (C_i^4)^2]^{\frac{1}{2}}, \quad C_i^1 = \arctan(C_i^4/C_i^3)$$

Employing previously introduced designations, introducing some new ones (obvious in their meaning) and taking into account relationships of Eq. (2.38) we obtain a Newton-Euler system of equations of motion in plane XOY

$$\begin{aligned} M^C \ddot{x}_0 + \sum_{j=1}^n C_j \ddot{\varphi}_j &= \sum_{j=1}^n D_j \dot{\varphi}_j^2 + N_x + \sum_{j=1}^n F_{jx}; \\ C \ddot{y}_0 + \sum_{j=1}^n D_j \ddot{\varphi}_j &= - \sum_{j=1}^n C_j \dot{\varphi}_j^2 - M^C g + N_y + \sum_{j=1}^n F_{jy}; \\ C_i \ddot{x}_0 + D_i \ddot{y}_0 + \sum_{j=1}^n A_{ij} \ddot{\varphi}_j &= \sum_{j=1}^n B_{ij} \dot{\varphi}_j^2 - g D_i + U_i^*, \quad i = \overline{1, n}; \end{aligned} \quad (2.50)$$

where

$$U_i^* = U_i + z'_{1i} F_{2i} - z'_{2i} F_{1i} + \sum_{j=i+1}^n \mu_{ji} P_{ij};$$

and $\underline{z}'_i = \underline{z}_i + \underline{\rho}_{ci} = z'_{1i} \underline{\varepsilon}_1^{(i)} + z'_{2i} \underline{\varepsilon}_2^{(i)}$ — vector connecting joint i and origin of force \underline{F}_i (i.e. its point of application). For moments P_{ij} we have

$$P_{ij} = \underline{k} \cdot (\underline{r}_i \times \underline{F}_j) = l_i F_j^0 \sin(\varphi_j - \varphi_i + F_j^1) = l_i (F_{jx} \cos \varphi_i + F_{jy} \sin \varphi_i),$$

where $F_j^0 = |\underline{F}_j| = [(F_{1j})^2 + (F_{2j})^2]^{\frac{1}{2}}$, $F_j^1 = \arctan(F_{2j}/F_{1j})$ — absolute value and inclination angle of \underline{F}_j in basis $\bar{e}^{(j)}$.

Let us now reformulate for planar motion relationships for moment of momentum and kinetic energy for bases $\bar{e}^{(0)}$, $\bar{e}^{(H_1)}$, $\bar{e}^{(c)}$ correspondingly

$$\begin{aligned} K_O &= \sum_{i=1}^n \sum_{j=1}^n A_{ij} \dot{\varphi}_j + \sum_{i=1}^n [(D_i x_0 - C_i y_0) \dot{\varphi}_i + D_i \dot{y}_0 + C_i \dot{x}_0] + \\ &\quad + M^C (x_0 \dot{y}_0 - y_0 \dot{x}_0); \\ K''_{H_1} &= \sum_{i=1}^n \sum_{j=1}^n A_{ij} \dot{\varphi}_j, \quad k = \sum_{i=1}^n \sum_{j=1}^n [A_{ij} - (D_i D_j + C_i C_j)/M^C] \dot{\varphi}_j; \\ T &= \frac{1}{2} \sum_{i=1}^n \sum_{j=1}^n A_{ij} \dot{\varphi}_i \dot{\varphi}_j + \sum_{i=1}^n (C_i \dot{x}_0 + D_i \dot{y}_0) \dot{\varphi}_i + \frac{1}{2} M^C (\dot{x}_0^2 + \dot{y}_0^2); \\ T'' &= \frac{1}{2} \sum_{i=1}^n \sum_{j=1}^n A_{ij} \dot{\varphi}_i \dot{\varphi}_j, \quad T' = \frac{1}{2} \sum_{i=1}^n \sum_{j=1}^n [A_{ij} - (D_i D_j + C_i C_j)/M^C] \dot{\varphi}_i \dot{\varphi}_j. \end{aligned} \quad (2.51)$$

And for potential energy

$$\Pi = \left(M^C y_0 - \sum_{i=1}^n C_i \right) g, \quad \Pi'' = \Pi - M^C g y_0. \quad (2.52)$$

Moment of momentum increment and full energy theorems under absence of external forces F_i take the following form

$$\left\{ \begin{aligned} \dot{K} &= x_0 N_y - y_0 N_x - M^C x_c g + M_1, \quad \dot{k} = \sum_{i=1}^n (N_x C_i - N_y D_i) + M_1, \\ \dot{E} &= \sum_{i=1}^n \dot{\varphi}_i U_i + \dot{x}_0 N_x + \dot{y}_0 N_y, \quad \dot{T}' = \sum_{i=1}^n [U_i - (C_i N_x + D_i N_y)/M^C] \dot{\varphi}_i. \end{aligned} \right. \quad (2.53)$$

As a check on motion Eq. (2.50), we can proposed direct differentiation of kinetic potential $L = T - \Pi$ with generalized coordinates vector $q = (x_0, y_0, \varphi_1, \dots, \varphi_n)^T$. Here one should employ Lagrange equations of the 2-nd kind.

Further, along with generalized coordinates $\varphi = (\varphi_1, \dots, \varphi_n)^T$, we will use interelement angles $\psi = (\psi_1, \dots, \psi_n)^T$. Coordinates φ and ψ are interrelated:

$$\psi = \mu^{-1} \varphi, \quad \varphi = \mu \psi. \quad (2.54)$$

Motion equations, Eq. (2.38) and Eq. (2.50) describe dynamics of an open kinematic chain with spherical joints for single-support phase of AM locomotion. These models are not too complex and therefore they can serve as preface to fuller and more complex models. The next section is devoted to more complex 3-D motion description.

2.5 System of Arbitrary Connected Bodies in 3-D Space

Anthropomorphic model with spherical joints is simpler in description and its use often proves to be correct. However, when one investigates dynamics of separate parts and there is need to spot subtle effects, supposition that model bodies are connected by joints with one fixed point turns out to be inadmissible.

Therefore, for description of a more complex model an “universal joint” is introduced. Its universality consists of the fact that it can restrict to any degree both rotational and progressive motions of the neighbouring body. It can as well impose no restriction at all.

For these purposes we will define two sets of vectors: $\{\rho_{ci}\}$ — radius-vector of mass center of body number i with respect to joint number i , which connects it with the nearest preceding in structure graph body, $\{s_i^{(l)}\}$ — radius-vector of joint number i with respect to mass center of body l , that precede body i in structure graph. Fig. 2.9 illustrates these definitions.

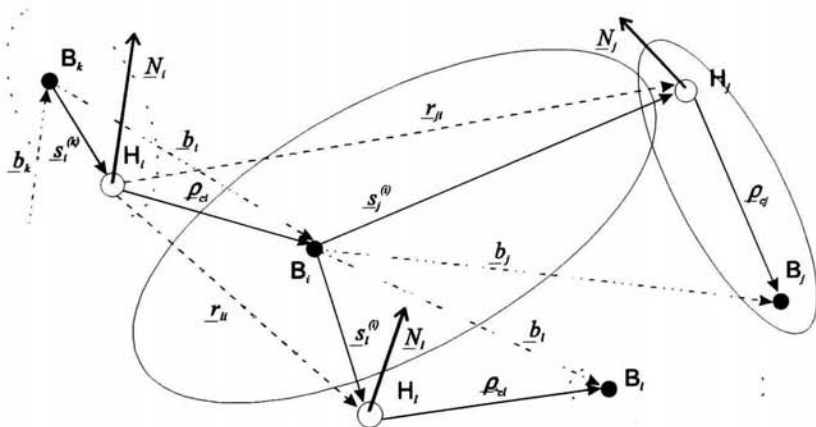


Fig. 2.9. Body with arbitrary joints.

It is clear that $\underline{b}_i = \underline{\rho}_{ci} - \sum_{l=1}^{i-1} \mu_{il}^{(inc)} \underline{s}_i^{(l)}$. We remind ourselves that the sum from

$l = 1$ to $i - 1$ is only a vector $\underline{s}_i^{(l)}$ choice rule. For vectors $\underline{\rho}_{ci}$ and $\underline{s}_i^{(l)}$ we assume that $\underline{\rho}_{ci}$ is defined in $\bar{e}^{(i)}$ basis strictly connected with body i and $\underline{s}_i^{(l)}$ is defined in $\bar{e}^{(l)}$ basis. The matrix μ is constructed as in Sec. 2.4. A restriction used here is that point B_i coincides with mass center of body. The matrix $\mu^{(inc)}$ is inverse with respect to μ . As soon as we have numerated elements of structure graph matrix $\mu^{(inc)}$ can be written very easily. Diagonal elements of $\mu^{(inc)}$ are units (1), element with subscript ij equals minus unit (-1) if body number j is nearest to the preceding body number i and zero (0) otherwise.

Separate element motion equations, stated earlier (Sec. 2.3), do not depend on the type of junctions. In this paragraph we shall derive motion equations for a system of bodies connected by universal joints. In order to make references easier, let us write the main equations anew. Then, the center of mass motion equation is as follows

$$m_i \dot{\underline{v}}_{ci} = \underline{V}_i^a + \underline{N}_i^* \quad (2.55)$$

and the law of resultant moment of momentum change with respect to the center of mass results in

$$\underline{J}_{ci} \cdot \dot{\underline{\omega}}_i + \underline{\omega}_i \times \underline{J}_{ci} \cdot \underline{\omega}_i = \underline{M}_{ci}^a + \underline{M}_i^* + \underline{M}_{ci}^H. \quad (2.56)$$

In Eq. (2.55), just as before, \underline{V}_i^a is the resultant vector of external forces, \underline{N}_i^* is the resultant vector of reaction forces at junctions H_{α_s} . In Eq. (2.56) \underline{M}_{ci}^a is the moment of system of external couples and forces with respect to center of mass, \underline{M}_i^* and \underline{M}_{ci}^H are the moment of system of couples and the moment of system reaction forces at junctions H_{α_s} with respect to the center of mass. In accordance with definitions of Fig. 2.9

$$\underline{M}_{ci}^H = -\underline{\rho}_{ci} \times \underline{N}_i + \sum_{k=i+1}^n \mu_{ki}^{(inc)} \underline{s}_k^{(i)} \times \underline{N}_k. \quad (2.57)$$

Taking into account the following equations describing joint reactions and resultant reaction forces

$$\underline{N}_i = \sum_{k=i}^n \mu_{ki} \underline{N}_k^*, \quad \underline{N}_i^* = \sum_{k=i}^n \mu_{ki}^{(inc)} \underline{N}_k, \quad (2.58)$$

$$\underline{M}_i = \sum_{k=i}^n \mu_{ki} \underline{M}_k^*, \quad \underline{M}_i^* = \sum_{k=i}^n \mu_{ki}^{(inc)} \underline{M}_k, \quad (2.59)$$

let us write the expression for \underline{M}_{ci}^H

$$\underline{M}_{ci}^H = -\sum_{k=i}^n (\mu_{ki} \underline{\rho}_{ci} - \sum_{l=i+1}^k \mu_{li}^{(inc)} \mu_{kl} \underline{s}_l^{(i)}) \times \underline{N}_k^* = \sum_{k=i}^n \underline{r}_{ki} \times \underline{N}_k^*. \quad (2.60)$$

Substitution of \underline{N}_i^* from equation of the center of mass motion Eq. (2.55) into Eq. (2.56) allows one to write system motion equations in terms of acceleration of

the center of mass $\dot{\underline{v}}_{ci}$ and angular accelerations $\dot{\underline{\omega}}_i$ of bodies. Upon this substitution Eq. (2.56) will take the following form:

$$\sum_{k=i}^n m_k \underline{r}_{ki} \times \dot{\underline{v}}_{ck} + \underline{J}_{ci} \cdot \dot{\underline{\omega}}_i + \underline{\omega}_i \times \underline{J}_{ci} \cdot \underline{\omega}_i = \underline{M}_{ci}^a + \underline{M}_i^* + \sum_{k=i}^n \underline{r}_{ki} \times \underline{V}_k^a. \quad (2.61)$$

Vectors \underline{r}_{ki} , introduced when defining moments with respect to the center of mass of the body number i , are in fact either vectors connecting joint number i with the joints connecting the body with the succeeding one in AM structure, or zero vectors. Radius-vector of the center of mass of the body number i can be written differently:

$$\begin{aligned} \underline{R}_{ci} &= \underline{r}_0 + \sum_{j=1}^i \mu_{ij} (\underline{\rho}_{cj} - \sum_{l=1}^j \mu_{jl}^{(inc)} \underline{s}_j^{(l)}) = \\ &= \underline{r}_0 + \sum_{j=1}^i (\mu_{ij} \underline{\rho}_{cj} - \sum_{l=j+1}^i \mu_{lj}^{(inc)} \mu_{il} \underline{s}_l^{(j)}) = \\ &= \underline{r}_0 + \sum_{j=1}^i \underline{r}_{ij} = \underline{r}_0 + \underline{\rho}_{ci} + \sum_{j=1}^{i-1} \underline{r}_{ij}. \end{aligned} \quad (2.62)$$

Comparing Eq. (2.62) with Eq. (2.18) it is not difficult to understand that Eq. (2.62) is a generalisation of Eq. (2.18). It is important for future discussions to note that first index of vector \underline{r}_{ij} corresponds to number of the joint at which it points whereas the second one corresponds to the number of basis in which it is described. Using theorems of point velocity and acceleration summation for compound motion and taking into account the note which we have made about vector indexation formulas for body center of mass velocity, acceleration vectors can be rewritten in the following neat and clear form:

$$\underline{v}_{ci} = \dot{\underline{r}}_0 + \sum_{j=1}^i (\overset{\circ}{\underline{r}}_{ij} + \underline{\omega}_j \times \underline{r}_{ij}), \quad (2.63)$$

$$\dot{\underline{v}}_{ci} = \ddot{\underline{r}}_0 + \sum_{j=1}^i (\overset{\circ\circ}{\underline{r}}_{ij} + 2 \underline{\omega}_j \times \overset{\circ}{\underline{r}}_{ij} + \dot{\underline{\omega}}_j \times \underline{r}_{ij} + \underline{\omega}_j \times (\underline{\omega}_j \times \underline{r}_{ij})). \quad (2.64)$$

In these equations we have used quite common way of designation of time derivative with respect to not fixed basis: $\overset{\circ}{\underline{r}}^{(j)}$. Substituting Eq. (2.64) into Eq. (2.61) we obtain a generalisation of the second equation in system Eq. (2.30)

$$\begin{aligned} &\underline{C}_i \times \ddot{\underline{r}}_0 + \sum_{j=1}^n (\underline{A}_{ij} \cdot \dot{\underline{\omega}}_j + (\underline{\omega}_j \times \underline{A}_{ij} - \underline{\omega}_j \underline{B}_{ij}) \cdot \underline{\omega}_j) + \\ &+ \sum_{k=i}^n \sum_{j=1}^k m_k \underline{r}_{ki} \times (\overset{\circ\circ}{\underline{r}}_{kj} + 2 \underline{\omega}_j \times \overset{\circ}{\underline{r}}_{kj}) = \underline{M}_i^* + \underline{M}_{ci}^a + \sum_{k=i}^n \underline{r}_{ki} \times \underline{V}_k^a, \end{aligned} \quad (2.65)$$

where

$$\underline{C}_i = \sum_{k=i}^n m_k \underline{r}_{ki}, \quad (2.66)$$

$$\underline{A}_{ij} = \underline{J}_{ci} \delta_{ij} + \sum_{\substack{k=1 \\ k \neq j}}^n m_k (\underline{E} \underline{r}_{kj} \cdot \underline{r}_{ki} - \underline{r}_{kj} \underline{r}_{ki}), \quad (2.67)$$

$$\underline{B}_{ij} = \sum_{\substack{k=1 \\ k \neq j}}^n m_k \underline{r}_{ki} \times \underline{r}_{kj}. \quad (2.68)$$

If we take into account Eq. (2.64) and Eq. (2.68), then Eq. (2.55) can be rewritten as follows

$$\begin{aligned} m_i \ddot{\underline{r}}_0 + m_i \sum_{j=1}^i \dot{\underline{\omega}}_j \times \underline{r}_{ij} + m_i \sum_{j=1}^i (\underline{\omega}_j \underline{\omega}_j - \underline{E} \underline{\omega}_j^2) \cdot \underline{r}_{ij} + m_i \sum_{j=1}^i (\overset{\circ}{\underline{r}}_{ij} + 2 \underline{\omega}_j \times \overset{\circ}{\underline{r}}_{ij}) = \\ = \underline{N}_i^* + \underline{V}_i^a. \end{aligned} \quad (2.69)$$

Summing over index i we obtain a generalisation of the first equation in Eq. (2.30) which corresponds to the theorem of system (AM) center of mass motion in an inertial basis

$$M^c \ddot{\underline{r}}_0 + \sum_{j=1}^n \dot{\underline{\omega}}_j \times \underline{C}_j = \sum_{j=1}^n (\underline{\omega}_j^2 \underline{E} - \underline{\omega}_j \underline{\omega}_j) \cdot \underline{C}_j - \sum_{j=1}^n (\overset{\circ}{\underline{C}}_j + 2 \underline{\omega}_j \times \overset{\circ}{\underline{C}}_j) + \underline{N}_0 + \underline{V}^a \quad (2.70)$$

The last equation establishes links between kinematic characteristics and external forces (active ones as well as constraint reaction force in point B_0).

Analogous result can be obtained for Eq. (2.65) after summation over index i .

$$\begin{aligned} \sum_{i=1}^n \underline{C}_i \times \ddot{\underline{r}}_0 + \sum_{i=1}^n \sum_{j=1}^n (\underline{A}_{ij} \cdot \dot{\underline{\omega}}_j + (\underline{\omega}_j \times \underline{A}_{ij} - \underline{\omega}_j \underline{B}_{ij}) \cdot \underline{\omega}_j) + \\ + \sum_{i=1}^n \sum_{k=i}^n \sum_{j=1}^k m_k \underline{r}_{ki} \times (\overset{\circ}{\underline{r}}_{ij} + 2 \underline{\omega}_j \times \overset{\circ}{\underline{r}}_{ij}) = \underline{M}_0 + \sum_{i=1}^n \underline{M}_{ci}^a + \sum_{i=1}^n \sum_{k=i}^n \underline{r}_{ki} \times \underline{V}_k^a. \end{aligned} \quad (2.71)$$

Equations (2.55) and Eq. (2.61) or Eq. (2.69) and Eq. (2.65) are based on the method of obtaining of closed system of equations describing motion of basic AM with tree-like structure.

In order for the system of motion equations to be closed it is necessary to describe concrete type of AM bodies junctions, defining \underline{r}_{ij} or \underline{N}_i^* and \underline{M}_i^* .

It is clear that it is more convenient to determine internal forces \underline{N}_i^* and moments \underline{M}_i^* via determination of forces in junctions. In order to do so we can use Eq. (2.58) and Eq. (2.59) and substitute \underline{N}_i^* and \underline{M}_i^* into, for example, Eq. (2.69) or Eq. (2.65).

However, substitution of Eq. (2.69) and Eq. (2.65) into expressions for \underline{N}_i and \underline{M}_i , proves to be more effective:

$$\sum_{k=i}^n \mu_{ki} m_i \ddot{\mathbf{r}}_0 + \sum_{k=i}^n \sum_{j=1}^k \mu_{ki} m_k (\dot{\boldsymbol{\omega}}_j \times \mathbf{r}_{kj} + (\boldsymbol{\omega}_j \boldsymbol{\omega}_j - \underline{E} \omega_j^2) \cdot \mathbf{r}_{kj} + (\overset{\circ}{T}_{ij} + 2 \boldsymbol{\omega}_j \times \overset{\circ}{\mathbf{r}}_{ij})) = \underline{N}_i + \sum_{k=i}^n \mu_{ki} \underline{V}_k^a, \quad (2.72)$$

$$\begin{aligned} & \sum_{k=i}^n \mu_{ki} \underline{C}_k \times \ddot{\mathbf{r}}_0 + \sum_{k=i}^n \sum_{j=1}^n \mu_{ki} (\underline{A}_{kj} \cdot \dot{\boldsymbol{\omega}}_j + (\boldsymbol{\omega}_j \times \underline{A}_{kj} - \boldsymbol{\omega}_j \underline{B}_{kj}) \cdot \boldsymbol{\omega}_j) + \\ & + \sum_{l=i}^n \sum_{k=l}^n \sum_{j=1}^k m_k \mu_{li} \underline{T}_{kl} \times (\overset{\circ}{T}_{lj} + 2 \boldsymbol{\omega}_j \times \overset{\circ}{\mathbf{r}}_{lj}) = \underline{M}_i + \sum_{l=i}^n \mu_{li} \underline{M}_{cl}^a + \sum_{l=i}^n \sum_{k=l}^n \mu_{li} \underline{T}_{kl} \times \underline{V}_k^a, \end{aligned} \quad (2.73)$$

The system of equations obtained from Eq. (2.69) and Eq. (2.65) via transformations is a system of equations including theorems of conservation of moment and moment of momentum with respect to center of mass of AM subsystem, containing AM bodies located further in kinematic chain than joint i .

For absolute angular velocities $\boldsymbol{\omega}_j$ and their derivations, relations linking them with relative angular velocities (accelerations) calculated with respect to previous body in the kinematic chain can be stated as follows:

$$\boldsymbol{\omega}_i = \sum_{k=1}^i \mu_{ik} \underline{\boldsymbol{\Omega}}_k, \quad \underline{\boldsymbol{\Omega}}_i = \sum_{k=1}^i \mu_{ik}^{(inc)} \boldsymbol{\omega}_k, \quad (2.74)$$

$$\dot{\boldsymbol{\omega}}_i = \sum_{k=1}^i \mu_{ik} \dot{\underline{\boldsymbol{\Omega}}}_k = \sum_{k=1}^i \mu_{ik} (\dot{\underline{\boldsymbol{\Omega}}}_k + \boldsymbol{\omega}_k \times \underline{\boldsymbol{\Omega}}_k), \quad \dot{\underline{\boldsymbol{\Omega}}}_i = \sum_{k=1}^i \mu_{ik}^{(inc)} \dot{\boldsymbol{\omega}}_k. \quad (2.75)$$

The problem of system of solid bodies dynamics modelling has been studied in its various aspects by many researchers. These investigations were caused by the necessity for solving different and special problems of robotics, engineering, space technology and modelling of human motion in space and in different environment conditions as well as in connection with general problem consideration in the framework of development of universal programs for CAD. Even the simplest model of human SMA remains a ramified kinematic chain only in the freefall phase and until there is no kinematic loops formed (as it can be, for example, when a sportsman holds with his hands to his shanks in somersault motion).

Interaction with the environment and attempts to model SMA by a more complex model make it necessary to consider closed kinematic chains. Special considerations require those constraints which are not satisfied due to current values of some generalized coordinates. The next section is devoted to these questions.

2.6 Additional Restrictions on the Base Model

In the terms of analytical dynamics restrictions on displacements, velocities and accelerations of the system points are called constraints. These constraints are classified according to the form of analytical description of restrictions. We shall be using this classification further on. In case the reader is not familiar with the terminology used, we recommend to read (or reread) one of the text books on classical mechanics fundamentals [55].

Let us assume that restrictions on the system of bodies of the base model, described by a structural graph of the "tree-like" type, can be nonstationary restraining, holonomic and non-holonomic constraints of the first and second order. This means that in the most general case of those considered, the bind equation (called further on constraint equation) has the following form:

$$\Phi_j(\{q_i\}, \{\dot{q}_i\}, \{\ddot{q}_i\}, t; \{u_s\}) = 0. \quad (2.76)$$

Here $\{q_i\}$, $\{\dot{q}_i\}$, $\{\ddot{q}_i\}$ are vector-columns of generalized coordinates, velocities and accelerations and $\{u_s\}$ is vector-column of functions which form is defined when the constraint is described in detail.

It should be noted that the system with non-restraining constraints can be considered as a system with changing in time structure of restraining constraints. Therefore, in the framework of our approach to modelling of dynamics of system of bodies, Eq. (2.76) describes all possible situations.

The problem of taking into account the constraints that bind the bodies of the base model has two aspects. The first one consists in formulating of possible constraints in quite a general form. It is obvious, that Eq. (2.76) has a form that is too general and cannot be used for description of kinematic or force restrictions on the system of bodies. Therefore it is important to carry out classification of possible restrictions and write them in a convenient for perception and analysis form.

The second aspect of the problem is connected with creation of an effective procedure which would take into account constraint equations of the form Eq. (2.76) when solving problems of analysis and synthesis of AM motions. Traditional separation of dynamics of system of bodies problems into the direct one (analysis) and the inverse one (synthesis) only in a few cases leads to the pure problems of differentiation of generalized coordinates or integration of system of differential equations. During experiment observable coordinates of certain points, their velocities, accelerations and angles of rotation of body parts, usually do not correspond with the chosen system of generalized coordinates of the base universal model. The relation between the generalized coordinates and the observable ones often is described by implicit nonlinear equations. In order to change from one system of coordinates to the other, one should integrate a system of differential-algebraic equations (DAE). Methods of integration of such systems is at present an actively investigated field of numerical analysis [34].

In chapter 3 we overview the up-to-date state of the problem and present our own

approach to its solution. In the following section we shall give a brief description of typical constraints using introduced definitions.

2.6.1 Linear Constraints

Equations which introduce linear link between generalized coordinates, velocities and accelerations do not always have clear physical meaning, but due to their simplicity they prove useful in universal anthropomorphic model. One of the most general descriptions of such equations is

$$\sum_{i=1}^n (L_{0i} q_i + L_{1i} \dot{q}_i + L_{2i} \ddot{q}_i) - f_{1j}(t) = 0. \quad (2.77)$$

Here L_{0i} , L_{1i} , L_{2i} are rectangular matrices with fixed parameters elements.

2.6.2 Preset Distance between Certain Points of Two Bodies

This type of constraint determines character of preset behaviour of distance between certain points of two AM elements. In order to widen parametric scope of this constraint the corresponding equation is written as a linear combination of derivatives (with respect to time variable) of distance $|r_i - r_k|$

$$L_{0j} \Phi_j + L_{1j} \dot{\Phi}_j + L_{2j} \ddot{\Phi}_j = 0, \quad (2.78)$$

where

$$\Phi_j = |r_i - r_k| - f_{2j}(t) = 0, \quad (2.79)$$

$$\dot{\Phi}_k = \frac{(v_i - v_k) \cdot (r_i - r_k)}{|r_i - r_k|} - \dot{f}_{2j}(t) = 0, \quad (2.80)$$

$$\begin{aligned} \ddot{\Phi}_j = & \frac{(\dot{v}_i - \dot{v}_k) \cdot (r_i - r_k)}{|r_i - r_k|} + \frac{(v_i - v_k) \cdot (v_i - v_k)}{|r_i - r_k|} - \\ & - \frac{(v_i - v_k) \cdot (r_i - r_k)(v_i - v_k) \cdot (r_i - r_k)}{|r_i - r_k|^3} - \ddot{f}_{2j}(t) = 0. \end{aligned} \quad (2.81)$$

The preset behaviour pattern of distance between a marker and some point is described by such constraint. If measurement accuracy is high enough, distance derivatives behaviour can be also included in the equations. Equations (2.79)–(2.81) can also be used for muscles modelling.

2.6.3 Preset Behaviour of Certain Point Radius Vector Projection onto Fixed Direction in Selected Basis

As in previous section, we will use Eq. (2.78) with an eye to universalise constraint description, but the role of Φ_j will play radius-vector projection onto fixed direction

$l_j^{(\alpha)}$ in certain selected basis $\underline{e}^{(\alpha)}$. Identities for Φ_j and its derivatives will be of the following form:

$$\Phi_j = (\underline{r}_i - \underline{r}_k) \cdot l_j^{(\alpha)} - f_{3j}(t) = 0, \quad (2.82)$$

$$\dot{\Phi}_j = (\underline{v}_i - \underline{v}_k - \underline{\omega}_\alpha \times (\underline{r}_i - \underline{r}_k)) \cdot l_j^{(\alpha)} - \dot{f}_{3j}(t) = 0, \quad (2.83)$$

$$\begin{aligned} \ddot{\Phi}_j = & (\underline{w}_i - \underline{w}_k - \underline{\varepsilon}_\alpha \times (\underline{r}_i - \underline{r}_k) - \underline{\omega}_\alpha \times (\underline{v}_i - \underline{v}_k) - \\ & - \underline{\omega}_\alpha \times (\underline{v}_i - \underline{v}_k - \underline{\omega}_\alpha \times (\underline{r}_i - \underline{r}_k))) \cdot l_j^{(\alpha)} - \ddot{f}_{3j}(t) = 0. \end{aligned} \quad (2.84)$$

Such type of constraints allow to preset dynamics of marker position or velocity detector (accelerometer) reading with respect to selected basis.

2.6.4 Preset Behaviour of Two Bodies Relative Angular Velocity Projection onto Fixed Direction in Selected Basis

Constraints of such type allow to predetermine direction of relative rotation of two bodies of the system. Such constraints allow to describe the following motions: body rotation with preset pattern of behaviour of angular velocity or angular acceleration with respect to selected basis.

$$\Psi_j = (\underline{\omega}_k - \underline{\omega}_j) \cdot l_j^{(\alpha)} - f_{4j}(t) = 0, \quad (2.85)$$

$$\dot{\Psi}_j = (\dot{\underline{\omega}}_k - \dot{\underline{\omega}}_j - \underline{\omega}_\alpha \times (\underline{\omega}_k - \underline{\omega}_j)) \cdot l_j^{(\alpha)} - \dot{f}_{4j}(t) = 0. \quad (2.86)$$

2.6.5 Preset Surface Shapes of Two Adjoined Bodies

Constraints of that type can be used as an additional possibility to describe two AM elements junction (e.g. joint contact surface shape) or external restrictions (e.g. shape of the surface, along which one of the system bodies can move)

$$\underline{\Phi}_j = (\underline{R}_{ck} + \underline{\rho}_{kj}(u_k, v_k) - (\underline{R}_{ci} + \underline{\rho}_{ij}(u_i, v_i))) - \underline{f}_{5j}(t) = 0, \quad (2.87)$$

$$\dot{\underline{\Phi}}_j = (\dot{\underline{R}}_{ck} + \dot{\underline{\rho}}_{kj}(u_k, v_k) - (\dot{\underline{R}}_{ci} + \dot{\underline{\rho}}_{ij}(u_i, v_i))) - \dot{\underline{f}}_{5j}(t) = 0, \quad (2.88)$$

$$\ddot{\underline{\Phi}}_j = (\ddot{\underline{R}}_{ck} + \ddot{\underline{\rho}}_{kj}(u_k, v_k) - (\ddot{\underline{R}}_{ci} + \ddot{\underline{\rho}}_{ij}(u_i, v_i))) - \ddot{\underline{f}}_{5j}(t) = 0. \quad (2.89)$$

Here we assume as in differential geometry that

$$\underline{\rho}_{kj} = \underline{\rho}_{kj}(u_k, v_k) \quad (2.90)$$

is a two-paramerical vector of contact surface. The next two equalities define its first and second derivatives:

$$\dot{\underline{\rho}}_{kj}(u_k, v_k) = \underline{\omega}_k \times \underline{\rho}_{kj} + \frac{\partial \underline{\rho}_{kj}}{\partial u_k} \dot{u}_k + \frac{\partial \underline{\rho}_{kj}}{\partial v_k} \dot{v}_k, \quad (2.91)$$

$$\ddot{\underline{\rho}}_{kj}(u_k, v_k) = \dot{\underline{\omega}}_k \times \underline{\rho}_{kj} + \underline{\omega}_k \times (\underline{\omega}_k \times \underline{\rho}_{kj}) + 2\underline{\omega}_k \times \left(\frac{\partial \underline{\rho}_{kj}}{\partial u_k} \dot{u}_k + \frac{\partial \underline{\rho}_{kj}}{\partial v_k} \dot{v}_k \right) +$$

$$+ \frac{\partial \rho_{kj}}{\partial u_k} \ddot{u}_k + \frac{\partial \rho_{kj}}{\partial v_k} \ddot{v}_k + \frac{\partial^2 \rho_{kj}}{\partial u_k^2} \dot{u}_k^2 + 2 \frac{\partial^2 \rho_{kj}}{\partial u_k \partial v_k} \dot{u}_k \dot{v}_k + \frac{\partial^2 \rho_{kj}}{\partial v_k^2} \dot{v}_k^2. \quad (2.92)$$

The equalities Eq. (2.87), Eq. (2.88), and Eq. (2.89) determine relative position, velocity, and acceleration vectors for surface points. In case $f_{5j}(t) \equiv 0$ these are relations for contact point kinematics determination. Additional conditions are as follows:

tangent contact

$$\Phi_{uj} = \left(\frac{\partial \rho_{kj}}{\partial u_k} \times \frac{\partial \rho_{kj}}{\partial v_k} \right) \cdot \frac{\partial \rho_{ij}}{\partial u_i} = 0, \quad \Phi_{vj} = \left(\frac{\partial \rho_{kj}}{\partial u_k} \times \frac{\partial \rho_{kj}}{\partial v_k} \right) \cdot \frac{\partial \rho_{ij}}{\partial v_i} = 0, \quad (2.93)$$

relative slip absence in point of contact, if necessary,

$$\Psi_{uj} = \left(\frac{\partial \rho_{kj}}{\partial u_k} \dot{u}_k + \frac{\partial \rho_{kj}}{\partial v_k} \dot{v}_k - \left(\frac{\partial \rho_{ij}}{\partial u_i} \dot{u}_i + \frac{\partial \rho_{ij}}{\partial v_i} \dot{v}_i \right) \right) \cdot \frac{\partial \rho_{ij}}{\partial u_i} = 0, \quad (2.94)$$

$$\Psi_{vj} = \left(\frac{\partial \rho_{kj}}{\partial u_k} \dot{u}_k + \frac{\partial \rho_{kj}}{\partial v_k} \dot{v}_k - \left(\frac{\partial \rho_{ij}}{\partial u_i} \dot{u}_i + \frac{\partial \rho_{ij}}{\partial v_i} \dot{v}_i \right) \right) \cdot \frac{\partial \rho_{ij}}{\partial v_i} = 0, \quad (2.95)$$

relative rotation bodies around normal in absence of contact point, if necessary,

$$\Psi_{\Omega kij} = \left(\frac{\partial \rho_{kj}}{\partial u_k} \times \frac{\partial \rho_{kj}}{\partial v_k} \right) \cdot (\omega_k - \omega_i) = 0. \quad (2.96)$$

2.6.6 Preset "Force" Constraint

A researcher can sometimes preset a priori behaviour pattern of constraints reactions or reading of force detectors. Being included in the set of constraints, these equations impose additional constraints on motions of the system of bodies. Linear combination of the model dynamic equations will allow us to obtain an identity for a force in certain point or a moment applied to certain body. Behaviour pattern of this linear combination is then the "force" constraint equation. Analytically such constraint can be written as follows:

$$K^T(A\ddot{q} + B - F) - Q(t) = 0. \quad (2.97)$$

It should be noted that requirement that such restriction be satisfied can, for example, be equivalent to satisfaction of the law of momentum increment, law of moment of momentum with respect to certain point increment, law of total energy of system or subsystem variation.

2.6.7 Generalised Form of Constraint Equations

Of course, these standard constraints do not describe all possible elements links and restrictions on their motion which can be encountered by a researcher. In this case it is possible to provide for individual description of these specific constraints by modelling

software user. We do not exclude from consideration such situations. Constraint equations of the first type will satisfy most peculiar requirements. Certainly, the user in this case bears responsibility for the quality of introduced constraint.

On the other hand, combining of constraints determined as standards allows us to formulate and to solve variety of problems of mechanical and biomechanical systems modelling. Employment of standard constraints for systems varying with time elements linkage structure extends considerably the sphere of modelled phenomena.

All these types of constraints can be written in the form of Eq. (2.76). However it is more convenient for further computer realisation to distinguish constraints as follows: equations which do not contain derivatives with respect to time variable

$$\Phi_j(\{q_i\}, t; \{u_s\}) = 0, \quad (2.98)$$

which contain first order derivatives with respect to time

$$\Psi_j(\{q_i\}, \{\dot{q}_i\}, t; \{u_s\}) = 0, \quad (2.99)$$

which contain second order derivatives with respect to time

$$\Omega_j(\{q_i\}, \{\dot{q}_i\}, \{\ddot{q}_i\}, t; \{u_s\}) = 0. \quad (2.100)$$

2.7 AM Equations in Generalized Coordinates

We can write system of Eq. (2.72), Eq. (2.73) in view of relation between vectors of absolute and relative angular accelerations (Eq. (2.75)). We shall consider this system as a system of $6 \times n$ vector linear equations with respect to vectors $\vec{r}_0, \dot{\vec{\Omega}}_j, (j = \overline{1, n}), \ddot{\vec{\rho}}_{cj}, (j = \overline{1, n}), \ddot{\vec{s}}_k^{(j)}, (k \leq n)$. Each of vectors $\ddot{\vec{\rho}}_{cj}$ can be submitted as linear function of not more than three generalized accelerations $\ddot{u}_{i\alpha}, (\alpha = \overline{1, n_i}, n_i \leq 3)$. The vectors $\ddot{\vec{s}}_k^{(j)}$ can be written as functions of generalized accelerations $\ddot{u}_{k\beta}, (\beta = \overline{1, n_k}, n_k \leq 3)$ and $\ddot{\varphi}_{ik\gamma}, (\gamma = \overline{1, n_{ik}}, n_{ik} \leq 3)$ — second derivatives of parameters determining angular orientation of the body with number i with respect to the element with number k . For each of the connections of two adjacent bodies, the total number of generalized coordinates does not surpass six, i. e. $n_i + n_k + n_{ik} \leq 6$. Let us project system of Eq. (2.72) and Eq. (2.73) in tangential space of generalized accelerations [78] $w = (\{\ddot{u}_{i\alpha}\}, \{\ddot{u}_{k\beta}\}, \{\ddot{\varphi}_{ik\gamma}\})$, and we shall receive system of equations of motion of base anthropomorphic model of the following form

$$A(y, t)w + B(y, v, t) - F(y, v, t) = 0,$$

which structure we shall discuss in more detail in Sec. 3.3.

At this point we finish description of generalized base model and its simpler modifications. In the following chapter we shall discuss additional aspects, arising in connection with construction of imitational dynamic anthropomorphic model.

CHAPTER 3
THE IMITATIONAL MODELLING ATTRIBUTES

3.1 Experimental Data Processing

Formalization of mathematical model in motion equations of the form Eq. (2.38) and Eq. (2.50) with constraints makes possible solution of direct and inverse problems of kinematics and dynamics if the researcher processes reliable information on model parameters, as well as forces and moments controlling the motion. Such information is, as a rule, available in robotics but in human SMA motion analysis AM geometrical and mass-inertia characteristics (GMIC) and controlling moments can be only estimated as statistical averages [102] obtained through regression analysis of data received from many people tested. Experimental data processing incorporates videoregistrated motion analysis, strain gauge and accelerometer monitoring plus additional GMIC measurements. Let us consider in more detail data processing and analysis.

3.1.1 Filmed or Video-taped Motion Processing

Frames of filmed or video-taped motion shot at high speed are processed by means of automatic comparator (or scanned information is fed directly into computer). Analysis in the plane of motion gives $2(n+3)$ numbers for each frame — Cartesian coordinates of AM joints in comparator basis (i, j) . Frame axes $(\underline{e}_1, \underline{e}_2)$ and comparator axes may not coincide and their mutual position may change from frame to frame which should be taken into account in determination of generalized coordinates φ_i . Horizontal ($G=1$) and vertical ($G=2$) straight line sections of fixed length are used to determine scale and orientation in the frame. Main designations employed hereafter are given in Fig. 3.1.

Let us introduce the following designations: $x^k o^k y^k, X^k O^k Y^k$ — frame and comparator coordinate systems correspondingly; R_i^G, R_j^G — radius vectors setting horizontal and vertical directions correspondingly; $\underline{R}_i, i = \overline{1, n}$ — radius-vectors of joints defined in comparator basis. Directly from Fig. 3.1 there follows

$$\begin{aligned} x &= r \cdot \underline{e}_1, \quad y = r \cdot \underline{e}_2, \quad l_i = |r_i|; \\ \varphi_i &= \arccos(-\underline{e}_1^{(i)} \cdot \underline{e}_2) \operatorname{sign}((\underline{r}_i \times \underline{e}_2) \cdot \underline{k}), \quad i = \overline{1, n}, \end{aligned} \quad (3.1)$$

where

$$\underline{k} = \underline{e}_1 \times \underline{e}_2, \quad \arccos(\alpha) \in [0, \pi], \quad \operatorname{sign}(\alpha) = \begin{cases} 1, & \alpha \geq 0; \\ -1, & \alpha < 0. \end{cases}$$

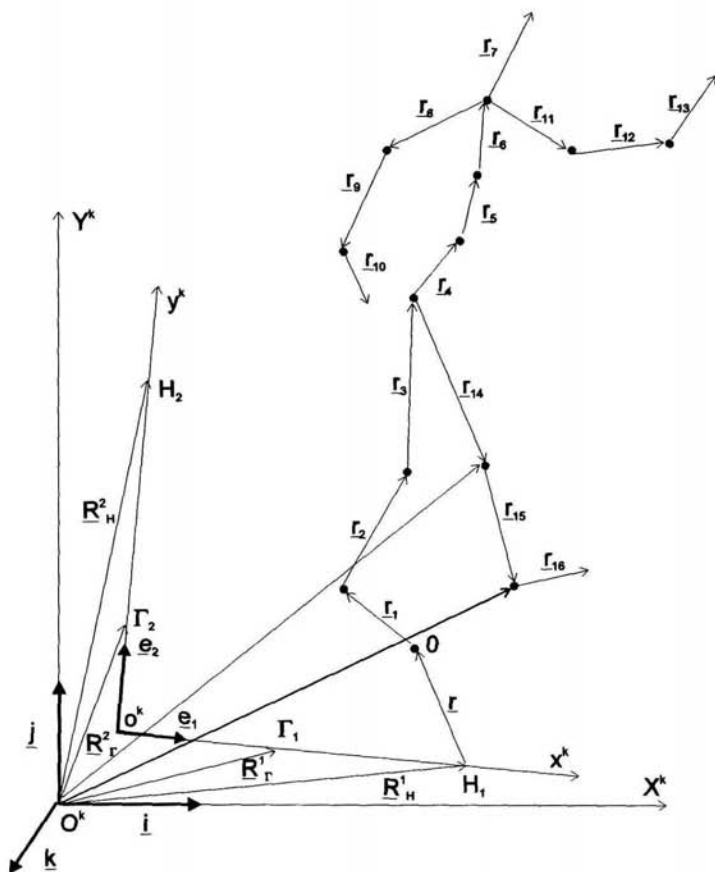


Fig. 3.1. Filmed or video-taped motion processing.

In order to determine x, y, l_i, φ_i values we shall rewrite some vectors in comparator basis (i, j) . For the frame unit vectors we can write

$$\underline{e}_G = (R_H^G - R_R^G) / |R_H^G - R_R^G|, \quad \underline{e}_{(3-G)} = \underline{\Theta}_G \cdot \underline{e}_G, \quad G = \overline{1, 2}, \quad (3.2)$$

where $\underline{\Theta}_G$ — is rotation tensor and

$$\underline{\Theta}_1 = \underline{\Theta}_2^T = \underline{\Theta}_2^{-1} = -i \underline{j} + j \underline{i} + k \underline{k},$$

with matrix

$$\Theta_1 = \begin{pmatrix} 0 & -1 & 0 \\ 1 & 0 & 0 \\ 0 & 0 & 1 \end{pmatrix}$$

Taking into account expressions for rotation tensor we can rewrite relationships Eq. (3.2) in the following form

$$\underline{e}_G = e_{G1} \underline{i} + e_{G2} \underline{j}, \quad \underline{e}_{(3-G)} = (-1)^G (e_{G2} \underline{i} - e_{G1} \underline{j}), \quad (3.3)$$

where

$$e_{Gi} = (R_{H_i}^G + R_{R_i}^G) / L_{R_v}^*, \quad e_{(3-G)(3-i)} = (-1)^{G+1} e_{Gi}, \\ L_{R_v}^* = [(R_{H_1}^G - R_{R_1}^G)^2 + (R_{H_2}^G - R_{R_2}^G)^2]^{\frac{1}{2}}.$$

Here index i corresponds to projection onto axis $O^k X^k$ ($i=1$) or $O^k Y^k$ ($i=2$); $L_{R_v}^*$ — horizontal or vertical straight line unit section length in comparator unit measure. Relationships allowing to determine r_i in comparator basis are obtained from equation

$$\sum_{i=1}^j \mu_{ji} r_i = \underline{R}_j - \underline{R}_0, \quad j = \overline{1, n},$$

from which it follows that

$$r_i = \sum_{k=1}^i \mu_{ik}^{-1} (\underline{R}_k - \underline{R}_0) = \sum_{k=1}^i \mu_{ik}^{-1} \underline{R}_k, \quad i = \overline{2, n}; \quad (3.4) \\ r_1 = \underline{R}_1 - \underline{R}_0, \quad r = \underline{R}_0 - \underline{R}_H.$$

Substitution of expressions Eq. (3.3) and Eq. (3.4) into Eq. (3.1) allows to obtain final result for each frame. For initial data check we can propose calculation of average length of each AM element during frames processing according to equations

$$l_{iav}^1 = l_i^1, \quad l_{iav}^k = \left(\sum_{j=1}^k l_i^j \right) / k = [(k-1)l_{iav}^{k-1} + l_i^{k-1}] / k, \quad i = \overline{1, n}, \\ k = \overline{2, k^*},$$

where k, k^* — frame number and total number of frames correspondingly. It is not always possible to mark out the shooting zone during motion videoregistration, however surrounding objects can substitute marking lines. In such a case the following relationships serve to determine R_r and R_H :

$$\underline{R}_r = \underline{R}_1^H - \varepsilon_H |\underline{R}_r - \underline{R}_1^H| = \underline{R}_1^H - \frac{\underline{R}_1^H - \underline{R}_2^H}{|\underline{R}_1^H - \underline{R}_2^H|} \cdot \frac{D_L}{L_{et}} |\underline{R}_4 - \underline{R}_3|, \quad \underline{R}_H = \underline{R}_1^H.$$

Here $\underline{R}_1^H, \underline{R}_2^H$ — radius vectors of two arbitrary points within frame positioned on one vertical line (and analogously for horizontal marking line); $\underline{R}_3, \underline{R}_4$ — radius vectors of so called standard AM element joints (standard AM element is the element which length can be most accurately measured and which motion is most strictly planar), L_{et} — standard element length (in meters), D_L — distance between H and Γ points (in meters).

In automatic processing of shot AM motion one can determine not only generalized coordinates of certain basic AM model (BM) but also assess relative (interelement) velocities and, if they prove to be too small, recommend reduction of AM freedom degrees number. That will require GMIC reassessment for AM elements. A measure of relative displacement can be introduced as follows

$$\Psi_i^2 = \frac{\sum_{j=1}^{k^*} [\tilde{\psi}_i(t_j) - \psi_i(t_j)]^2 + (\Omega_i \tau)^2}{k^* - 2}, \quad (3.5)$$

$$\tilde{\psi}_i(t) = \Omega_i t + \psi_i^0, \quad i = \overline{1, \nu},$$

where $\tilde{\psi}_i(t)$ — linear regression estimate of relative (interelement) displacement i with constant coefficients Ω_i, ψ_i^0 ; τ — observation time. If Ψ_i — is relatively small we assume $\Omega_i = 0$ which corresponds to imposition of confining constraint $\psi_i = \psi_i^0$.

3.1.2 GMIC and Reduction of AM Degrees of Freedom

In the basis of algorithms described below lie results of statistical information processing and elementary mechanics formulas. Let us assume that constraints can be imposed only on adjoining AM elements which have become adjoining due to imposed constraints. Complex AM locomotions characterized by constraints imposition/lifting during motion performance (walking, gymnast exercise on the horizontal bar or bars etc.) can be described by uniform dynamics equations due to redetermination of structure matrix and GMIC in case of support point transference. This considerably facilitates such locomotions computer modelling. BM geometry is defined by: vectors \underline{r}_i linking joints; ρ_{ci} — center of mass radius vectors in basis $\bar{e}^{(i)}$, \underline{r}_0 — support point radius vector. Hereafter we will also be employing the following variables: $l_i, m_i, J_{ci}, a_{1i}, a_{2i}$ which were introduced above.

BM GMIC assessment is carried out for instance by means of least squares analysis of experimental data received from considerable number of tests. Comparative analysis of various and quite numerous human GMIC determination methods is found in [102]. For example, this work gives description of the most accurate method — radioisotopy. According to research done by authors this method error averages about 3-5%. Numerous measurements carried out on persons of different build allowed us to compile charts of multiple regression equations coefficients which in turn make possible to assess 16-element AM GMIC by given integral characteristics (height, weight, etc.). According to [102] GMIC are calculated as follows

$$P_{ij}^k = \sum_{q=0}^l B_{qij}^k F_q, \quad (3.6)$$

where $F_0 = 1$, F_q , $q = \overline{1, l}$ — integral characteristics of the person tested (1-height, 2-weight, 3, 4... — other anthropomorphic data); $k = 1, 2$ — corresponds to different sexes; $i = \overline{1, n}$ — AM element number, $j = \overline{1, f} \leq 7$ — element characteristic number; B_{qij}^k — coefficients which values are given in Ref. [102].

Let us assume that there are S holonomic stationary constraints imposed on BM which confine mutual position of adjoining AM elements as follows

$$\varphi_i - \varphi_j - \psi_{ij} = 0, \quad (3.7)$$

where ψ_{ij} — constants. Let us also assume that support point is located at the end of AM element k ($k = \overline{0, n}$), (here $k = 0$ corresponds to standard support location, for instance, at the beginning of the first element). Constraints imposition and support point transference can occur simultaneously or in some arbitrary succession. System degrees of freedom number (without those due to possible support mobility) is $q = (n - S)$. Constraints of the Eq. (3.7) type can be viewed as resulting in new AM which consists of reduced number of solid bodies, each of which has no more than two joints. Thus we can still use structure matrix for mechanism's elements and their arrangement description and remain in the framework of AM model which has been considered above.

Let us designate GMIC values corresponding to this new AM model — result of Eq. (3.7) type constraints imposition on BM — with the following sign: ($'$). Algorithm of formation of new structure matrix μ' and attendant chart of AM elements groups comprising new AM elements is obvious. Let us give an auxiliary formula for further GMIC calculation. Element i radius vector in structure μ is determined as follows

$$R_i^p = r + \sum_{k=1}^{i-1} \mu_{ik} r_k + p r_i, \quad i = \overline{1, n}, \quad (3.8)$$

where $p = \{0 - \text{the beginning} \mid 1 - \text{the end}\}$ of element i .

Element j center of mass radius vector in μ : $\underline{R}_{cj} = \underline{R}_j^0 + \underline{\rho}_{cj}$, where $\underline{R}_j^0 = \underline{R}_j^p$ when $p = 0$. Then element j center of mass radius vector in structure μ with respect to the beginning of element i :

$$\underline{R}_{cji} = \underline{R}_{cj} - \underline{R}_i^0 = \underline{R}_j^0 + \underline{\rho}_{cj} - \underline{R}_i^0 = \sum_{k=1}^{i-1} (\mu_{jk} - \mu_{ik}) \underline{r}_k + \sum_{k=i}^{j-1} \mu_{jk} \underline{r}_k + \underline{\rho}_{cj}. \quad (3.9)$$

With an eye to simplify working out of the algorithm and further calculation based on information on every group of elements comprising a new element (a solid body) we will form one-dimensional information array (Table 3.1).

Table 3.1. Information array.

| | | | | | |
|-------|-------|-------|-------|-----|-------------|
| 1 | 2 | 3 | 4 | ... | $S_1 + 2$ |
| S_1 | S_2 | S_3 | S_4 | ... | S_{S_1+2} |

In Table 3.1 we resort to the following designations:

S_1 — total number of AM elements comprising a group;

S_2 — number of AM element one of which joints is at the same time a second joint of the new element (for new element length assessment);

S_3 — number of AM element which is the first in the group;

S_{k+3} , $k = \overline{1, S_1 + 2}$ — numbers of elements comprising the group.

As soon as this group information vector is formed, weight, height and center of mass coordinates of the new AM element are determined. Its weight

$$m'_i = \sum_{k=1}^{S_1} m_{S_{k+2}}. \quad (3.10)$$

If $S_2 = 0$, the element's length can be adopted to be of arbitrary value because the element in this case is located at the end of kinematic chain and does not influence other elements displacement and as for motion equation of the end element it does not include elements length. If $S_2 \neq 0$, then

$$l_i'^2 = |r_i'|^2, \quad r_i' = \underline{R}_{S_2}^0 - \underline{R}_{S_3}^0 = \sum_{k=S_3}^{S_2} \mu_{S_2 k} \underline{r}_k \quad (3.11)$$

in case if $S_2 = k$ (number of the element at which end there is the support point) we can write

$$r_i' = \sum_{j=S_3}^{S_2-1} \mu_{S_2 j} \underline{r}_j + \underline{r}_k.$$

Center of mass radius vector

$$M_i' \underline{\rho}'_{ci} = \sum_{k=1}^{S_1} R_{cS_{k+2}S_3} M_{S_{k+2}} = \\ = \sum_{k=1}^{S_1} M_{S_{k+2}} \left[\sum_{j=1}^{S_3-1} (\mu_{S_{k+2}j} - \mu_{S_3j}) \underline{r}_j + \sum_{j=S_3}^{S_{k+2}-1} \mu_{S_{k+2}j} \underline{r}_j + \underline{\rho}_{cS_{k+2}} \right].$$

Its projections in basis $\bar{e}^{(i)}$

$$a'_{1i} = \begin{cases} |\underline{\rho}'_{ci}|, & S_2 = 0; \\ \underline{r}'_i \cdot \underline{\rho}'_{ci} / l'_i, & S_2 \neq 0; \end{cases} \quad a'_{2i} = \begin{cases} 0, & S_2 = 0; \\ (|\underline{\rho}'_{ci}|^2 - a'^2_{1i})^{1/2}, & S_2 \neq 0. \end{cases} \quad (3.12)$$

Moment of inertia with respect to rotation axis S_3 is determined as follows

$$J'_i = \sum_{k=1}^{S_1} [M_{S_{k+2}} |\underline{R}_{cS_{k+2}S_3}|^2 + J_{cS_{k+2}}], \quad (3.13) \\ J'_{ci} = J'_i - M'_i |\underline{\rho}'_{ci}|^2.$$

Vector $\underline{R}_{cS_{k+2}S_3}$ is determined from formula Eq. (3.9).

Quantities in relationships Eq. (3.10)–Eq. (3.13) are calculated for given (with accuracy of number of new degrees of freedom) AM configuration which depends on values of ψ_{ij} from Eq. (3.7). These quantities are invariable with respect to new generalized coordinates. System of solid bodies GMIC assessment at discrete moments of time (for each frame of filmed motion) allows to plot how GMIC depend on time. Specifically, for each group of solid bodies position of its center of mass and moment of inertia change with time. Quantities $J'(t)$ and $\underline{\rho}'_c(t)$ can be used for approximate description of a group of AM elements motion. Linear regression estimate of Eq. (3.5) type makes possible to substitute a group of AM elements with one solid body with averaged across the sample characteristics if structure μ' parameters are relatively stable.

When support point is translated to the end of element k new structure matrix μ^k is formed from μ' according to the following algorithm. First, line k is considered and components μ'_{ki} are analyzed for $j = \overline{k, (-1), 1}$. If $\mu'_{ki} = 1$, then element j is given a new number in order of increase (starting from $k=1$) and quantities a^k_{1j} , a^k_{2j} , J^k_j , φ^k_j are recalculated according to obvious formulas as $\bar{e}^{(j)}$ basis position has changed. Structure matrix components μ^k_{ij} are put equal to 1 for $i = \overline{1, n_1}$, $j = \overline{1, i}$, where n_1 — number of non-zero components in line k of μ' . The rest of μ^k_{ij} components are put to be non-zero if μ'_{ij} and μ'_{kj} values do not coincide for $i, j = \overline{1, q}$ (q — number of freedom degrees).

In conclusion, let us note that the proposed approach, in contradistinction from traditional one employing Lagrange multipliers technique in order to describe constraints influence, allows to work out relatively simple solution algorithm.

3.1.3 Trajectories Smoothing

Experimental data processing and motion synthesis problems are related to determination of model structure (number of freedom degrees, incidence matrix) and AM elements and interelement junctions characteristics parametrization. The most general approach seems to rely on computer determination of ranges within which these parameters lie or possibly even their concrete values. At the same time we should note that most contemporary experimental units allow to monitor only displacements and obtain some additional fragmentary data from strain gauges and accelerometers. On the whole, question whether concrete AM model adequately reflects real human SMA motion remains open. Hereafter we suggest to consider some quantity depending on discrepancy of experimental data received from strain gauges (or accelerometers) and corresponding modelled data on AM behaviour as model adequacy criterion.

Processing of experimental data often includes function derivatives calculation when the only information available is function value. In general case there are no exhausting recommendations as to how smoothly approximate a function which behaviour is given in table form. However, taking into account uniform character of measurements characteristics for filmed motion, let us employ cubic smoothing splines [89]. An essential feature of procedure proposed below is that spline coefficients depend on smoothing parameter p . Value of p lies within $[0, \infty)$ range which corresponds to a set of curves of class C_2 — from interpolation curve to a straight line plotted according to the least squares method (LSM).

Let us assume that y_i — given values of function $y(t)$ in ν uniformly located at interval h nodes: $t_i = t_1 + (i - 1)h, i = \overline{1, \nu}$. We will approximate $y(t)$ behaviour at each of $(\nu - 1)$ intervals with a cubic polynomial which coefficients depend on parameter p .

$$f_i(t) = a_i + b_i(t - t_i) + c_i(t - t_i)^2 + d_i(t - t_i)^3, \quad (3.14)$$

$$i = \overline{1, \nu - 1}, \quad t \in [t_i, t_{i+1}].$$

Let f_i belong to the class C_2 , i.e. for each internal node there hold true relationships

$$f_{i-1}^{(k)}(t_i) = f_i^{(k)}(t_i), \quad k = 0, 1, 2; \quad i = \overline{2, \nu - 1} \quad (3.15)$$

and measurement error at each observation point is one and the same and equal to δ (equal accuracy). Then $f(t)$ discrepancy and continuity of its derivatives criterion can be introduced as follows

$$I = p \int_{t_1}^{t_\nu} [f^{(2)}(t)]^2 dt + \sum_{i=1}^{\nu} [f(t_i) - y(t_i)]^2 / \delta^2 \quad (3.16)$$

Obviously, for interpolation spline ($p = 0$) and for least squares straight line ($p \rightarrow \infty$) correspondingly second and first terms take their minimal value — zero. Intermediate values of parameter p allow to plot a smoothing spline which would combine derivatives continuity and closeness to experimental data y_i .

Let the following relationships be true

$$f_0(t_i) = f_1(t_1) = a_1, \quad f_{\nu-1}(t_\nu) = f_\nu(t_\nu) = a_\nu, \quad f_0^{(3)}(t_1) = f_\nu^{(3)}(t_\nu) = 0. \quad (3.17)$$

Then, taking into account formula Eq. (3.14), expression for functional I can be rewritten as follows

$$I = p[f_{\nu-1}^{(2)}(t_\nu)f_{\nu-1}^{(1)}(t_\nu) - f_1^{(2)}(t_1)f_1^{(1)}(t_1)] + \sum_{i=1}^{\nu} \{pa_i[f_i^{(3)}(t_i) - f_{i-1}^{(3)}(t_i)] + (a_i - y_i)^2/\delta^2\}. \quad (3.18)$$

Putting functional derivatives with respect to a_i equal to zero for $i = \overline{1, \nu}$ we get

$$\delta^2 p[f_i^{(3)}(t_i) - f_{i-1}^{(3)}(t_i)] = 2(y_i - a_i), \quad i = \overline{1, \nu}. \quad (3.19)$$

Finally we obtain a closed system of linear algebraic equations. To $(4\nu - 2)$ unknown quantities a_i , c_i , $i = \overline{1, \nu}$, b_i , d_i , $i = \overline{1, \nu-1}$, $(4\nu-6)$ Eq. (3.15), Eq. (3.19) and the additional four following equations correspond

$$f_{\nu-1}(t_\nu) = a_\nu, \quad f_1^{(2)}(t_1) = c_1 = \text{const}_1, \\ f_\nu^{(2)}(t_\nu) = c_\nu = \text{const}_2, \quad f_{\nu-1}^{(2)}(t_\nu) = c_\nu.$$

Omitting intermediate transformations we will write this system of equations in matrix form. First, let us introduce $\nu \times (\nu - 2)$ matrix Q and $(\nu - 2) \times (\nu - 2)$ matrix T as follows

$$Q^T = \begin{pmatrix} 1 & -2 & 1 & 0 & \dots & 0 & 0 & 0 \\ 0 & 1 & -2 & 1 & \dots & 0 & 0 & 0 \\ 0 & 0 & 1 & -2 & \dots & 0 & 0 & 0 \\ \vdots & \vdots & \vdots & \vdots & \dots & \vdots & \vdots & \vdots \\ 0 & 0 & 0 & 0 & \dots & 1 & -2 & 1 \end{pmatrix}, \\ T = \begin{pmatrix} 4 & 1 & 0 & \dots & 0 & 0 \\ 1 & 4 & 1 & \dots & 0 & 0 \\ 0 & 1 & 4 & \dots & 0 & 0 \\ \vdots & \vdots & \vdots & \dots & \vdots & \vdots \\ 0 & 0 & 0 & \dots & 1 & 4 \end{pmatrix}$$

and $(\nu \times 1)$ columns $C^{**} = (-c_1, c_1, 0, \dots, c_\nu, -c_\nu)^T$, $a = (a_1, \dots, a_\nu)^T$, $y = (y_1, \dots, y_\nu)^T$, and $(\nu - 2) \times 1$ columns $C^* = (c_1, 0, \dots, 0, c_\nu)^T$, $C = (c_2, \dots, c_{\nu-1})$. Then

$$3Q^T a = h^2(TC + C^*), \\ \delta^2 p(QC + C^{**}) = h(y - a). \quad (3.20)$$

From Eq. (3.20) we can obtain a system of linear algebraic equations for determination of column C

$$(3p\delta^2 Q^T Q + h^3 T)C = 3hQ^T y - 3p\delta^2 Q^T C^{**} - h^3 C^*. \quad (3.21)$$

It is obvious that matrix $(3p\delta^2 Q^T Q + h^3 T)$ is symmetric, positive definite and five diagonal which simplifies finding solution C . Let us note that if $p = 0$ matrix becomes three-diagonal which corresponds to the well-known cubic spline-interpolation problem [89]. From Eq. (3.20) we obtain the following expression for coefficients a

$$a = y - p\delta^2(QC + C^{**})/h, \quad (3.22)$$

and the rest of coefficients are found from continuity conditions

$$\begin{aligned} b_i &= (a_{i+1} - a_i)/h - c_i h - d_i h^2, \\ d_i &= (c_{i+1} - c_i)/(3h), \quad i = \overline{1, \nu - 1}. \end{aligned} \quad (3.23)$$

If $p \rightarrow \infty$, cubic spline asymptotically transforms into a straight line plotted according to the least squares analysis. It is clear that in this case we should put $c_1 = c_\nu = 0$, and then Eq. (3.22) can be rewritten as follows

$$a = [E - Q(Q^T Q)^{-1} Q^T] y, \quad (3.24)$$

where E — identity matrix; coefficients b_i are found from Eq. (3.23). Spline interpolation properties are characterized by quantity S .

$$S = (a - y)^T (a - y) / \delta^2 = p^2 \delta^2 (QC + C^{**})^T (QC + C^{**}) / h. \quad (3.25)$$

The c_1 and c_ν values estimation (if they are not preset) is essential in spline coefficients determination. Estimation can be done either by differentiation of formulas which directly interpolate experimental data y_i or by setting initial values of c_1 and c_ν (e.g. equalizing them to zero) and preliminary smoothing of experimental data. However, thoroughness of boundary conditions evaluation is only necessary for small data samples ($\nu < 10$). Otherwise c_1 and c_ν can be adopted to be equal to zero as their values significantly influence interpolation polynomial behaviour only as far as several nodes from the boundary (this fact has been proved by multiple test calculations). Most valuable in the spline coefficients determination procedure described above is that functional dependence is brought down to a single-parameter one which is highly important for a system with many freedom degrees. On the other hand, such approach may lead to excessive smoothing, i.e. disappearance of relatively large but actually present velocities and accelerations values. Bearing this in mind there can be suggested stipulation of parameter p value range or its calculation based on additional considerations and physical conditions described by experimenter. As for parameter optimal value, it should be determined from AM behaviour and human SMA real motion closeness criterion.

3.2 Choice of the Optimal Model Parameters

In practice, as a basis for optimal choice of parameters of mathematical models mostly serve different methods of minimization of functions of several variables. Most effective of them with respect to the convergence speed usually incorporate calculation of

the functional derivatives. These methods become less effective if the derivatives are to be computed numerically. In addition, due to the complexity of AM models, even for the simplest form of the functional its convexity cannot be established. The same reason leads to considerable errors in gradients calculation. Therefore let us consider two well-known methods which do not require derivatives calculation.

So called regular methods which allow to carry out directional search do not work well when it is necessary to find the global extremum of a function of many variables. So, it is suggested to use a method of pseudo-stochastic search based on generation of LP- τ sequences in the space characterized by the dimension of the field of arguments [88]. According to authors research this method gives best results in comparison with other methods generating sequences of uniform distribution and is effective in finding the global extremum or a starting point for regular methods. The simplicity of its realisation together with possibility of generating sequences meeting given constraints allow to use this method to get out of deadlock situations which may occur when using methods of directional search.

Let us write out formulas for LP- τ sequences generation using "numerators tables" $r_j^{(e)}$ [88]. First, we find the value of $m = 1 + [\ln(i)/\ln(2)]$, where i — is the number of the sequence. Then we generate vector number i , which has n components and is in fact the current point of K^n space,

$$q_{ij} = \sum_{k=1}^m 2^{-k+1} \left\{ \frac{1}{2} \sum_{l=k}^m [2\{i2^{-l}\}] [2\{r_j^{(l)} 2^{k-1-l}\}] \right\}, \quad j = \overline{1, n}. \quad (3.26)$$

In Eq. (3.26) symbols $[z]$, $\{z\}$ stand for integer and fractional part of z correspondingly. Note, that when programming in FORTRAN, for effective use of Eq. (3.26) one should rather use one-dimensional array instead of a two-dimensional one and appropriate successive extracting of the array items coupled by explicit calculation of the 2-D address and addition in place of raising to a power (which is possible since we use addition instead of multiplying by 2).

Use of pseudostochastic search methods is justified in case of absence of *a priori* information about possible behaviour of the function or some estimation calculations. The advantages of this method, which make it undependable on the topology of the problem under consideration (due to the independence of neighbouring stochastic vectors), lead at the same time to some overestimation of the function being minimized. Moreover, with increase of the sequence number i , the total number of operations to calculate one pseudostochastic vector q_{ij} , $j = \overline{1, n}$ increases correspondingly to the change of the parameter m (this number becomes rather big when $i = 1024$). For continuation of sequence generation one should start from the number corresponding to the end of the previous sample, which leads to different computer time needed for realisation of neighbouring samples of the same length. It is worth mentioning that as a rule 1000 is in fact the limit "sensible" number of tests used in practice, especially for not very effective computers.

In order to get more precise values of the extreme points we use a slightly altered

procedure from that given by Himmelblau in [42]. From the analytical geometry it is known that coordinates of vertexes of the regular simplex are defined by the matrix D . This matrix columns-vertexes are numbered from 1 to $(n + 1)$ and its lines-coordinates can be presented as follows

$$D = \begin{pmatrix} 0 & d_1 & d_2 & \dots & d_2 \\ 0 & d_2 & d_1 & \dots & d_2 \\ \cdot & \cdot & \cdot & \dots & \cdot \\ \cdot & \cdot & \cdot & \dots & \cdot \\ 0 & d_2 & d_2 & \dots & d_1 \end{pmatrix}, \quad \begin{aligned} d_1 &= \frac{t}{n\sqrt{2}}(\sqrt{n+1} + n - 1), \\ d_2 &= \frac{t}{n\sqrt{2}}(\sqrt{n+1} - 1), \end{aligned} \quad (3.27)$$

where $t = |d_1 - d_2|\sqrt{2}$ — is the distance between any two arbitrary vertexes. The modification of the regular simplex, allowing for change of the distance between different vertexes and resulting in adaptation of the method to the topology of the problem under consideration, was called the method of the deformed polyhedron.

Let $\bar{x}_i^k = (x_{i1}^k, \dots, x_{in}^k)$, $i = \overline{1, n+1}$ — be the i -th vertex in the E^n space at the k -th search stage ($k = 0, 1, 2, \dots$). Let $f(\bar{x}_i^k)$ — be the value of the aim function and

$$f(\bar{x}_h^k) = \max_{i=\overline{1, n+1}} \{f(\bar{x}_i^k)\}, \quad f(\bar{x}_l^k) = \min_{i=\overline{1, n+1}} \{f(\bar{x}_i^k)\}.$$

Since a polyhedron in the E^n space has $(n + 1)$ vertexes $\bar{x}_1, \dots, \bar{x}_{n+1}$, let \bar{x}_{n+2} be the centroid of n of them (except for \bar{x}_h), then its coordinates are

$$x_{n+2, j}^k = \frac{1}{n} \left[\left(\sum_{i=1}^{n+1} x_{ij}^k \right) - x_{hj}^k \right], \quad j = \overline{1, n}, \quad (3.28)$$

then the procedure of finding the vertex in the polyhedron where $f(\bar{x})$ is minimum consists of the following operations:

1. *Reflection or projection* of the \bar{x}_k through the centroid.

$$\bar{x}_{n+3}^k = \bar{x}_{n+2}^k + \alpha(\bar{x}_{n+2}^k - \bar{x}_h^k), \quad \alpha > 0. \quad (3.29)$$

2. *Expansion*. If $f(\bar{x}_{n+3}^k) \leq f(\bar{x}_l^k)$, then the $(\bar{x}_{n+3}^k - \bar{x}_{n+2}^k)$ vector is elongated:

$$\bar{x}_{n+4}^k = \bar{x}_{n+2}^k + \gamma(\bar{x}_{n+3}^k - \bar{x}_{n+2}^k), \quad \gamma > 1. \quad (3.30)$$

If $f(\bar{x}_{n+4}^k) < f(\bar{x}_l^k)$, then \bar{x}_h^k is substituted by \bar{x}_{n+4}^k and the procedure is carried out anew from the first operation (with $k := k + 1$). Otherwise \bar{x}_h^k is substituted by \bar{x}_{n+3}^k (followed by the same switch to the 1-st operation with $k = k + 1$).

3. *Compression*. If $f(\bar{x}_{n+3}^k) > f(\bar{x}_l^k)$, for all $i \neq h$, then the $(\bar{x}_h^k - \bar{x}_{n+2}^k)$ vector is shortened

$$\bar{x}_{n+5}^k = \bar{x}_{n+2}^k + \beta(\bar{x}_h^k - \bar{x}_{n+2}^k), \quad (3.31)$$

where $0 < \beta < 1$. Then we substitute \bar{x}_h^k by \bar{x}_{n+5}^k and switch over to the 1-st operation for continuation of the search at step number $(k + 1)$.

4. *Reduction.* If $f(\bar{x}_{n+3}^k) > f(\bar{x}_h^k)$, then all $(\bar{x}_i^k - \bar{x}_l^k)$, $i = \overline{1, n+1}$ vectors are reduced two times starting from the \bar{x}_i^k

$$\bar{x}_i^k = \bar{x}_l^k + (\bar{x}_i^k - \bar{x}_l^k)/2, \quad i = \overline{1, n+1}. \quad (3.32)$$

Then we turn back to the operation number 1.

For termination criteria the following ones may serve

$$\begin{aligned} f(\bar{x}_l^k) < \varepsilon, \quad f(\bar{x}_h^k) - f(\bar{x}_l^k) < \varepsilon, \\ \sum_{i=1}^n \sum_{j=1}^{n+1} (x_{ji}^k - x_{n+2,i}^k)^2 < \varepsilon, \quad \|\bar{x}_h^k - \bar{x}_l^k\| < \varepsilon n^2, \end{aligned} \quad (3.33)$$

where $\|\dots\|$ is the Euclidean norm of a vector.

Concrete values of reflection (α), expansion (γ) and compression (β) parameters are chosen empirically.

Combining of the pseudostochastic and directional search methods in one procedure allows for principal possibility of determination of the global extremum with the necessary precision level. Some technical problems, which may arise in concrete problems, can be resolved by introducing an interactive dialogue with the user or supplying periodical information on the current state of the procedure work with an option of its termination or switching to further stage of the problem solving algorithm. Anyhow, there always should be a possibility of presetting of the maximum iteration number. An option of switching from one termination criterion to another Eq. (3.33) also helps very essentially in "dead lock" situations which happen when dealing with an arbitrary function with many local extremums. Later we will consider such an example when the aim function is a "convolution" of several criteria in the form of a linear combination.

Modelling of human SMA motion by differential Eq. (2.50) implies certain idealisation of the real motion of the human body. As it has been mentioned before, the main supposition is that SMA parts can be presented as a system of solid bodies connected by joints. The AM is modelled as a system with localised parameters. In case of a planar model these are the position of the center of mass of the body a_{1i} , a_{2i} , its "length" l_i ; mass m_i and the central moment of inertia J_{ci} .

GMIC measurement errors are passed on the generalised coordinates φ_i , ψ_i , $i = \overline{1, n}$ causing serious distortion of the motion energy and forces behaviour picture. Let us recall the AM motion equations. Let $\varphi = (\varphi_1, \dots, \varphi_n)^T$, $\dot{\varphi} = (\dot{\varphi}_1, \dots, \dot{\varphi}_n)^T$, $\text{diag} \dot{\varphi} \dot{\varphi} = (\dot{\varphi}_1^2, \dots, \dot{\varphi}_n^2)^T$, where $\text{diag} \dot{\varphi} \dot{\varphi} = \{\delta_{ij} \varphi_i^2\}$, δ_{ij} — the Kronecker symbol and $C = (C_1, \dots, C_n)^T$, $D = (D_1, \dots, D_n)^T$, $B = \{B_{ij}\}$, $A = \{A_{ij}\}$, where C_i , D_i , A_{ij} , B_{ij} , $i, j = \overline{1, n}$ are defined by Eq. (2.49). Then from Eq. (2.50)

$$\hat{A}\ddot{q} = \hat{B}\text{diag} \dot{\varphi} \dot{\varphi} + g\hat{D} + Q, \quad (3.34)$$

where

$$\hat{A} = \begin{pmatrix} M^c & 0 & C \\ 0 & M^c & D \\ C & D & A \end{pmatrix}, \quad \hat{B} = \begin{pmatrix} D \\ -C \\ B \end{pmatrix}, \quad \hat{D} = \begin{pmatrix} 0 \\ -M \\ -D \end{pmatrix},$$

$$Q = \left(N_x + \sum_{j=1}^n F_{jx}, N_y + \sum_{j=1}^n F_{jy}, U_1^*, \dots, U_n^* \right)^T,$$

$$\tilde{q} = (\tilde{x}_0, \tilde{y}_0, \tilde{\varphi})^T$$

\hat{A} is the kinetic energy matrix and its components, as well as of \hat{B} and \hat{D} , depend only on the generalized coordinates φ . From Eq. (3.34) we get

$$Q = \hat{A}\tilde{q} - \hat{B}\text{diag}\dot{\varphi}\dot{\varphi} - g\hat{D}, \quad (3.35)$$

i.e. the solution of the direct dynamics problem on condition that all variables and parameters on the right side of Eq. (3.35) are known. The matrices elements depend linearly on the GMIC measurement and calculation errors

$$C_i^3 = a_{1i}m_i + l_i \sum_{k=i+1}^n m_k \mu_{ki}, \quad C_i^4 = a_{2i}m_i, \quad (3.36)$$

$$A_{ij}^3 = a_{1i}\mu_{ij}m_i + l_i \sum_{k=i+1}^n m_k \mu_{ki}\mu_{kj}, \quad A_{ij}^4 = a_{2i}\mu_{ij}m_i.$$

Therefore, Q is also a linear function of these errors. As for the errors in $\dot{\varphi}$ and \tilde{q} determination, which are due to numerical differentiation, they will appear in Eq. (3.35) with the factor $1/h^2$, where h — is the observation step ($1/h = v$ — the frequency of film recording). Thus, we can assume that when solving the direct dynamics problem, one should first of all estimate the trajectory smoothing parameters and only then choose the GMIC. Note that with the increase of the parameter v value GMIC calculation errors almost do not change (except possibly for l_i if they are defined as sample averages, say, from the relation given above). On the contrary, estimation errors of $\dot{\varphi}$ and \tilde{q} may grow due to the film recording frequency nonstability, decrease of the film resolution ability and other technical reasons.

Use of smoothing splines depending on one parameter gives a chance to get through its variation best $\dot{\varphi}$, \tilde{q} and U_i^* , $i = \overline{1, n}$ values estimations. We consider N_x , N_y , F_{jx} , F_{jy} values to be given or measured during the experiment. One of the most simple test experiments is when a free fall is shot. The AM center of mass moves along the ballistic trajectory and $N_x = N_y = F_{jx} = F_{jy} = M_1 = 0$. First two equations of Eq. (3.34) can be used for experimental determination of N_x , N_y with estimation of the GMIC and trajectory smoothing parameters. The theorem on the system moment of momentum change can obviously be used in this case. During the motion moment of momentum should not change. This equation supplements essentially the adequacy criterion, since taking into account of only N_x , N_y leads to

demand of fulfilment of the theorem of the center of mass motion which does not depend on the errors of J_{ci} estimation.

Let us now consider a single-support phase of motion, supposing that we have information on the ground reaction \underline{N} behaviour (i.e. we possess measurements of the force platform graduated and synchronized with the film record). We also suppose that except for the main shots and measurements, a few shots at the very beginning and the end have been made. This is necessary to avoid "boundary effects" when using splines and defining the start point velocity. Then for the center of mass (CM) coordinates we will have

$$\begin{aligned} x_c(t) &= x_{c0} + \dot{x}_{c0}(t - t_0) + \frac{1}{M^c} \int_{t_0}^t \int_{t_0}^{\tau} N_x(q) dq d\tau, \\ y_c(t) &= y_{c0} + \dot{y}_{c0}(t - t_0) - g \frac{(t - t_0)^2}{2} + \frac{1}{M^c} \int_{t_0}^t \int_{t_0}^{\tau} N_y(q) dq d\tau, \end{aligned} \quad (3.37)$$

where x_{c0} , \dot{x}_{c0} , y_{c0} , \dot{y}_{c0} are the starting coordinates and velocity projections. The integrals are calculated numerically using table values of N_x , N_y . Upon differentiating of Eq. (3.37) we get expressions for velocities and accelerations of the CM

$$\begin{aligned} \dot{x}_c(t) &= \dot{x}_{c0} + \frac{1}{M^c} \int_{t_0}^t N_x(\tau) d\tau, \\ \dot{y}_c(t) &= \dot{y}_{c0} - g(t - t_0) + \frac{1}{M^c} \int_{t_0}^t N_y(\tau) d\tau, \\ \ddot{x}_c(t) &= N_x(t)/M^c, \quad \ddot{y}_c(t) = N_y(t)/M^c - g. \end{aligned} \quad (3.38)$$

On the other hand, their values can be expressed as functions of the AM parameters (further on we will use the tilde sign to designate them). Let us choose the criterion of adequacy of the model to the experiment as follows

$$\begin{aligned} J &= \int_{t_0+t_1}^{T-t_1} \{ \lambda_1(x_c - \tilde{x}_c)^2 + \lambda_2(y_c - \tilde{y}_c)^2 \} dt + \\ &+ \int_{t_0+t_2}^{T-t_2} \{ \lambda_3(\dot{x}_c - \tilde{\dot{x}}_c)^2 + \lambda_4(\dot{y}_c - \tilde{\dot{y}}_c)^2 \} dt + \end{aligned}$$

$$+ \int_{t_0+t_3}^{T-t_3} \{ \lambda_5(\ddot{x}_c - \tilde{\ddot{x}}_c)^2 + \lambda_6(\ddot{y}_c - \tilde{\ddot{y}}_c)^2 + \lambda_7(M_1 - \tilde{M}_1)^2 \} dt, \quad (3.39)$$

where $(T - t_0)$ — the observation interval; t_i — observation interval used for neutralisation of the splining “boundary effect”; λ_i , $i = \overline{1, 7}$ — weight coefficients. The integrals in Eq. (3.39) are calculated numerically.

The functional value J of the adequacy criterion depends actually on the model dimension n , the GMIC parameters ($4n$) and smoothing splines parameters $(n + 2)$. The weight coefficients and values of t_i are set based on results of concrete research. The experiment yields directly only displacements. Therefore, the largest value in Eq. (3.39) will be that of the third item reflecting the difference in acceleration values. Apparently, in order to get a balanced criterion J behaviour, one should choose second and third integrals from Eq. (3.39) proportional to h and h^2 correspondingly. Practical results show that for estimation of energy and forces behaviour picture one can leave only the third integral in Eq. (3.39) (i.e. differences in displacements and velocities values stay within measurement errors boundaries).

Let us give here one practical recommendation. In order to process the displacements received from experiments there should be a possibility of their correction by use of the criterion

$$J_1 = \lambda_1(x_c - \tilde{x}_c)^2 + \lambda_2(y_c - \tilde{y}_c)^2 \quad (3.40)$$

Minimization of this difference at each point of time is carried out through solving of the inverse kinematics problem with respect to coordinates taking into account constraints on phase coordinates. Specifically, using expressions for \tilde{x}_c , \tilde{y}_c (which depend on $q = (x_0, y_0, \varphi)$) we resolve the nonlinear algebraic system of equations $\tilde{x}_c(q) = x_c$, $\tilde{y}_c(q) = y_c$ by the least square method, minimising J_1 .

Naturally, this correction of experimental data brings about additional oscillations in the behaviour of generalized coordinates. However, this does not influence essentially the behaviour of generalized velocities and accelerations if we resort to smoothing splines. Moreover, x_c , y_c mean values correspond to those of the experiment with a very high precision.

Thus, the problem of AM optimal parameters estimation, which positive solution allows to confirm model adequacy to the real motion of human SMA, was reduced to a problem of multiparametric minimization with constraints. Methods of its solution have been described above. We find it necessary to underline once more the necessity of parameter field ranging. The number of degrees of freedom of the system is chosen out of preliminary considerations, involving demand of smallness of relative angular displacements (see criteria Eq. (3.5)). This is one of the steps of the first stage which is carried out off-line, when the experimental data have been preliminary processed. Upon imposing of constraints of the Eq. (3.7) type, applying of the reduction procedure and calculation of new GMIC we get a new base model.

Then follows correction of generalized coordinates (using Eq. (3.40) criterion) and choosing of trajectory smoothing parameters $(n + 2)$. This stage is the most labori-

ous, since for each new set of smoothing parameters new sets of splines coefficients are built. The upper bound for smoothing parameters values can be defined using relations for spline interpolation properties estimation Eq. (3.25). It can be shown that when S is set, the problem reduces to finding numerical solution of this equation with respect to smoothing parameter p (which can be done using for example the Newton method).

Search of the optimal GMIC is carried out in the diapason defined by the errors of their measurements. Since this diapason is as a rule quite small (3–5%) and for calculation of a new set of GMIC one only needs to calculate (using the Eq. (3.26) formula) the coefficients of motion equations, this stage takes much less time.

Optimization can be continued to find more precise values of smoothing parameters using the last iteration values as starting ones. Apparently, a conclusion cannot be made on the global conversion of this process, but practical investigations show decrease of the functional Eq. (3.39) value by several orders with respect to its “worst” value. This result can easily be detected numerically after estimation of the base of the initial simplex by the method of LP- τ sequences, since then both best and worst combinations of the GMIC and smoothing parameters can be determined. This is another advantage of use of a pseudostochastic search method at the first stage.

Results of direct dynamics problem solution can be verified by substitution of the calculated values in the Eq. (3.34) with following motion equations integration. This can be done also for estimation of adequacy of the model. The character of relation $Q(t)$ should be such as not to cause “disintegration” of results of integration of differential Eq. (3.34). Note that since the experimental data is processed using an averaged model, $Q(t)$ should correspond to some averaged motion. Experimental displacements derivatives oscillations will be surely passed on $Q(t)$. This, however, should not cause nonstability of results of numerical integration of the motion equations. One of the methods used to improve stability of numerical integration methods is to introduce in the right part of the motion equations new items proportional to the generalized velocity and considered as addition to the generalized forces (i.e. they are calculated taking into account that the generalized velocities are functions of time). These items bring about some dissipation of the energy produced by the generalized forces but this improves stability characteristics of the AM and of the numerical solution as well.

Successive solution of the direct and inverse dynamics problems allows to make conclusions on the model adequacy. It is important to underline here how the solution of each of these two problems can be used for the other one. Importance of differentiation results verification (it is differentiation that brings about the largest errors) by use of integration has been shown above. As for the integration results, it is practically impossible to notice their “disintegration” without following differentiation and substitution in the motion equations. This is due to the fact that all numerical integration methods in their choice of the integration step are based on local estimation and cannot guarantee precise solution.

Exchange of information between these two problems is also useful for testing of the procedure of search for optimal parameters based on results of processing of noise-damaged phase picture. We get this picture upon equations integration and introducing a uniformly distributed (within a circle of a preset radius) "noise" distorting the real positions of joints of the AM. This distortion imitates measurements errors (in the process of the experimental film processing, etc.). In the same way the GMIC can be altered. By regulating the noise amplitude (or the distribution circle radius) one can assess effectiveness of both smoothing methods and procedure of multiparametric optimization as a whole.

3.3 Control Structure

3.3.1 Stationary Control

Solving of the direct and inverse dynamics problems for the AM mathematical model described by the system Eq. (2.38) is connected with the structure of the resultant moment vector \underline{U}_i^* , namely, with hypotheses of its dependence on external and internal forces and constraints reactions. When we have "accurate" information about the number of links n , their mass-inertia characteristics (m_i , ρ_{ci} , r_i , \underline{J}_{ci}) and all the joints are of the ball-and-socket type, the direct dynamics problem yields the $\underline{U}_i^*(t)$ functions. However, the real motion is a result of action of both external and internal forces and moments, depending on the positions of links $\bar{r} = (r_1, \dots, r_n)^T$, vectors r_0 , $\bar{\omega}$ and constraint parameters. From the synthesis point of view (i.e. building of motion with preset kinematic characteristics) it seems expedient to provide for different ways of the moment $\underline{U}_i^*(t, \bar{r}, \bar{\omega})$ formation. Let us point out three of them: interelement moments $\bar{M} = \mu^T \underline{U}$, external forces and moments, external and internal constraint reactions.

Real motion of the AM can be a result of one of these three factors action. But from the point of view of interelement control moments synthesis it is possible to construct a motion with preset kinematic characteristics by correct choice of only external forces and constraints. Then one can get the \bar{M}_i value from the direct problem solution (in case of absence of other factors). This approach to simple motions synthesis seems to be the most "economical" (in comparison, for example, with solution of the inverse kinematics problem by use of nonlinear programming methods). Moreover, introduction of external forces into the equations of motion can serve as a stabilisation factor for the problem of numerical integration. Motion synthesis with help of interelement moments and/or constraint equations [53] can bring one to the problem of dealing with statically non-stable systems. Such problems as a rule are solved by use of general integration methods with an automatic choice of the method order and step.

Let us consider some example of control formation. For model with spherical joints

the resultant moment vector is defined by formula

$$\underline{U}_i = \sum_{k=i+1}^n \mu_{ki}^{-1} \underline{M}_k + (\underline{\rho}_{ci} + \underline{z}_i) \times \underline{F}_i + \underline{r}_i \times \sum_{k=i+1}^n \mu_{ki} \underline{F}_k + \underline{Q}_i, \quad (3.41)$$

where μ_{ki}^{-1} — the components of the matrix inverse to the matrix μ , \underline{F}_i — external forces (the gravity force is taken into account separately), \underline{M}_k — interelement moments, \underline{Q}_i — resultant moment of constraint reaction forces. Synthesis of kinematics with respect to inertial basis is typical for problems when the grip of a robot's arm should move along a preset trajectory with certain orientation in space. Synthesis of such a motion through variation of the $\underline{M}_k(t)$ moment is difficult without solution of the inverse kinematics problem. Use of external forces and moments acting on the principle of a negative feed-back with respect to absolute displacements and velocities brings additional oscillations into the system. Therefore errors in the motion performance are quite large. However, the advantage of this approach is that additional differential equations do not appear and one has to work with the system Eq. (2.38) alone. Additional equations appear if the system is subjected to holonomic and/or nonholonomic constraints which, however, results in essentially more precise performance of the preset grip motion.

Results of analysis or, in other words, solution of the direct dynamics problem yields generalized forces, in particular, ground reactions as functions of time. Then supposing that they can be presented in the form

$$N_x = -c_x x - \beta_x \dot{x}, \quad N_y = -c_y y - \beta_y \dot{y} \quad (3.42)$$

(where x, y are projections of the relative displacement of the support point), we can assess the values of $c_x, c_y, \beta_x, \beta_y$, for example, calculating them for each film frame and doing a linear regression estimation over the whole sample.

For planar model motion we can consider an important specific case when there is only one external force \underline{F}_k (except for support reaction \underline{N}) applied to the AM at given point of element k . Bearing in mind the ordered numeration of AM elements and taking into account the triangular form of μ matrix we will see that Eq. (2.50) with $i = \overline{1, k-1}$ contain moment $U_i^k = \mu_{ki}(\underline{r}_i \times \underline{F}_k) \cdot \underline{k}$, equation number k contains moment $U_k^k = ((\underline{\rho}_k + \underline{z}_k) \times \underline{F}_k) \cdot \underline{k}$. As for the rest of equations, they will not contain \underline{F}_k in explicit form. Let us note that for a ramified kinematic chain $\mu_{ki} = 0$ for those elements of AM which do not belong to the chain linking support and element k and this leads to exclusion of \underline{F}_k from corresponding equation (equation i). Radius vector of the force origin (point of its application) in basis $\bar{e}^{(0)}$ is defined as follows

$$\underline{P}_k = \underline{r}_0 + \sum_{i=1}^{k-1} \mu_{ik} \underline{r}_k + \underline{\rho}_{ck} + \underline{z}_k.$$

Now, the simplest way to describe and study multisupport phase of AM locomotion consists in representation of \underline{F}_k in the following form $\underline{F}_k = -f(|\underline{P}_k - \underline{\hat{P}}_k|)$, where

$f > 0$ is arbitrary function. For $f(|P_k - \tilde{P}_k|) = c_k|P_k - \tilde{P}_k|$ with $c_k > 0$ this corresponds to negative linear feedback with respect to deviation \underline{P}_k from nominal trajectory \tilde{P}_k . Let us note that c_k value, defining support stiffness coefficient, is chosen empirically with an eye to minimize maximum value of relative displacement $|P_k - \tilde{P}_k|$ and assigning to c_k too high a value may cause undesirable free oscillations due to introduction of confining constraint. In order to model AM behaviour with additional support more adequately one can introduce feedback with respect to velocity. Although this will lead to some AM motion energy dissipation, such a move allows to get rid of undesirable oscillations in the system and creates a stabilizing factor in numerical integration of motion equations.

For interelement moments estimation formula such as Eq. (3.42) does not hold, since the AM model imposes certain constraints on the values of interelement angles. Let us consider one interelement moment model with non-linear elastic behaviour. Let the angle constraints have the form $\psi \in [\psi_1, \psi_2]$, and let there be a stable point at $\psi_0 \in (\psi_1, \psi_2)$.

Let the interelement moment M satisfy the constraint: $M \in [M_1, M_2]$, where $M_1 < 0$, $M_2 > 0$ — are some constants specific for each joint (N.B. these constants not to be taken for \underline{M}_1 , \underline{M}_2 — first and 2-nd interelement moments). Now, let the moment M change according to equation

$$M = -A \tan(d_1\psi + d_2) - d_3, \quad (3.43)$$

where A , d_1 , d_2 , d_3 — are positive parameters, chosen so as to provide tending of the M value to its marginal value when ψ tends to its corresponding limit. This allows to avoid discontinuities in the right part of motion equations, which is important when integrating with an alternating step. Taking into account that periodical function $\tan(x)$ has discontinuities at $x \rightarrow \pm\pi/2$, let us write down equations for definition of unknown parameters from Eq. (3.43)

$$\begin{aligned} d_1\psi_1 + d_2 &= e_2 = -\arctan(M_2/A) < 0, \\ d_1\psi_2 + d_2 &= e_1 = -\arctan(M_1/A) > 0, \end{aligned} \quad (3.44)$$

where $e_1 \rightarrow \pi/2$, $e_2 \rightarrow -\pi/2$, as the absolute values of M_1 , M_2 increase. Then

$$d_1 = (e_1 - e_2)/(\psi_2 - \psi_1), \quad d_2 = (e_1 + e_2 - d_1(\psi_1 + \psi_2))/2 \quad (3.45)$$

and out of the condition that M be equal to zero at $\psi = \psi_0$

$$d_3 = -A \tan(d_1\psi_0 + d_2). \quad (3.46)$$

Then, when $M_i \rightarrow \pm\infty$ we get

$$d_3 = -A \tan\{\pi[\psi_0 - (\psi_1 + \psi_2)/2]/(\psi_2 - \psi_1)\},$$

i.e. M will be equal to zero at the middle of the $[\psi_1, \psi_2]$ interval. Let for simplicity $M_2 = -M_1 = M^* > 0$. Then $e_1 = -e_2 = e = \arctan(M^*/M)$ and

$$\begin{aligned} d_1 &= 2e/(\psi_2 - \psi_1), \quad d_2 = -d_1(\psi_1 + \psi_2)/2 = -e(\psi_1 + \psi_2)/(\psi_2 - \psi_1), \\ d_3 &= -A \tan(d_1\psi_0 + d_2) = -A \tan\{2e[\psi_0 - (\psi_1 + \psi_2)/2]/(\psi_2 - \psi_1)\}. \end{aligned} \quad (3.47)$$

Thus, setting for every hinge-joint values of M^* , A , ψ_1 , ψ_2 , β , we get non-linear visco-elastic behaviour of the interelement moment

$$M = \beta \dot{\psi} - A \tan(d_1\psi + d_2) - d_3, \quad (3.48)$$

where $\beta > 0$ is a characteristic of energy dissipation in the hinge-joint.

Control of the AM by means of interelement moments is in fact certain idealisation of the real forces that perform the useful work. In motions of human SMA the main propelling force is surely that of contracting muscles. So, the biomechanics of muscle contraction should be taken into account for determination of interelement moments limit values. Hill equations [41, 99] express a constraint on power of muscles work and have the form

$$v(P + a) = b(P_0 - P), \quad (3.49)$$

v — is the velocity of the muscle contraction; P — the force at the time of observation; a — heat loses for a unit of the muscle length change; b — the coefficient reflecting type of muscles at work; P_0 — the maximum force value. Let us consider how the Eq. (3.49) formula can be used on example of two elements junction presented schematically on Fig. 3.2 and brought into motion by a flexor and extensor muscle correspondingly.

Substituting into Eq. (3.49) $v = \dot{l}$, where l — is the muscle length, and using designations of Fig. 3.2, pinpointing the places of muscles fixation, we will have

$$\begin{aligned} Q_1(\psi, \dot{\psi}) &= [\dot{\psi} a_1(\psi) + b_1(\psi) Q_0^1(\psi)] / [b_1(\psi) - \dot{\psi}] \geq 0, \\ Q_2(\psi, \dot{\psi}) &= [\dot{\psi} a_2(\psi) + b_2(\psi) Q_0^2(\psi)] / [\dot{\psi} - b_2(\psi)] \leq 0, \end{aligned} \quad (3.50)$$

where

$$\begin{aligned} a_1(\psi) &= a^1 C_1 d \sin(\psi) / l_1, \quad b_1(\psi) = b^1 l_1 / [C_1 d \sin(\psi)]; \\ Q_0^1(\psi) &= P_0^1 C_1 d \sin(\psi) / l_1, \quad l_1 = [C_1^2 + (d)^2 + 2C_1 d \cos(\psi)]^{\frac{1}{2}}; \\ a_2(\psi) &= a^2 C_2 d \sin(\psi - \beta) / l_2, \quad b_2(\psi) = b^2 l_2 / [C_2 d \sin(\psi - \beta)]; \\ Q_0^2(\psi) &= P_0^2 C_2 d \sin(\psi - \beta) / l_2, \quad l_2 = [C_2^2 + (d)^2 + 2C_2 d \cos(\psi - \beta)]^{\frac{1}{2}}; \end{aligned}$$

and parameters a^i , b^i , P_0^i , $i = 1, 2$ correspond to designations of the Eq. (3.49) equations. Derivation of Eq. (3.50) required implementation of some obvious geometrical relationships.

Therefore, power constraints on the interelement moments will have the following form

$$Q_2(\psi, \dot{\psi}) \leq M \leq Q_1(\psi, \dot{\psi}). \quad (3.51)$$

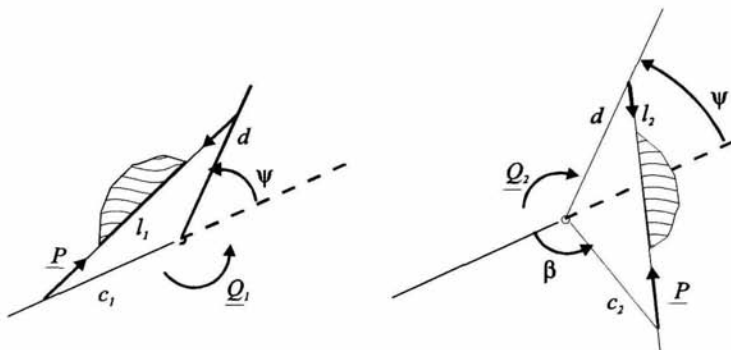


Fig. 3.2. Joint linking two elements. Flexor and extensor muscles.

Let us note one peculiarity in the control synthesis problem setting. Motion equations depend linearly on the resultant moment of external forces U . So, the simplest way of the optimal control problem solution would be mere testing of different U values. It is assumed that u_i must satisfy $u_i^1 \leq u_i \leq u_i^2$ or in the matrix form

$$U^1 \leq U \leq U^2, \quad (3.52)$$

where $U = (u_1, \dots, u_n)^T$ — is the control vector; U^1, U^2 — its limit values. Since $M = \mu^T U$, for interelement moments we get

$$\mu^{-T} M^1 \leq M \leq \mu^{-T} M^2, \quad (3.53)$$

and for their limit values

$$\mu^{-T}(M^2 - M^1) \geq 0. \quad (3.54)$$

This formula can be considered as a condition of static equilibrium in a single-support phase. This means that amplitude values of the interelement moments should decrease as we move from the support to branches of the kinematic chain. Let for example $-M^1 = M^2 = M^*$, then

$$\mu^{-T} M^* \geq 0, \quad (3.55)$$

and in the scalar form

$$M_i^* > - \sum_{k=i+1}^n \mu_{ki}^{-1} M_k^*, \quad i = \overline{1, n}, \quad (3.56)$$

and after recalling that $-\mu_{ki}^{-1}$ is equal either to 1 or 0, and that $M^* > 0$, $i = \overline{1, n}$ in the sense of inequalities Eq. (3.54), Eq. (3.55) becomes obvious. Note that in a free-fall phase these conditions do not hold (in particular, the first interelement moment will be equal to 0).

Solution of AM control synthesis problems implies integration of systems of ordinary differential equations of the general type. Difficulties arising are of both mechanical and numerical nature (e.g. non-linear oscillations with small energy dissipation and large system dimensions, wide parameters values spread). Numerical problems are caused by the fact that the expanded matrix of kinetic energy is ill conditioned. Methods used for solution of systems of differential equations of the general type are most fully presented in the monograph [61]. Universal methods can be used only after the system has been transformed to the standard form (i.e. to a system of equations of the first order). However, since this has been done, one can use well-tested integration packages with automatic choice of the order and step of the method being used. For robotics problems, when the behaviour of the generalized forces is well-known one can use special methods [53, 87] which essentially speed up the procedure of the inverse dynamics problem solution. But the constancy of the integration step characteristic to these methods often results in the necessity of considerable efforts to choose the optimal step value. In the framework of the optimal control theory, synthesis problems solution includes numerous integration of motion equations of the Eq. (2.38) and Eq. (2.50) type. But in this case control variation, even within fields of a small measure, can "wreck" the integration procedure and cause essential distortion of the optimality criterion value or phase constraints violation. This is another argument in favour of use of universal integration packages when developing software for analysis and synthesis of AM motions.

3.4 Integration of Motion Equations for Mechanical System with Constraints

The problem of mathematical (and computer) modelling of human motion has existed as one the mechanics problems since development of first human-like automatic mechanisms. With time anthropomorphic models have become more complex, however they are still based on the model of system of solid bodies connected by rigid and visco-elastic junctions [29, 101, 107]. Progress in development of adequate anthropomorphic models depends on the quality of motion videoregistration system, accuracy of determination of geometric and mass-inertia characteristics of human body elements, measurements of external forces appearing through interaction with environment, and internal forces, controlling muscle forces and joint reactions. Therefore an open, sensitive to additional experimental data computer anthropomorphic model should allow for parametric adjustment and should be universal in the sense of possibility of modelling of wide motions variety. The problem of modelling can consist either in traditional analysis (determination of muscle forces from results of

videoregistration and tensometry) and synthesis (determination of motion characteristics from given behaviour of motion controlling forces) problems or in the mixed problem solution. In development of contemporary computer packages for system of solid bodies dynamics modelling various systems of generalized coordinates are used and suppositions on the character of junctions between bodies can be either fixed or changed with time during motion performance. But even in the latter case it is often not possible to satisfy all the restrictions and constraints on motion. It should be also noted that even in solution of classical analysis problem registered kinematics can seldom be presented in the form of explicit dependencies of generalized coordinates from time. That is why in creation of computer anthropomorphic mechanism model some base anthropomorphic model is used and a system of additional constraints and solution of set problems is brought down to integration of a system of differential-algebraic equations (DAE). One of the central points of modelling is choice of integration method. Universal optimal integration method choice problem remains open [66]. In this section we describe the original approach to DAE solution. One is development of modern methods which have been used in codes for simulation systems bodies dynamics.

3.4.1 Implicit Form of Equations for Mechanical System with Constraints

System of differential equations, describing the dynamics of an open kinematic chain written for generalized coordinates is described by the following equation

$$H(y, v, w; t) = A(y; t)w + B(y, v; t) - F(y, v; t) = 0. \quad (3.57)$$

Such a form of differential equations presentation is convenient for both plain model and universal model. Here H — matrix-column of n differential motion equations written in an implicit form, $y \equiv q, v \equiv \dot{q}, w \equiv \ddot{q}$ — matrices-column of generalized coordinates, velocities and accelerations correspondingly, A — square nonsingular symmetric positive-definite matrix. B, F — matrices-columns of generalized inertia forces and external forces. Motion equations of a system restricted by constraints Eq. (2.98)–Eq. (2.100) can be represented in the form of differential-algebraic equations system

$$H_w(y, v, w; t; \lambda, \mu, \nu) = A\ddot{q} + B - F + C_0\lambda + C_1\mu + C_2\nu = 0, \quad (3.58)$$

$$H_\lambda(y, v, w; t) = \Omega(q, \dot{q}, \ddot{q}; t) = 0, \quad (3.59)$$

$$H_\mu(y, v; t) = \Psi(q, \dot{q}; t) = 0, \quad (3.60)$$

$$H_\nu(y; t) = \Phi(q; t) = 0. \quad (3.61)$$

Rectangular matrices C_0, C_1, C_2 in Eq. (3.58) are correspondingly of the following dimensions: $(n \times n_\lambda), (n \times n_\mu), (n \times n_\nu)$. These matrices elements are result of partial

derivation of constraint equations Eq. (3.59), Eq. (3.60) and Eq. (3.61)

$$\begin{aligned} C_0^T &= \frac{\partial}{\partial w^T}(H_\lambda), \\ C_1^T &= \frac{\partial}{\partial v^T}(H_\mu), \\ C_2^T &= \frac{\partial}{\partial y^T}(H_\nu), \end{aligned} \quad (3.62)$$

and λ, μ, ν — are matrices-columns of the following dimensions $(n_\lambda \times 1)$, $(n_\mu \times 1)$ and $(n_\nu \times 1)$. The system of Eq. (3.58)-Eq. (3.61) is assigned with differential index 2 according to the commonly accepted classification system DAE [34]. It can be solved via employment of BDF methods [33] or Runge-Kutta methods [77]. It should be noted that the explicit integration method use requires calculation of inverse matrix of coefficients at generalized accelerations and Lagrange multipliers for each call of differential equations system right parts computing subroutine. Therefore implicit predictor-corrector methods are more attractive. Let us consider in detail algorithm of corrections calculation when DAE system Eq. (3.58)–Eq. (3.61) is solved.

3.4.2 Corrections Calculation for Arbitrary Constraints

Multistep method is described by the following equation

$$y_k = h_k \beta \dot{y}_k + \sum_{j=1}^p (\alpha_j y_{k-j} + h_k \beta_j \dot{y}_{k-j}), \quad (3.63)$$

and we can always rewrite this equation as follows

$$y_k = h_k \beta \Delta \dot{y}_k + y_k^*, \quad (3.64)$$

where y_k^* is an approximation of y_k obtained on prediction step.

For the following differential matrix equation of the second order

$$\begin{aligned} H(y, v, \dot{v}; t) &= 0, \\ v - \dot{y} &= 0 \end{aligned} \quad (3.65)$$

application of Eq. (3.63) allows to write down formulas for correction process

$$\dot{v}_k = w_k = \xi_w + w_k^*, \quad v_k = h_k \beta \xi_w + v_k^*, \quad y_k = h_k^2 \beta^2 \xi_w + y_k^*. \quad (3.66)$$

Substituting Eq. (3.66) into Eq. (3.65) for $t = t_k$ leads us to the equation for ξ_w determination

$$H(y_k^* + h_k^2 \beta^2 \xi_w, v_k^* + h_k \beta \xi_w, w_k^* + \xi_w; t_k) = 0. \quad (3.67)$$

Application of the described approach to a system of differential- algebraic equations Eq. (3.58)–Eq. (3.61) brings us to necessity of solving of a system $(n + n_\lambda + n_\mu + n_\nu)$ nonlinear equations

$$H_w(y_k^* + h_k^2\beta^2\xi_w, v_k^* + h_k\beta\xi_w, w_k^* + \xi_w; t_k; \lambda_k, \mu_k, \nu_k) = 0, \quad (3.68)$$

$$H_\lambda(y_k^* + h_k^2\beta^2\xi_w, v_k^* + h_k\beta\xi_w, w_k^* + \xi_w; t_k) = 0, \quad (3.69)$$

$$H_\mu(y_k^* + h_k^2\beta^2\xi_w, v_k^* + h_k\beta\xi_w; t_k) = 0, \quad (3.70)$$

$$H_\nu(y_k^* + h_k^2\beta^2\xi_w; t_k) = 0. \quad (3.71)$$

Solution of the system of Eq. (3.68)–Eq. (3.71) is found employing Newton-Raphson method. Taking into account behavior of $H_w, H_\lambda, H_\mu, H_\nu$ as functions of ξ_w , system of linear equations with respect to correction term $\zeta = (\zeta_w, \zeta_\lambda, \zeta_\mu, \zeta_\nu)$ at one iteration step can be presented by the following system of equations

$$\begin{aligned} \bar{A}\zeta_w + C_0\zeta_\lambda + C_1\zeta_\mu + C_2\zeta_\nu + H_w &= 0, \\ \bar{C}_0^T\zeta_w + H_\lambda &= 0, \\ \beta h\bar{C}_1^T\zeta_w + H_\mu &= 0, \\ \beta^2 h^2\bar{C}_2^T\zeta_w + H_\nu &= 0. \end{aligned} \quad (3.72)$$

In Eq. (3.72) we used the following nomenclature:

$$\begin{aligned} \bar{A} &= \frac{\partial}{\partial w^T}(H_w) + \beta h \frac{\partial}{\partial v^T}(H_w) + \beta^2 h^2 \frac{\partial}{\partial y^T}(H_w), \\ \bar{C}_0^T &= C_0^T + \beta h \frac{\partial}{\partial v^T}(H_\lambda) + \beta^2 h^2 \frac{\partial}{\partial y^T}(H_\lambda), \\ \bar{C}_1^T &= C_1^T + \beta h \frac{\partial}{\partial y^T}(H_\mu), \\ \bar{C}_2^T &= C_2^T, \end{aligned} \quad (3.73)$$

$$\begin{aligned} \frac{\partial}{\partial w^T}(H_w) &= A + \frac{\partial}{\partial w^T}\left(\frac{\partial}{\partial w}(H_\lambda)^T\lambda\right), \\ \frac{\partial}{\partial v^T}(H_w) &= \frac{\partial}{\partial v^T}(B - F + \frac{\partial}{\partial w}(H_\lambda)^T\lambda + \frac{\partial}{\partial v}(H_\mu)^T\mu), \\ \frac{\partial}{\partial y^T}(H_w) &= \frac{\partial}{\partial y^T}(Aw + B - F + \frac{\partial}{\partial w}(H_\lambda)^T\lambda + \frac{\partial}{\partial v}(H_\mu)^T\mu + \frac{\partial}{\partial y}(H_\nu)^T\nu). \end{aligned} \quad (3.74)$$

It should be noted that parameter h may be not equal to actual integration step h_k . We should consider now that h is a parameter of iterations.

Transformation of the system Eq. (3.72) will give

$$\zeta_w = -\bar{A}^{-1}(H_w + C_0\zeta_\lambda + C_1\zeta_\mu + C_2\zeta_\nu), \quad (3.75)$$

$$\begin{aligned}
 \sigma_{00}\zeta_\lambda + \sigma_{01}\zeta_\mu + \sigma_{02}\zeta_\nu &= H_\lambda & -\tilde{C}_0^T \tilde{A}^{-1} H_w, \\
 \sigma_{10}\zeta_\lambda + \sigma_{11}\zeta_\mu + \sigma_{12}\zeta_\nu &= H_\mu/(\beta h) & -\tilde{C}_1^T \tilde{A}^{-1} H_w, \\
 \sigma_{20}\zeta_\lambda + \sigma_{21}\zeta_\mu + \sigma_{22}\zeta_\nu &= H_\nu/(\beta^2 h^2) & -\tilde{C}_2^T \tilde{A}^{-1} H_w,
 \end{aligned} \tag{3.76}$$

where

$$\sigma_{ij} = \tilde{C}_i^T \tilde{A}^{-1} C_j, \quad i, j = \overline{0, 2}. \tag{3.77}$$

Finally, solution of system Eq. (3.72) in matrix form

$$\begin{aligned}
 \zeta_w &= (\tilde{A}^{-1} C \sigma^{-1} \tilde{C}^T - E) \tilde{A}^{-1} H_w - \tilde{A}^{-1} C (\sigma^{-1} (\hat{H}_\lambda + \hat{H}_\mu/(\beta h) + \hat{H}_\nu/(\beta^2 h^2)) + V u), \\
 \zeta &= -\sigma^{-1} \tilde{C}^T \tilde{A}^{-1} H_w + \sigma^{-1} (\hat{H}_\lambda + \hat{H}_\mu/(\beta h) + \hat{H}_\nu/(\beta^2 h^2)) + V u,
 \end{aligned} \tag{3.78}$$

where

$$C^T = \begin{pmatrix} C_0^T \\ C_1^T \\ C_2^T \end{pmatrix}, \quad \hat{H}_\lambda = \begin{pmatrix} H_\lambda \\ 0 \\ 0 \end{pmatrix}, \quad \hat{H}_\mu = \begin{pmatrix} 0 \\ H_\mu \\ 0 \end{pmatrix}, \quad \hat{H}_\nu = \begin{pmatrix} 0 \\ 0 \\ H_\nu \end{pmatrix}$$

— matrices columns of dimension $(n_\lambda + n_\mu + n_\nu)$, u — arbitrary vector of dimension n , $V = (E - \sigma^{-1} \sigma)$ — matrix orthogonal to σ , and σ^{-1} — in general case, semi-inverse matrix to σ , satisfying the following equation

$$\sigma = \sigma \sigma^{-1} \sigma. \tag{3.79}$$

If rank of σ is equal to $(n_\lambda + n_\mu + n_\nu)$, then $\sigma^{-1} = \sigma^{-1}$, $V \equiv 0$. Formulas of Eq. (3.78) give general expression for ζ_w acceleration correction terms and for Lagrange multipliers $\zeta_\lambda, \zeta_\mu, \zeta_\nu$ at the current s -th iteration of correction step. In correspondence with Eq. (3.66) values of unknown variables at each iteration are calculated by the following formula

$$w_k^{(s)} = w_k^{(s-1)} + \zeta_w^{(s)}, \quad v_k^{(s)} = v_k^{(s-1)} + h_k \beta \zeta_w^{(s)}, \quad y_k^{(s)} = y_k^{(s-1)} + h_k^2 \beta^2 \zeta_w^{(s)}, \tag{3.80}$$

$$\lambda_k^{(s)} = \lambda_k^{(s-1)} + \zeta_\lambda^{(s)}, \quad \mu_k^{(s)} = \mu_k^{(s-1)} + \zeta_\mu^{(s)}, \quad \nu_k^{(s)} = \nu_k^{(s-1)} + \zeta_\nu^{(s)}. \tag{3.81}$$

3.4.3 Holonomic Constraints

Let the constraints imposed on the system are holonomic and defined by Eq. (3.61). If smoothness conditions on function Φ are fulfilled, we can impose additional to Eq. (3.61) constraint equations

$$\dot{\Phi} = \frac{\partial}{\partial q^T}(\Phi) \dot{q} + \frac{\partial}{\partial t}(\Phi) = 0, \tag{3.82}$$

$$\ddot{\Phi} = \frac{\partial}{\partial q^T}(\Phi) \ddot{q} + \frac{\partial}{\partial t} \left(\frac{\partial}{\partial q^T}(\Phi) \dot{q} + \frac{\partial}{\partial t}(\Phi) \right) + \frac{\partial}{\partial q^T} \left(\frac{\partial}{\partial q^T}(\Phi) \dot{q} + \frac{\partial}{\partial t}(\Phi) \right) \dot{q} = 0. \tag{3.83}$$

For the type of constraints under consideration Eq. (3.73) and Eq. (3.74) can be presented as follows (using Eq. (3.82), Eq. (3.83) and Lagrange identities)

$$\tilde{A} = A + \beta h \frac{\partial}{\partial v}(H_w) + \beta^2 h^2 \frac{\partial}{\partial y}(H_w), \quad \tilde{C}_0^T = C_0^T + 2\beta h \dot{C}_0^T + \beta^2 h^2 \ddot{C}_0^T, \quad (3.84)$$

$$\tilde{C}_1^T = C_0^T + \beta h \dot{C}_0^T, \quad \tilde{C}_2^T = C_0^T,$$

$$\frac{\partial}{\partial v}(H_w) = \frac{\partial}{\partial v}(B - F), \quad (3.85)$$

$$\frac{\partial}{\partial y}(H_w) = \frac{\partial}{\partial y}(Aw + B - F + C_0\lambda + C_0\mu + C_0\nu),$$

where

$$\dot{C}_0^T = \frac{\partial}{\partial q^T}(\dot{\Phi}), \quad \ddot{C}_0^T = \frac{\partial}{\partial q^T}(\ddot{\Phi}). \quad (3.86)$$

Let us write down equation setting the relation between the block matrix \tilde{C}_0^T and matrices $C_0^T, \dot{C}_0^T, \ddot{C}_0^T$

$$\tilde{C}^T = \begin{pmatrix} E & 2E & E \\ E & E & 0 \\ E & 0 & 0 \end{pmatrix} \begin{pmatrix} E & 0 & 0 \\ 0 & \beta h E & 0 \\ 0 & 0 & \beta^2 h^2 E \end{pmatrix} \begin{pmatrix} C_0^T \\ \dot{C}_0^T \\ \ddot{C}_0^T \end{pmatrix} = E_3 D \hat{C}_0^T, \quad (3.87)$$

where E — is unit matrix. Then σ^- can be presented as follows

$$\sigma^- = (\hat{C}_0^T \tilde{A}^{-1} C_0 e_3)^- D^{-1} E_3^{-1} = \hat{\sigma}^- D^{-1} E_3^{-1}, \quad (3.88)$$

where $e_3 = (E, E, E)$.

Substituting Eq. (3.88) in Eq. (3.78) we shall obtain the formula for ζ_w and ζ

$$\begin{aligned} \zeta_w &= (\tilde{A}^{-1} C_0 e_3 \hat{\sigma}^- \tilde{C}_0^T - E) \tilde{A}^{-1} H_w - (\beta h)^{-2} \tilde{A}^{-1} C_0 e_3 (\hat{\sigma}^- \hat{H}_\zeta + (\beta h)^2 V u), \\ \zeta &= -\hat{\sigma}^- \tilde{C}_0^T \tilde{A}^{-1} H_w + (\beta h)^{-2} (\hat{\sigma}^- \hat{H}_\zeta + (\beta h)^2 V u), \end{aligned} \quad (3.89)$$

where

$$\hat{H}_\zeta = \begin{pmatrix} \Phi \\ (\dot{\Phi}\beta h - \Phi)/(\beta h) \\ (\ddot{\Phi}(\beta h)^2 - 2\dot{\Phi}\beta h + \Phi)/(\beta h)^2 \end{pmatrix}. \quad (3.90)$$

The received form of solution presentation is convenient for further analysis and allows to assess effectiveness of possible variants of its application. Traditional for analytical solution approach to the problem with holonomic constraints is based on joint solution of system of Eq. (3.58) and Eq. (3.83). This is done under supposition that at any time, including the starting point, constraint equations Eq. (3.61) and Eq. (3.82) are satisfied. Repeating speculations for this particular case, or making necessary redefinitions directly in Eq. (3.88) and Eq. (3.89), we get

$$\begin{aligned} \zeta_{w0} &= (\tilde{A}^{-1} C_0 \sigma_{00}^- \tilde{C}_0^T - E) \tilde{A}^{-1} H_w - \tilde{A}^{-1} C_0 (\sigma_{00}^- \ddot{\Phi} + V u), \\ \zeta_\lambda &= -\sigma_{00}^- \tilde{C}_0^T \tilde{A}^{-1} H_w + \sigma_{00}^- \ddot{\Phi} + V u, \end{aligned} \quad (3.91)$$

where $\sigma_{00} = \tilde{C}_0^T \tilde{A}^{-1} C_0$.

If constraint equations in Eq. (3.83) are linearly independent then $\text{rank } C_0 = n_\lambda$, matrix σ_{00} is nonsingular and semi-inverse matrix $\sigma_{00}^- = \sigma_{00}^{-1}$. If rank of matrix C_0 is less than number of constraints of equation then only a generalized solution can be found. And in case system Eq. (3.83) is compatible it will be the solution of the problem. Otherwise, problem of correctness (compatibility) of constrains system Eq. (3.83) should be studied.

When dealing with integration of system of equations with holonomic constraints equations we face different variants of constraint equations formulation : Eq. (3.82) or Eq. (3.61). For Eq. (3.82) the solution is as follows

$$\begin{aligned} \zeta_{w1} &= (\tilde{A}^{-1} C_0 \sigma_{10}^- \tilde{C}_1^T - E) \tilde{A}^{-1} H_w - (\beta h)^{-1} \tilde{A}^{-1} C_0 (\sigma_{10}^- \dot{\Phi} + \beta h V u), \\ \zeta_\mu &= -\sigma_{10}^- \tilde{C}_1^T \tilde{A}^{-1} H_w + (\beta h)^{-1} \sigma_{10}^- \dot{\Phi} + V u, \end{aligned} \quad (3.92)$$

where $\sigma_{10} = \tilde{C}_1^T \tilde{A}^{-1} C_0$, and for Eq. (3.61) it is of the following form .

$$\begin{aligned} \zeta_{w2} &= (\tilde{A}^{-1} \tilde{C}_0 \sigma_{20}^- C_2^T - E) \tilde{A}^{-1} H_w - (\beta h)^{-2} \tilde{A}^{-1} C_0 (\sigma_{20}^- \Phi + (\beta h)^2 V u), \\ \zeta_\nu &= -\sigma_{20}^- \tilde{C}_2^T \tilde{A}^{-1} H_w + (\beta h)^{-2} \sigma_{20}^- \Phi + V u, \end{aligned} \quad (3.93)$$

where $\sigma_{20} = \tilde{C}_0^T \tilde{A}^{-1} C_0$.

It should be noted that matrix $\hat{\sigma}$ introduced in Eq. (3.88) due to redundance of system of constraint Eq. (3.61), Eq. (3.82) and Eq. (3.83) is singular even if $\text{rank } C_0 = n_\lambda$ and solution of Eq. (3.89) is a generalized one. If we choose pseudo-inverse matrix for semi-inverse matrix to $\hat{\sigma}$

$$\hat{\sigma}^+ = \frac{1}{3} e_3^T (C_0^T \tilde{A}^{-T} \hat{C}_0 \hat{C}_0^T \tilde{A}^{-1} C_0)^{-1} C_0^T \tilde{A}^{-T} \hat{C}_0, \quad (3.94)$$

then solution at some iteration step

$$\begin{aligned} \zeta_w &= (\tilde{A}^{-1} C_0 e_3 \hat{\sigma}^+ \hat{C}_0^T - E) \tilde{A}^{-1} H_w - (\beta h)^{-2} \tilde{A}^{-1} C_0 e_3 \hat{\sigma}^+ \hat{H}_\zeta, \\ \zeta &= -\hat{\sigma}^+ \hat{C}_0^T \tilde{A}^{-1} H_w + (\beta h)^{-2} \hat{\sigma}^+ \hat{H}_\zeta \end{aligned} \quad (3.95)$$

and satisfies system of equations Eq. (3.72) in sence of the quadratic norm minimum [13, 27]. The problem of convergence of iteration process for non-linear system of equations of the Eq. (3.68)–Eq. (3.71) type in case of their compatibility is quite well reflected in the literature [20].

3.4.4 Nonholonomic Constraints of the First Order

Equations of kinematic and nonholonomic constraints in general case can be described by relations Eq. (3.60). As in previous section, we suggest that these relations are differentiable with respect to time and require that the following identity holds

$$\dot{\Psi} = \frac{\partial}{\partial \dot{q}^T}(\Psi) \dot{q} + \frac{\partial}{\partial q^T}(\Psi) \dot{q} + \frac{\partial}{\partial t}(\Psi) = 0. \quad (3.96)$$

For the type of constraints being considered, equalities Eq. (3.73) and Eq. (3.74) take the following form (if Lagrange identity is taken into account)

$$\begin{aligned}\bar{A} &= A + \beta h \frac{\partial}{\partial v^T}(H_w) + \beta^2 h^2 \frac{\partial}{\partial y^T}(H_w), \\ \hat{C}_0^T &= C_1^T + \beta h(\dot{C}_1^T + C_{11}^T) + \beta^2 h^2 \dot{C}_{11}^T, \\ \hat{C}_1^T &= C_1^T + \beta h C_{11}^T,\end{aligned}\tag{3.97}$$

$$\begin{aligned}\frac{\partial}{\partial v^T}(H_w) &= \frac{\partial}{\partial v^T}(B - F + \frac{\partial}{\partial v}(\Psi)^T \lambda + \frac{\partial}{\partial v}(\Psi)^T \mu), \\ \frac{\partial}{\partial y^T}(H_w) &= \frac{\partial}{\partial y^T}(A w + B - F + C_1 \lambda + C_1 \mu),\end{aligned}\tag{3.98}$$

where

$$C_1^T = \frac{\partial}{\partial \dot{q}^T}(\Psi), \quad \dot{C}_1^T = \frac{d}{dt} \left(\frac{\partial}{\partial \dot{q}^T}(\Psi) \right), \quad C_{11}^T = \frac{\partial}{\partial q^T}(\Psi), \quad \dot{C}_{11}^T = \frac{\partial}{\partial q^T}(\dot{\Psi}).\tag{3.99}$$

Let us write in matrix form the link between \hat{C}^T and C_1^T , \dot{C}_1^T , C_{11}^T , \dot{C}_{11}^T

$$\hat{C}^T = \begin{pmatrix} E, & E \\ E, & 0 \end{pmatrix} \begin{pmatrix} E, & 0 \\ 0, & \beta h E \end{pmatrix} \begin{pmatrix} C_1^T + \beta h C_{11}^T \\ \dot{C}_1^T + \beta h \dot{C}_{11}^T \end{pmatrix} = E_2 D_2 \hat{C}_1^T.\tag{3.100}$$

Then σ^- can be expressed as follows

$$\sigma^- = (\hat{C}_1^T \bar{A}^{-1} C)^- D^{-1} E_2^{-1} = \hat{\sigma}_2^- D^{-1} E_2^{-1}\tag{3.101}$$

Substituting Eq. (3.101) into Eq. (3.72) we obtain formulas for determination of ζ_w and ζ :

$$\begin{aligned}\zeta_w &= (\bar{A}^{-1} C \hat{\sigma}_2^- \hat{C}_1^T - E) \bar{A}^{-1} H_w - (\beta h)^{-1} \bar{A}^{-1} C (\hat{\sigma}_2^- \hat{H}_{C_2} + \beta h V u), \\ \zeta &= -\hat{\sigma}_2^- \hat{C}_0^T \bar{A}^{-1} H_w + (\beta h)^{-1} \hat{\sigma}_2^- \hat{H}_{C_2} + V u,\end{aligned}\tag{3.102}$$

where

$$\hat{H}_{C_2} = \begin{pmatrix} \Psi \\ (\dot{\Psi} \beta h - \Psi) / (\beta h) \end{pmatrix}\tag{3.103}$$

If we use pseudo-inverse matrix as a semi-inverse one, we obtain results similar in form to Eq. (3.95). It is also clear that using one of the two equations: Eq. (3.60) and Eq. (3.96) we can derive classical solution (for the case of the system of independent constraint equations) analogous to solution Eq. (3.91).

3.4.5 Regularization According to Baumgarte

If we use system of constraint equations in differential form, equations for correction terms (Eq. (3.83) and Eq. (3.96)) yield classical solution. However, there appears problem of keeping point on the constraint surface (in case of nonholonomic constraint the constraint surface is considered in the phase space). Employment of redundant system of constraints Eq. (3.61), Eq. (3.82) and Eq. (3.83) or Eq. (3.60) and Eq. (3.96) is one of the approaches to solution of this problem. However, as it is clear from previous results, this approach leads to necessity of generalized solution utilization.

Alternative approach, suggested by Baumgarte is based on usage of a regularizing operator and substitution of Eq. (3.83) or Eq. (3.96) by the following one

$$\ddot{\Phi} + 2n\dot{\Phi} + k^2\Phi = 0 \quad (3.104)$$

or by equation

$$\dot{\Psi} + 2n\Psi = 0. \quad (3.105)$$

Substituting Eq. (3.104) in the generalized solution of Eq. (3.78) and making supposition that C_0 is non-singular we get

$$\begin{aligned} \zeta_w &= (\tilde{A}^{-1}C_0\sigma_{B_*}^{-1}\tilde{C}_{B_*}^T - E)\tilde{A}^{-1}H_w - \tilde{A}^{-1}C_0\sigma_{B_*}^{-1}\frac{\ddot{\Phi} + 2n\dot{\Phi} + k^2\Phi}{1 + 2n\beta h + k^2\beta^2 h^2}, \\ \zeta &= -\sigma_{B_*}^{-1}\tilde{C}_{B_*}^T\tilde{A}^{-1}H_w + \sigma_{B_*}^{-1}\frac{\ddot{\Phi} + 2n\dot{\Phi} + k^2\Phi}{1 + 2n\beta h + k^2\beta^2 h^2}, \end{aligned} \quad (3.106)$$

where

$$\sigma_{B_*} = \tilde{C}_{B_*}^T\tilde{A}^{-1}C_0,$$

and

$$\tilde{C}_{B_*} = C_0 + \frac{2\beta h(1 + \beta hn)}{1 + 2\beta hn + \beta^2 h^2 k^2}\dot{C}_0 + \frac{\beta^2 h^2}{1 + 2\beta hn + \beta^2 h^2 k^2}\ddot{C}_0. \quad (3.107)$$

Substituting Eq. (3.105) in the generalized solution of Eq. (3.78) and making supposition that C_1 is non-singular we get

$$\begin{aligned} \zeta_w &= (\tilde{A}^{-1}C_1\sigma_{B_*}^{-1}\tilde{C}_{B_*}^T - E)\tilde{A}^{-1}H_w - \tilde{A}^{-1}C_1\sigma_{B_*}^{-1}\frac{\dot{\Psi} + 2n\Psi}{1 + 2n\beta h}, \\ \zeta &= -\sigma_{B_*}^{-1}\tilde{C}_{B_*}^T\tilde{A}^{-1}H_w + \sigma_{B_*}^{-1}\frac{\dot{\Psi} + 2n\Psi}{1 + 2n\beta h}, \end{aligned} \quad (3.108)$$

where

$$\sigma_{B_*} = \tilde{C}_{B_*}^T\tilde{A}^{-1}C_1,$$

and

$$\tilde{C}_{B_*} = C_1 + \beta h C_{11} + \frac{\beta h}{1 + 2\beta hn}\dot{C}_1 + \frac{\beta^2 h^2}{1 + 2\beta hn}\ddot{C}_{11}. \quad (3.109)$$

Comparison of Eq. (3.91), Eq. (3.92), Eq. (3.93) and Eq. (3.106) brings one to conclusion that under supposition

$$\tilde{C}_0 = \tilde{C}_1 = \tilde{C}_{B_*} = C_0,$$

Baumgarte regularization consists in calculation of the correction term as weighted average of these solutions according to the formula

$$\zeta_{w_B} = \frac{\zeta_{w0} + 2n\beta h\zeta_{w1} + k^2\beta^2 h^2\zeta_{w2}}{1 + 2n\beta h + k^2\beta^2 h^2}. \quad (3.110)$$

If we choose n and k in accordance with researchers recommendations [74], then the weighted average will be

$$\zeta_{w_O} = \frac{\zeta_{w0} + \sqrt{2}k\beta h\zeta_{w1} + k^2\beta^2 h^2\zeta_{w2}}{1 + \sqrt{2}k\beta h + k^2\beta^2 h^2}. \quad (3.111)$$

Choice of parameters value recommended in paper [3] gives

$$\zeta_{w_D} = \frac{\zeta_{w0} + ST_p\beta\zeta_{w1} + ST_p\beta^2 h\zeta_{w2}}{1 + ST_p\beta + ST_p\beta^2 h}. \quad (3.112)$$

And finally we can compare these results with solution given by the least squares method (LSM) under traditional suppositions about matrix $C^T = \tilde{C}^T = e_3^T C_0^T$:

$$\zeta_{w_D} = \frac{\zeta_{w0} + \zeta_{w1} + \zeta_{w2}}{3}. \quad (3.113)$$

It is clear that when $n = 1/(2\beta h)$ and $n = k/2$ the regularization method according to Baumgarte is equivalent to LSM.

Describing in this chapter some aspects of imitational dynamic anthropomorphic model we aspired to reflect those difficulties and peculiarities which arise in model application. We did not aspire to give the detailed description of all used algorithms and methods and their detailed logic interrelation. We have only stopped at those aspects, which from our view have importance for adequate physical interpretation of results of modeling. In particular these are problems of smoothing of experimental data, description of muscular "drives", of multicriterial optimization and numerical integration of systems of differential-algebraic equations. In the following chapters results of employment of our system of imitational modeling of anthropomorphic mechanisms for the analysis, synthesis and optimization of some human motions are discussed.

CHAPTER 4

ANALYSIS

Experimental data analysis is one of the main tools of adequate mathematical modelling of human motion. Part of this data can be used for calculations reliability control and parametric adjustment of mathematical model (MM). Employment of ramified kinematic chain dynamics equations with constraints as MM can be taken as a basis for solution of the direct, inverse and mixed (direct and inverse problems in combination) problems of dynamics.

Creation of MM of skeletal-muscular apparatus starts, as a rule, from motion video-registration, estimation of model elements velocities and accelerations via video-frames processing. Then follows solution of the direct dynamics problem with an eye to estimate energy-force picture of motion. Such an approach to experimental data analysis is historically accepted. Quality of such analysis essentially depends on quality and quantity of experimental data and researcher expertise in choice of anthropomorphic model (AM) structure. In this chapter there will be considering some examples of such analysis and examples of MM parametric adjustment methodology employment.

4.1 Basic Principles

Development of mathematical model (MM) of skeletal-muscular apparatus (SMA) is based on analysis of data obtained through registration of real motion and following processing of this information. Analysis includes several stages and, as a rule, is an iteration procedure. In previous chapters problems of development of MM reflecting characteristic features of SMA, possible types of its motion, methodology of structural and parametric MM adjustment have been considered. In this chapter we consider several examples of the proposed methodology employed for processing of real experimental data and of synthesized motions data as well.

In the analysis examples there are reflected main features of employment of adequacy criteria of the Eq. (3.39) type. Influence of dynamic components of the criterion on energy-force characteristics of modelled motion is also shown. These examples also prove applicability of criteria of the Eq. (3.39) type. Combination of motion synthesis and the following analysis under various assumptions about synthesized data distortion allows one to come closer to correct formulation of the problem of development of adequacy criteria which allow to solve MM identification (i. e. its structural and parametric adjustment) problem for minimal additional information about the motion.

Before considering calculated results let us name the main varied quantities. Direct motion observation or its video-registration allow to give preliminary estimate number of SMA model elements needed for adequate modelling, which relative motion produces SMA motion as a whole. Hereafter we imply that MM used is a model of system of bodies. The number and position of markers should be predetermined, which coordinates allow to calculate generalized coordinates for each video frame. It is obvious that for various types of motion minimal required number of markers is different. The number of markers is closely linked with the number of freedom degrees of chosen MM.

If videoframes are processed with employment of a computer, it is possible to automate the process of freedom degrees number determination. This can be done, for example, on the basis of criterion Eq. (3.5), if we take for the basis model a system of bodies with redundant number of freedom degrees. Such an approach requires development of automatic markers recognition procedure. Besides, there appears need in large memory for storage of digital information on position of markers for each frame.

It is clear that the number of freedom degrees is one of the main parameters influencing the model adequacy. There certainly exist some upper and lower limits of optimal freedom degrees number, which depend on measurements accuracy and the type of motion modelled. Usually, however, this number is chosen judging from model capabilities (structure of the basis model) and computer resources.

Other important parameters are the number of markers and frames frequency. These parameters depend on the video-registration systems capabilities. Standard frame frequency is about 100 frames per second. Necessary frames frequency depends on maximum values of generalized velocities and accelerations. Estimates of velocities increments allow to determine acceleration values, which, in turn, allow to assess energy-force characteristics of motion. Let us consider, for example, pushing-off phase of the long running jump. Observation time is approximately 0.13 s, maximal values of angular velocities and accelerations of the thigh of the swinging leg are correspondingly 25 rad/s and 300 rad/s²

Empirical estimate of minimal motion registration frequency corresponds to the value of maximal angular acceleration. For pushing-off phase of the long jump at least 30 frames should be shot, which approximately corresponds to frames frequency of 300 rad/s. It is important to note that even motions performed within short period of time can be of significantly heterogenic structure. For example, at the moment of landing in long jump an impact-like interaction of SMA with the ground is observed, which is characterized by a sharp increase of vertical component of the ground impulse. This rapid process of landing takes up about 0.01–0.02 s only. Certainly, investigation of this phase of motion requires increase in the frames shooting frequency to at least 1000 frames per second and more.

Video-registration of motion allows to estimate generalized coordinates behaviour. Numerical differentiation of coordinates allows one to assess generalized velocities and

accelerations. One parameter of numerical differentiation is the weight coefficient in the functional of the Eq. (2.22) type. It is also called the splining parameter. Its direct choice for each generalized coordinate cannot be practically realized because its value influences behaviour of other generalized coordinates and their derivatives as functions of time. Received estimation of generalized velocities and accelerations distribution should yield reliable assessments of such integral characteristics of motion as displacement, velocity and acceleration of the center of mass, increment of moment of momentum, full energy increment.

Special additional measurements for one or several generalized coordinates allow for coordinate-wise decomposition of the numerical differentiation procedure. When creating corresponding universal software, these additional measurements can be taken into account in the functional of the Eq. (3.39) type, analogously to M_1 . Essential corrections in the smoothing procedure for a finite number of measurements can be achieved by estimation of boundary conditions for the smoothing spline. In this case additional information can prove to be especially useful (for example, angular velocity at the boundaries of the observation interval). As it has been noted earlier, the effect of rough boundary conditions setting disappears at the interval of about 5–10 reading points from the boundary, which can prove to be too “expensive” if the frames number is limited.

One more point showing the necessity of boundary conditions setting is that there is a possibility of “appearing of velocities leap” (especially for a low frequency of measurements). In this case motion (for example, the foot landing on the support) is processed by splitting into several observation and analysis intervals. Then, the accuracy of velocities and/or accelerations estimation at the boundaries is very essential. In practice, for increasing of displacements numerical differentiation accuracy we recommend widening of the observation interval. This can be done upon condition that the character of motion remains the same over this interval.

Thus, for example, for the support phase of motion, prolongation of the observation interval over some period of time after taking-off is acceptable, because it does not involve any shock (in contradistinction to landing on the support). All mentioned parameters are connected with assessment of motion kinematics and their choice influences a great deal adequacy of motion description by means of MM.

For MM with given structure and kinematics varied parameters are geometric and mass-inertia characteristics (GMIC). Namely, these are the mass, coordinates of the center of mass and tensor of inertia components for each solid body considered as an element of the SMA. Let us note, that positions of spherical joints are verified at the stage of calculation of generalized coordinates from markers positions. Variation of GMIC within their error margins should be considered as precision increasing procedure, since influence of these errors on the value of the adequacy criterion of the Eq. (3.39) type is essentially less than influence of errors in kinematics. This fact is due to actual noncorrectness of the numerical differentiation procedure.

Let us also note, that GMIC variation (even within their error margin values)

should be carried out under additional condition that the integral mass and moments of inertia (for some fixed SMA position) remain the same. As one of the variants for finding more precise GMIC values, frame by frame minimization procedure can be suggested with criterion of the Eq. (3.39) type followed by averaging of the GMIC values over the whole sample. This approach can prove to be much more effective for a large number of degrees of freedom and processed film frames. It should also be mentioned that for Eq. (3.39) adequacy criterion \underline{R}_c , \hat{R}_c , and \check{R}_c values do not depend on values of tensor of inertia components and, therefore, moments of inertia variation has sense only if $\lambda_7 \neq 0$, or if additional experimental data are available depending on this tensor components values.

Except for the varied parameters mentioned above Eq. (3.39) criterion contains: intervals of nonsensitiveness (t_i) of the criterion items; weighted coefficients λ_i , allowing to receive a weighed sum of different criteria. Analysis and choice of these parameters depends essentially on quality and quantity of additional measurements. It seems *a priori* obvious that for estimation of dynamic characteristics of motion the adequacy criterion should contain components depending on generalized accelerations (for example, $\lambda_i \neq 0$, $i = 5, 6, 7$ for Eq. (3.39)). Analysis examples considered further on prove acceptability of the proposed criterion and its parameters.

Estimation of parameters influence depends essentially on the reliability of additional measurements with respect to which MM identification is carried out. For elimination of influence of errors of this type, let us use results of computer synthesis of goal-oriented motions in supposition that the synthesized motion is distorted by noise. In other words, functional dependencies (displacements) and parameters (GMIC, shooting frequency) are stochastically varied. Obviously, such analysis can be carried out without synthesis problem solution, but in this case, considered motion can prove to be not anthropomorphic or of too simple structure (small number of freedom degrees, inadequate interelement displacements). Therefore, it will be hard to interpret results of such analysis with respect to real motions.

4.2 Analysis of the Synthesized Motion

First, let us consider a 7-element AM which motion kinematics is presented in Fig. 4.1. Modelled GMIC values can be found in Table 4.1.

Motion begins from a half squatting position, toe stand. Motion goal is a jump at a small height of $\Delta h = 0.3$ m. Time before taking off is restricted by $\Delta t = 0.6$ s. It is assumed that there is no friction at the support point, which does not distort dynamics but allows for better kinematics presentation (Fig. 4.1). AM dynamics at the support phase was controlled by the value and form of vertical component of the ground reaction force (R_y), presented in Fig. 4.2. Its horizontal component and interelement ankle moment were set equal to zero ($R_x = 0$, $M_1 = 0$). As a result of synthesis of this goal-oriented motion distribution of interelement moments controlling the motion of the open kinematic loop was received. In Fig. 4.3 graphics

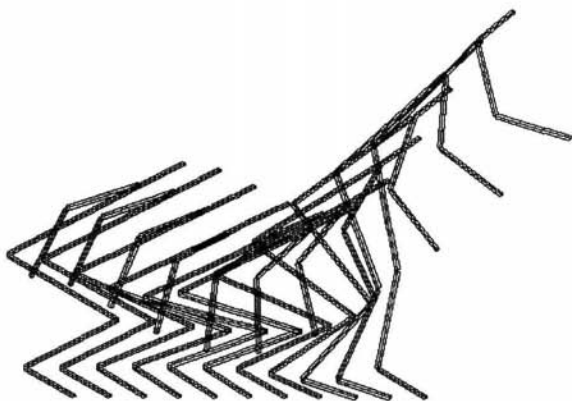


Fig. 4.1. Kinematic scheme of the 7-element model motion (high jump, arms motion is preset beforehand).

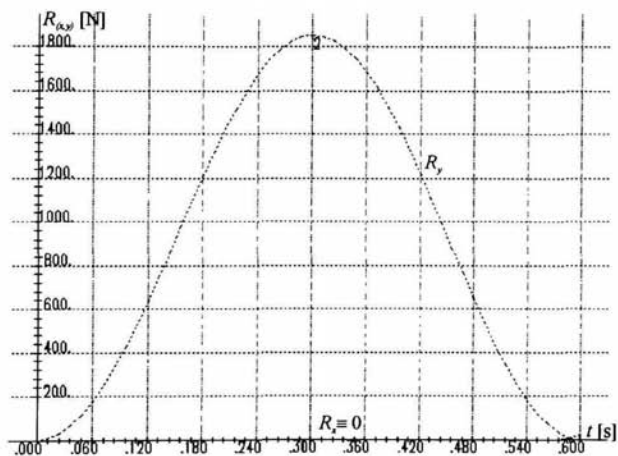


Fig. 4.2. Horizontal (1) and vertical (2) components of the support reaction force.

Table 4.1. 7-element model GMIC distribution (elements numeration from support point: 1-feet, 2-shanks, 3-thighs, 4-trunk, 5-shoulders, 6-forearms, 7-head).

| N link | mass, kg | length, m | a_{1i} , m | a_{2i} , m | J_{ci} , kg·m ² |
|----------|----------|-----------|--------------|--------------|------------------------------|
| 1 | 2.00 | .20 | .14 | .0 | .1 |
| 2 | 5.18 | .36 | .21 | .0 | .26836 |
| 3 | 23.29 | .44 | .27 | .0 | 1.08616 |
| 4 | 34.16 | .52 | .27 | .0 | 3.58974 |
| 5 | 5.37 | .27 | .13 | .0 | .09725 |
| 6 | 4.3 | .27 | .14 | .0 | .03172 |
| 7 | 3.52 | .17 | .17 | .0 | .20627 |

of the shin-ankle (2), knee (3) and hip (4) moments ($M_1 \equiv 0$) are presented. Other moments have considerably smaller amplitudes and do not play principal role for the motion considered.

It is essential to note that initial horizontal position of AM center of mass was $\Delta x_c = -0.01$ m with respect to the support point. Because of absence of horizontal component of the ground reaction, this relative position did not change. As result of this and of zero value of the interelement moment M_1 , moment of momentum increment (k_c increment) with respect to the AM center of mass behaves as it is depicted in Fig. 4.4. This behaviour is in exact correspondence with Eq. (2.53) relations. Positive value of k_c at the moment of push-off is in accordance with the technique of rotational motions with one point of support.

Kinetic energy increment (T_k) is given in Fig. 4.5. Taking into account kinetic energy of horizontal motion of the whole AM with the velocity of $V_{cx} = 2$ m/s, total kinetic energy at the moment of push-off $T_k = 240$ J.

Synthesized motion was used as experimental data for the analysis problem. Joint coordinates data was for test purpose distorted by noise equally distributed in a circle of given radius (~ 0.01) m. Acceleration of the center of mass and data on M_1 were used without "noise" addition as additional "experimental" data for adequacy criterion of the Eq. (3.39) type.

Generalized coordinates with noise and their estimates obtained by means of smoothing splines are given in Fig. 4.6–Fig. 4.8.

As a result of application of parameters of trajectories smoothing optimization procedure when all additional information was used ($\lambda_5, \lambda_6, \lambda_7 \neq 0$ in Eq. (3.39)), distribution of relative angular velocities (Fig. 4.9) and accelerations (Fig. 4.10) was obtained which minimize noise discrepancy caused by the ground reaction and first joint moment.

Final distribution of interelement moments M_1 – M_4 is given in Fig. 4.11. Small oscillations of M_1 about zero practically cannot be eliminated using splines on the whole observation interval because of the integral form of the criterion. Let us note

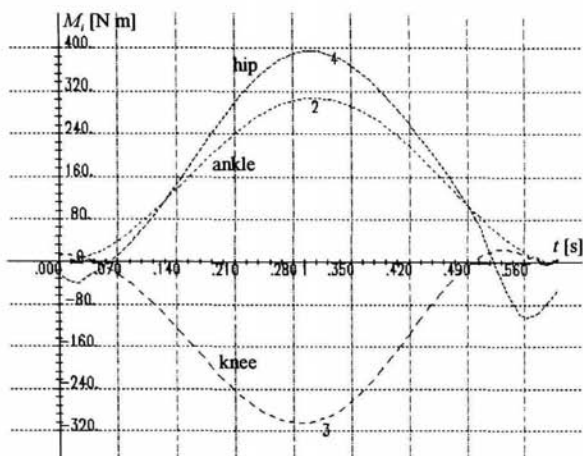


Fig. 4.3. Synthesised ankle (2), knee (3) and thigh (4) moments behaviour.

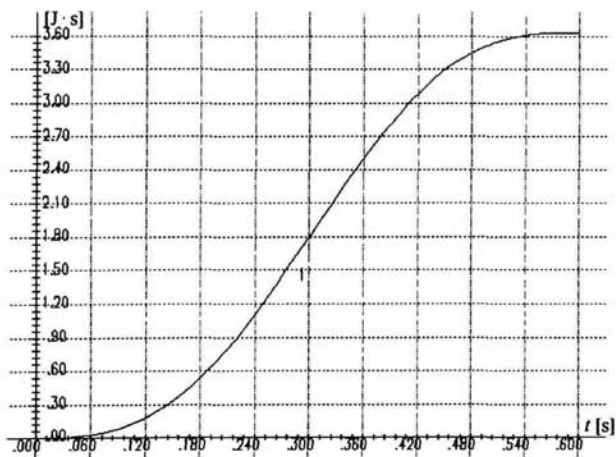


Fig. 4.4. Moment of momentum with respect to the centre of mass.

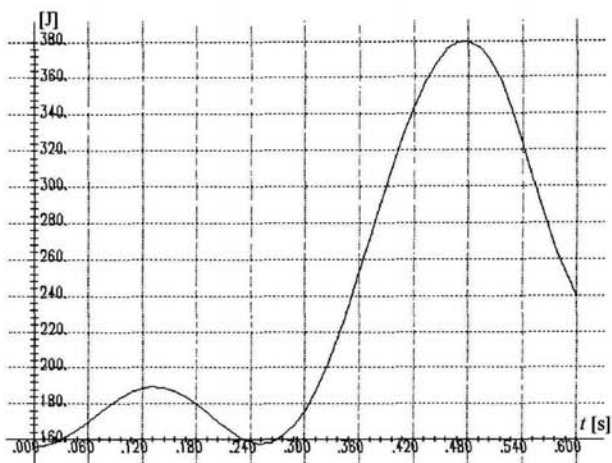


Fig. 4.5. Kinetic energy chart taking into account horizontal component of centre of mass velocity.

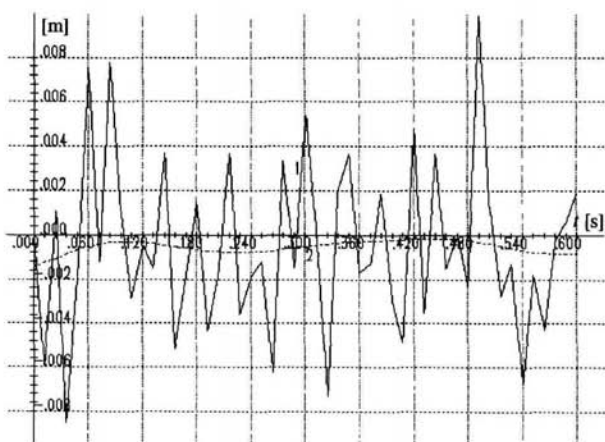


Fig. 4.6. Vertical displacement of the support point (experimental and smoothed curves).

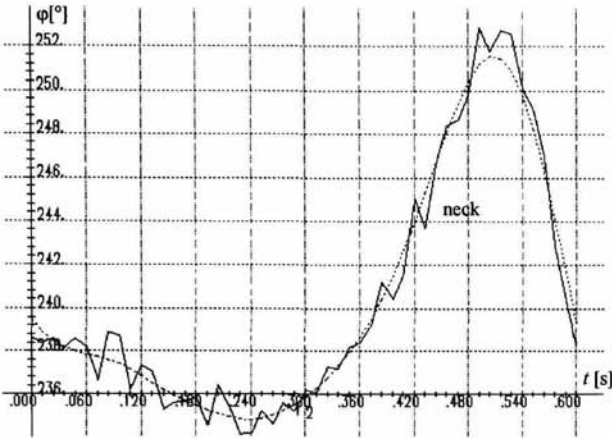


Fig. 4.7. Behaviour of inter-element angle in the neck joint (experimental and smoothed curves).

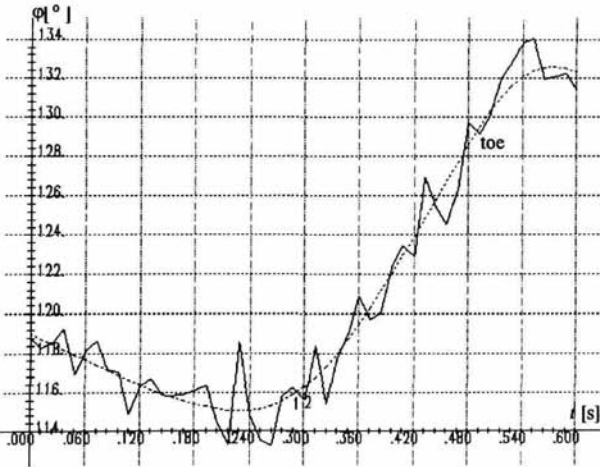


Fig. 4.8. Behaviour of inter-element angle in the first joint (experimental and smoothed curves).

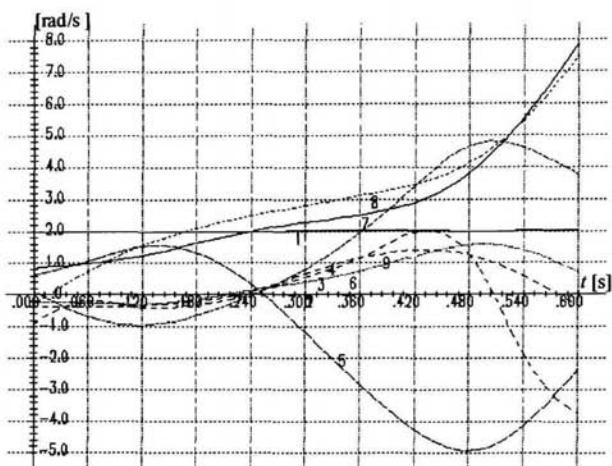


Fig. 4.9. Absolute velocities distribution.

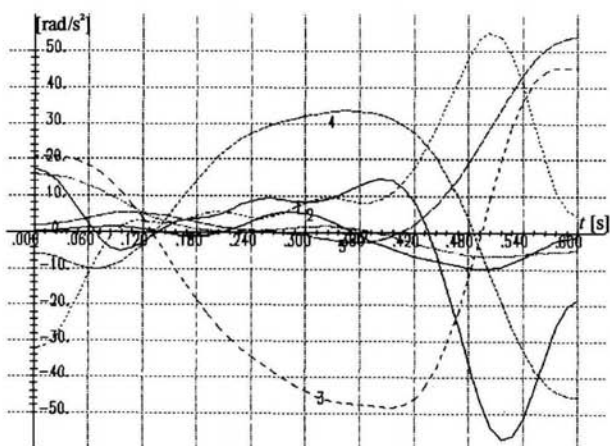


Fig. 4.10. Inter-element angular accelerations distribution.

that for this example 61 points of observation were used which corresponds to frames frequency of 100 frames per second. In order to cope with the boundary effect, it was assumed that generalized accelerations at interval ends are known exactly. Results of this idea application are demonstrated in Fig. 4.11. In Fig. 4.12 we presented interelement moments behaviour without this supposition. Acceleration components of the center of mass are depicted in Fig. 4.13.

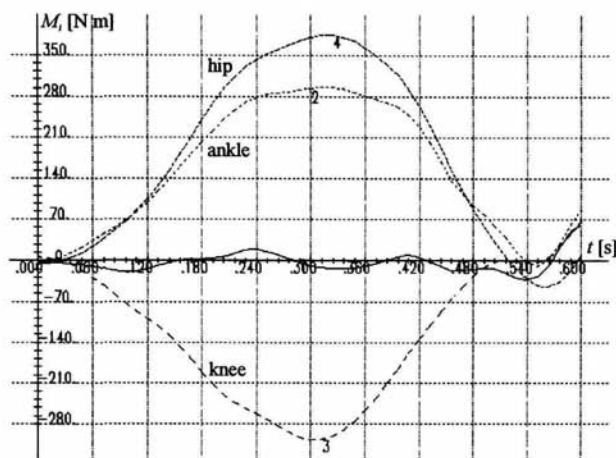


Fig. 4.11. Smoothed inter-element moments ($\lambda_5, \lambda_6, \lambda_7 \neq 0$).

Let us consider now the case of partial or complete elimination of dynamic components from the adequacy criterion. Successively putting λ_i in Eq. (3.39) equal to zero for $i = 7$; $i = \bar{5}, \bar{7}$; $i = \bar{3}, \bar{7}$, we obtain different smoothing procedure results. Characteristic behaviour of the center of mass acceleration is given in Fig. 4.14–Fig. 4.16. Corresponding changes in interelement moments values are reflected in Fig. 4.17–Fig. 4.19.

Analysis of obtained curves shows that attempts to assess energy-force characteristics of motion require inclusion of dynamic components into the adequacy criterion.

For accelerations estimation in examples considered above, double smoothing by means of cubic splines was used. Figure 4.10 reflects smooth character of accelerations behaviour for this method. Second smoothing parameter value can be also varied with an eye to achieve better adequacy. However, this parameter does not significantly influence the adequacy criterion value, so that computer resources required for realization of this idea prove to be too large with respect to the effect obtained. Variation of GMIC, as it was noted above, also allows to improve processing results from the point of view of the adequacy criterion J (Eq. (3.39)), but for the phase

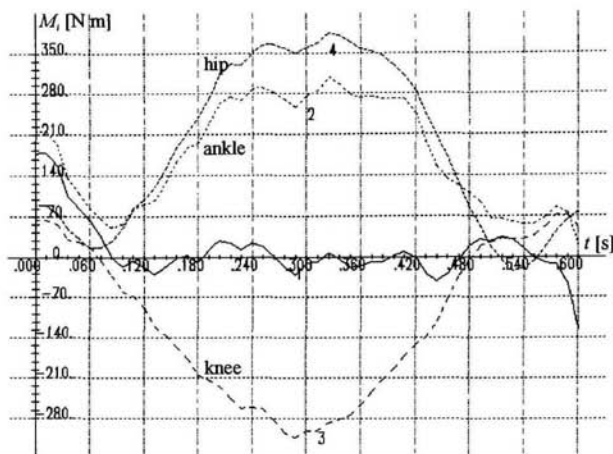


Fig. 4.12. Smoothed inter-element moments ($\lambda_5, \lambda_6, \lambda_7 \neq 0$, boundary angular accelerations are not preset).

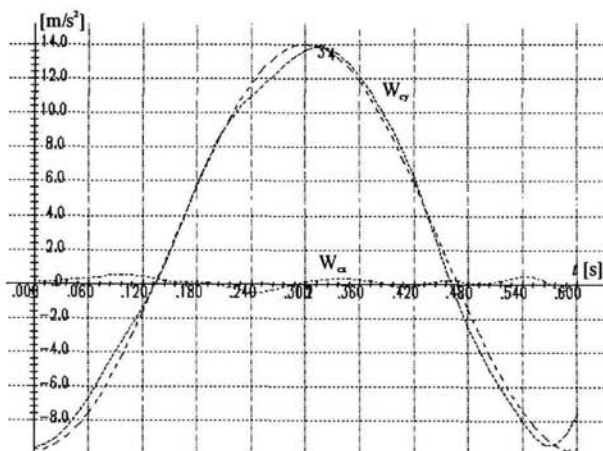


Fig. 4.13. Smoothed centre of mass accelerations ($\lambda_5, \lambda_6, \lambda_7 \neq 0$, boundary angular accelerations are not preset).

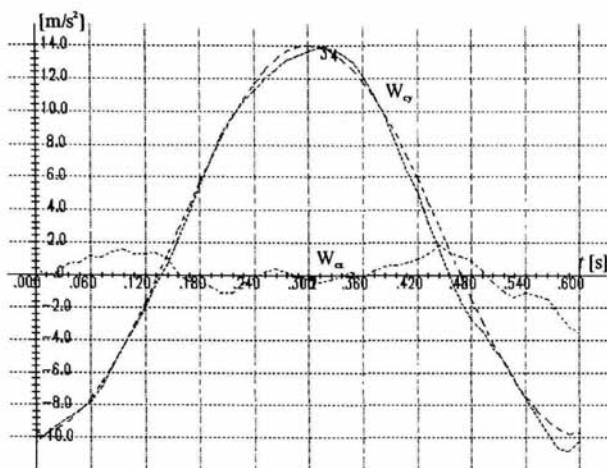


Fig. 4.14. Smoothed centre of mass accelerations ($\lambda_7 = 0$, boundary angular accelerations are not preset).

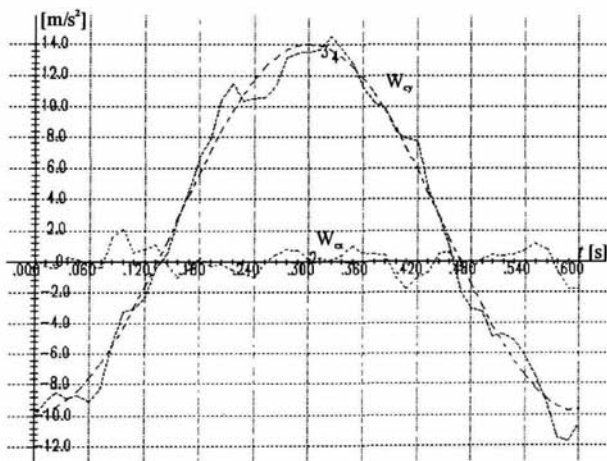


Fig. 4.15. Smoothed centre of mass acceleration components ($\lambda_i = 0$, $i = \overline{5, 7}$, boundary angular accelerations are not preset).

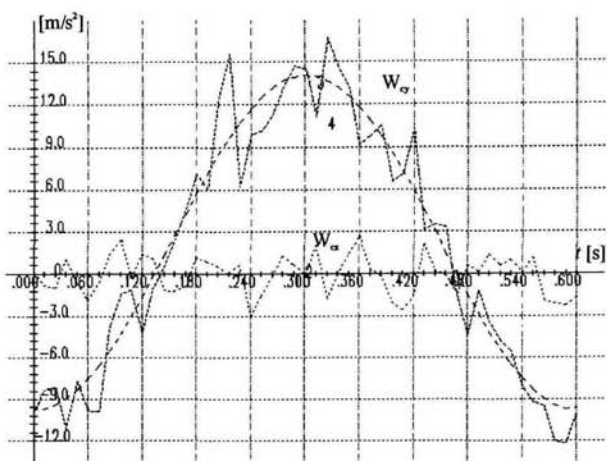


Fig. 4.16. Smoothed centre of mass acceleration components ($\lambda_i = 0$, $i = \overline{3,7}$, boundary angular accelerations are not preset).

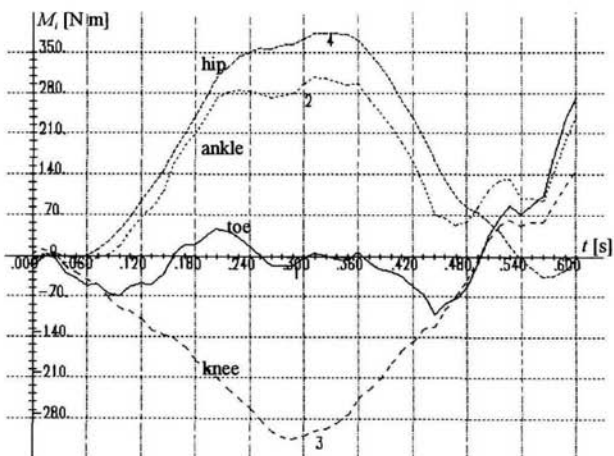


Fig. 4.17. Inter-element moments behaviour ($\lambda_7 = 0$, boundary angular accelerations are not preset).

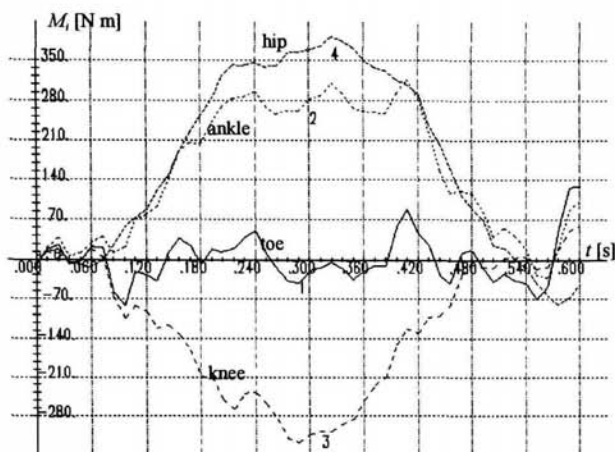


Fig. 4.18. Inter-element moments behaviour ($\lambda_i = 0$, $i = \overline{5,7}$, boundary angular accelerations are not preset).

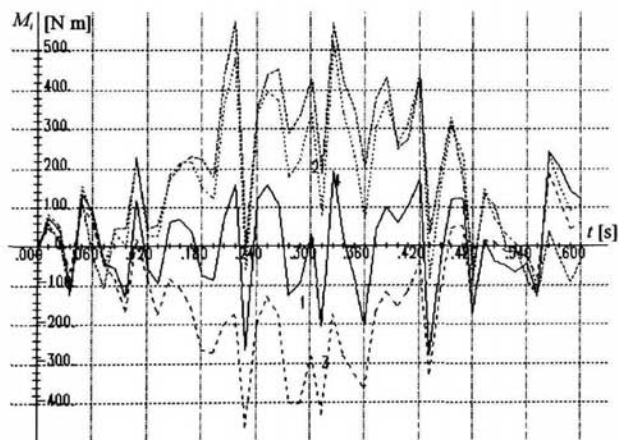


Fig. 4.19. Inter-element moments behaviour ($\lambda_i = 0$, $i = \overline{3,7}$, boundary angular accelerations are not preset).

picture distorted by noise, preliminary determination of kinematic quantities, even for exact GMIC values, does not minimize J value to zero. Further variation of GMIC can lead to decrease in J value with respect to value calculated from exact GMIC data.

Therefore GMIC variation is sensible when these characteristics are known within large error margin. For the example being considered, interelement moments values after GMIC variation are given in Fig. 4.20. Despite decrease of J value, calculation results show significant redistribution of moment maximums with respect to original moments behaviour.

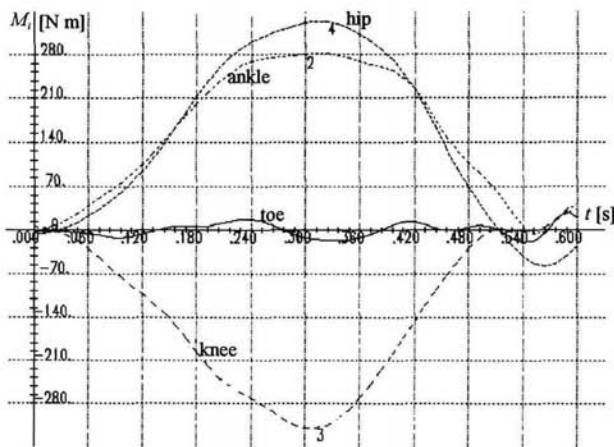


Fig. 4.20. Smoothed inter-element moments after GMIC variation ($\lambda_i = 0$, $i = \overline{3,7}$, boundary accelerations are not set) for 7-element model, arms motion is not preset.

In the considered example influence of different parameters was shown, except for the freedom degrees number (n) and the frequency of motion registration (ν), on computer motion analysis. As for ν variation, it is easy to show that some relative error in this parameter value leads to corresponding relative errors in coordinates values, the influence of which on motion analysis has been already considered.

Variation of n is a much more difficult procedure because it means AM structure variation and, correspondingly, variation of the structure of motion equations system. Increase of n value gives proportional increase in number of parameters which variation allows to improve MM adequacy, but there also appear additional errors, which elimination is our main goal.

We will come back to the question of n variation in the next chapter when we will

be considering synthesis of adequate models, where increase of number of freedom degrees is not linked with additional measurement errors (although numerical calculation errors grow) and, therefore, can be used for improvement of MM adequacy.

In the next example we consider previous model performing similar motion (see Fig. 4.21), but with essentially different form of the ground reaction (Fig. 4.22).

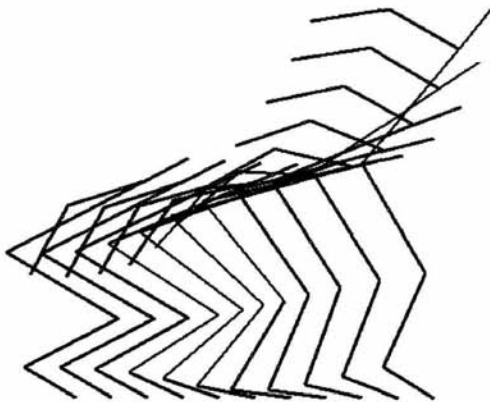


Fig. 4.21. Kinematic scheme of 7-element model motion (high jump; arms motion is not preset).

Sharp leap of vertical component of the ground reaction N_y (under noise distortion with noise level of 0.01 m for joints coordinates) cannot practically be “reconstructed” (modelled) even if accelerations are known without error at the observation interval beginning and end. One of the possible variants of ground reaction behaviour after optimization of smoothing parameters is given in Fig. 4.23.

Behaviour of interelement moments according to analysis results is depicted in Fig. 4.24. Knee moment sign change (with respect to Fig. 4.3) is connected with intensive swing back of arms and with presence of horizontal component of ground reaction. Practical impossibility of “reconstruction” of the sharp leap of the vertical component of the ground reaction is due to relatively low frequency of frames with respect to rapid accelerations change.

4.3 Analysis of a Real Experiment

Let us now consider results of real experimental data processing. This data is obtained via motion video-registration and measurement of the ground reaction with help of

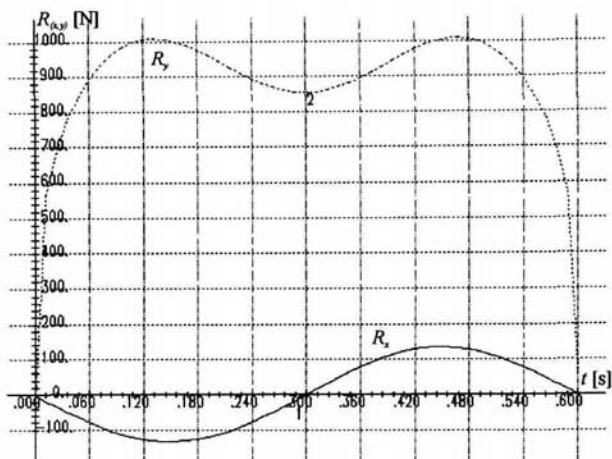


Fig. 4.22. Horizontal (1) and vertical (2) components of the support reaction force.

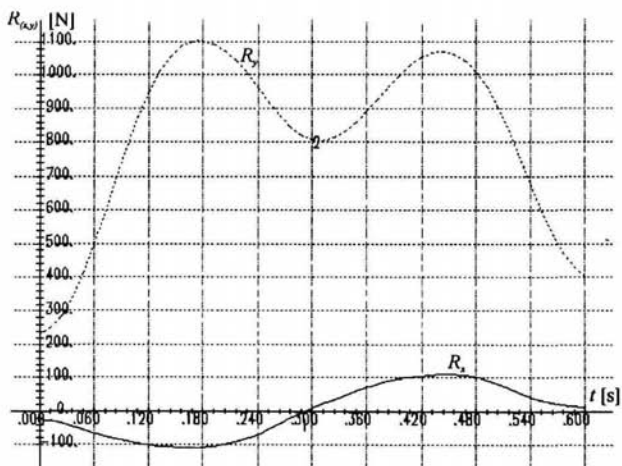


Fig. 4.23. Smoothed horizontal (1) and vertical (2) components of the support reaction force.

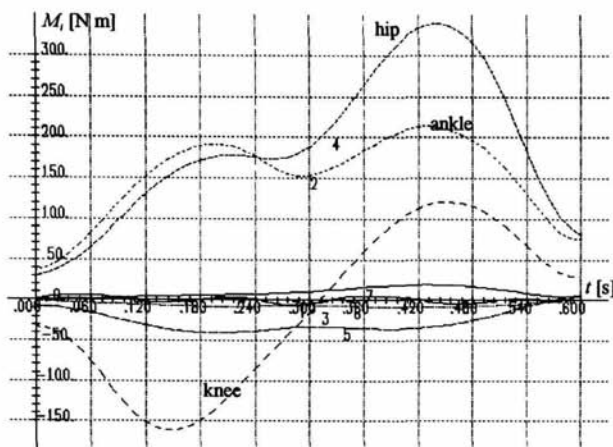


Fig. 4.24. Smoothed inter-element moments behaviour after GMIC variation (boundary angular accelerations are preset).

the force platform. We investigated a jump down from relatively small height onto the force platform with a successive jump upward approximately 0.5 m high. Mass-inertia characteristics of the motion performer (his height was 1.6 m, weight — 60 kg) calculated by means of regressional estimates [102] are given in Table 4.2.

The motion was filmed with frequency of 54 frames per second. Force platform readings were registered with frequency of 250 Hz. As a result of preliminary analysis of relative motion in AM joints, a 6-element model was selected. Its motion kinematics is depicted in Fig. 4.25. Maximal error of coordinates determination was observed for the ankle joint. Charts of experimental and smoothed displacements are given in Fig. 4.26. Among specific features of this motion impact-like interaction of the AM with the support at the moment when the heel touches the ground should be noted. This was registered by the force platform (Fig. 4.27), but was not reflected in the model motion due to low frequency of video-registration. Graphics depicting smoothed behaviour of the center of mass acceleration components are given in Fig. 4.27. Support phase period of motion was about 0.4 s, which corresponds to approximately 22 points of coordinates readings for frames frequency of 54 frames per second.

As a result of optimal smoothing parameters search, distributions of relative angular velocities and accelerations which are depicted in Fig. 4.28 and Fig. 4.29 correspondingly were obtained. Comparison of these charts with previous examples (Fig. 4.9, Fig. 4.10) shows that values of variables are of the same order. Interelement

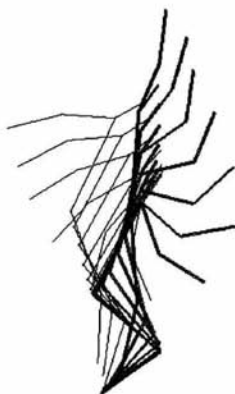


Fig. 4.25. Kinematic scheme of 6-element model motion (high jump, arms motion is not preset).

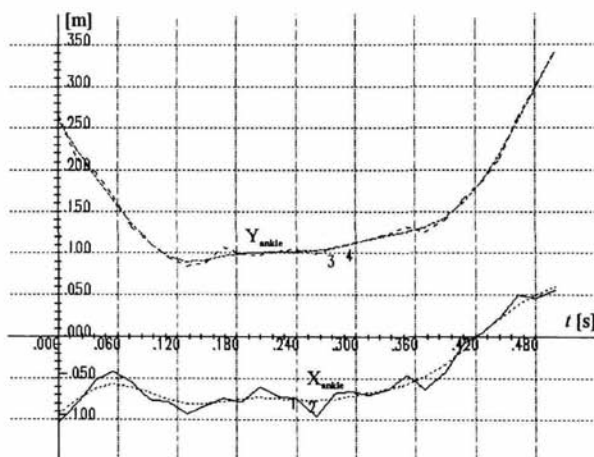


Fig. 4.26. Ankle joint displacement (experimental and smoothed curves).

Table 4.2. 6-element model GMIC distribution (elements numeration from support point: 1-shanks, 2-thighs, 3-trunk, 4-shoulders, 5-forearms, 6-head).

| N element | mass, kg | length, m | a_{1i} , m | a_{2i} , m | J_{ci} , kg·m ² |
|-------------|----------|-----------|--------------|--------------|------------------------------|
| 1 | 7.18 | .36 | .21 | .0 | .26836 |
| 2 | 23.29 | .44 | .27 | .0 | 1.08616 |
| 3 | 34.16 | .52 | .27 | .0 | 3.58974 |
| 4 | 5.37 | .27 | .13 | .0 | .09725 |
| 5 | 4.3 | .27 | .14 | .0 | .03172 |
| 6 | 3.52 | .17 | .17 | .0 | .20627 |

moments behaviour is given in Fig. 4.30 (for the ankle, knee and hip joints).

Qualitative behaviour of moments completely coincides with the one for Fig. 4.3. Greater amplitudes of moments are due to the higher jump upward ($\Delta h \sim 0.2$ m higher), which can be seen from energy losses comparison (1400 J and 800 J correspondingly).

This example is one of the classic experiments allowing to assess possibilities of employment of AM with low number of freedom degrees for estimation of the energy-force picture of real motion. Calculations show that even when there is additional data available accuracy of such estimation is not high because motion registration frequency is limited, which leads to serious errors in velocities and accelerations.

If we also take into account errors in GMIC values, then we finally face necessity of finding of a principally different approach to experimental data analysis. Specifically, we can refuse from direct experimental data processing and use this data, along with possibly other data, for constraint equations in the mixed problem of dynamics (inverse and direct problems in combination) solution. Modelling error problem becomes especially acute when the researcher tries to assess contribution of small solid bodies to general motion. For example, this is the case when we attempt to model AM motion taking into account foot motion (foot can be modelled by one body or a system of solid bodies). Serious errors in measurement of the foot displacement lead to necessity of strong smoothing, which distorts significantly total energy-force picture of motion.

4.4 Analysis of Grand Circles on the Horizontal Bar

Grand circles on the horizontal bar can serve as one of the most speaking examples of small displacements influence. Due to the necessity to differentiate experimental data, attempts to take into account motion of the bar lead to large values of the first interelement moment M_1 (the moment between the palm and the bar). For example, for a 3-element model M_1 can attain a higher value than other joint moments, which is

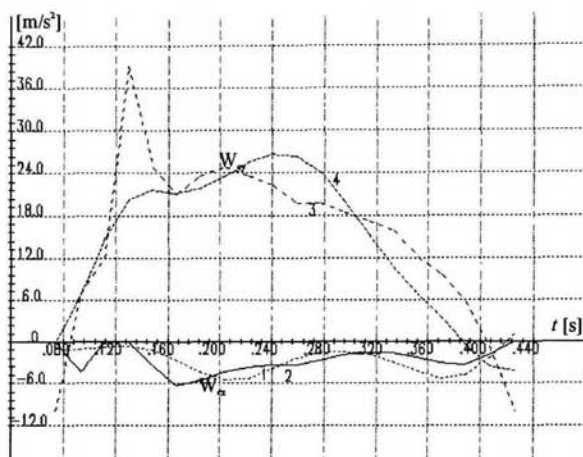


Fig. 4.27. Horizontal (1) and vertical (2) components of the centre of mass acceleration.

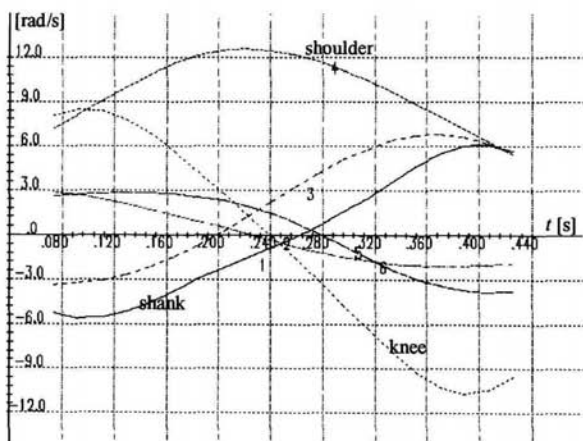


Fig. 4.28. Inter-element angular velocities distribution.

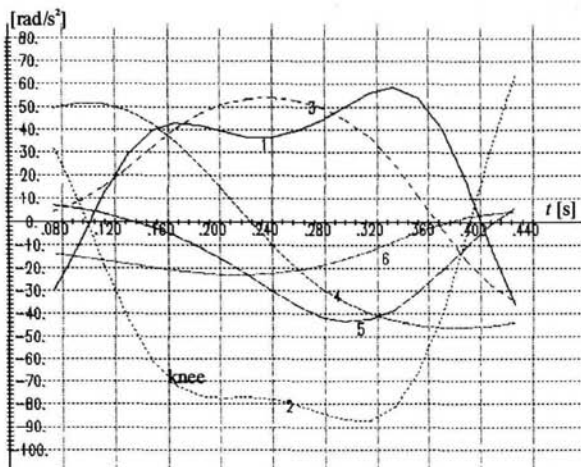


Fig. 4.29. Inter-element angular accelerations distribution.

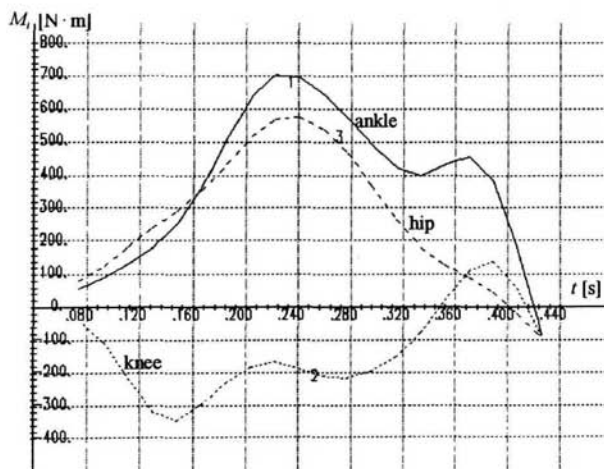


Fig. 4.30. Smoothed inter-element moments after GMIC variation (boundary angular accelerations are preset).

apparently a result of significant errors in determination of the bar position, velocity and acceleration.

The degree of influence of errors in joint coordinates can be investigated analogously to the approach described in the first example of this chapter. Let us also note that absolute error in determination of joints coordinates is of the same order for all joints. However, joint angle value error is in inverse proportion to the distance between the joints, as it is clear from Fig. 4.31.

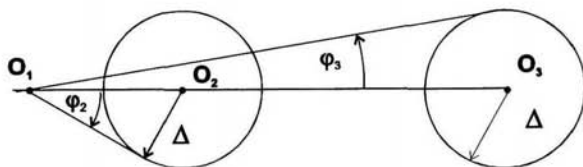


Fig. 4.31. Joint displacements measurements error influence on the joint angle value.

This fact makes clear necessity of construction of AM model from a set of elements with close values of geometric and mass-inertia characteristics. In the example considered below, most interesting is analysis of the bar position error influence on values of interelement moments. As experimental data we used results of backward grand circles synthesis for the 3-element model, which kinematic scheme is presented in Fig. 4.32. Corresponding GMIC can be found in Table 4.4.

Table 4.3. 3-element model GMIC (elements numeration from the horizontal bar: 1-arms, 2-trunk, 3-legs).

| N element | mass, kg | length, m | a_{1i} , m | a_{2i} , m | J_{ci} , kg·m ² |
|-------------|----------|-----------|--------------|--------------|------------------------------|
| 1 | 7.02 | .63 | .39 | .0 | .26126 |
| 2 | 33.24 | .67 | .21 | .0 | 2.08912 |
| 3 | 19.74 | .84 | .35 | .0 | 1.30985 |

Visco-elastic properties of the bar were regulated by linear coefficients of viscosity ($\beta = 500$ N s/m) and elasticity ($C = 18000$ N/m). Synthesis of grand circles was carried out by presetting of the hip joint angular displacement. Synthesized values of interelement moments are presented in Fig. 4.33 (moment $M_1 \equiv 0$). As it

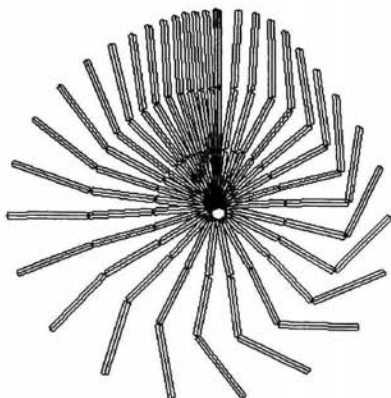


Fig. 4.32. Kinematic scheme of the 3-element model motion (grand circles on the horizontal bar, first circle).

is seen from charts of interelement moments power increment (Fig. 4.34), most significant contribution in kinematic energy increase (Fig. 4.35) is due to the hip joint moment.

Synthesized “accelerating” circle and additional data on the bar reaction force behaviour (Fig. 4.36) were used for testing of the analysis problem solution. It was adopted that joints coordinates data is distorted by equally distributed (within a circle of given diameter) noise. Results of the optimization procedure (for frames frequency of 20 frames per second and noise amplitude approximately equal to 0.006 m) are depicted in Fig. 4.37.

Obviously, these results can be considered satisfactory. However, optimal parameters values have been received for $\lambda_7 \neq 0$ in the adequacy criterion (that means that the value of M_1 was used). If the Eq. (2.47) criterion is used, optimal values of smoothing parameters for $\lambda_7 = 0$ give the best result for the reaction force discrepancy, although, they yield essentially less exact values of interelement moments. As one of the reasons of such nonsatisfactory smoothing we see low frequency of displacements registration (20 frames per second).

An important advantage of the considered analysis example is possibility of variation of “measurements” parameters in order to estimate significance of errors of different parameters groups in calculation of interelement moments. Thus, by GMIC variation it can be seen that their measurement error is about 10 times less “important” than that for velocities and accelerations of given displacements. We also

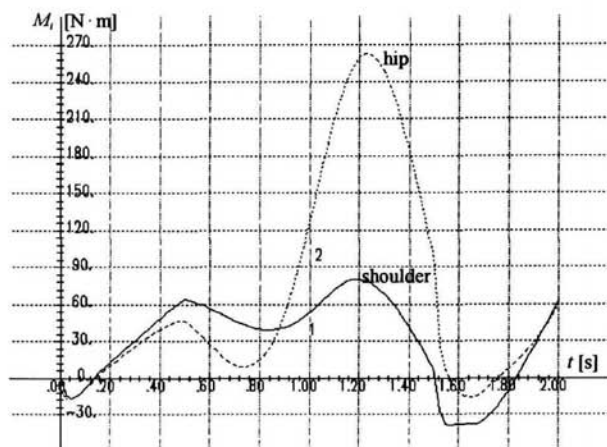


Fig. 4.33. Synthesized inter-element moments behaviour.

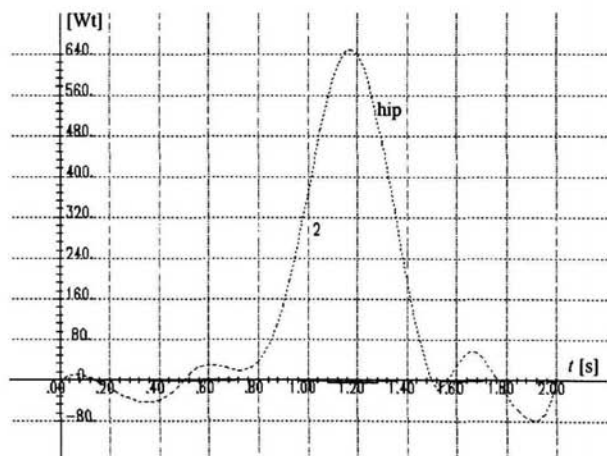


Fig. 4.34. Power of synthesized inter-element moments.

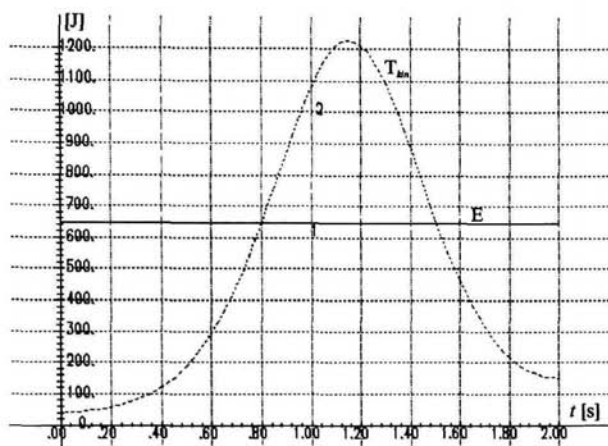


Fig. 4.35. Energy balance and kinetic energy behaviour.

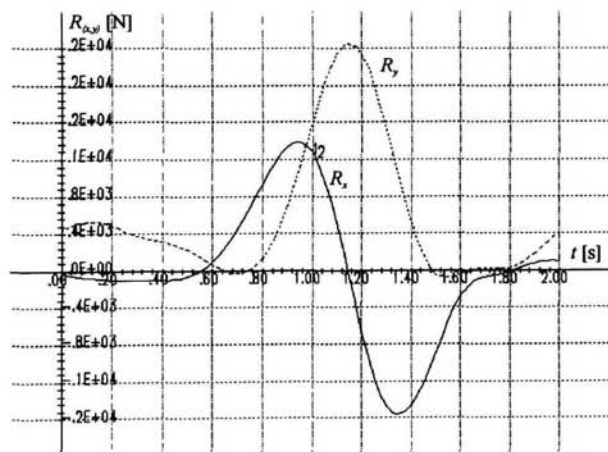


Fig. 4.36. Behaviour of horizontal bar reaction force components.

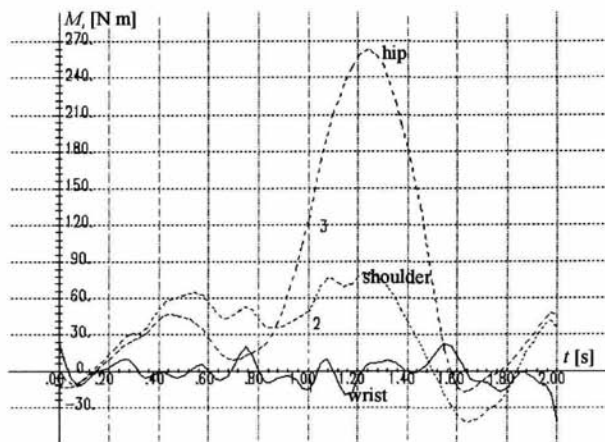


Fig. 4.37. Smoothed inter-element moments.

found out that an essential error in moments calculation is due to nonstability of the registration frequency, which can be easily explained by distortion of the whole kinematic picture.

Most significant errors, as mentioned above, appeared in data on the horizontal bar position. Imitation of such errors can be easily done by increasing the lower boundary for values of smoothing splines parameters for components of the bar displacement. It is important to note that in relative values the bar position change of 0.01 m does not influence significantly the center of mass position. In Fig. 4.38 initial and smoothed values of the bar displacement components are given. Increase of the lower boundaries for smoothing parameters leads to displacement of the bar towards its neutral position (in other words, decrease of the bar displacement along the whole trajectory (Fig. 4.39)). Results of the smoothing procedure, taking into account mentioned above constraints, are presented in Fig. 4.40–Fig. 4.42.

Good coincidence of the initial and modelled center of mass accelerations (see Fig. 4.40) obviously provides for good coincidence of velocities and displacements. In particular, moment of momentum increment k_c (Fig. 4.41) coincides almost exactly with that for the initial nondistorted motion.

In Fig. 4.42 interelement moments as functions of time are presented. They show large amplitude value of the wrist interelement moment ($\max |M_1| \approx 160 \text{ N} \cdot \text{m}$). The amplitude values of M_2 , M_3 almost repeat that of Fig. 4.33.

Let us demonstrate the reason of such essential change in M_1 in contradistinction with $M_1 \equiv 0$ (Fig. 4.33). Directly from the theorem of increment of the moment of

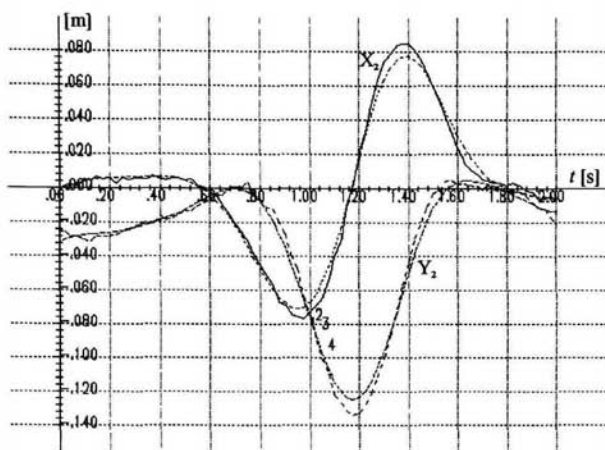


Fig. 4.38. Initial and smoothed behaviour of the bar displacement components (with respect to time variable).

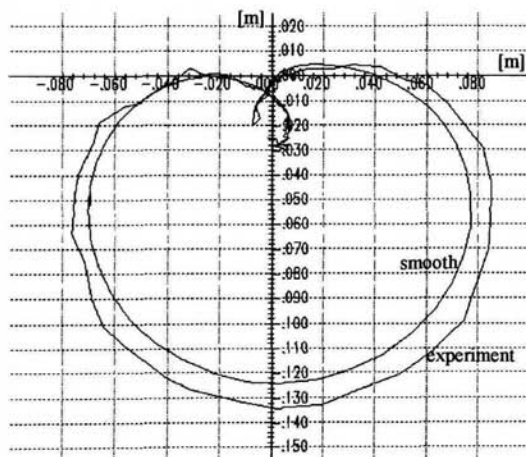


Fig. 4.39. Initial and smoothed horizontal bar trajectory.

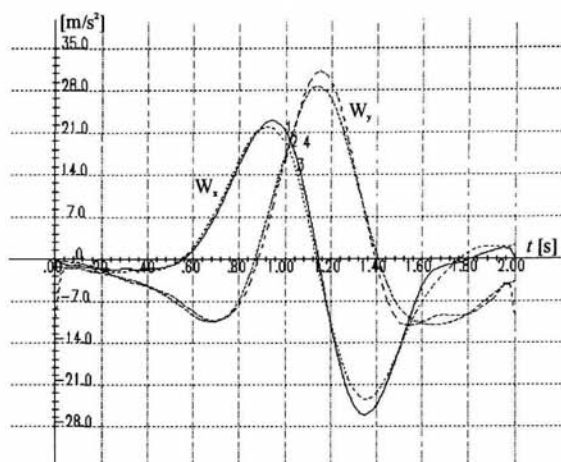


Fig. 4.40. Behaviour of centre of mass acceleration components.

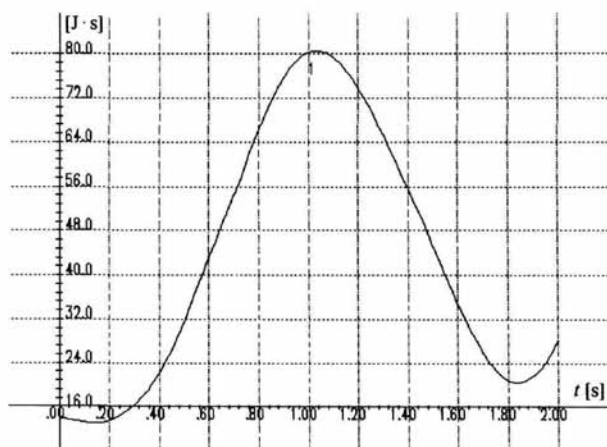


Fig. 4.41. Moment of momentum with respect to the centre of mass.

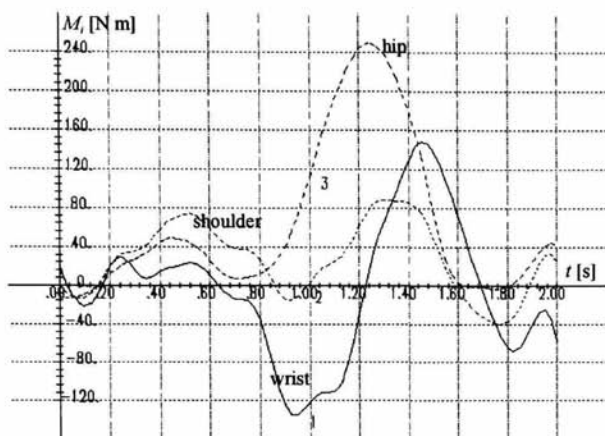


Fig. 4.42. Smoothed inter-element moments behaviour.

momentum with respect to the center of mass Eq. (2.42), taking into account the reaction force \underline{N}_1 and external moment \underline{M}_1 , we have:

$$\underline{M}_1 + (\underline{r}_0 - \underline{R}_c) \times \underline{N}_1 = \dot{\underline{k}}_c, \quad (4.1)$$

where \underline{r}_0 , \underline{R}_c — vectors of the bar position and the AM center of mass, correspondingly. Let $\underline{r}'_0 = \underline{r}_0 + \Delta \underline{r}_0$ — be a new bar position.

Then, supposing that $\underline{N}_1 = -C \underline{r}_0 - \beta \dot{\underline{r}}_0$, where $C = 18000 \text{ N/m}$ we receive: $\beta = 500 \text{ N}\cdot\text{s/m}$, $\underline{N}'_1 = \underline{N}_1 + \Delta \underline{N}_1 = \underline{N}_1 - C \Delta \underline{r}_0$.

Then, directly from Eq. (4.1) we have

$$\underline{M}'_1 - \underline{M}_1 = \Delta \underline{M}_1 = C(\underline{r}_0 - \underline{R}_c) \times \Delta \underline{r}_0. \quad (4.2)$$

Received expression Eq. (4.2) allows one to estimate behaviour of the error in \underline{M}_1 calculation. For the case of planar motion, which is being considered, we have $|\underline{r}_0 - \underline{R}_c| \approx 1 \text{ m}$, $|\Delta \underline{r}_0| \approx 0.01 \text{ m}$. At the moment of $t \approx 1 \text{ s}$ the angle between vectors $(\underline{r}_0 - \underline{R}_c)$ and $\Delta \underline{r}_0$ is approximately equal $3\pi/2$. Therefore \underline{M}_1 projection on the axis z (perpendicular to the motion plane) $M_{1z} \approx -18000 \cdot 1 \cdot 0.01 = -180 \text{ N}\cdot\text{m}$. Change of the interelement moment sign at $t = 1.4 \text{ s}$ corresponds to a new relative position of the vectors under consideration.

Let us also note that from the $\dot{\underline{k}}_c$ behaviour graphic (Fig. 4.41) it follows that at $t = 1 \text{ s}$, $\dot{\underline{k}}_c$ reaches its maximal value. Then, at this moment $\dot{\underline{k}}_c \approx 0$ and error $\Delta \underline{M}_1$ is mostly due to the error in calculation of $\Delta \underline{N}_1 = -C \Delta \underline{r}_0$. The analysis carried

out shows that most significant errors are ones appearing when calculating positions of joints, among which, for one-support phase, essential contribution to the integral error is due to errors in position of the support point determination.

4.5 Some Conclusions

Let us summarize the examples considered above of AM motion experimental data analysis.

Traditional approach to this data processing implies calculation of generalized coordinates from motion videoregistration data for MM with a fixed structure and GMIC. Then follows coordinates differentiation in order to obtain full kinematic picture of motion.

Numerical differentiation is connected with smoothing process and can be carried out for each generalized coordinate independently. However, most reliable smoothing criterion seems to be direct comparison of corresponding calculated and measured quantities.

Obtaining reliable estimates of dynamic motion characteristics requires additional measurements of dynamic quantities or trustable suppositions on their behaviour (as, for example, in supportless phase of motion).

Minimal frequency of motion registration depends on maximal values of AM accelerations increment, i.e. on the third derivative of coordinates.

For a short time series of AM coordinates functions, knowledge of boundary velocities or/and accelerations (or approximation of their values) proved quite useful. This allows to essentially lessen negative boundary effect for approximating splines.

Influence of errors in GMIC values calculation is considerably less significant in comparison with that of errors in determination of markers coordinates, because generalized coordinates are differentiated twice. Differentiation error is in inverse proportion to motion registration frequency.

Maximal error, when calculating interelement (motion controlling) moments, is observed for the external moment value (first interelement moment). It is especially so when there are real external forces applied to MM. These forces values satisfy equation Eq. (4.1) and even a small error (up to 5°) in value of the angle between the vector connecting the center of mass with the support point ($r_0 - \underline{R}_c$) and the vector of the support reaction \underline{N}_1 , leads to a significant error in \underline{M}_1 value.

Mentioned above peculiarities of the problem of analysis of experimental data should be taken into account when working with computer programmes for choice of adequate anthropomorphic model. Most suitable variant of such software creation is reserving of MM of maximum structure complexity. Then follows parametric adjustment of the MM by the criterion of coincidence of main integral (over the observation period) characteristics calculated from model and experimental data. This procedure is carried out for minimal possible number of freedom degrees.

Most resources-requiring blocks of software realizing these ideas are connected

with:

- a) building of smooth approximations of generalized coordinates given in the table form;
- b) solution of the direct dynamics problem for each time point, which is included in the estimation of the MM integral adequacy;
- c) realization of the procedure of multicriteria optimization;
- d) user interface development.

Let us note that upon solution of the analysis problem according to the classical scheme, practically all MM parameters and functions do not coincide with corresponding values of the real AM. This is due to integral character of the adequacy criterion of the Eq. (3.39) type and abundant number of MM parameters with respect to the number of criteria in the multicriteria approach.

In the next chapter we will consider one more possible approach to creation of an adequate AM. It is based on solution of the mixed dynamics problem with non-stationary constraints, which can be formulated on the basis of additional experimental data.

CHAPTER 5

SYNTHESIS

In this chapter main attention is paid to formulation and solution of anthropomorphic mechanisms (AM) motion synthesis problem. Such synthesis can be carried out if we have developed mathematical model (MM) in the form of differential-algebraic motion equations system, which was considered in the previous chapter. Variation of generalized forces, with employment of various forms of external and internal forces and moments parameterization, allows to synthesize required kinematics of AM at several points of time as well as for the whole interval of motion. Proposed approach to AM motion synthesis is based on solution of mixed problem of dynamics. Parameteration of constraint equations allows to discuss ways of goal-oriented motion optimization problem solution.

Employment of kinematic and/or dynamic characteristics of motion for imposition of constraint equations makes possible such parametric MM adjustment which takes into account results of various additional measurements. Considering motion synthesis problem as an iteration of MM identification process we state the necessity of superelement approach to MM structure description. Thus, formulation and solution of AM motion synthesis problem appears to be one of basic elements of a more general problem — MM identification, which the topic this book is mainly devoted to.

5.1 General Points (Fundamentals)

Mathematical modelling of human and animal SMA (skeletal-muscular apparatus) in various biomechanics problems is aimed at solution of motion analysis and synthesis tasks and construction of new anthropomorphic mechanisms. Classical field of MM application is motion analysis, i. e. processing of experimental data obtained through motion videoregistration and, possibly, other additional measurements (data on velocities, accelerations, forces values). This processing allows one to obtain kinematic and energy-force picture of motion which reflects real motion at certain level of adequacy. Choice of the adequacy criterion is usually based on comparison of kinematic and dynamic quantities of common dimension which values are obtained through measurements and calculations.

Presently measurement devices capabilities are essentially widened via employment of computers in experiments proper. Therefore problems concerning use of additional measurements for adequate modelling become topical. Only development

of reliable procedure of complexly coordinated motion synthesis allows to realize a regular approach to formulation of the problem of the best adequacy criterion and choice of MM with minimal number of parameters. Possibility to synthesize AM motion with required kinematic and dynamic characteristics gives all the necessary data for analysis problem or, to be more precise (taking into account varying model structure), identification problem. As soon as a researcher has synthesized certain motion, he can consider the problem of minimization of variety and volume of additional measurements required for development of MM adequately describing real SMA motion.

In this chapter main attention is paid to “technology” of dynamic modelling of human SMA which is intended not only to enable employment of complex MM but also to structurize control so that motion goal would be used directly as control factor. In the simplest case this is programmed motion. In general case MM is a system of differential-algebraic equations, reflecting dynamics of a system of bodies with constraints [54, 101].

Problems of control structurization in biomechanics have common points with principles of control formation in problems of system of bodies dynamics [46, 107]. Consideration of these problems is necessitated by requirement on SMA motion synthesis that constraints on controlled quantities be not only satisfied but also mutually coordinated and realizable through strictly internal (e. g. muscular) control.

Proposed approach to SMA motion control formation will be considered for a MM of general type. We will represent SMA as a system of bodies [101], but it is suggested to employ superelement description of the model structure, i. e. SMA is considered to consist of a set of bodies [101], each of which can itself consist of some other set of bodies and so on. This approach can be realized most easily for two-level model. At the first stage number of elements and their mutual configuration are set in order to reflect main freedom degrees of SMA. Then AM elements are presented as successive kinematic chains of certain form. Examples of systems with such structure will be given in the following sections.

Superelement approach simplifies the process of model initial data formation (preparation) and also allows to employ parametric control under condition of small deformations in “internal” joints of superelements. Besides, if we introduce viscosity and elasticity in these “internal” superelements joints, then we can model elastic behavior of superelements while remaining in the framework of dynamics of solid bodies systems.

One of the possible variants of realization of concentrated in superelements joints visco-elastic properties is to use non-linear (with respect to generalized coordinates) dependency $U_k(q, \dot{q})$

$$U_k(q, \dot{q}) = -\beta_k \dot{q}_k - A_k \tan(d_{1k} q_k + d_{2k}) - d_{3k}, \quad k = \overline{1, n}, \quad (5.1)$$

where coefficients β_k , A_k , d_{1k} , d_{2k} , d_{3k} are chosen in the same way as corresponding coefficients in relation Eq. (3.43).

Different values of the coefficients can be chosen for various AM positions. Relation Eq. (5.1), for example, allows to model visco-elastic character of superelement model contact with external obstacles described as geometric constraints. In particular, human SMA interaction with nonlinear visco-elastic support is described as a set of external forces acting upon AM when a set of points of AM "attempt" to cross geometric line corresponding to support level. If this set of points consists of superelements joints then the character of interaction depends on structure, shape and internal visco-elastic properties of superelements. One of the simplest variants of superelement modelling consists in description of interaction of an elastic rod of given shape with visco-elastic support. Motion equations of general type with non-stationary constraints can be stated as follows:

$$\begin{cases} A(q)\ddot{q} = B(q, \dot{q}, t) + U(q, \dot{q}, t), \\ F(q, t) = 0, \\ G(q, \dot{q}, t) = 0, \end{cases} \quad (5.2)$$

where $q = \{q_1, \dots, q_n\}^T$ — vector-column of generalized coordinates, \dot{q} , \ddot{q} — its derivatives with respect to time; $A(q)$ — $(n \times n)$ — matrix of kinetic energy; $B(q, \dot{q}, t)$ — $(n \times 1)$ — vector-column of inertia items; $F(q, t)$, $G(q, \dot{q}, t)$ — $(m \times 1)$, $(l \times 1)$ — vector-columns, describing holonomic and non-holonomic non-stationary constraints, $U(q, \dot{q}, t)$ — $(n \times 1)$ — vector-column of generalized forces. Method of formation of this column determines capability of motion synthesis process. Let us note that in relation Eq. (5.2) it is implied that via method of multipliers constraint equations enter expression for $U(q, \dot{q}, t)$. Details of this method are given by Wittenburg [101].

Differentiation of constraint equations, calculation of P' — Jacobian matrix of these equations and following solution of system of linear algebraic equations:

$$(P'^T A^{-1} P')\lambda = P'^T A^{-1} B + D(q, \dot{q}, t), \quad (5.3)$$

where $P' = (F'_q, G'_q)^T$ — $(n \times (m+1))$ — Jacobian matrix of constraint equations, $\lambda = (\lambda_1, \dots, \lambda_{m+l})^T$ — vector-column of Lagrange multipliers, allows to deal with linearly-dependent constraints. Solution of the system Eq. (5.3) by means of modernized Gauss method makes necessary calculation of only $\lambda = (\lambda_1, \dots, \lambda_r)^T$ Lagrange multipliers (where $r \leq (l+m)$, if matrix $M = (P'^T A^{-1} P')$ rank is equal to r) because $(m+l-r)$ constraint equations follow from the first r of them. Additive structure of items corresponding to each constraint in expression for $U(q, \dot{q}, t)$ allows to put $\lambda_i = 0$, $i = r+1, m+l$. In relation Eq. (5.3) column $D(q, \dot{q}, t)$ is of $(m+l)$ dimension. This vector-column consists of items which do not depend explicitly on \ddot{q} . It is obvious that D can be divided into 2 items as follows

$$D(q, \dot{q}, t) = D_1(q, \dot{q}) + D_2(t), \quad (5.4)$$

where $D_2(t)$ corresponds to program motion with respect to various freedom degrees, as well as combination of such program motions intended for realization of some motion goal.

Let us return to the discussion on item $U(q, \dot{q}, t)$ in relation Eq. (5.2). Inverse problem of dynamics solution requires that U be of the form $U = U_1(t)$. Parametric control of SMA model via selection of characteristics of springs and dampers in joints, in its turn, requires that U be of the form $U = U_2(q, \dot{q})$. And, finally, non-stationarity of constraint equations actually requires that equation $U = U_3 = -P'\lambda$ be satisfied, where λ is calculated from Eq. (5.3) for each moment of time t , that is $\lambda = \lambda(q, \dot{q}, t)$. Thus, structure of generalized forces column $U(q, \dot{q}, t)$ should be as follows:

$$U(q, \dot{q}, t) = U_1(t) + U_2(q, \dot{q}) - P'\lambda(q, \dot{q}, t). \quad (5.5)$$

Solution of the direct problem of dynamics (analysis problem) yields U only as $U(t)$. Any further steps can be done if we take certain hypothesis on $U(t)$ structure. In particular, it can be of such structure as in Eq. (5.1) or Eq. (5.5). However, reliability of the hypothesis can be checked only if there are made additional measurements of quantities being calculated.

Let us consider in more detail the third item in Eq. (5.5). Modeling of certain motion with use of non-stationary feed-back allows us to formulate a problem of synthesis in a space of geometric and kinematic of parameters, which are more natural for the researcher. From analytical mechanics point of view we are speaking of solution of the mixed problem of dynamics. Most universal approach to its solution is to write down desired (program) motion in the form of constraint equations and then to solve differential-algebraic system of equations. Peculiar feature of human motion is that SMA transition is performed only by means of internal control. Therefore, for motion synthesis it is required not only to write down kinematic constraint equations but also to solve them jointly with equations of dynamics theorems of SMA motion.

As result of differentiation of constraint equations we obtain a system of differential equations of the second order (additional to system Eq. (5.2)). According to this method let us link up to Eq. (5.2) theorem of center of mass motion and theorem of moment of momentum increment written for the whole SMA and for any set of its elements. This will allow to obtain synthesized motion with desired behaviour of ground reaction and/or external with respect to SMA moment (e. g. we may require that this moment be equal to zero).

Employment of this approach to synthesis of supportless phases of motion will thus imply that along with kinematic non-stationary constraint equations, we should write (as additional constraints) theorems of center of mass motion and moment of momentum preservation. In this case among possible realizations of certain kinematics, the one which can be performed only by means of "internal" control will be chosen.

In conclusion, let us underline importance of non-stationary items in constraint equations of Eq. (5.2) type. It is due to the non-stationarity that there appears possibility to synthesize motion with required ground reaction behaviour and/or relative displacements of selected SMA points. This motion can be dynamically corrected, i. e. motion goal can be changed during motion.

The proposed approach to motion synthesis does not require pre-setting of generalized forces values (for example, interelement moments) which allows to increase number of freedom degrees and vary SMA structure. Thus we obtain a number of sets of test problems used in identification algorithm of analysis problems.

In the next section we will consider examples of various non-stationary constraints.

5.2 Typical Non-Stationary Constraints

Before we start considering typical constraint equations that were used for synthesis of most number of motions, let us give some useful formula allowing for direct realization of non-stationary item $D_2(t)$ in Eq. (5.4). Realization of a preset absolute or relative displacement is often described by only boundary conditions on initial ($t = 0$) and final ($t = T$) displacements and velocities (x_0, v_0, x_T, v_T — correspondingly). When investigating periodical motions for variation parameter, oscillation amplitude (x_*) or position of a generalized coordinate at given time point (for example, $x(\frac{T}{2}) = x_0 + x_*$) can be taken. For realization of conditions mentioned above in form of time function a polynomial function of the 4-th order can be suggested:

$$x(t) = at^4 + bt^3 + ct^2 + v_0t + x_0, \quad (5.6)$$

where a, b, c — coefficients depending on above mentioned parameters $T, x_0, v_0, x_T, v_T, x_*$. Differentiating of function Eq. (5.6) with respect to time variable t and taking into account of additional boundary conditions will yield

$$\begin{aligned} aT^4 + bT^3 + cT^2 &= d_1, \\ 4aT^3 + 3bT^2 + 2cT &= d_2, \\ aT^4 + 2bT^3 + 4cT^2 &= 16d_3, \end{aligned} \quad (5.7)$$

where $d_1 = x_T - x_0 - v_0T$, $d_2 = v_T - v_0$ and $d_3 = x_* - v_0\frac{T}{2}$. Solution of the system of linear algebraic equations Eq. (5.7) gives the following formula

$$\begin{aligned} a &= (-8d_1 + 2Td_2 + 16d_3)/T^4, \\ b &= (14d_1 - 3Td_2 - 32d_3)/T^3, \\ c &= (-5d_1 + Td_2 + 16d_3)/T^2. \end{aligned} \quad (5.8)$$

In particular, if $v_0 = v_T$ and $x_* = (x_T - x_0)/2$, but $x_0 \neq x_T$ then $a = 0$. This means that $\ddot{x}(t) = 6bt + 2c$. It can be seen that acceleration is, in this case, a linear function of time and

$$T^3b = -2(x_T - x_0) + 2Tv_0, \quad T^2c = 3(x_T - x_0) - 3Tv_0. \quad (5.9)$$

In another example of start-stop motion (periodical with respect to position and velocity) we have $x_0 = x_T$, $v_0 = v_T = 0$, but $x_* \neq 0$, and therefore

$$T^4 a = 16x_*, \quad T^3 b = -32x_*, \quad T^2 c = 16x_*. \quad (5.10)$$

Then acceleration can be written as follows $\ddot{x}(t) = 32x_*(6t(t-T) + T^2)/T^4$

In case of a less number of parameters, for example, if x_* is not known, Eq. (5.8) take a simpler form, and, omitting several relations, we will have

$$\begin{aligned} a &= 0, \\ -T^3 b &= 2(x_T - x_0) - T(v_T + v_0), \\ -T^2 c &= -3(x_T - x_0) + T(v_T + 2v_0). \end{aligned} \quad (5.11)$$

Linear dependence of accelerations on time in Eq. (5.9) and Eq. (5.11) allows for realization of typical start-stop trajectories. However, when modelling some complex motions by a combination of start-stop trajectories there appear disruption points in acceleration functions at points of different trajectories linking (with respect to displacements and velocities). There are no conditions of accelerations continuity directly in Eq. (5.8). However, it is possible to provide for their continuity by use of parameter x_* , which for given $\ddot{x}(0)$ can be determined from the following relation

$$16x_* = 0.5T^2 \ddot{x}(0) + 5(x_T - x_0) - T(v_T - v_0) + 3v_0 T, \quad (5.12)$$

which can be received directly from the formula for coefficient c in Eq. (5.8), taking into account definitions introduced in Eq. (5.7). Substituting Eq. (5.12) in formula for coefficients a , b we receive polynomial coefficients values, providing for acceleration continuity when modelling trajectories are characterized by a set of parameters.

The relations given above are very useful for synthesis of complex motions employing a consequence of fixed coordinates and velocities values at fixed time moments. Meanwhile, acceleration values are usually not set. However, for motion smoothness it is necessary to have continuous accelerations at trajectories linking points. As generalization of relations considered, polynomial spline approximations can be employed. However, for large number of equations the data volume needed for approximation essentially grows.

Polynomial character of non-stationarity for trajectories described above can obviously be enriched by other nonlinear functions if we take into consideration, for example, nonlinear behaviour of the ground reaction and/or controlling moments. Thus for description of ground reaction behaviour there, for example, can be used following functions

$$\begin{aligned} R_x(t) &= A_x \cdot A_1 \cdot \sin(\alpha_x 2\pi t/T), \\ R_y(t) &= A_1((4t(T-t)/T^2)^{\alpha_1} - A_2(4t(T-t)/T^2)^{\alpha_2}). \end{aligned} \quad (5.13)$$

By choosing different combinations of parameters $A_1, A_x, \alpha_1, \alpha_2, \alpha_x$ values one can receive a wide diapason of possible variations in the ground reaction behaviour. In particular, ground reaction function R_y , characterized by two peaks (which is typical for walking, running, jumps etc.) can be received. Obviously, if measurements of the variable being modelled is available, in the table form, one should employ spline approximation method or some nonlinear regression estimation algorithm. For example, for this purpose least square method can be used, which realization details can be based on the minimization procedure described in the third chapter. Some concrete examples of non-stationarity will be analyzed further on.

Let us now describe several variants of constraint equations for the AM from Sec. 2.6. One of the simplests variants is based on programming of motion for every generalized coordinate or closed set of coordinates. The "closed set" term implies that the number of constraint equations is equal to the number of coordinates present in them. Let us show how such type of constraint equations will influence general equations Eq. (5.2) and Eq. (5.3).

With no harm to generality let us assume that m constraints are imposed on first m generalized coordinates. Otherwise, the coordinates can be renumerated. Then we can rewrite Eq. (5.2) as follows

$$\begin{pmatrix} A_m & c \\ c^T & A_{n-m} \end{pmatrix} \begin{pmatrix} \ddot{q}_m \\ \ddot{q}_{n-m} \end{pmatrix} = \begin{pmatrix} B_m \\ B_{n-m} \end{pmatrix} + \begin{pmatrix} F_{q_m} \\ \emptyset_{n-m} \end{pmatrix} (\lambda_m), \quad (5.14)$$

$$F_{q_m}^T \ddot{q}_m = D_m,$$

where F_{q_m} — $(m \times m)$ non-singular Jacobian matrix of constraint equations; \emptyset_{n-m} — zero column of length $(n - m)$. According to general methodology of taking into account of constraint equations, let us transform first m motion and constraint equations in Eq. (5.14)

$$\ddot{q}_m = A_m^{-1}(B_m - c\ddot{q}_{n-m} + F_{q_m}\lambda_m), \quad (5.15)$$

$$F_{q_m}^T A_m^{-1}(B_m - c\ddot{q}_{n-m} + F_{q_m}\lambda_m) = D_m.$$

From which we receive the following formula for λ_m

$$\lambda_m = (F_{q_m}^T A_m^{-1} F_{q_m})^{-1} (D_m - F_{q_m}^T A_m^{-1} (B_m - c\ddot{q}_{n-m})).$$

Then, taking into account that F_{q_m} is a square, non-singular matrix we can write: $(F_{q_m}^T A_m^{-1} F_{q_m})^{-1} = F_{q_m}^{-1} A_m F_{q_m}^{-T}$. And, therefore, substituting λ_m in first m equations of Eq. (5.15) we shall have $\ddot{q}_m = F_{q_m}^{-T} D_m$.

Thus, having employed general technology of constraint equations utilization, we obtained that programmed motion along q_m coordinates will take place. This motion corresponds to the following "closed" system of constraint equations: $F_{q_m}^T \ddot{q}_m = D_m$. In particular, for $m = n$ we receive solution of the direct dynamics problem upon condition that $F_{q_n} = \text{diag}(\alpha_i)$ or $F_{q_n} = E_n$, (F_{q_n} is a diagonal or unit matrix). In

particular most simple type of constraint equations $f_i = q_i - \tilde{q}_i(t) = 0$, where $\tilde{q}_i(t)$ — is programmed motion along coordinate number i , is characterized by diagonal form of F_{qm} .

For the AM considered in paragraph 2.5 for generalized coordinates absolute elements rotation angles $q_i = \varphi_i$ were taken. If desired interelement angles behaviour is given, constraint equations take the following form $\psi_k - \tilde{\psi}_k(t) = 0$ or $\varphi_k - \varphi_{\nu_k} - \tilde{\psi}_k(t) = 0$, where ν_k — is a component of structure vector, containing information on elements linking order. Thus, as a good generalization constraint equations, containing linear combinations of generalized coordinates can be considered:

$$\varphi_k - \alpha_k \varphi_{\nu_k} - \tilde{\psi}_k(t) = 0, \quad (5.16)$$

where $\alpha_k \geq 0$ — parameter determining fixed increment of interelement ($\alpha_k = 1$) or absolute ($\alpha_k = 0$) rotation angle of element number k .

Behaviour of generalized coordinates as functions of time is, as a rule, known for relatively simple models of human SMA. The most general case is when absolute or relative motion of certain AM points, for example, its joints is preset. If the number of freedom degrees is large, then a researcher can introduce fictitious elements in MM, which makes possible to control motion of any AM point under supposition that it is a joint point. Thus, constraint equations in form of linear combinations of joints coordinates allow to realize desired kinematics of AM arbitrary point.

In particular, for two arbitrary joints with corresponding numbers k and j , vector constraint equation is:

$$\underline{R}_k - \alpha_k \underline{R}_j - \underline{R}_k^0(t) = 0, \quad (5.17)$$

where $\underline{R}_k, \underline{R}_j$ — radius-vectors of joints k and j ; $\alpha_k \geq 0$ — parameter, used analogously to the parameter in relation Eq. (5.16), $\underline{R}_k^0(t)$ — non-stationary item, which actually corresponds to desired motion. For planar model with cylindrical joints (see Sec. 2.4) we can write:

$$\underline{R}_i = \underline{r}_0 + \sum_{k=1}^i \mu_{ik} \underline{r}_i. \quad (5.18)$$

Taking derivative of constraint Eq. (5.17) twice and taking into account Eq. (5.18) we obtain

$$\ddot{\underline{r}}_0(1 - \alpha_k) + \sum_{i=1}^k \mu_{ki} \ddot{\underline{r}}_i - \alpha_k \sum_{i=1}^j \mu_{ji} \ddot{\underline{r}}_i - \ddot{\underline{R}}_k^0(t) = 0. \quad (5.19)$$

If we use generalized coordinates $x_0, y_0, \varphi_i, i = \overline{1, n}$ then $\underline{r}_0 = x_0 \underline{i}_x + y_0 \underline{i}_y$, $\underline{r}_i = l_i(\sin \varphi_i \underline{i}_x - \cos \varphi_i \underline{i}_y)$, where $\underline{i}_x, \underline{i}_y$ — unit vectors of absolute (inertial) basis. Differentiation in this case gives:

$$\begin{aligned}\ddot{\mathbf{r}}_0 &= \ddot{x}_0 \dot{i}_x + \ddot{y}_0 \dot{i}_y, \quad \ddot{\mathbf{R}}_k^0 = \ddot{x}_k^0(t) \dot{i}_x + \ddot{y}_k^0(t) \dot{i}_y, \\ \ddot{\mathbf{r}}_i &= l_i ((-\sin \varphi_i \dot{\varphi}_i^2 + \cos \varphi_i \ddot{\varphi}_i) \dot{i}_x + (\cos \varphi_i \dot{\varphi}_i^2 + \sin \varphi_i \ddot{\varphi}_i) \dot{i}_y).\end{aligned}\quad (5.20)$$

Substituting expressions from Eq. (5.20) directly into Eq. (5.19) we obtain projections of differentiated constraint equation onto unit vectors of inertial basis (\dot{i}_x, \dot{i}_y):

$$\begin{aligned}\ddot{x}_0(1 - \alpha_k) + \sum_{i=1}^k \mu_{ki} l_i \cos \varphi_i \ddot{\varphi}_i - \alpha_k \sum_{i=1}^j \mu_{ji} l_i \cos \varphi_i \ddot{\varphi}_i &= D_{kx}(t, \varphi, \dot{\varphi}), \\ \ddot{y}_0(1 - \alpha_k) + \sum_{i=1}^k \mu_{ki} l_i \sin \varphi_i \ddot{\varphi}_i - \alpha_k \sum_{i=1}^j \mu_{ji} l_i \sin \varphi_i \ddot{\varphi}_i &= D_{ky}(t, \varphi, \dot{\varphi}),\end{aligned}\quad (5.21)$$

where D_{kx}, D_{ky} — functions of time, generalized coordinates and velocities (see also Eq. (5.4)), which contain all items which did not enter the left part of differentiated constraint equations — Eq. (5.21). Rectangular Jacobian matrix of dimension $(2 \times (n + 2))$ contains elements which can be taken directly from Eq. (5.21) — these are factors which generalized accelerations ($\ddot{x}_0, \ddot{y}_0, \ddot{\varphi}_i, i = \overline{1, n}$) are multiplied by.

Jacobian formation can be most conveniently realized algorithmically via successive accumulation of algebraic sums of components, which corresponds to summing over k and j indexes. Such algorithmic approach allows to easily handle arbitrary linear combination of joints coordinates:

$$\sum_{i=1}^n \alpha_{ki} \ddot{R}_i - \ddot{R}_k^0(t) = 0, \quad k \leq n. \quad (5.22)$$

Here $\alpha_{ki} \geq 0$ — components of a rectangular matrix. In particular, for $\ddot{R}_k^0 \equiv 0$, $k = \overline{1, n}$ and $\{\alpha_{ki}\} = \text{diag}\{\alpha_{ii}\}$, that is in case of diagonal form of this matrix, it is assumed that if $\alpha_{ii} \neq 0$, then the position of corresponding joint with radius-vector \mathbf{R}_i is fixed.

Let us consider one essential aspect concerning constraint equations. It is obvious that even for such relatively simple forms of constraint equations as Eq. (5.14), Eq. (5.17) and Eq. (5.22) degeneracy of constraint equations and/or their incompatibility can occur. Degeneracy of constraint equations can be caused by, for example, linear dependency of some constraint equations.

One of the ways to handle such a situation was considered above. Much more difficult to handle is the case when constraint equations are mutually incompatible with kinematic capabilities of MM. As an example, we can consider the situation when $\ddot{R}_k^0(t)$ sets joint position out of AM reaching zone. This situation practically cannot be predicted beforehand. Thus, there appears necessity to introduce in the software an additional block which would allow one to analyze whether constraint equations are solvable or not. If the system of constraints is not solvable those which impede motion realization should be dynamically eliminated.

As a sign that system of constraint equations is incompatible it can serve “end-less” decreasing of integration step in the procedure of numerical integration of motion equations together with the constraint equations. In particular, geometric incompatibility of constraints makes it impossible to carry out numerical integration. Dynamic incompatibility (which, as a rule, is observed in some vicinity of the points of geometric incompatibility) shows itself in sharp decreases and increases in velocities and acceleration values which requires periodic check of their values with respect to maximal and minimal allowable values, especially if procedure of numerical integration is relatively slow.

Special cases of geometric and dynamic incompatibility of constraint equations are due to writing these equations directly in differentiated form, for example, in form of motion equations corresponding to general theorems of dynamics of the whole system and/or its subset. In this case energy expenditures of AM necessary for realization of desired change of external forces and moments (taking into account AM current configuration and elements velocities distribution) can serve as motion realizability criterion.

Let us further consider some variants of constraint equations in differential form. Directly from theorems of center of mass motion and increment of moment of momentum with respect to radius-vector r_0 (named support point) we obtain:

$$\begin{aligned} (\ddot{\underline{R}}_c - \underline{g})M^c - \underline{N}_1 &= 0, \\ \dot{\underline{K}}'' - M^c(\underline{R}_c - r_0) \times (\underline{g} - \ddot{r}_0) - \underline{M}_1 &= 0. \end{aligned} \quad (5.23)$$

Relations in Eq. (5.23) contain nomenclature used in derivation of Eq. (2.39) under supposition that there is only one external force \underline{N}_1 (support reaction) and one external moment \underline{M}_1 applied to SMA.

Employment of generalized coordinates in Eq. (5.23) allows to consider these relations as non-stationary constraint equations. Non-stationary part is determined by $\underline{N}_1 = \underline{N}_1(t)$ and $\underline{M}_1 = \underline{M}_1(t)$. Relations in Eq. (5.23) yield six scalar constraint equations. Formally $\underline{N}_1 = \underline{N}_1(t, q, \dot{q})$, and $\underline{M}_1 = \underline{M}_1(t, q, \dot{q})$, i. e. \underline{N}_1 and \underline{M}_1 can be arbitrary functions of phase variables. For example the case when $\underline{N}_1 = -c\underline{r}_0 - \beta\dot{\underline{r}}_0$ corresponds to linear visco-elastic behaviour of reaction force.

Most clear is how to use constraint equations of Eq. (5.23) type for modelling of supportless phases of motion with kinematics described by constraint equations of Eq. (5.22) type, where $\underline{N}_1 = \underline{M}_1 \equiv 0$. Absence of additional constraint equations in Eq. (5.23) in general case leads to non-zero values of \underline{N}_1 , \underline{M}_1 , which, obviously, cannot be realized in the supportless phase.

As one more useful vector constraint equation, theorem of increment of moment of momentum with respect to the center of mass can be proposed:

$$\dot{\underline{k}} - (r_0 - \underline{R}_c) \times \underline{N}_1 - \underline{M}_1 = 0. \quad (5.24)$$

This constraint allows to directly control value of moment of momentum \underline{k} , for

example, through variation of mutual position of vectors ($r_0 - \underline{R}_c$) and \underline{N}_1 when $\underline{M}_1 \equiv 0$ in single-support phase of motion. It is especially important to be able to control value of \underline{k} when we consider combination of supportless and single-support (or multi-support) phases. As follows from Eq. (5.24) $\underline{k} = \text{const}$ if $\underline{N}_1 = \underline{M}_1 \equiv 0$. This constant determines potential for performance of rotational motions in supportless phase.

Concrete forms of constraint equations depend on generalized coordinates choice. For example, for planar AM (see Sec. 2.7) system of constraint equations consists of two equations from Eq. (2.50) and a third one which is a sum of the rest of motion equations:

$$M^c \ddot{x}_0 + \sum_{j=1}^n C_i \ddot{\varphi}_j = \sum_{j=1}^n D_j \dot{\varphi}_j^2 + N_x(t, \varphi, \dot{\varphi}),$$

$$M^c \ddot{y}_0 + \sum_{j=1}^n D_i \ddot{\varphi}_j = - \sum_{j=1}^n C_j \dot{\varphi}_j^2 - M^c g + N_y(t, \varphi, \dot{\varphi}), \quad (5.25)$$

$$\sum_{i=1}^n C_i \ddot{x}_0 + \sum_{i=1}^n D_i \ddot{y}_0 + \sum_{j=1}^n \left(\sum_{i=1}^n A_{ij} \right) \ddot{\varphi}_j = \sum_{i=1}^n \sum_{j=1}^n B_{ij} \dot{\varphi}_j^2 - g \sum_{i=1}^n D_i + M_1(t, \varphi, \dot{\varphi}).$$

Jacobian matrix elements can be, as it is clearly seen, calculated simultaneously with calculation of components C_i , D_i , A_{ij} . This essentially helps to save time resources.

One of the first two vector equations in Eq. (5.23) for $\underline{N}_1 \neq 0$ should be combined with one of the equations in Eq. (5.22). For example, it can be $r_0 = r_0(t)$, which determines motion of the support-point and behaviour of reaction force ($\underline{N}_1 = \underline{N}_1(t)$). If we use only force constraint, the resulting motion will be determined by action of all external forces (including gravity force) and force constraint, which can lead to undesired displacement of some points of AM (for example, support point). Analogous consideration can be related to the second equation in Eq. (5.23).

On the whole, peculiarities of constraint equations realization determine to a great extent the constraints set for concrete software employed by a researcher. It is clear, that additional calculations in order to take into account constraint equations are needed. However, constraint equations can often even precipitate modelling (integration) process due to stabilizing influence on motion with respect to some generalized coordinates. In particular, stabilization of AM strongly oscillating motion with respect to one of the coordinates frees numerical method being employed from necessity to make calculations with small integration step (interval).

Practical recommendations on constraint equations realization were mainly presented in Chapter 3. Let us only note here that classical variant, when constraint equations are written in form of Eqs. (5.2)–(5.4), can also be realized quite efficiently. Basically, at each integration step it is necessary to decompose the kinetic energy matrix A and present it as multiplication of two triangular matrices LU . This is

done in order to find constraint multipliers. Then we have to solve one system of equations of the form $AH = B$ and $(m + l)$ equation systems of the form $AY = P'$, where $Y = (n \times (m + l))$ solution matrix and P' corresponds to nomenclature used in Eq. (5.3). Later we should also solve system of Eq. (5.3) characterized by potentially degenerate matrix $M = (P'^T A^{-1} P')$ (as it has been noted above) and then we finally find corrected values of accelerations by solving system of equations $A\ddot{q} = B - P'\lambda$ (LU decomposition of kinetic energy matrix is already known by this time).

It should be noted that dealing with constraint equations according to this methodology should take place after formation of column $B(t, q, \dot{q})$, that is all external and internal forces and moments must be already taken into account. Constraint equations just correct values of accelerations. This can be used for parametric correction of constraints action distribution. Right-hand side of Eq. (5.3) depends on $B = B(t, q, \dot{q})$ and therefore parametric form of visco-elastic generalized forces, for example of the Eq. (5.1) type, makes possible redistribution of values λ through variation of parameters in Eq. (5.1). Thus, motion with required kinematics can be formed via variation of parameters which determine visco-elastic properties of joints.

What actually such variation can yield depends essentially on number of redundant freedom degrees and number of simultaneously "active" constraint equations. Alongside with parametric corrections, corrections based on the principle of local variations can also be carried out. It consists of introducing some time-functions in the right-hand side of motion equations. However, for high number of freedom degrees this method proves to be not very effective and difficult for solving.

The realization of typical constraint equations in mathematical model considered above allows one to deal with various possible cases of MM applications to adequate modelling of human SMA. Methodology of this modelling is oriented on a multi-level superelement model with the following possibilities:

- 1) parametrical description of visco-elastic properties of joints;
- 2) constraints on displacements of some points (which are realized by means of a feed-back with respect to displacements and velocities);
- 3) parametrical equations of geometric, kinematic and force (e.g. of Eq. (5.23)) type constraints.

It should be noted, that among the possibilities listed above of MM parameters variation, constraint equations allow one to receive most constructive results in synthesis of new motions as well as for adequate modelling of concrete motions (since the adequacy criterion implies employment of additional measurements which can be used as constraint equations).

Hereafter we shall consider some examples of application of the methodology described above.

5.3 Synthesis of Grand Circles on the Horizontal Bar (3-element model)

Modelling of grand circles on the horizontal bar is one of the classical problems employing motion equations of rigid bodies. Interest to this motion is, first of all, due to possibility to describe precisely enough a complex motion using a model with a few number of elements and MM freedom degrees. Assessment of the quality of grand circle performance is connected with requirement of preservation of relative position of body elements.

Obviously, such motion is possible only under certain initial conditions. If we take into account energy losses, due to the viscosity of the bar, friction and air resistance, it becomes clear that there is need in energy restoration which is possible only as a result of coordinated motion of AM elements at "internal" joints. The problem of grand circles synthesis includes necessity of building of motion control, which would provide at least for cyclic character of this motion with minimal dissipation of energy due to external factors (viscosity, friction, air resistance etc.).

Since these energy losses can be estimated beforehand (at least their order can be estimated) the problem actually comes down to synthesis of so-called "speeding-up" circles, which provide for certain energy increment if we do not take into account external factors. Modelling of the gymnast body by successive kinematic chain with cylindric joints (in other words by a planar AM) allows for essential simplification of the problem of synthesis. Mechanical energy losses in such a model (for zero value of the wrist moment M_1) can be estimated as follows

$$E_{in} = \int_0^T \sum_{i=2}^n M_i \cdot \dot{\psi}_i dt, \quad (5.26)$$

where $M_i(t)$, $\dot{\psi}_i(t)$, $i = \overline{2, n}$ — functions of interelement moments and angular velocities correspondingly; T — period of one grand circle.

Analysis of this formula shows that energy increment depends not so much on M_i values as on the sign of momentary power value $P_i(t) = M_i(t) \cdot \dot{\psi}_i(t)$ for each degree of freedom and also on their sum over all "internal" joints. So, the term "coordinated motion of AM elements" means such distribution of moments signs which provides for positiveness of the sum in Eq. (5.26). In this case, the mechanical energy increment will be also positive.

The problem of AM energy losses optimization usually is connected with the so-called biomechanical criteria, calculated according to relations of the following type:

$$E_1 = \int_0^T \sum_{i=2}^n |M_i \cdot \dot{\psi}_i| dt, \quad E_2 = \int_0^T \sum_{i=2}^n (M_i)^2 dt, \quad (5.27)$$

where E_i does not always have the dimension of energy.

Analysis of the formula Eq. (5.26) shows that coordinated behaviour of interelement moments provides increase of integral energy. At the same time biomechanical criterion E_1 drops to its minimal value, since there are no elements characterized by negative sign of $M_i\dot{\psi}_i$ value. Let us note, that coordinated behaviour of interelement moments is most simply realized when we have alternating joints and intervals of motion with $M_i > 0$ if $\dot{\psi}_i > 0$ and $M_i \simeq 0$ if $\dot{\psi}_i < 0$. This means, in particular, use of flexor-muscles during flexing and relaxing of these muscles for straightening under inertia forces.

The example considered below was used in paragraph 4.4 for analysis of parameters of adequate modelling. Let us explain some details of synthesis of grand circles by means of a 3-element model (Fig. 4.32).

Visco-elastic properties of the support were described by a linear function with rigidity coefficient $C = 18000$ N/m and viscosity coefficient $\beta = 500$ N·s/m, which were chosen from constraints on statical displacement of the bar and damping of proper oscillations of the bar-AM system.

Concentrated at joints non-linear dampers and springs of the Eq. (5.1) type provided for stable behaviour of so-called uncontrollable degrees of freedom. For the 3-element model this is shoulder joint. It is assumed that in the first (wrist) joint there are no external forces or control moments. As for external moments (friction, resistance, etc.), they were also taken equal to zero by setting of corresponding parameters. However, zero values of active (stationary and non-stationary) components do not necessarily result in zero value of integral wrist moment, since the AM geometric constraints of the Eq. (5.16) type were also imposed. Therefore, for realization of condition $M_1 = 0$, we also used the theorem of moment of momentum behaviour Eq. (5.23) (second relation).

Formation of preset AM motion for grand circles was actually provided by 3 successive time periods characterized by different behaviour of function $\psi_3(t)$. Differentiated constraint equations and non-stationary relations of the Eq. (5.6) type were also used. Presence of three successive periods can be, for example, seen in graphics of function $\dot{\psi}_3(t)$ (Fig. 5.1, $t \in [0, 2]$). From the same figure it follows that grand circles were performed with $\dot{\psi}_1(t) > 0$ and $\dot{\psi}_2(t) \simeq 0$ over the whole time interval $t \in [0, 4]$.

In Fig. 5.1 graphics of interelement angular velocities, corresponding to two circles with periods of $T_1 \simeq T_2 \simeq 2$ s are presented. Actually the motion was controlled by changing of $\psi_3(t)$, that is by flexing and straightening at the hip joint performed at given time moments, corresponding to adopted technique of this motion performance. The leap in $\dot{\psi}_3(t)$ value at $t = 2$ s corresponds to the start of the second circle (vertical position of the gymnast) and shows necessity of working with disruptions in acceleration functions, which was reflected in interelement moments graphics (Fig. 5.2).

Programmed motions for the first and second circle almost coincide (Fig. 5.1). However, as it can be seen from Fig. 5.2, $M_3(t)$ has a smaller peak value for the

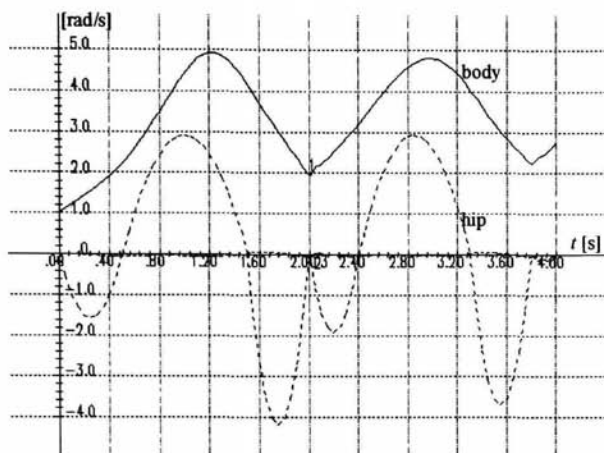


Fig. 5.1. Angular velocities in model joints (two circles interval).

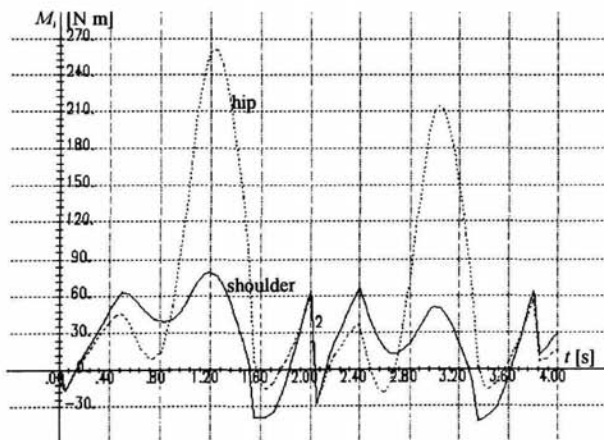


Fig. 5.2. Inter-element moments (two circles interval).

second circle, which resulted in decreasing of area under the power function graphic (Fig. 5.3), and since $P_2 = M_2 \cdot \dot{\psi}_2 \approx 0$ ($\psi_2 \approx 0$, Fig. 5.1), decreasing of P_3 leads to a smaller increment of kinetic energy over the second circle in comparison with the first one ($\Delta T_{kin}^1 \approx 100$ J, $\Delta T_{kin}^2 \approx 50$ J correspondingly, see Fig. 5.4). The described effect is reflected to some extent in Fig. 5.1, where maximum ψ_1 at $t \approx 3$ s. (lower position of AM) is less than ψ_1 at $t \approx 1.2$ s.

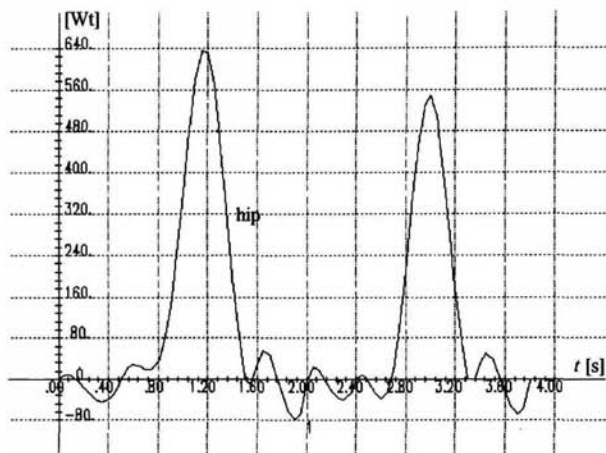


Fig. 5.3. Behaviour of power of the hip joint moment (two circles interval).

The analysis conducted above, shows in particular, that the technique of grand circles performance with equal increments of absolute velocity (energy) over every circle should vary depending on the initial angular velocity ($\psi_1(0) = 1\text{ s}^{-1}$, $\dot{\psi}_1(2) = 2\text{ s}^{-1}$) of the whole body.

Let us note one more important moment, connected with employing of the quality criteria Eq. (5.27) for assessment of effectiveness of the performance technique. In Fig. 5.2 it can be seen that $M_2(t) \neq 0$ over the whole motion interval. However, since $\dot{\psi}_2(t) \approx 0$ (Fig. 5.1), E_1 and E_2 criteria (Eq. (5.27)) will be of significantly different values.

Obviously, the fact that $M_2 \neq 0$ plays the role of counterbalance against dynamic bending moment, which, no doubt, requires energy expenditures from real motion performer. However, this is not taken into account in calculation of mechanical (E_{in}) or biomechanical (E_1) energy losses.

The considered above example, in spite of simplicity of the AM, allowed to underline basic principles of synthesis of grand circles employing variation for formation of given motion. As an alternative approach to this motion synthesis variants of

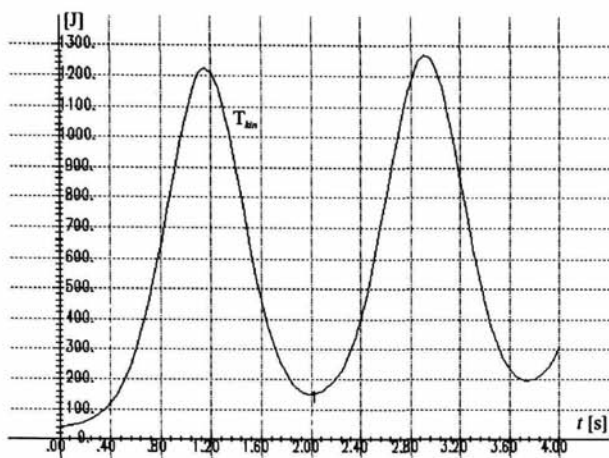


Fig. 5.4. Kinetic energy (two circles interval).

$M_i(t)$, $i = \overline{1,3}$ formation are often considered. In spite of small number of freedom degrees ($n = 3$) this methodology implies variation of time functions, which essentially complicates the process of construction of the given motion.

The main difficulty of this variant of modelling is estimation of initial distribution of $M_i^*(t)$, which is usually then varied during the synthesis process. Attempts to receive distribution of $M_i^*(t)$ from experimental data have already been assessed in the fourth chapter, where it was noted that $M_1(t)$ can be significantly distorted. For this method of variation there are simply realized constraints on $M_i(t)$. However, there appear difficulties with fulfillment of geometric (relative position of bodies) and kinematic (velocities distribution) constraints.

For experiments conducted in laboratory conditions, values of ground reaction components and of the first interelement moment can be quite accurately measured, which allows one to consider two variants of using this additional information. A researcher can either vary parameters of AM and trajectories smoothing procedures (Chapter 4), or use constraint equations of Eq. (5.23) type for exact coincidence of the measured experimental data with corresponding values calculated from the model. Errors in measured experimental data (for example, result of videoregistration data conversion to digital data) can be used for parametric adjustment of the AM.

Let us note, that we have just described a principally new conception of AM parametric adjustment which allows one to use experimental data depending on their quality. Obviously, the basis of the suggested method of synthesis is the procedure of numerical integration of the system of differential-algebraic equations, which has

been considered in detail in preceeding paragraphs and in Chapter 3. As it has been noted above, difficulties here are expected in connection with possible local incompatibility of constraint equations which depends on the character of non-stationarity in constraint equations. In this case, there is need for a procedure for ranging of additional experimental data and its successive employment as constraint equations.

Hereafter we will consider some more examples of synthesis and optimization of motions, in which we discuss some details of problems of synthesis and optimization solution.

5.4 Single-Support Motion (7-element model)

As it was noted in Sec. 5.1, control $U(q, \dot{q}, t)$ structure (Eq. (5.2)) determines motion synthesis prospects. In this section we will consider some details of synthesis process which was already considered in Sec. 4.2. Let the seven-element AM, which kinematic scheme is depicted in Fig. 4.1 and mass-inertia characteristics are given in Table 4.1, perform jumping motion to a relatively small height. In initial position, the legs are half-bent at knees. Let us, for example, set initial ($t = 0$) AM pose to be as in Fig. 4.1 (left picture). Let initial generalized velocities be equal to zero, toes in initial pose touch support under zero value of support reaction.

These restrictions are not of principal character. However, they allow us to assess main motion parameters. During jumping-up to a small height or simply raising-up from squatting position the motion performer easily controls vertical position of his body (even if he wears rollers), which means that near zero value of moment of momentum (with respect to the center of mass) is preserved. Even for this rather simple motion we note that it can be performed with different trajectories of various AM parts. For example, palms can move along various trajectories and even fingers motion can be taken into account. As a rule, complexly coordinated motion can be decomposed in an obvious way, which is achieved by man in complex motion performance studying process (that is during multiple attempts to perform it).

Synthesis of motion for anthropomorphic model is linked with alteration of control as function of time. For example, for the 7-element model $M_i(t)$, $i = \overline{1, 7}$; $t \in [0, T]$, i.e. control moments in joints should be determined. Direct variation of $M_i(t)$, $i = \overline{2, n}$; ($M_1 \equiv 0$), as noted above, is possible only for low n (≤ 3), because it becomes very difficult to choose coordinated behaviour of $M_i(t)$ so that the AM would not push-off the support or even fall down before straightening up. This problem is not simple even for a two freedom degrees case.

Functions of time variation is reduced, as a rule, to parameters variation, which leads to some increase of the upper limit of n value. As one of the possible variants we can propose to use relation Eq. (5.1) if we assume that neutral position of non-linear springs corresponds to straightened-up position of the AM. Then, the initial AM position corresponds to a compressed spring position and the task is to choose distribution of joint springs and dampers parameters to ensure anthropomorphic

character of motion and its integral characteristics behaviour.

Difficulties of such approach to motion synthesis are connected with possible achievement of limit value by one or several joint angles "ahead of schedule", because parameter values of various joints springs and dampers are not interconnected. Besides, parameters being varied do not determine support reaction value (\underline{N}_1). Then, according to Eq. (4.1), even for $\underline{M}_1 \equiv 0$, increment of moment of momentum with respect to the center of mass is determined by relation $\dot{\underline{k}}_c = \underline{N}_1 \times (\underline{R}_c - \underline{r}_0)$, which leads to its uncontrollability. As a result of this for relatively low number of freedom degrees ($n \leq 5$) it is possible to obtain required kinematics of motion employing coordinate-by-coordinate descent method (variation of two-three parameters when the rest are fixed). However, support reaction projection values and time of push-off phase (T) can significantly differ from experimental data.

In this approach question of AM foot interaction with the support is left out. It is obvious that this significantly influences synthesized motion characteristics. However, even in supposition of one-point contact with the support (for example by toes), introduction of visco-elastic parameters which describe support reaction significantly complicates synthesis of goal-oriented motion of AM.

Considered variants of motion synthesis are successfully used when good initial approximation $M_i^*(t)$ of $M_i(t)$ is available, especially in problems of optimal control with relatively low number of freedom degrees and when motion characteristics under small joint displacements and high number of freedom degrees are assessed. Visco-elastic properties "concentrated" in joints and determined by relations of Eq. (5.1) type allow to model the so-called superelements of elastic constructions and, in particular, to solve problems of interaction of the foot with the support [107], to assess values located at joints and distributed along elements shearing forces and bending moments.

Returning to the theme of this section, let us underline that goal-oriented variation of parameters of interelement controls requires introduction of constraints which realize this goal.

As first constraint equation, vector equation of the type $\underline{r}_0 = 0$, which implies fixation of the support point can be proposed. Moment of this constraint lifting (T) can depend, for example, on value and sign of N_{1y} (vertical projection of \underline{N}_1) or can be fixed. Various standing-up motion can be organized because angular displacements are varied as functions of time. The main criterion which allows to choose one of the multiple variants is positivity of the support reaction. To be more precise, active raising of the center of mass will take place until the support reaction is greater than the gravity force (for the support reaction of the form depicted in Fig. 4.2). Active zone of the support reaction action lies in the interval $t \in [0.12, 0.48]$.

Let us use the center of mass motion theorem in the following form:

$$M^c(\underline{R}_c - \underline{g}) = \underline{N} \quad (5.28)$$

to carry out formal analysis of the support reaction \underline{N} action.

It is obvious that intensity of motion performance depends on the form and value of base impulse $\underline{P}(T) = \int_0^T \underline{N}(t) dt$. Support point is fixed and no work is performed at it. After scalar multiplication of Eq. (5.28) by $\dot{\underline{R}}_c$ and integration over all interval of motion we obtain:

$$\frac{1}{2} M^c \dot{\underline{R}}_c^2(t) - M^c \underline{g} \cdot \underline{R}_c(t) = \int_0^t \underline{N} \cdot \dot{\underline{R}}_c dt + E_0, \quad (5.29)$$

where $E_0 = \frac{1}{2} M^c \dot{\underline{R}}_c^2(0) - M^c \underline{g} \cdot \underline{R}_c(0)$ — full energy of the “frozen system” at the initial moment $t = 0$.

Relation Eq. (5.29) gives exhausting information for analysis of influence of support reaction \underline{N} upon AM motion. The term “frozen system” implies absence of internal motion (with respect to relative generalized coordinates). This means that AM center of mass motion is considered as motion of a particle with mass M^c .

It is obvious that if motion goal is achievement of maximal velocity or maximal distance (for example, in jumping), then the center of mass motion determines main trajectory characteristics.

Potential and kinetic energy of the “frozen system” can be written as follows:

$$E_k(t) = \frac{1}{2} M^c \dot{\underline{R}}_c^2(t), \quad E_p = -M^c \underline{g} \cdot \underline{R}_c(t), \quad (5.30)$$

and $E_z(t) = E_k(t) + E_p(t)$. It should be noted that $E_p(t)$ is not the full potential energy of AM because the system includes springs (located elasticities) described by relations of the type Eq. (5.1). Thus, it follows from Eq. (5.29) that condition of increase of full energy $E_z(t)$ is that momentary power of the “frozen system”

$$Q(t) = \underline{N}(t) \cdot \dot{\underline{R}}_c(t) \quad (5.31)$$

be mainly positive. That means that the quantity

$$A(t) = \int_0^t Q(t_1) dt_1 \quad (5.32)$$

should be positive. If we take into account that the motion being considered implies that $\dot{R}_{cy} > 0$, then it follows that condition $N_y > 0$ ensures increase of energy $E_z(t)$.

Conducted analysis of this concrete motion gives *a priori* obvious result, because the model and motion considered are very simple. However, the relations written above hold for AM with arbitrary structure complexity. Therefore, relations of the Eq. (5.29)–Eq. (5.32) type allow to assess strategy of AM motion control formation.

Possibility of addition of non-stationary vector constraint equations of the Eq. (5.28) type into motion equations system allows to synthesize motion so that the support re-

action behaviour corresponds to the desired one. Then, if we model support reaction behaviour according to the following law:

$$\underline{N}(t) = \frac{p(t)\dot{\underline{R}}_c(t)}{\underline{R}_c^2(t)}, \quad (5.33)$$

where $p(t) \geq 0$, $t \in [0, T]$, we will obtain *a priori* known value of full energy increase for the “frozen system” because $E_z(T) = \int_0^T p dt + E_0$.

Later we will consider results of synthesis of such “optimal” motions, but first let us describe the rest of constraint equations for the example being considered.

If there are no kinematic constraints of the Eq. (5.17) type imposed upon AM motion, then preset behaviour of the support reaction yields necessary results — the desired motion. In particular, if $N_x \equiv 0$, $N_y(t)$ is of the form depicted in Fig. 4.2 and horizontal position of the center of mass is close to zero, then, according to Eq. (5.24), $\dot{\underline{R}}_c \simeq 0$ if $\underline{M}_1 = 0$. That means that the employed constraint equations will provide for strictly vertical ascent of the center of mass with zero value (due to chosen initial conditions) of moment of momentum. Situation changes if additional constraints upon AM motion are imposed. It could be, for example, constraints concerning palm motion during raising-up. Constraint equation for the considered model will be as follows:

$$\underline{R}_7(t) - \underline{R}_7^*(t) = 0, \quad (5.34)$$

where $\underline{R}_7(t)$ is expressed in scalar form as function of generalized coordinates, $\underline{R}_7^*(t)$ — desired trajectory of palms.

Constraint of the Eq. (5.34) type is equivalent to application to AM of external force which is a known function of time. Such constraint can lead to non-zero value of first interelement moment \underline{M}_1 in an open kinematic loop. We considered single-point support, therefore, in order to “neutralize” constraint Eq. (5.34) effect, additional constraint of the Eq. (5.23) type (second equation) where $\underline{M}_1 \equiv 0$ should be introduced.

Thus, we finally impose 4 geometric constraints (similar to $r_0 = 0$ and Eq. (5.34)) and 3 force constraints (center of mass motion theorem and moment of momentum increment theorem) upon system with 9 freedom degrees (planar motion of 7-element model). It is obvious, that the left “reserve” of freedom degrees will not allow the motion to be quite arbitrary. In particular, palms motion in some calculations variants was constrained by only one equation or, under intensive character of $\underline{N}(t)$ behaviour, we even had to “free” palms motion.

The example discussed above allowed us to show some details of constraint equations employed which was aimed at ensuring anthropomorphic and goal-oriented character of motion. It is important to note that in contradistinction to independent parametric method of motion synthesis (see above), increase of AM freedom degrees

number widens possibilities of performance by AM of multiple-goal functions formalized via constraint equations. This creates a base for a principally new approach to parametric adjustment of AM, including AM structure variation.

Second, no less important aspect of constraint equations application consists in possibility of AM motion optimization with clear strategy of control variation through motion goal variation. Let us consider this on concrete examples.

In the two examples considered below, of synthesis of a high jump from standing position we employ the same 7-element AM. These examples illustrate possibilities of consecutive development of optimal motion. No additional constraints on arms motion are imposed. For the initial slow motion $t \in [0, 0.6]$, which kinematics is depicted in Fig. 5.5, such constraints on arms motion would not bring any essential changes, whereas for the second motion ($t \in [0, 0.25]$, Fig. 5.6), such constraints lifting allows to significantly precipitate optimal motion synthesis process.

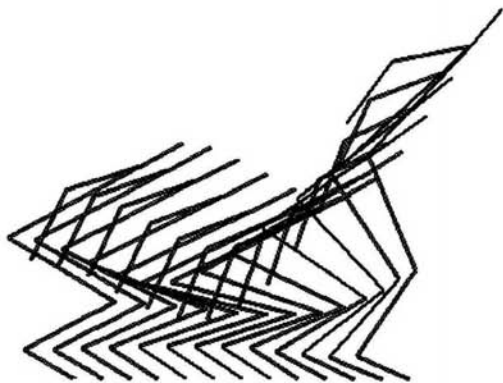


Fig. 5.5. Kinematic scheme of the 7-element model motion (slow motion, high jump, arms motion is not preset).

Let us make parallel analysis of both motion synthesis results. In both cases upon 7-element AM, 5 non-stationary constraints (2 geometric of the $r_0 = 0$ type and 3 force constraints of the $|\underline{M}_1| \equiv 0$ type; $\underline{N}(t)$ is available) were imposed. Charts reflecting behaviour of support reaction are given in Fig. 5.7 and Fig. 5.8 for slow and rapid motion correspondingly. Form, amplitude and time of action of the support reaction were the main parameters being varied in order to increase height of the jump.

It is obvious that under condition of preservation of moment of momentum, which

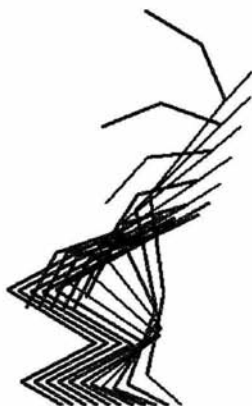


Fig. 5.6. Kinematic scheme of the 7-element model motion (fast motion, height jump, arms motion as not preset).

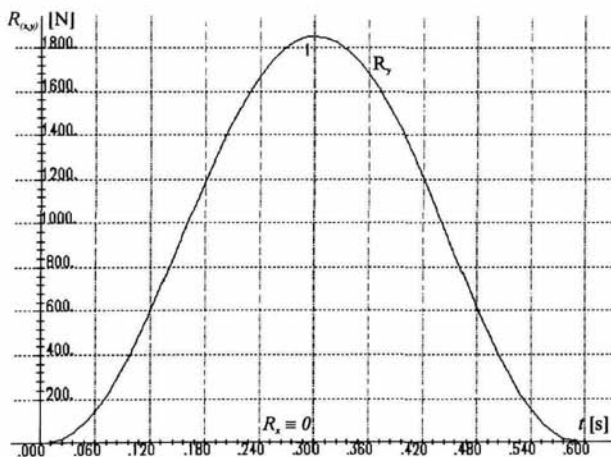


Fig. 5.7. Vertical component of the support reaction force (slow motion).

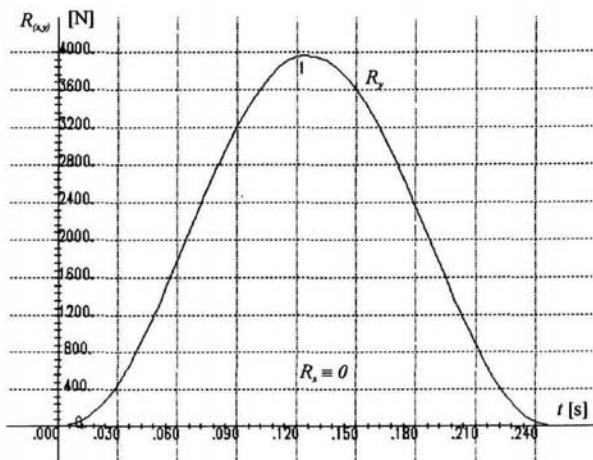


Fig. 5.8. Vertical component of the support reaction force (fast motion).

value is near zero, the main strategy of optimal motion choice consists in achievement of maximal velocity of the center of mass, before distance between the center of mass and toes acquires its maximal possible value (total straightening-up). Taking into account constraint on horizontal motion of the center of mass ($N_x \equiv 0$), we see that for the model being considered relative position of the center of mass corresponds to the absolute one because it is positioned strictly on one vertical line. Center of mass elevation achieves its maximal value for fully straightened-up position of AM (with hands up).

Optimization of the reaction impulse form requires that $\underline{N}(t)$ be close in behaviour to the law of the Eq. (5.33) type. However, center of mass velocity $\underline{\dot{R}}_c$ depends on $\underline{N}(t)$ by itself. Therefore, in order to decrease the time interval when $\dot{R}_{cy} < 0$ (in Fig. 5.9 it corresponds to $t \in [0, 0.25]$), steepness of the reaction impulse at the beginning of motion should be increased.

On the other hand, in order to decrease the center of mass velocity loss at the moment of push-off ($N_y < M^c g$), steepness of reaction impulse N_y at the end of pushing-off phase should be increased. Results of correction of the forefront and backfront of N_y are reflected in the chart of vertical velocity of center of mass for the fast motion (Fig. 5.10). Direct comparison of Fig. 5.9 and Fig. 5.10 shows a decrease in velocity loss from ~ 1 m/s to ~ 0.1 m/s, i. e. by about ten times. Amplitude value of velocity at the moment of push-off increased correspondingly by 3.5 times (from 1.3 m/s to 4 m/s).

Amplitude value of velocity wholly depends on intensity of support reaction im-

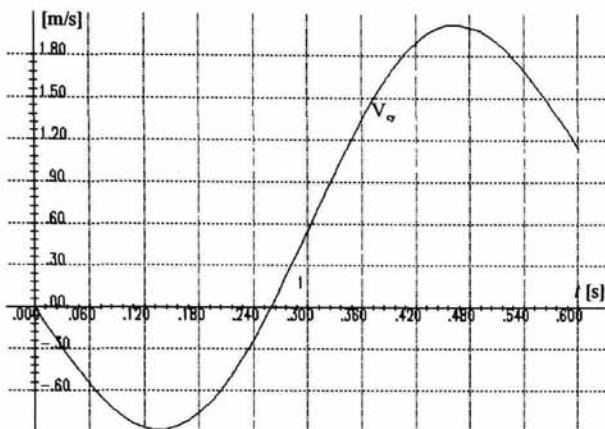


Fig. 5.9. Behaviour of vertical component of the centre of mass velocity (slow motion).

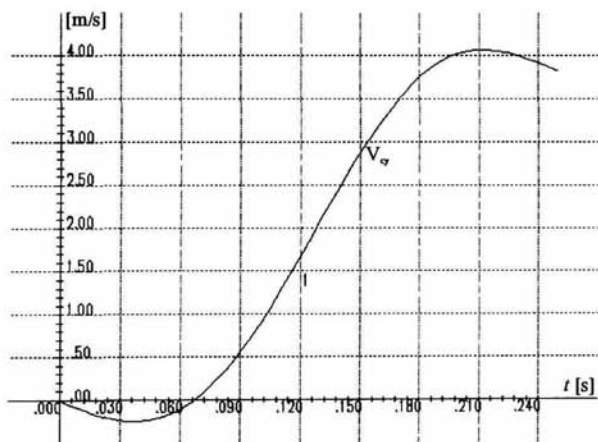


Fig. 5.10. Behaviour of vertical component of the centre of mass velocity (fast motion).

pulse i.e. impulse amplitude divided by impulse duration. It is obvious that decrease of impulse duration brings AM interaction with support nearer to impact-like interaction ($\Delta t \leq 0.01$ s corresponds to impact) which under condition of positiveness of impulse amplitude leads to positive velocity increment with no disruption in displacements. Such an impulse is called in mechanics an impulse of the first order. There are a number of research works devoted to this aspect of AM motion formation [31]. In the case being considered, minimal time of interaction with support is limited by AM power reserve and motion goal. However $\underline{N}(t)$ behaviour should be close to impact-like which means that push-off phase interval should be decreased, whereas impulse amplitude should be increased, which allows to satisfy the main geometric constraint upon center of mass relative displacement.

Naturally, such mechanical analysis of control formation strategy should include integral energy constraints and energy-force constraints for each controllable degree. Besides, analysis of feasibility of each optimization iteration step can include analysis of values of shearing forces and bending moments in superelements of the model.

For the considered motions behaviour of kinetic energy increment and mechanical work $A(t)$

$$A(t) = \int_0^T \sum_{k=1}^n M_i \dot{\psi}_i dt \quad (5.35)$$

is depicted in Fig. 5.11 and Fig. 5.12. Full energy $E_z(t)$ and kinetic energy $E_k(t)$ gains for the “frozen systems” are given in Fig. 5.13 and Fig. 5.14 correspondingly.

Analysis of these charts allow, in particular, to assess AM performance coefficient in support-phase for each of the two motions. If we consider useful energy to be the energy which contributes to the height of jump, spent energy — full energy of AM, then relation $k(t) = E_k(t)/T_{kin}(t)$ will help assess “unproductive” energy expenditures during performance of work $A(t)$ from Eq. (5.35). From kinetic energy increment charts (Fig. 5.11–Fig. 5.14) we can state for the push-off moment:

$$k_s = \frac{\Delta E_k}{\Delta T_k} \approx \frac{200 - 160}{260 - 160} \approx 0.4, \quad k_f \approx \frac{760 - 160}{1560 - 160} \approx 0.43,$$

where k_s, k_f correspond to slow and fast motions (remind that $T_{kin0} = 160$ J because $V_x = 2$ m/s).

Obtained values of coefficients show that even for the case of significant increase of the jump height (to about 1 meter) synthesized motion coordination (technique) is analogous to the initial one. Coefficient of “unproductive” energy expenditures remains approximately the same.

Analysis of charts reflecting behaviour of interelement moments (see Fig. 5.15 and Fig. 5.16) confirms time concertion of main peaks of interelement moments. However, in Fig. 5.16 significant change in values of hip (M_3) and arm (M_4) moments before pushing off the support ($t \in [0.18, 0.25]$) is observed. Especially important appeared

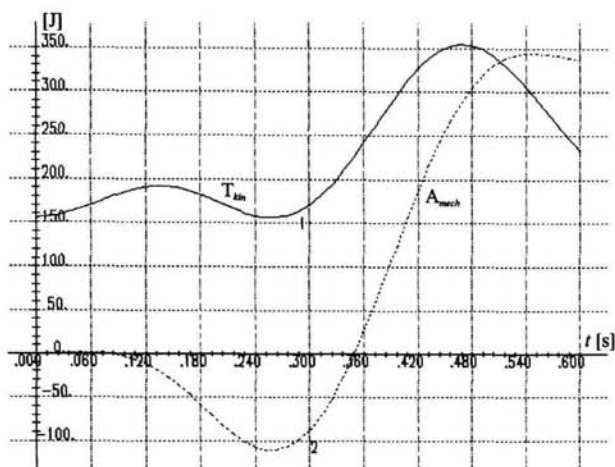


Fig. 5.11. Kinetic energy (1) and mechanical work (2) (slow motion).

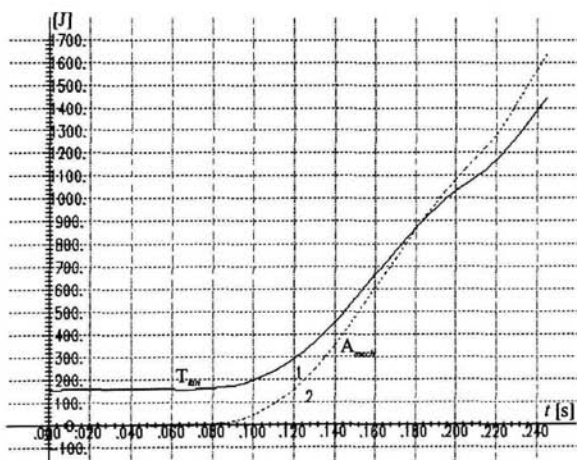


Fig. 5.12. Kinetic energy (1) and mechanical work (2) (fast motion).

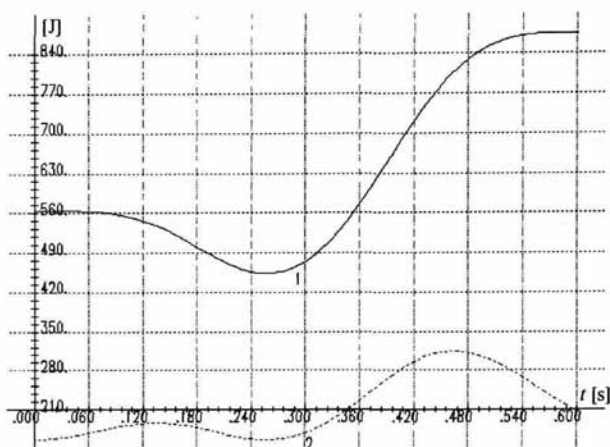


Fig. 5.13. Increment of full (1) and kinetic (2) energy of the "frozen" system (slow motion).

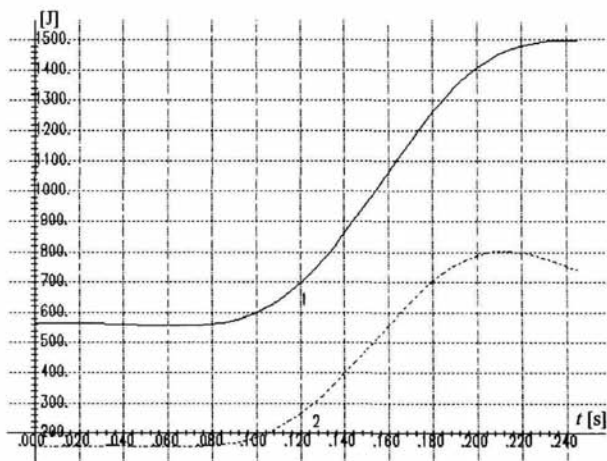


Fig. 5.14. Increment of full (1) and kinetic (2) energy of the "frozen" system (fast motion).

to be contribution of M_4 at the final stage of motion to the total mechanical energy gain because $P_4(t) = M_4(t)\dot{\psi}_4(t) > 0$ for $t \in [0.19, 0.25]$ (see Fig. 5.17 and Fig. 5.18 depicting interelement moment power behaviour).

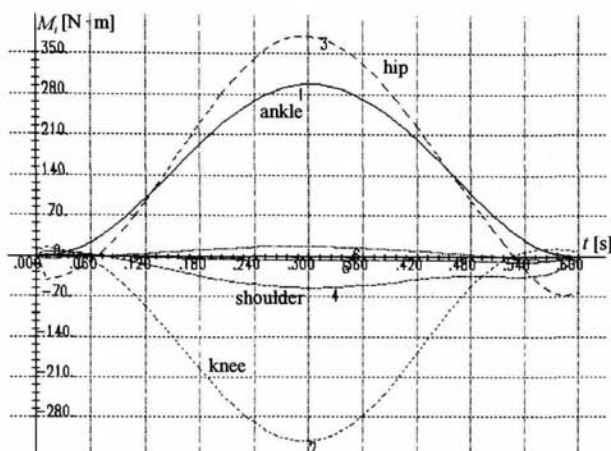


Fig. 5.15. Inter-element moments behaviour (slow motion).

On the other hand, significant scattering of power over joints at the end of support phase which can lead to non-feasibility of motion is observed. From the point of view of motion optimization or simply new motion synthesis every feasibility constraint should be taken into account either by variation of already imposed constraint equations parameters or by introduction of new constraint equations accompanied by possible increase of AM freedom degrees number.

Optimal motion synthesis in the push-off phase is not a simple problem even for relatively simple motions. At the end of this section let us consider one of the motion synthesis variants. Motion synthesized is the same as before, but there is no constraint on horizontal displacement of the center of mass. Support point fixation constraint is preserved.

Introduction of such freedom in AM motion under preservation of the form of the vertical component of support impulse leads to non-zero value of its horizontal component (Fig. 5.19) and consequently non-zero moment of momentum k_c with respect to the center of mass even if constraint providing for $|\underline{M}_1| \equiv 0$ is not lifted. Finally, distribution of interelement moments depicted in Fig. 5.20 shows significant redistribution of moments peaks positions and values. Consequently, in considered example by the moment of push-off AM received increment of horizontal component

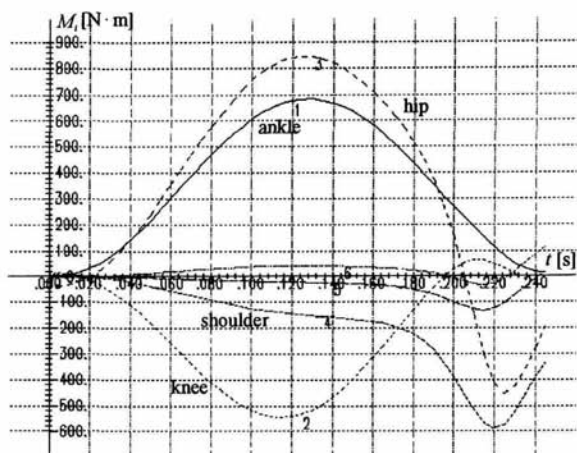


Fig. 5.16. *Inter-element moments behaviour (fast motion).*

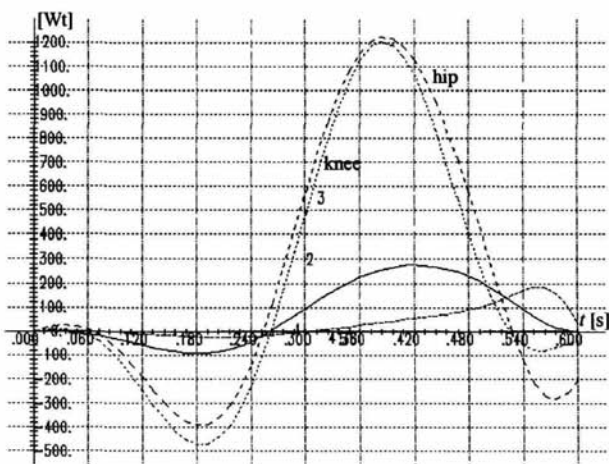


Fig. 5.17. *Behaviour of inter-element moments power (slow motion).*

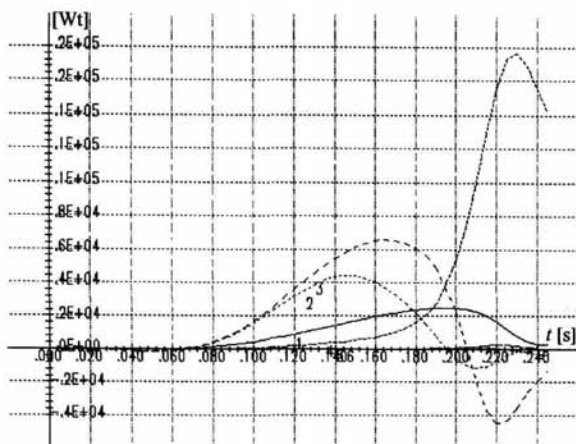


Fig. 5.18. Behaviour of inter-element moments power (fast motion).

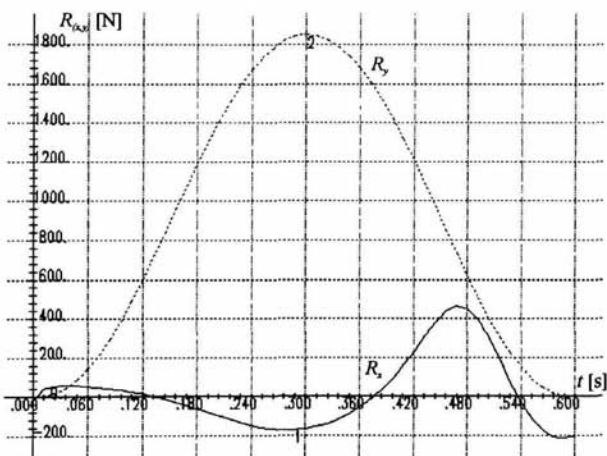


Fig. 5.19. Support reaction components behaviour (slow motion, horizontal component is not preset).

of velocity $\Delta V_{cx} \simeq 0.2$ m/s. Moment of momentum $k_c(0.6) \simeq 15$ kg·m²/s (m·N·s) caused anticlockwise AM rotation during flying phase of motion.

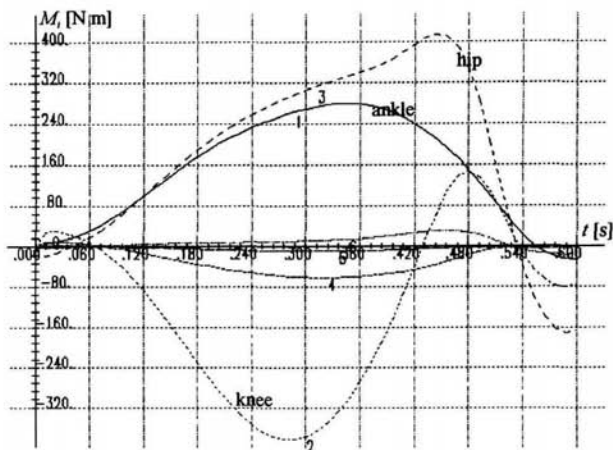


Fig. 5.20. Inter-element moments behaviour (slow motion, horizontal component of support reaction is not preset).

Analysis of graphics of power of interelement moments (Fig. 5.21) and their comparison with corresponding ones in Fig. 5.17 show significant “effectiveness” energy losses at the knee joint (M_3) and especially at the hip joint (M_4) (if the motion goal is still vertical jumping up at a small height with no body rotation during the free-fall phase). Besides, uncontrolled amplitude and phase changes of the ground reaction force component $N_x(t)$ (Fig. 5.19) resulted in the fact that at the moment when $N_x \simeq -200$, N_y turns to zero ($t = 0.6$ s). But this cannot be realized for usual non-confining support and dependency of the friction force on N_y value.

Thus, conducted detailed analysis showed necessity and effectiveness of employment of constraint equations of different types for realization of goal-oriented motions. The most vulnerable point of this methodology is that there can be such systems of constraint equations which are locally incompatible. But this can be taken into account in computer model of AM with constraints.

The incompatibility problem can be partially solved if one employs for constraint equations real experimental data of human motion. Amplitude and phase characteristics of such motion and additional measurements (for example, accelerations measuring units, force platform data) correspond to displacements of real ramified kinematic chain. It is especially important to use information of this kind for synthesis of unique (record) motions, since they, as a rule, are performed with maximum employment of

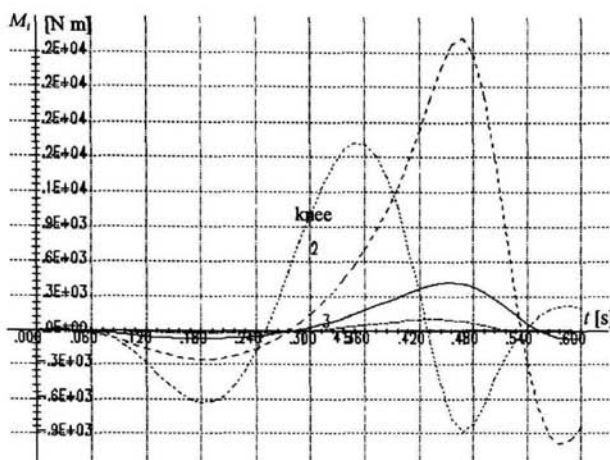


Fig. 5.21. *Inter-element moments power behaviour (slow motion, horizontal component of support reaction is not preset).*

human capabilities. Examples of such motions synthesis will be considered further on.

5.5 Walking

Solution of the problem of two-leg walking is connected with several aspects of motion synthesis by means of AM. From one hand walking is a cyclic motion, from the other hand starting moments are characterized by significant non-stationarity, depending on intensity of the motion. From the point of view of walking synthesis, it is important that we have a two-support phase of motion, which relative duration depends on the average motion velocity.

Let us now consider two examples of walking synthesis, considering starting phase and the basic regular cycle of motion. Kinematic scheme of the AM performing first step is presented in Fig. 5.22. Mass-inertia characteristics of 11-element model are given in Table 5.1.

Numeration of AM elements starts from the foot of the support leg and corresponds to the following human body parts. Support leg: 1—foot; 2—shin; 3—thigh. The body consists of the loin (element 4) and the chest (5), which can be presented as superelements consisting of two and more subelements. The swinging leg, just as the support one, consists of the thigh (6), the shin (7) and the foot (8). The last three elements are the head (9), the shoulder (10) and arms (11).

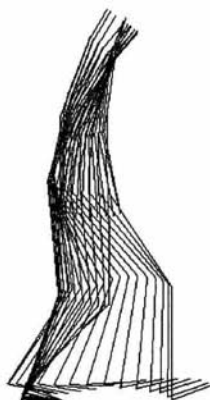


Fig. 5.22. Kinematic scheme of the 11-element model motion (walking, 1-st step).

Table 5.1. Mass-inertia characteristics of the 11-element model (elements number 1, 8—feet; 2, 7—shanks; 3, 6—thighs; 4, 5—trunk parts; 9—head; 10—shoulders; 11—forearms and palms).

| N element | mass, kg | length, m | a_{1i} , m | a_{2i} , m | J_{ci} , kg·m ² |
|-------------|----------|-----------|--------------|--------------|------------------------------|
| 1 | 1.0 | .18 | .09 | .0 | .5e-2 |
| 2 | 5.0 | .5 | .30 | .0 | .1500 |
| 3 | 10. | .5 | .30 | .0 | .2500 |
| 4 | 1.0 | .1 | .05 | .0 | .1e-3 |
| 5 | 26. | .52 | .26 | .0 | .5000 |
| 6 | 10. | .5 | .30 | .0 | .2500 |
| 7 | 5.0 | .5 | .30 | .0 | .1500 |
| 8 | 1.0 | .18 | .09 | .0 | .5e-2 |
| 9 | 2.0 | .14 | .07 | .0 | .1e-1 |
| 10 | 7.0 | .36 | .18 | .0 | .2000 |
| 11 | 5.0 | .36 | .18 | .0 | .1000 |

Any element (for example, the feet) can be presented by a superelement with successive or ramified structure. As it has been noted above, presentation of elements by a superelement with visco-elastic distributed over its joints properties at least allows us to estimate distribution of stresses appearing in the element due to shifting force and bending moment action.

For two-leg walking significant interest presents problem of modelling of motion on artificial prostheses. Thus, for example, modelling of prosthesis insert by a ramified superelement allows us to solve problems of the insert form optimization for different gates, running and jumping. For example, in Fig. 5.23 four variants of insert for artificial foot, corresponding to constructions of the flex-foot type [28] are presented.

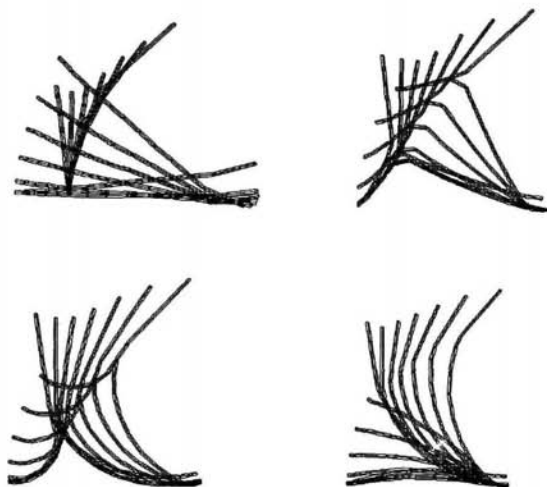


Fig. 5.23. *Insert shape variants for artificial foot of flexfoot type.*

For investigation of dependance of recuperation properties of the insert on its form a ramified superelement, consisting of up to 21 superelement [85] was used. Analysis of these calculation results does not belong to the framework of this work, but let us only note the principal possibility of such cases when the upper part of AM models general human body motion (macro-motion), whereas the element under detailed consideration (for example, a foot) is presented as an independent system of bodies.

Employment of constraint equations for macro-motion synthesis, for modelling approach when AM is described by a single system of motion equations, is connected with certain difficulties since displacements of AM points depend on changes of generalized coordinates of the superelement. This results in the fact that constraint

reactions in the motion equations correspond not only to main controllable degrees of freedom, but also to joints of visco-elastic elements. For correct problem solution, in this case, important additive components of generalized forces in motion equations, which provide for visco-elastic control of the Eq. (5.1) type are present.

Choice of coefficient values in these relations allows to realize a differential approach to control formation. As it has been noted, the influence of constraint equations on the AM motion is analogous to imposing of external and internal forces and moments. Therefore, qualitative analysis allows one to make the conclusion that constraint equations will be first of all fulfilled due to those joint displacements, which result rather from constraint reactions than from the action of none generalized forces.

When these joints displacement values reach their natural (depending on the joint type) or artificial (additional constraints) margins, the main constraint equations will be fulfilled by means of action of reaction forces at "uncontrollable" joints. Thus, the basic strategy of motion control formation for such combined AM consists of, for example, employment of essentially different visco-elastic characteristics at controllable and uncontrollable joints and satisfying of constraints on motion realization ability.

Therefore, methodology of modelling can be split at least at two stages. The first stage is modelling of the basic motion in supposition that all elements are rigid bodies. At this stage it is essential to have so-called "motion margin" If small variations of constraint equations lead to the loss of motion ability to be realized, additional freedom degrees should be introduced into the system. The second stage is presentation of certain element (e. g. a foot) by a superelement. At this stage, as a rule, a small correction is needed in constraint equations, depending on how adequate are the initial element and the superelement.

Regularization of the procedure of superelement introduction consists of successive increase of its degrees of freedom. For adequacy criterion of parameters of motion of the current model and the reduced one (that is the one which corresponds to one of preceding models) can serve as comparison.

The motion under consideration (walking) belongs to the class of non-intensive ones (in contradistinction with support phases of running and jumping) and can be performed by a large number of different ways. This implies wide range of variation of parameters of constraint equations and of the superelement form.

In spite of great variety of gaits, there are some common features characteristic to all of them, which are quite well described in the scientific literature. Let us consider, so-called, normal walking, which is characterized by a certain form of ground reaction function, rhythm and tempo. Let us concentrate on modelling of one-support phase of walking. Modelling of the two-support phase of motion, which takes place from the start of motion to about 20% of the walking cycle period, can be realized either by employment of additional constraint equations, or (which is simpler) by application to the second foot of distributed external force, appearing when the foot support point crosses the support surface of a given form. In a general case the contact problem of elasticity theory should be considered.

The first step of the motion can be performed by many different ways. Let at the first moment AM be motionless and the needed first step length be about 0.4 meter. For performance of this motion, presented in Fig. 5.22, seven constraint equations were introduced. Three stationary constraints provide for stillness of the support foot toe ($r_0 = 0$) and zero value of external interelement moment ($|M_1| = 0$), which is very important, since on the ankle joint of non-support leg non-stationary constraint is imposed providing for motion of the ankle along a given trajectory with zero value of absolute velocity at the final moment.

Fixing of the support foot toe is realized by employment of pre-set non-stationary functions of ground reaction components (Fig. 5.24) for constraint equations. If

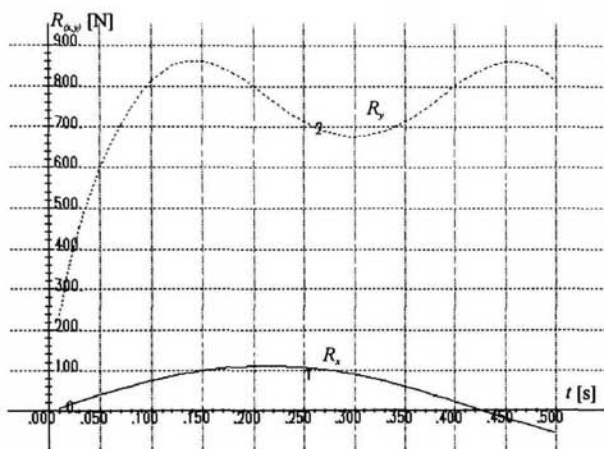


Fig. 5.24. Support reaction force components behaviour (walking, 1st step).

the support point is not fixed, there appear additional problems analogous to those considered at the end of the preceding section. Presence of two peaks in the graphic of vertical component of the support reaction is usual for the main motion cycle as a result of foot rolling from the heel to the toe followed by taking off of the heel from the support. In our case such character of function N_y allows to provide for necessary vertical displacement of the center of mass. The function N_y can be changed for real experimental data.

Presented in Fig. 5.24 behaviour of the horizontal component of the ground reaction force ($N_x > 0$) provides not only for transference of the non-support leg for 0.4 m forward, but also for certain reserve of the horizontal component of velocity (Fig. 5.25) and, correspondingly, kinetic energy (Fig. 5.26). This energy reserve is

sufficient for “rolling” of the leg over the foot upon touching of the leg on the support.

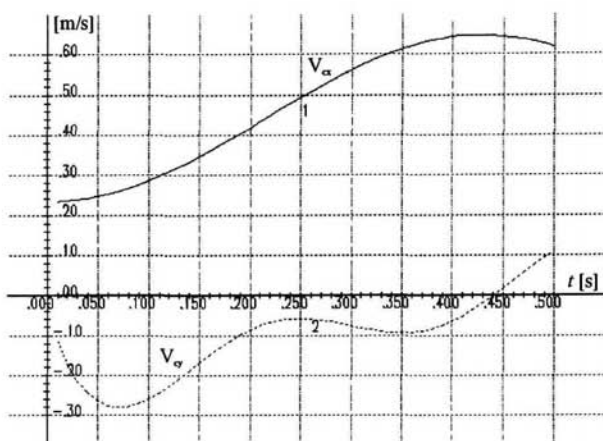


Fig. 5.25. Centre of mass velocity components behaviour (walking, 1st step).

Modelling of the described motion faces difficulties of bringing into concert of constraint equations requirements with traditional description of AM elements motion, when they are not subjected to constraint equations. In particular, requirement of zero velocity at the moment of landing should be in coordination with the step length. In case of a relatively long first step (≥ 0.7 m) impactless walking is achieved by means of active motion of body and arms. As support reaction form is to some extent arbitrary, motion in this case can be essentially different from traditional step technique.

Distribution of interelement moments for the considered step motion is given in Fig. 5.27. Peak values of interelement moments reflect, on one hand, the necessity to realize desired support reaction and, on the other hand, ensure impactless step. It is quite important that relative motion of hands is almost negligible (Fig. 5.22), which shows that there is enough “motion reserve” for gait variation. Characteristic behaviour of interelement moment (M_2) is mostly due to simple foot model (one element model), which directly transmits impulse form (Fig. 5.24) under zero value of moment M_1 .

Let us now consider the second step (or so-called double step), which determines rhythmical gait. Naturally, we use the same AM which kinematic scheme is depicted in Fig. 5.28.

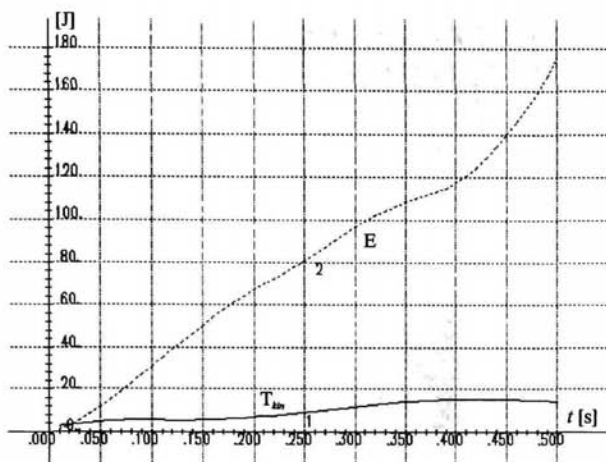


Fig. 5.26. Full and kinetic energies of the “frozen” system (walking, 1st step).

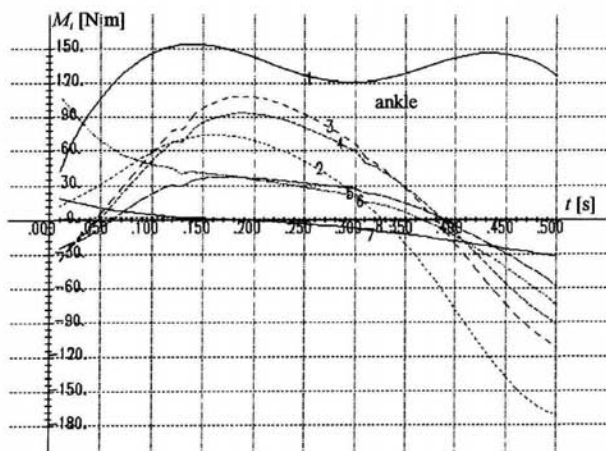


Fig. 5.27. Inter-element moments (walking, 1st step). 11-element model: walking, second step.

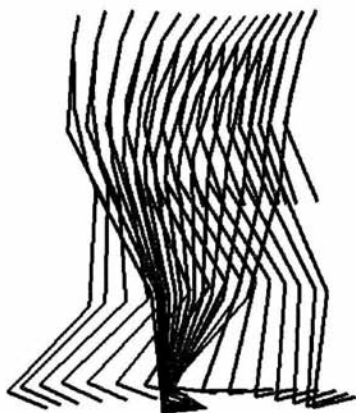


Fig. 5.28. Kinematic scheme of the 12-element model motion (walking, second step).

Walking cyclicity requires repetition of the AM pose and relative velocities distribution at the moments of step beginning and ending. Certainly, some deviation of coordinates and velocities values is possible, which is easily corrected via interelement moments values variation. Kinematic scheme depicted in Fig. 5.28 corresponds to a single-support phase of motion (from the moment of separation of the swinging leg toe from the support to the moment when the swinging leg heel touches the support surface). It will be shown later that double-support phases of walking motion (at the beginning and at the end of the step) can also be considered in the framework of this motion.

Initial distribution of interelement angular velocities (Fig. 5.29) for fixed position of the support leg toe allows for the horizontal component of the center of mass velocity V_{cx} to achieve a value of 1.8 m/s, which exceeds regular walking velocity (approximately 1.5 m/s). Motion was mainly synthesized by employing non-stationary constraint equations, which allow to preset the swinging leg shank-foot motion and behaviour of support reaction components (depicted in Fig. 5.30). Synthesized foot motion determines the step length (~ 0.7 m) and allows for impactless swinging leg foot landing. It is clear, that such constraint equations actually act like an external force, applied to the shank of the swinging leg. Therefore, for synthesis of anthropomorphic motions (controlled by means of interelement moments) constraint equations were added with relations Eq. (5.23), first of which describes preset behaviour of the ground reaction, and the second one describes absence of external, with respect to AM, moment \underline{M}_1 (in case we put $\underline{M}_1 = 0$).

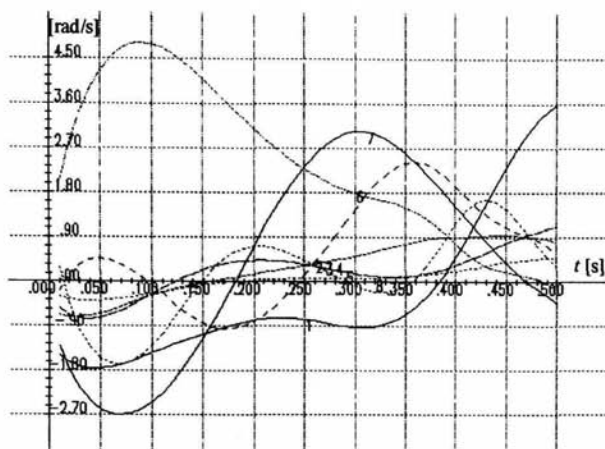


Fig. 5.29. *Inter-element angular velocities distribution (walking, second step).*

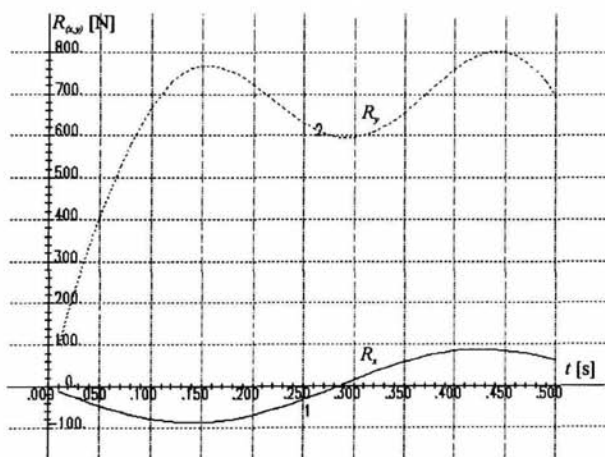


Fig. 5.30. *Support reaction force components behaviour (walking, second step).*

For two-leg walking start of the double-support phase of motion corresponds to the moment of taking off of the support leg “heel” and landing of the “heel” of the swinging leg. End of this phase corresponds to the moment of taking off of the “toe” of the support leg and landing of the “toe” of the former swinging leg. Of course, the technique of walking can vary, but we should note that single-support phase is modelled not till the moment when the vertical component of the reaction turns to zero, but till the moment of its decrease after the second peak of the double peak graphic of this reaction component. Therefore, in Fig. 5.30 the end of modelling is connected with a “slump” of the ground reaction components.

Obviously, the period of the double-support phase is closely connected with the horizontal velocity of motion and can decrease to such a limit value as zero ($V_{cx} \approx 12$ m/s). Finally, for synthesis of the necessary motion, 4 geometric and 3 force constraints were imposed on the initial 12-link model possessing 14 degrees of freedom.

The rest of freedom degrees allow one to make a conclusion on the level of compatibility of constraint equations upon condition of preserving of cycle character of motion. In particular, let us note, that absence of constraint equations on motion of arms or trunk can lead, for certain combinations of constraint equations, to intensive motion over all freedom degrees. The AM in such case performs aimless swinging of arms and trunk motion. Meanwhile, normal walking is characterized by absence of such motions. This means that parameters of constraint equations should be varied so as to exclude parasite motions.

Of course, one can decrease the number of freedom degrees to its minimum (for example, take hands, the trunk and the head for one element), but these will make it impossible to satisfy constraint equations, which, as it has been noted above, takes much effort to overcome when creating software packages meant for employment of different models and modelling of different motions. Therefore a sensible arm motion can be used as an indicator of a good choice of constraint equations parameters.

Cycle character of motion, except for Fig. 5.28, can be noted from the graphic of moment of momentum \underline{k}_c increment with respect to the center of mass (Fig. 5.31). Result of synthesis problem solution is a set of interelement moments behaviour curves, depicted in Fig. 5.32. Amplitude values of interelement moments, taking into account angular velocities distribution (Fig. 5.29), can be presented graphically (see Fig. 5.33).

As it is obvious from Fig. 5.33, largest contribution to mechanical energy E_{in} (see Eq. (5.26)) and, correspondingly, biomechanical (E_1 in Eq. (5.27)) energy is due to moments at the hip joint of the swinging leg (at the beginning of motion) and at the ankle joint of the support leg. Charts depicting behaviour of mechanical (A_{mech}), kinetic (T_{kin}) and biomechanical (A_{bio}) energies are given in Fig. 5.34. Characteristic value of $A_{bio} \approx 200$ J for a cycle of two steps corresponds to data obtained by other authors [6, 28, 31]. However, it should be noted that this value can be yet corrected.

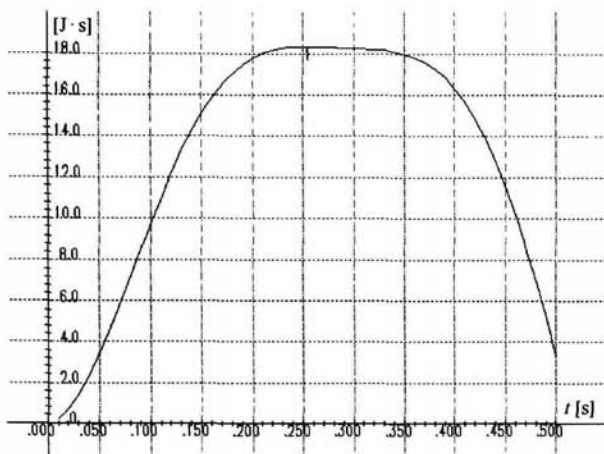


Fig. 5.31. *Increment of moment of momentum with respect to the centre of mass (walking, second step).*

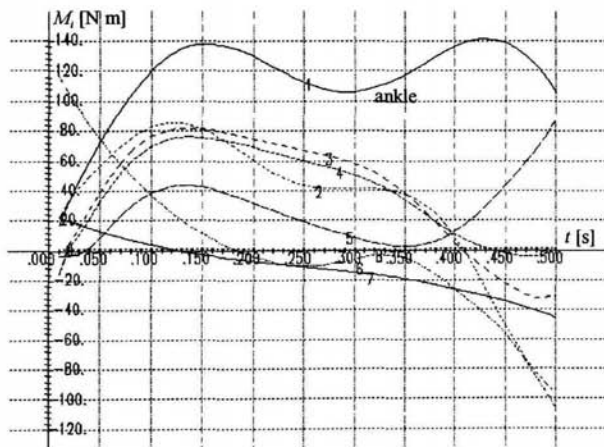


Fig. 5.32. *Inter-element moment (walking, second step).*

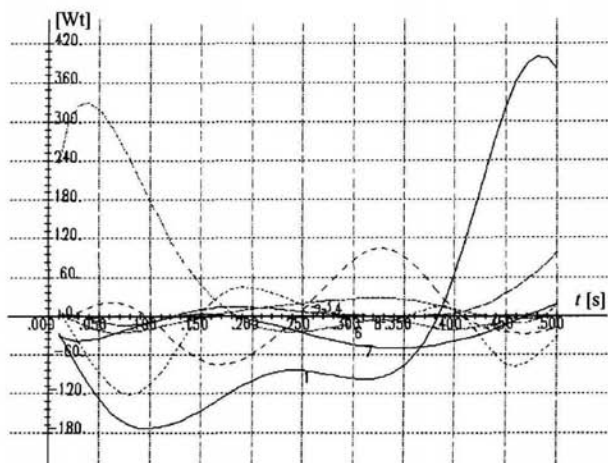


Fig. 5.33. *Inter-element moments power behaviour.*

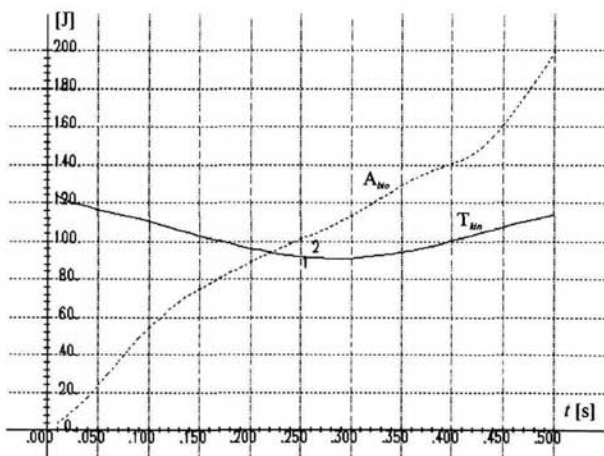


Fig. 5.34. *Kinetic energy of the "frozen" system and biomechanical work (walking, second step).*

As it was noted above, charts depicting behaviour of interelement moments (Fig. 5.32) are obtained in supposition that motion was performed by an open kinematic chain with preset motion (fixed position) of the support point. Under this supposition, distortion mostly concerns interelement moments values at joints closest to the support point. Let us show how the ankle moment M_2 should be corrected, if the support reaction moves during step motion from the heel to the toe. Let us also analyze character of M_2 behaviour if additional external support is present.

Correction term values can be assessed from the following model. Let us assume that the foot is a superelement which is linked to the shank of the support leg and rests on the support surface. There are external forces applied to this superelement (one-element foot is the simplest version). These are: support reaction \underline{N} with radius-vector ρ_1 with respect to the superelement center of mass C_1 , shank reaction force $-\underline{R}_2$ and ankle moment $-\underline{M}_2^0$. Introduced nomenclature is reflected in Fig. 5.35. Behaviour of $M_2^0(t)$ value for one-element foot model is given in Fig. 5.32.

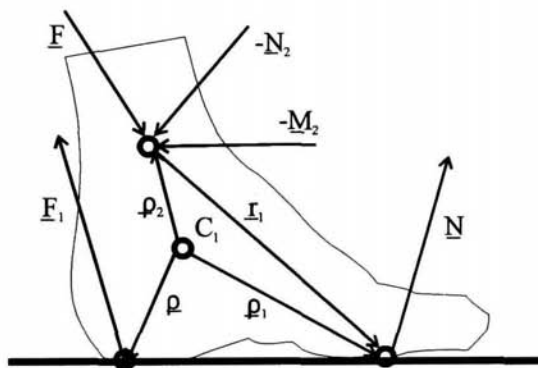


Fig. 5.35. Foot, nomenclature.

Let us employ moment of momentum \dot{k}_1 increment theorem for the whole superelement (foot model):

$$\dot{k}_1 = -\underline{M}_2^0 - \rho_2 \times \underline{R}_2 + \rho_1 \times \underline{N}. \quad (5.36)$$

In Eq. (5.36) it is taken into account that external, with respect to AM, moment \underline{M}_1 is equal to zero. \underline{M}_2^0 value corresponds to open kinematic chain model with fixed point of the support reaction \underline{N} application.

Let us further consider the case when $\underline{N} = \underline{F} + \underline{F}_1$, where \underline{F}_1 is applied to one of the foot elements at point with radius vector ρ , and \underline{F} is the sum of all external forces (except for \underline{F}_1) applied to AM elements (except for foot elements).

According to general rules of taking into account of external forces Eq. (2.39), the foot will be under action of additional force \underline{F} applied at the ankle. Therefore,

corrected formulation of the theorem of moment of momentum increment will have the following form

$$\dot{\underline{k}}_1 = -\underline{M}_2^1 - \underline{\rho}_2 \times (\underline{R}_2 - \underline{F}) + \underline{\rho} \times \underline{F}_1, \quad (5.37)$$

where \underline{M}_2^1 — corrected value of the ankle moment for a different behaviour from Eq. (5.36) of the ground reaction force. Directly from Eq. (5.36) and Eq. (5.37) we have

$$\underline{M}_2^1 = \underline{M}_2^0 + (\underline{\rho}_2 - \underline{\rho}_1) \times \underline{F} + (\underline{\rho} - \underline{\rho}_1) \times \underline{F}_1. \quad (5.38)$$

Let us denote $\underline{r}_1 = (\underline{\rho}_2 - \underline{\rho}_1)$ — radius vector, connecting certain point (not necessarily fixed one) with the ankle joint; $\underline{r}_1^1 = (\underline{\rho} - \underline{\rho}_1)$ — radius vector of varied length, pointing at the instant support point of the foot. Then, moments of external forces \underline{F}_1 and \underline{F} can be put down as follows $\underline{M}_F = -\underline{r}_1 \times \underline{F}$ and $\underline{M}_{F_1} = -\underline{r}_1^1 \times \underline{F}_1$.

Finally, we shall have the following structure of the ankle control moment

$$\underline{M}_2^0 = \underline{M}_2^1 + \underline{M}_F + \underline{M}_{F_1}. \quad (5.39)$$

For the case of planar motion, in projection on the axis perpendicular to the motion plane, we have

$$M_2^0 = M_2^1 + M_F + M_{F_1}. \quad (5.40)$$

Let us return to the analysis of contribution of interelement moment M_2^0 to motion formation (Fig. 5.28). Positive value of M_2^0 corresponds to straightening at the ankle joint. It is essential to note that, if \underline{F}_1 is directed to the foot along the normal vector of the contact surface, then $M_{F_1} \geq 0$ (M_2^0 is equal to zero when $\underline{\rho} = \underline{\rho}_1$). That means that part of the positive value of M_2^0 can be modelled only by a more adequate model of \underline{F}_1 influence in single-support phase.

Let us suppose that \underline{F} is part of ground reaction force of the second foot, then it is obvious that $M_F \geq 0$ ($M_F = 0$ if $|\underline{F}| = 0$ or if vector \underline{F} is colinear with vector \underline{r}_1). It is important to note that in this case value of M_F does not depend on position of the second support leg (ahead or behind) and for usual walking disposition of vectors \underline{r}_1 and \underline{F} moment M_F gives a positive contribution in relation Eq. (5.40).

From the carried out analysis, it follows that values of \underline{F}_1 and \underline{F} can be chosen so that \underline{M}_2^1 will be equal to zero. Considering the chart of A_{bio} (Fig. 5.34) it can be shown that distracting of area under curve reflecting behaviour of N_2 (i. e. about 60 J see Fig. 5.33) from total energy expenditures we obtain that energy required for one cycle of walking is about 140 J, which corresponds to some physiological investigations [6, 31].

Conducted analysis of ankle moment correction procedure can be checked in an obvious way, because, as it was noted in the beginning of this example, motion synthesis was actually conducted by means of variation of \underline{F}_1 and \underline{F} values, except that there was variated ankle position of the swinging leg instead of \underline{F} , and \underline{F}_1 was considered to be applied at the fixed support point.

Let us also note that conducted analysis of influence of $\underline{N} = \sum_i \underline{F}_i$ distribution upon change of interelement moments distribution can be applied to any element (superelement) if we take into account that relative position of support point can change according to the given law (support point is not fixed). The most significant correction require values of moments in joints which are close to the point which is considered to be immovable (support point). For example, for the considered walking motion moments of \underline{F} and \underline{F}_1 decrease with increase of distance from ankle because, in particular, new superelement center of mass position and mutual position of vectors r_1 , r_1^1 , \underline{F} , \underline{F}_1 significantly change, so that vector product of multiplication of \underline{F} by \underline{F}_1 tends to zero.

Analysis of relations Eq. (5.39) and Eq. (5.40) allows one to make one more important conclusion from synthesis point of view. Namely, M_2^0 value cannot be negative, because from inequalities $M_F \geq 0$, $M_{F1} \geq 0$ it follows that negative value of M_2^1 would necessarily lead to even higher negative values of M , which is possible only for actually fixed toe of the support leg (as, for example, in skiing).

Considered examples of the first and second step of walking allowed to carry out, along with the two-leg anthropomorphic walking synthesis problem, estimation of the necessary distribution of interelement control functions, energy losses and make conclusions on role of distributions of real external forces on AM motion control. Analysis also showed essential influence of the support superelement construction when calculating external (with respect to the superelement) interelement moment. The number of supports plays its role here only with respect to formation of the value and direction of external (with respect to the superelement) component (\underline{F}) of the resultant vector of all forces applied to the AM.

5.6 Gymnastic Exercises

In the previous section main principles of goal-oriented motions formation by means of non-stationary constraint equations were considered. Alongside with motion synthesis realization assessments of energy-force motion characteristics were made. On the whole, considered motions are characterized by low intensity (level of intensity is determined from momentary power value) necessary for motion performance and by significant variability, i. e. possibility to perform one motion differently. As intensity of the motion being performed grows, control parameters variation range becomes more narrow. Hereafter, in this and following sections we will consider synthesis of some unique (record beating) AM motions.

Alongside with motion intensity coefficient, typically used for push-off phase of various jump motions, quite essential motion characteristics are general energy expenditures and motion coordination. They can be assessed as optimal correlation between the "frozen system" kinetic energy (see Sec. 5.4) and moment of momentum at given point of time (for example, at the moment of hands letting off the bar during performance of grand circles with successive jump-off).

Let us consider now synthesis of double backward somersault performed in grouped position after running up. Kinematic scheme of motion of the 7-element AM used in this modelling problem is depicted in Fig. 5.36. AM mass-inertia characteristics are given in Table 4.1 (see Sec. 4.2).

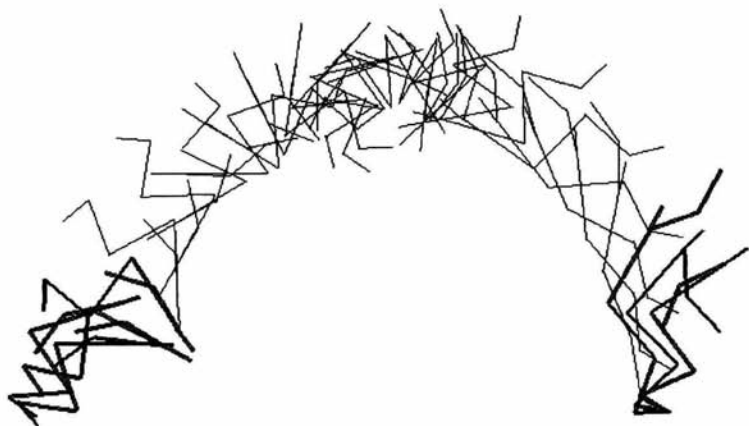


Fig. 5.36. Kinematic scheme of the 7-element model motion (backward double somersault).

After two-leg push off the support during support phase ($t \in [0, 0.15]$ s), center of mass moved along parabolic trajectory raising up to 2.2 meters above the floor and with horizontal displacement of 4 meters. Center of mass velocity projections at the moment of push-off were: $V_{cx} \approx -2.7$ m/s, $V_{cy} \approx 4.8$ m/s. During the flying phase of motion (duration approximately 1 s) non-stationary constraints upon AM were imposed, which allowed to model the needed grouping at the beginning in order to perform double somersault and landing onto feet toes at the end of motion.

At the moment of push-off moment of momentum was about 75 N·s/m, its value increased during support phase by about 45 N·s/m (Fig. 5.37). According to the law of moment of momentum preservation average value of central moment of inertia must be the following: $J=75/(4\pi) \simeq 6$ kg·m², which can be easily realized for the given flying phase time reserve. From Fig. 5.36 it is clear that grouping was not complete.

Main difficulties arise in synthesis of support phase of motion, i. e. in formation of required support reaction impulse and moment of momentum. In Fig. 5.38 charts reflecting behaviour of support reaction projections are depicted, where important sign change of horizontal projection, corresponding to the direction of motion being

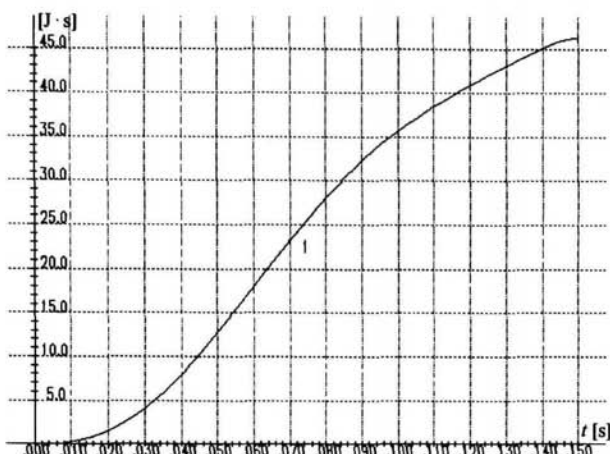


Fig. 5.37. Increment of moment of momentum with respect to the centre of mass (backward double somersault).

performed (backward somersault) is observed. Interelement moments behaviour is depicted in Fig. 5.39, from which it follows that maximal moments are developed in joints of support leg and shoulder. As it has been mentioned several times above, the very moment values do not much characterize motion dynamics as to give a set of momentary values of bending moments. Only analysis of relative angular velocities behaviour charts (Fig. 5.40) in combination with moments charts (Fig. 5.39) allows to make conclusions on contribution of motion in joints into energy balance.

Interelement moments power behaviour charts are given in Fig. 5.41. These chart analysis show individual contribution of work performed at each joint (areas under corresponding curves) into total energy balance. It is also seen from these charts that maximal values of joint power are “scattered” over all interval of motion. This shows that AM motion power in support phase is distributed pseudo-uniformly, which is better from the point of view of possibility of synthesis of this motion with interelement moments similar to that ones depicted in Fig. 5.39.

Energy expenditure in support phase is reflected in Fig. 5.42. It follows from there that biomechanical energy expenditure is about 2600 J, which requires biomechanical power value of about 15000 Wt if motion performance time is 0.15 s. Therefore, such motion is high-intensity motion, as similar quantity for walking motion is only about 400 Wt.

In order to make internal joints of AM “work” two constraint equations were imposed, fixing foot toe position and equalizing external moment to zero, with respect

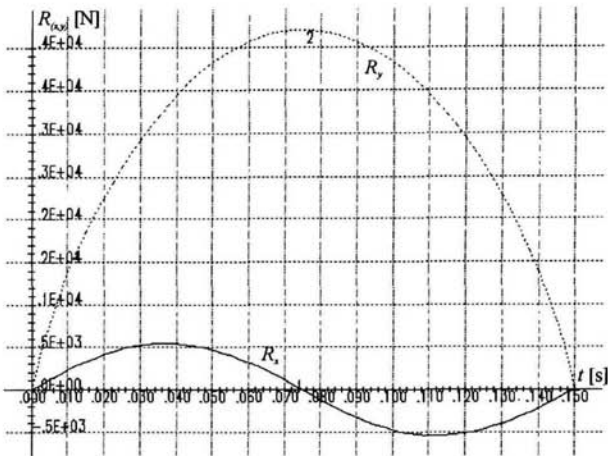


Fig. 5.38. Support reaction force components behaviour (backward double somersault).

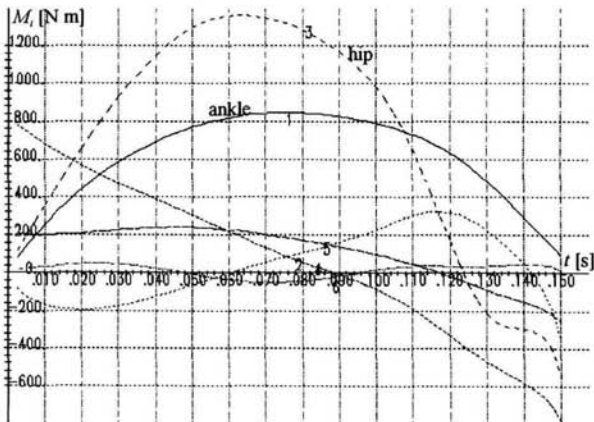


Fig. 5.39. Inter-element moments (backward double somersault).

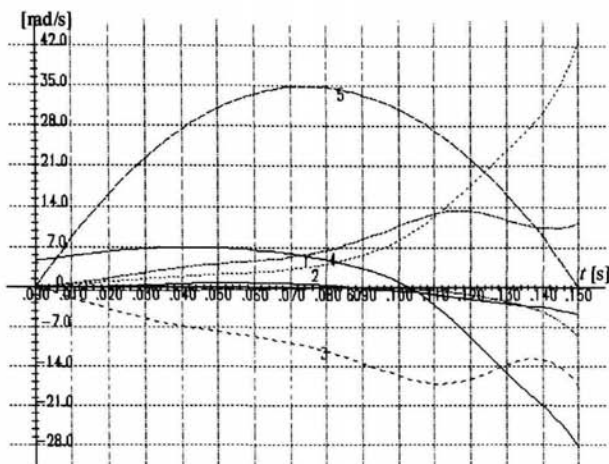


Fig. 5.40. *Inter-element angular velocities distribution (backward double somersault).*

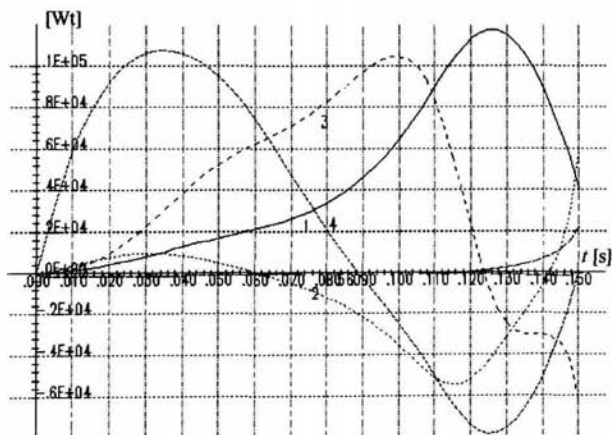


Fig. 5.41. *Inter-element moments power behaviour (backward double somersault).*

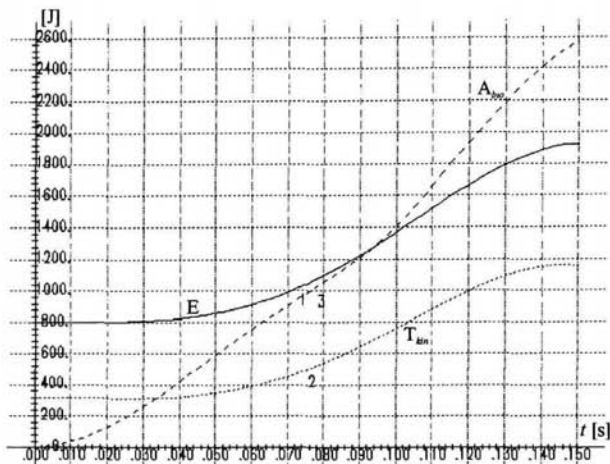


Fig. 5.42. Full and kinetic energies of the “frozen” system and biomechanical work (backward double somersault)

to AM. Difficulty of necessary arms motion coordination synthesis (arms swing) is solved by imposing corresponding constraints on palms motion. Required positive increment of moment of momentum is achieved due to “right” mutual position of the vector joining the center of mass with the support point and the support reaction vector.

In supportless phase the main synthesis problem consists of grouping motion formation so that the AM would land onto its feet. Several iterations of motion synthesis are enough for finding appropriate joint angles behaviour.

The scheme of double-somersault synthesis considered above can be employed for synthesis of record-beating types of motion (multisomersault motion, for example). It is important to take into account restriction on AM motion possibilities as well as initial distribution of elements positions and velocities.

In the next example we will consider synthesis of backward grand circles on elastic bar with following jump-off with performance of double-somersault in stretched out pose or four backward somersaults in grouped position.

Kinematics of 8-element AM motion in both cases is depicted in Fig. 5.43 and Fig. 5.44. Mass-inertia characteristics are given in Table 5.2. Elements numeration starts from arms (1st element), then shoulders — second element, chest and the rest of body — third and fourth elements, thighs, shanks, feet — correspondingly fifth, sixth and seventh elements, head — eighth element.

The 8-element model being considered possesses 10 degrees of freedom, which is

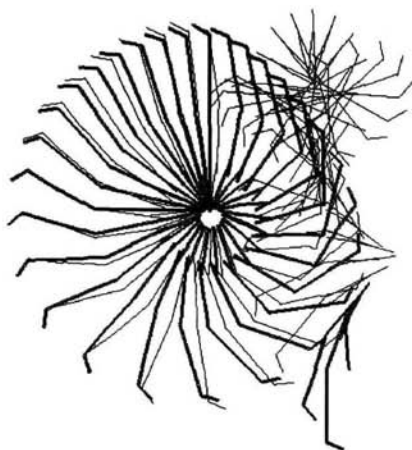


Fig. 5.43. Kinematic scheme of the 8-element model motion (two backward grand circles with following backward double somersault in stretched-out position).

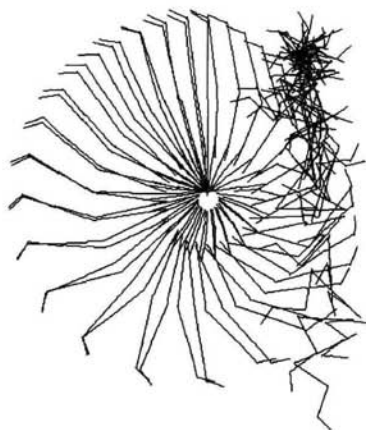


Fig. 5.44. Kinematic scheme of the 8-element model motion (two backward grand circles with following four backward somersaults in grouped position).

Table 5.2. Mass inertia characteristics of the 8-element model (element number 1-forearms and palms; 2-shoulders; 3,4-trunk parts; 5,6,7-thighs, shanks, feet; 8-head).

| <i>N</i> element | mass, kg | length, m | a_{1i} , m | a_{2i} , m | J_{ci} , kg m ² |
|------------------|----------|-----------|--------------|--------------|------------------------------|
| 1 | 4.3 | .27 | .14 | .0 | .03172 |
| 2 | 5.37 | .27 | .13 | .0 | .09725 |
| 3 | 34.16 | .52 | .27 | .0 | 3.58974 |
| 4 | 2.00 | .05 | .02 | .0 | .10000 |
| 5 | 23.29 | .44 | .27 | .0 | 1.08616 |
| 6 | 5.18 | .36 | .21 | .0 | .26836 |
| 7 | 2.00 | .20 | .14 | .0 | .10000 |
| 8 | 3.52 | .17 | .17 | .0 | .20627 |

quite important for accelerating circles phase and phase of grouping during jump-off (extent of grouping depends on required value of central moment of inertia). Let us note here that for the two motions being modelled, AM motion in support phase is the same. Variation in jump-off phase is achieved due to appropriate motion coordination during AM flying.

Linear visco-elastic properties of the bar lead to its deformation during grand circles performance (see Fig. 5.45). Viscosity coefficient $\beta=500$ N·s/m and elasticity coefficient $C=20000$ N/m are chosen so that under support reaction maximal value of about 4000 N (Fig. 5.46) bar displacement would not exceed 0.2 m (Fig. 5.45). Center of mass velocity projections behaviour for the motion considered in support phase is given in Fig. 5.47. It is seen from it, in particular, that motion was performed from handstand initial position with initial angular velocity of about 2.5 rad/s.

Analogously to earlier considered example of the 3-element model (see Sec. 5.3), initial energy reserve in this case is not sufficient for performance of a full grand circle. If we take into account that performance of somersaults during jump-off also requires additional energy reserve, it becomes obvious that there is a need in energy inflow into the system, which is possible only through concerted motion in system "internal" joints.

Theoretical fundamentals for synthesis of accelerating circles were considered earlier on the 3-element model. In that example kinematic control in hip joint and shoulder joint angle were subjected to variation, which is reflected in the charts of relative angular velocities depicted in Fig. 5.48. During support phase of motion AM should be accelerated intensively. For example, first element angular velocity increment after first circle was about 2 rad/s, while kinetic energy increment was about 200 J.

During second circle performance interelement angles at shoulder and hip joints were changed in such a manner that kinetic energy increased further as it is shown in Fig. 5.49. Interelement moments charts are given in Fig. 5.50. One can see, in particular, that shoulder moment significantly increased during the second circle

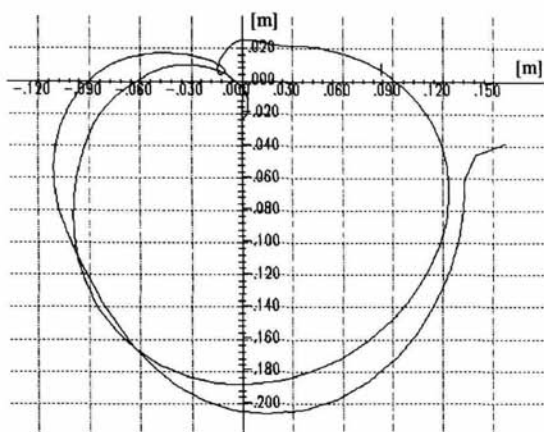


Fig. 5.45. The bar trajectory (two grand circles interval).

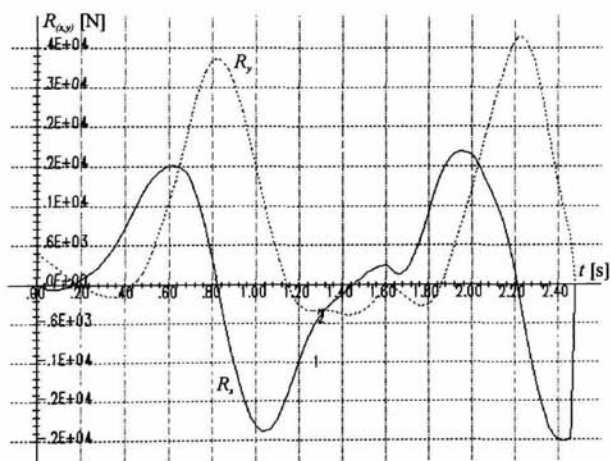


Fig. 5.46. Support reaction force components behaviour (two circles interval).

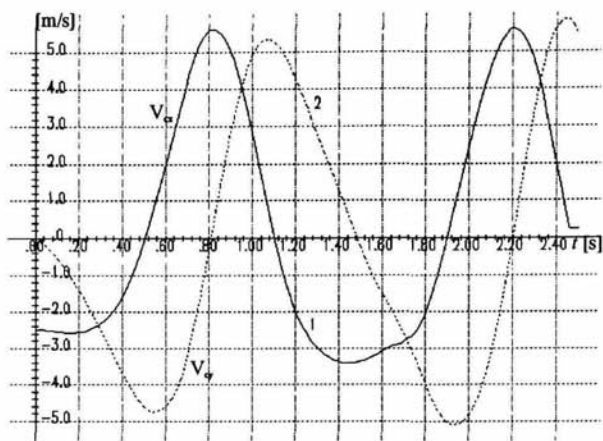


Fig. 5.47. Centre of mass velocity components behaviour (two circles interval).

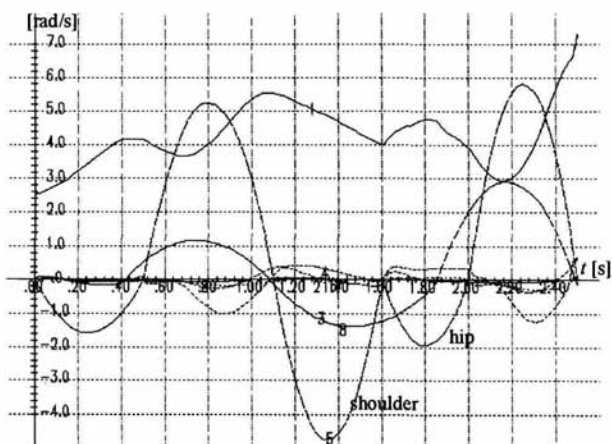


Fig. 5.48. Interelement angular velocities distribution (two circles interval).

with respect to its value after the first circle and with respect to all other interelement moments. This is due to requirement of increase of relative angular velocity at the shoulder joint with respect to the first circle (see Fig. 5.48).

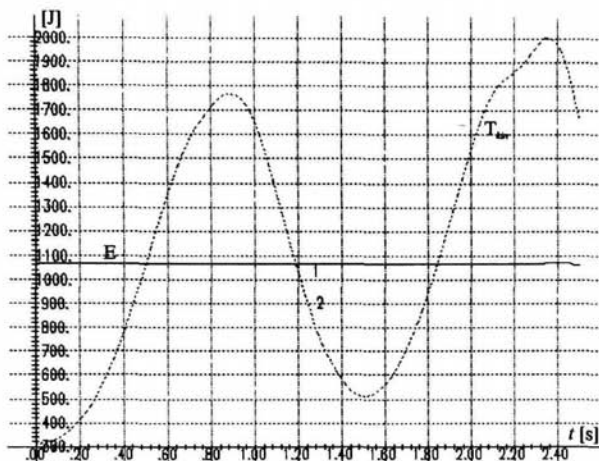


Fig. 5.49. Energy balance and kinetic energy behaviour (two circles interval).

This increase of angular velocity leads to trunk lagging behind arms (decrease of the shoulder joint angle with zero palm joint moment) which, in case of radial direction of the bar reaction \underline{N} (when \underline{N} is directed from the current bar position to its initial position), leads to positive value of product of multiplication of the center of mass relative position vector ($\underline{r}_0 - \underline{R}_c$) by the support reaction vector. In other words (see Eq. (4.1)) it leads to increase of positive value of moment of momentum with respect to the center of mass, which is important in supportless phase of motion.

Comparing synthesis of the motion being considered with synthesis of the 3-element model motion (see Sec. 5.3) one observes principally different structure of energy expenditures distribution. Main contribution into energy increase of the 8-element model is due to interelement moment work at the shoulder joint, which is obvious from charts of interelement moments powers, depicted in Fig. 5.51. From these charts we can also see significant increase of positive contribution into the total energy of the hip joint moment over the second circle with respect to the first one (Fig. 5.50).

After performance of almost two accelerating circles during time interval $t \in [0, 2.5]$ s, at the moment of letting off the bar horizontal and vertical velocity projections are: $V_{cx} \simeq 1$ m/s, $V_{cy} \simeq 5.5$ m/s (see Fig. 5.47); moment of momentum, with respect to the center of mass, $k_c \simeq 90$ J s. In Fig. 5.52 moment of momentum

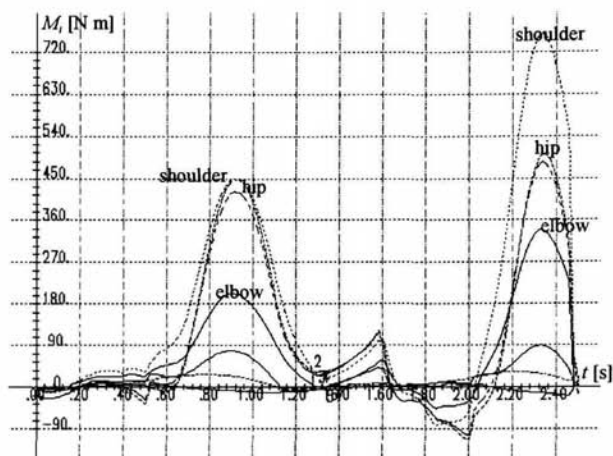


Fig. 5.50. *Inter-element moments (two circles interval).*

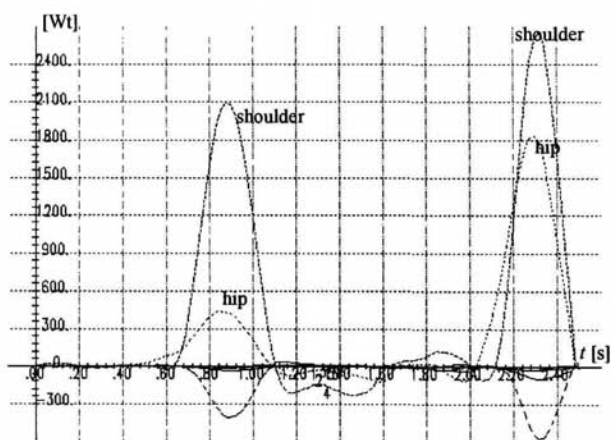


Fig. 5.51. *Inter-element moments power behaviour (two circles interval).*

k_c increment chart is depicted, initial value k_c^0 is about 20 J s. From Fig. 5.52 it is seen that in the flying phase of motion, moment of momentum is preserved (in this example the bar is located 2.5 meters above the floor, flying phase duration is about 1.25 s).

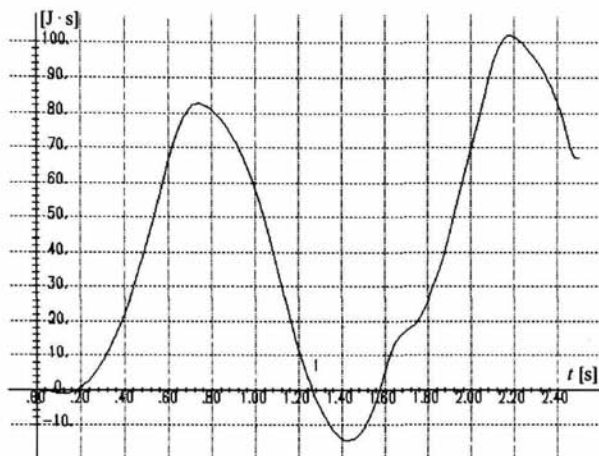


Fig. 5.52. Increment of moment of momentum with respect to the centre of mass (two circles interval).

At the moment of letting off the bar AM is slightly bent. Motion in the flying phase is determined by parameters of non-stationary items in constraint equations imposed for AM grouping and landing on the feet (see Fig. 5.43 and Fig. 5.44). Synthesis of considered motion was carried out as synthesis of one (support phase, flying phase, landing phase) complexly coordinated motion. In the synthesis process there were successively imposed (by groups) 23 constraint equations upon AM with 10 freedom degrees.

5.7 Running Long Jump

Having considered some examples of complexly coordinated motions synthesis using non-stationary constraint equations, let us now look at more intensive motion synthesis. Namely: running up phase of running long jump.

Support phase duration for experimental jumps is about 0.11 s. Increment of vertical projection of the center of mass velocity is about 4 m/s which, for an athlete of 80 kg weight, means average value of support reaction vertical projection about 3000 N and minimal value of power about 7000 Wt. Motion is performed with

horizontal velocity of about 10 m/s. Necessary support impulse can be developed only by means of concerted work of "internal" joints. Negative energy expenditures are inevitable, in particular, because it is necessary to preserve AM pose and motion performance technique (which should be kept in accordance with competitions requirements).

As it was shown above (see Sec. 5.4), support phase of the jump is most effective in case of vertical direction impact-like contact of AM with the support, followed by vertical velocity projection increase, but not accompanied by internal displacements in AM (impact of the first order). Therefore, mechanical and biomechanical works are equal to zero. Certainly, such ideal situation is practically impossible because the support cannot perform positive work. However, it is obvious that AM contact with the support is most effective when it is close to impact-like one, i. e. when the time period of contact is decreased and the support impulse amplitude is in its turn increased.

Two aspects should be underlined. First aspect is that during that short period of contact time AM motion should be highly coordinated, i. e. velocities and relative positions of elements should be governed by one goal — maximum value of vertical projection of the support impulse. Second aspect is that due to general restrictions on AM motion power the support impulse value should not be too sharply raising and falling afterwards, but it should rather be of a rectangular form.

In the example of synthesis considered below a 12-element AM with mass-inertia characteristics from Table 5.1 (see Sec. 5.5) is considered. Kinematic schemes of motion in support and flying phases are depicted in Fig. 5.53 and Fig. 5.54 correspondingly. Initial and final AM position in the support phase depend on the technique of pushing-off. Maximal motion amplitude is observed at the hip joint of the swinging leg and at the shoulder joint. Center of mass velocity projections behaviour is given in Fig. 5.55, from which it follows that horizontal velocity $V_{cx} \simeq 8.6$ m/s, vertical component increment is $V_{cy} \simeq 4$ m/s.

Concerning stabilization of general AM rotation in the flying phase of motion, it is important that moment of momentum with respect to the center of mass (Fig. 5.56) receive positive increment $\Delta k_c \simeq 20$ J s, because during impact-like contact with the support, AM receives negative increment of general angular velocity and, correspondingly, the value of k_c decreases. Such slump in k_c value can lead to AM falling forward if there was no general AM rotation in the opposite direction before contact with the support (see Fig. 5.53).

Analysis of angular velocity increment sign can be carried out on the simplest model of impact of a solid body against the support.

Let $\rho_0 = r_1 + \rho_1$ be the center of mass radius-vector of a solid body in inertial basis \bar{e} , where r_1 — radius vector of possible impact contact point (with respect to the origin of basis \bar{e}) and ρ_1 — relative position of the center of mass O . Let the body move in one plane. Impact takes place at point 1 and non-confining constraints of the following form are introduced: $x_1 \leq X_1$, $y_1 \geq Y_1$. At the point of impact there

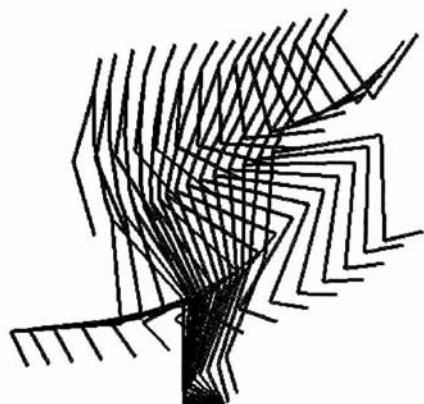


Fig. 5.53. Kinematic scheme of the 11-element model motion (support phase of the running long jump).



Fig. 5.54. Kinematic scheme of the 11-element model motion (support and free-fall phases of the running long jump).

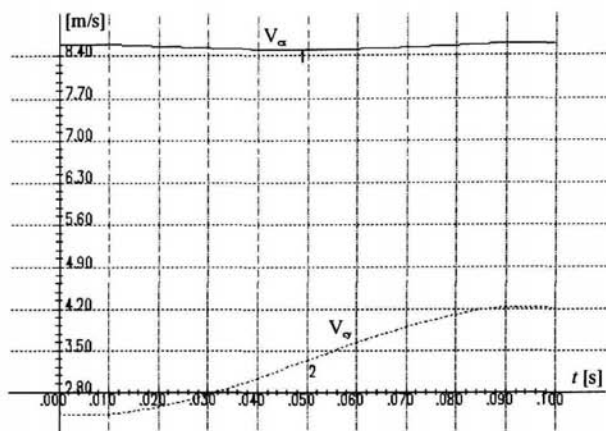


Fig. 5.55. Centre of mass velocity components behaviour (support phase).

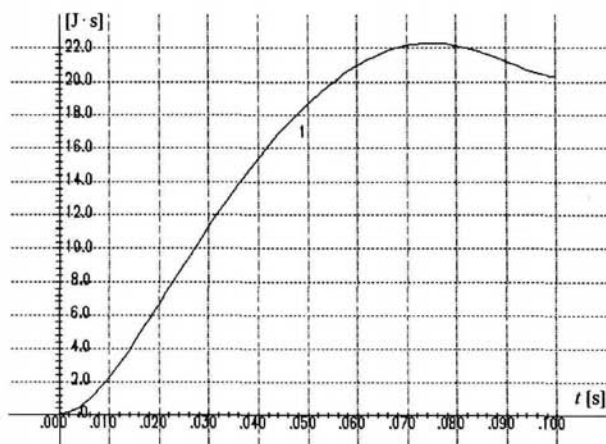


Fig. 5.56. Moment of momentum increment behaviour (with respect to the centre of mass).

appear constraint reactions λ_x, λ_y .

Integrating motion equations in the interval from $(t - \Delta t)$ to t , if Δt tends to zero, we obtain variation equations, which are linear with respect to velocities increments:

$$\begin{cases} J_0 \Delta \dot{\varphi} = \lambda_x \frac{C}{m} - \lambda_y \frac{D}{m}, \\ m \Delta \dot{x}_0 = -\lambda_x, \\ m \Delta \dot{y}_0 = \lambda_y, \end{cases} \quad (5.41)$$

where m, J_0 — mass and central moment of body inertia, $C = m(y_1 - y_0)$, $D = m(x_0 - x_1)$, $\Delta \dot{x}_0 = \dot{x}_0^+ - \dot{x}_0^-$, $\Delta \dot{y}_0 = \dot{y}_0^+ - \dot{y}_0^-$, $\Delta \dot{\varphi}_0 = \dot{\varphi}_0^+ - \dot{\varphi}_0^-$, “+” and “-” signify moments of time directly after and before the impact.

Let us assume that the impact is non-elastic in both directions, then $\dot{x}_1^+ = \dot{y}_1^+ = 0$. Employing this hypothesis further, we obtain:

$$\begin{aligned} \dot{x}_0^+ &= \frac{C}{m} \dot{\varphi}^+, \\ \dot{y}_0^+ &= \frac{D}{m} \dot{\varphi}^+. \end{aligned} \quad (5.42)$$

Solving systems Eq. (5.41) and Eq. (5.42) with an eye to find unknown quantities $\Delta \dot{x}_0, \Delta \dot{y}_0, \Delta \dot{\varphi}, \lambda_x, \lambda_y$, we obtain:

$$\Delta \dot{\varphi} = \frac{m}{J_1} (-y_0 - y_1) \dot{x}_1^- + (x_0 - x_1) \dot{y}_1^- = \frac{1}{J_1} (C \dot{x}_1^- + D \dot{y}_1^-), \quad (5.43)$$

where $J_1 = J_0 + (C^2 + D^2)/m$ — moment of body inertia with respect to the impact point.

Analysis of this relation allows one to make a conclusion on the sign of $\Delta \dot{\varphi}$ after the impact. Its sign corresponds to the sign of mixed product $\underline{e}_3 \cdot (\underline{\rho}_1 \times \dot{\underline{r}}_1^-)$, where \underline{e}_3 — unit vector orthogonal to the plane of motion. It is obvious that if $\underline{\rho}_1$ and $\dot{\underline{r}}_1^-$ (absolute velocity of the contact point) are colinear, then $\Delta \dot{\varphi} = 0$. However, for the running long jump one can usually write: $\dot{\underline{r}}_1^- = \underline{V}_1^- = V_{1x}^- \underline{e}_1 + V_{1y}^- \underline{e}_2$, where $V_{1x}^- > 0$ and $|V_{1x}^-| \gg |V_{1y}^-|$. Besides, $\underline{\rho}_1 = \rho_{1x} \underline{e}_1 + \rho_{1y} \underline{e}_2$ where $\rho_{1x} \approx -0.5$ m, $\rho_{1y} \approx 1$ m.

Thus, obvious assessments show that $\Delta \dot{\varphi} < 0$ and, therefore, during support phase AM attains negative increment of moment of momentum with respect to the center of mass. These assessments can be illustrated by the example of a tall solid body sliding on ice and meeting a horizontal obstacle, which can lead to falling over or jumping up of the body.

Let us write down some more useful relations for the considered model of impact-like contact with the support. Expressions for the impact impulses λ_x, λ_y are as follows:

$$\begin{aligned} \lambda_x &= -\frac{C}{J_1} (C \dot{x}_1^- + D \dot{y}_1^-) + m \dot{x}_1^-, \\ \lambda_y &= \frac{D}{J_1} (C \dot{x}_1^- + D \dot{y}_1^-) - m \dot{y}_1^-. \end{aligned} \quad (5.44)$$

From inequalities $\lambda_x < 0$, $\lambda_y > 0$ (non-confining constraint) one can calculate what limitations are imposed on velocity projections of the support foot at the moment of meeting the support (i. e. landing velocity projections): \dot{x}_1^-, \dot{y}_1^- . If $C < 0$, $D < 0$, then solving system of inequalities with respect to \dot{x}_1^-, \dot{y}_1^- , we obtain that when $\dot{x}_1^- > 0$, \dot{y}_1^- must satisfy at least one of the two inequalities

$$\dot{y}_1^- < \frac{mJ_0 + D^2}{CD} \dot{x}_1^-, \text{ or } \dot{y}_1^- < \frac{CD}{mJ_0 + C^2} \dot{x}_1^-, \quad (5.45)$$

Taking into account that $|D| = |m(x_0 - x_1)|$ is close to zero, more essential is the second from the two inequalities in Eq. (5.45), which implies that $\dot{y}_1^- \leq 0$, if $D > 0$ (at the moment of impact horizontal coordinate of the center of mass lies behind the support point).

Let us now assess kinetic energy losses connected with impact-like contact with the support. According to the theorem of Carnot (see for example [55], v.2), kinetic energy loss ($T^+ - T^-$) is equal to kinetic energy of lost velocities T_Δ with the inverted sign. One can calculate T_Δ from variation equations Eq. (5.41) and relations Eq. (5.44):

$$\begin{aligned} 2T_\Delta &= J_0 \Delta\dot{\varphi}^2 + m(\Delta\dot{x}_0^2 + \Delta\dot{y}_0^2) = \\ &= -\lambda_x(\Delta\dot{x}_0 - \frac{C}{m}\Delta\dot{\varphi}) + \lambda_y(\Delta\dot{y}_0 - \frac{D}{m}\Delta\dot{\varphi}) = \\ &= \lambda_x \dot{x}_1^- - \lambda_y \dot{y}_1^- = -\frac{1}{J_1}(C\dot{x}_1^- + D\dot{y}_1^-)^2 + m((\dot{x}_1^-)^2 + (\dot{y}_1^-)^2) = \\ &= -J_1 \Delta\dot{\varphi}^2 + m((\dot{x}_1^-)^2 + (\dot{y}_1^-)^2). \end{aligned} \quad (5.46)$$

Using relation Eq. (5.46) we finally obtain estimation of kinetic energy T^+ after the impact

$$T^+ = T^- + \frac{J_1}{2} \Delta\dot{\varphi}^2 - \frac{m}{2} ((\dot{x}_1^-)^2 + (\dot{y}_1^-)^2). \quad (5.47)$$

This relation shows that for non-elastic impact with the support part of kinetic energy corresponding to translation motion with the velocity of the contact point (\dot{x}_1^-, \dot{y}_1^-) is always lost, but kinetic energy of rotation increases, independently on the sign of $\Delta\dot{\varphi}$. It should be noted that $J_1 \Delta\dot{\varphi}^2 \leq m((\dot{x}_1^-)^2 + (\dot{y}_1^-)^2)$, since $T_\Delta \geq 0$. Relation Eq. (5.47), just as relation Eq. (5.43), confirms transformation of translation motion to rotation as a result of non-elastic impact.

Relations Eq. (5.41)–Eq. (5.47) hold true for impact of a system of bodies [56, 97]. Main theorems of dynamics of a system of bodies should be used then, instead of variation equations Eq. (5.41). Then, x_0, y_0 will stand for coordinates of the AM center of mass, J_0 — momentary value of the AM moment of inertia with respect to

the center of mass. Then, $\Delta\dot{\varphi}$ will correspond to increment of angular velocity of the vector ρ_1 , connecting the center of mass and the contact point.

All this allows to chose the strategy of the foot setting on the support when performing running jump. Significant difficulties in this strategy realization arise when constraints on maximum values of forces realizing conservation of the AM position at the impact moment are reached. Impact time of the support phase of the running jump is about 0.02-0.03 s and, in spite of possible positive influence of correct foot setting, this process is actually uncontrollable.

The rest of time of the support phase lasts for about 0.1 s and control functions should have simple structure. For motion synthesis trajectories of joint points and, correspondingly, angular displacements must have monotonous character, that is distribution of angular velocities should be quite smooth. In Fig. 5.57 distribution of angular velocities of the support leg and trunk elements is shown and in Fig. 5.58 — distribution of relative angular velocities of the rest of model limbs (arms, second leg) is shown.

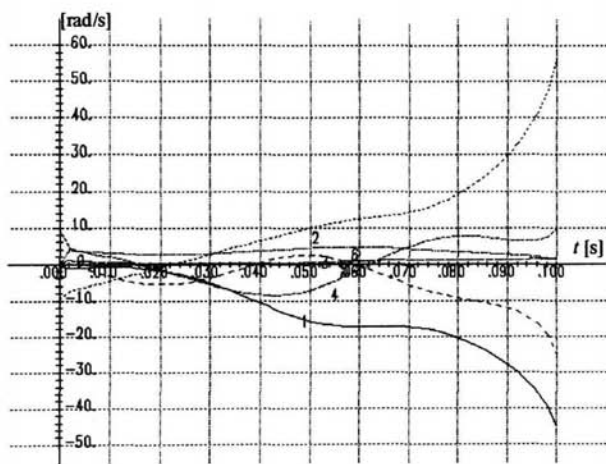


Fig. 5.57. Inter-element angular velocities distribution (support leg and trunk elements).

For initial approximation of synthesized motion results of real running jump for 7.5 meters were used. The strategy described above of the jump length optimization actually consists in successive increase of the vertical component of “the support impulse”, presented in Fig. 5.59, with parallel decrease of the support phase duration from 0.15 s to 0.1 s. There were preset trajectories of motion of the ankle of the swinging leg and arms with variation of values of velocities of these joints at the end

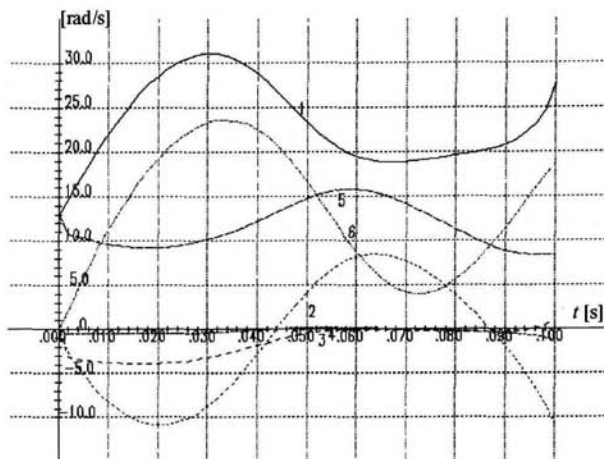


Fig. 5.58. Inter-element angular velocities distribution (arms and swinging leg elements).

of motion.

Main difficulties of synthesis, inspite of the short period of observation (~ 0.1 s), are connected with combination of kinematic constraint equations (regulating limbs motions) and force ones (ground reaction, moment of momentum). Not significant, at first glance, variations of constraints lead to impossibility of motion realization and essentially non-monotonous distribution of angular velocities.

In Fig. 5.60 is presented the final distribution of interelement control moments which resulted in achievement of the maximum value of the vertical component of the center of mass $V_{cy} = 4.1$ m/s, and jump length of 9.65 m. As it has been noted in preceding examples, the most informative value with respect to contribution to increase of mechanical energy is change of interelement powers, which graphics are presented in Fig. 5.61 (support leg and trunk elements) and Fig. 5.62 (other limbs). Analysis of these graphics shows that the most essential aspect with respect to energy losses is motion of the swinging leg at the hip joint (Fig. 5.62).

During the process of motion synthesis it turned out that increase of the maximum value of the ground reaction, along with decrease of the time period of the support phase, should be coupled by increase of the angular velocity of the swinging leg. By analyzing this fact we can conclude that increase of angular velocity of the swinging leg leads to increase of the inertia force pressing the model down and, therefore, allows to increase the work of the support impulse.

In Fig. 5.63 graphics of different energy functions are presented, among which

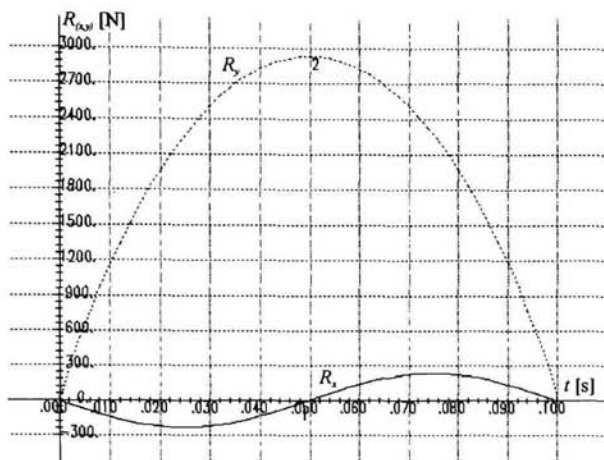


Fig. 5.59. Support reaction components.

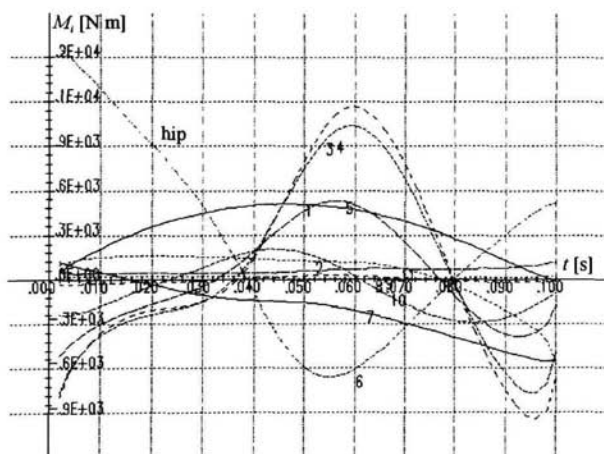


Fig. 5.60. Inter-element joint moments.

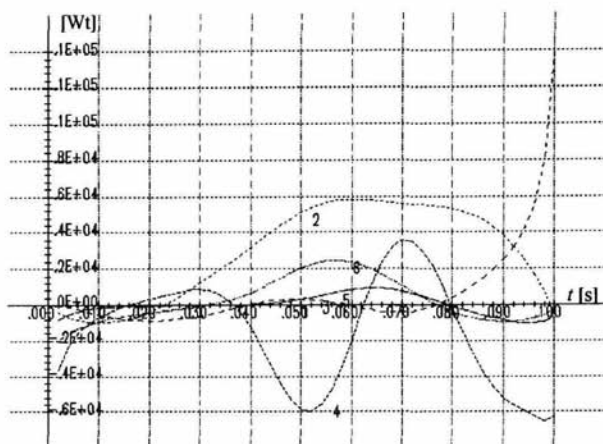


Fig. 5.61. *Inter-element moments power (support leg and trunk elements).*

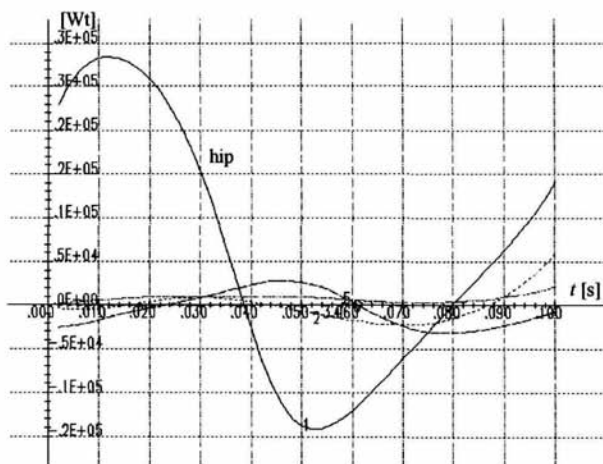


Fig. 5.62. *Inter-element moments power (arms and swinging leg elements).*

a strictly monotonous increase of kinetic energy of the “frozen” system should be noted, which means that direction of the ground reaction vector is close to that of the center of mass velocity. For ideal motion these directions should coincide (see paragraph 5.4). Availability of the biomechanical work function behaviour allows one to estimate average biomechanical power needed for performance of the support phase of motion, which turns out to be equal to about 25 kWt.

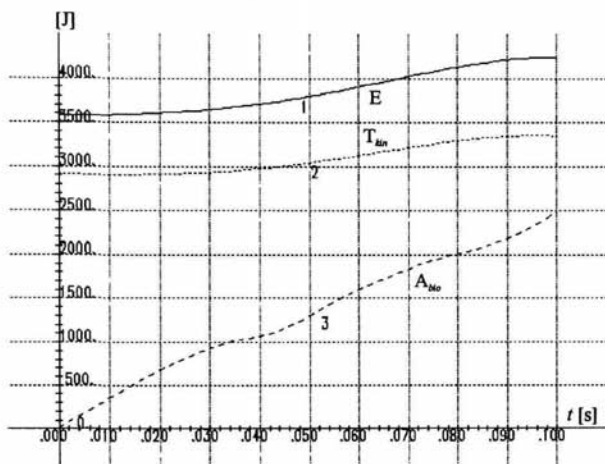


Fig. 5.63. Full, kinetic energy of the “frozen” system and biomechanical work.

Upon taking off of the AM from the support, the main synthesis problem consisted in compensation of the negative value of moment of momentum (about $-50 \text{ J}\cdot\text{s}$) by means of an intensive clockwise swing by arms (Fig. 5.54). Besides, in order to provide for the best position of AM elements at the moment of landing, equations of non-stationary kinematic constraints for flexing at the hip and knee joints were used. Synthesized motion is presented in Fig. 5.54.

For the considered motion, the problem of optimal control during the support phase of the running jump for non-confining constraints on interelement moments and constraints on kinematics was actually solved. It is essential to note, that for the considered approach it is possible to receive a continuous picture of interelement moments behaviour for increasing jump length (from 7.5 m up to 9.65 m and more), as well as for variation of the model structure by change of some elements for superelements. Strategy of control formation is based on including of integral motion characteristics into non-stationary constraint equations, which allows to find necessary directions of change of values of varied parameters, so as to provide for increase of the jump length.

5.8 Human Motion in Weightlessness and under Overloads

Results of investigation of human motions under zero-gravity and overloads show that, in spite of the change of the gravity field, the motion coordination is soon regained [18, 19, 90]. This motion coordination recovering is carried out by the human central neural system by means of control functions reconstruction. This leads to a change of inter-element moments.

In previous sections we have considered synthesis of a wide class of motions under gravity force. Main attention in motion modelling was paid to kinematic and dynamic constraints formulation. Energy-force characteristics of motion were assessed via solution of the direct problem of dynamics for open kinematic chain. This problem solution allows to assess controlling forces and moments in joints. However presence of external forces (e.g. in multi-support motions) brings about essential alterations in resulting values of joint moments.

Relations considered in this section allow to assess necessary correction terms for interelement joint moments for the case of external forces application directly to AM element which motion control should be corrected, as well as to an arbitrary AM element which motion is influenced by interelement moment being corrected.

One of the external forces is gravity force, which is distributed along all elements and depends on the value of gravity force acceleration g . Variation of g leads to significant redistribution of interelement controlling moments if we want to preserve motion kinematics. Relations, which are given in this section, allow to assess values of external forces and moments needed for compensation of gravity force acceleration g alteration. In the second chapter we considered how should external forces be taken into account in a general case. In this section we will concentrate on relations for a 2-element model, but they can be easily generalised.

Suppose that 2-element model depicted in Fig. 5.64 is subjected to external forces \underline{N}_1 , \underline{N}_2 , applied to the first element, and force \underline{F} , applied to the second element. The latter force application point is pinpointed by vector \underline{r}_2 .

Relations which we give here partially repeat in their succession motion equations derivation. In particular, using theorems of centre of mass motion and moment of momentum \underline{k}_{ci} , $i = \overline{1, 2}$ increment, we can write

$$\begin{aligned} \underline{F}_{k1} &= \underline{P}_1 + \underline{N}_1 + \underline{N}_2 - \underline{R}_2, \\ \underline{F}_{k2} &= \underline{P}_2 + \underline{R}_2 + \underline{F}, \end{aligned} \quad (5.48)$$

where for $i = \overline{1, 2}$: $\underline{F}_{ki} = m_i \ddot{\underline{R}}_{ci}$, $\underline{P}_i = m_i \underline{g}$ — gravity force; \underline{R}_2 — joint reaction force;

$$\begin{aligned} \underline{U}_1 &= \dot{\underline{k}}_{c1} = \underline{M}_1 - \underline{M}_2 + \underline{\rho}_{11} \times \underline{N}_1 + \underline{\rho} \times \underline{N}_2 - \underline{\rho}_{12} \times \underline{R}_2, \\ \underline{U}_2 &= \dot{\underline{k}}_{c2} = \underline{M}_2 + \underline{\rho}_{21} \times \underline{R}_2 + \underline{\rho}_{22} \times \underline{F}. \end{aligned} \quad (5.49)$$

In the last relations \underline{U}_i , $i = \overline{1, 2}$, is estimated from AM kinematics analogously to \underline{F}_{ki} , $i = \overline{1, 2}$, in Eq. (5.48). The nomenclature employed is reflected in Fig. 5.64.

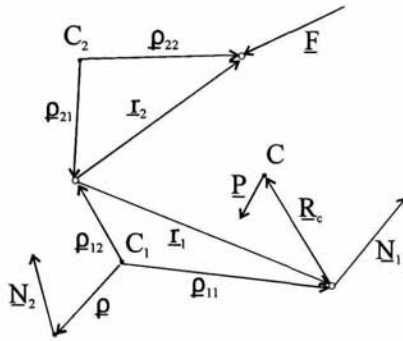


Fig. 5.64. Two element model (basic nomenclature).

Directly from the second relation in Eq. (5.49), if we take into account Eq. (5.48), it follows:

$$\underline{M}_2 = \underline{U}_{2k} + \rho_{21} \times \underline{P}_2 - r_2 \times \underline{F}, \quad (5.50)$$

where $\underline{U}_{2k} = \underline{U}_2 - \rho_{21} \times \underline{F}_{k2}$ — quantity calculated from AM motion kinematics. Equation (5.50) gives the general structure of relation between interelement moment \underline{M}_2 and external forces \underline{P}_2 , \underline{F} . The structure of this relation becomes more obvious upon receiving of analogous formula for \underline{M}_1 . Analogously to preceding speculations, summation of Eq. (5.48) and Eq. (5.49) with following substitution of \underline{N}_1 by corresponding combination of \underline{N}_2 and other external forces gives us

$$\begin{aligned} \underline{M}_1 &= \underline{U}_1 + \underline{U}_2 - \rho_{11} \times (\underline{F}_{k1} + \underline{F}_{k2} - \underline{P}_1 - \underline{P}_2 - \underline{F} - \underline{N}_2) - \\ &\quad - (\rho_{21} - \rho_{12}) \times (\underline{F}_{k2} - \underline{P}_2 - \underline{F}) - \rho_{22} \times \underline{F} = \\ &= \underline{U}_{1k} - (\rho - \rho_{11}) \times \underline{N}_2 + \rho_{11} \times \underline{P}_1 + (\rho_{11} + \rho_{21} - \rho_{12}) \times \underline{P}_2 + \\ &\quad + (\rho_{11} + \rho_{21} - \rho_{12} - \rho_{22}) \times \underline{F} = \\ &= \underline{U}_{1k} - (\rho - \rho_{11}) \times \underline{N}_2 - \underline{R}_c \times \underline{P} - r_F \times \underline{F}, \end{aligned} \quad (5.51)$$

where $\underline{P} = \underline{P}_1 + \underline{P}_2$ — gravity force acting on the AM, $r_F = r_1 + r_2$ — radius-vector of the point of application of the force \underline{F} with respect to the fixed basis; \underline{R}_c — radius-vector of the AM centre of mass.

In Eq. (5.51) the following variable is introduced:

$$\underline{U}_{1k} = \underline{U}_1 + \underline{U}_2 - \rho_{11} \times \underline{F}_{k1} - (\rho_{11} + \rho_{21} - \rho_{12}) \times \underline{F}_{k2} = \dot{k}_{c1} + \dot{k}_{c2} + M^c \underline{R}_c \times \ddot{\underline{R}}_c, \quad (5.52)$$

where $M^c = m_1 + m_2$ — AM total weight. It is obvious that \underline{U}_{1k} also depends only on AM kinematics.

Finally, we can put down for \underline{M}_1 :

$$\underline{M}_1 = \underline{U}_{1k} + (\rho_{11} - \rho) \times \underline{N}_2 - \underline{R}_c \times \underline{P} - r_F \times \underline{F}. \quad (5.53)$$

As it was noted above Eq. (5.53) and Eq. (5.50) are of analogous structure. This allows to easily consider also the case when external forces are applied to that AM part which motion is influenced by variation of interelement moments \underline{M}_j , $j = \overline{1, n}$. Let us introduce set Ω_j which includes numbers of all elements linked with joint j . Then

$$\underline{M}_j = \sum_{i \in \Omega_j} \dot{k}_{ci} + M_j^c R_c^j \times (\ddot{R}_c^j - \underline{g}) - \sum_{i \in \Omega_j} r_F^i \times F^i, \quad (5.54)$$

where M_j^c , R_c^j — total weight and centre of mass radius-vector of elements which numbers belong to Ω_j ; r_F^i , F^i — radius-vectors of application points and external forces applied to the AM part under consideration.

Relation Eq. (5.54) allows to make final correction of joint moments which were at first calculated for kinematic chain under no external forces. In particular, variation of g brings about necessity to vary r_F and F in order to compensate changes in M_j value if we want to preserve motion kinematics.

For investigation of motions under zero-gravity and overloads two approaches can be used. The first one, traditional for biomechanics, is solution of the direct dynamics problem, when from given motion kinematics forces and moments controlling this motion are found. The second approach utilises the methodology of imitational dynamic motion modelling described above, which allows for computer synthesis of goal-oriented human motions. Joint application of traditional methods and methods developed by researchers increased hope for reception of results illustrating changes in control moments behaviour providing for motion coordination preservation in the gravity field of varied intensity.

In the framework of the direct dynamics problem the following motions have been investigated: first — translation of objects of varied mass by the forearm; second — successive speeding up and slowing down as a result of interaction with the support, push off from the support.

The first motion is an elementary one, which is very common for astronauts physical activity. This simple example illustrates the general changes of control muscle moments for gravity fields of different intensity. The second motion is a jump off a low stand with a following jump up. This motion can be easily repeated for experimental purposes during the flight.

Both motions were registered by a special film-shooting equipment in the earth environment. The first motion was performed with arm fixation. The angle between the forearm and the arm was registered as a function of time $\varphi(t)$. For the second motion the behaviour of hip, knee and ankle interelement joints were registered.

Then mathematical investigations were carried out in order to solve the problem as to how the control moments should be changed, so that the motion kinematics remains the same under overloads and in weightlessness as it was in normal (earth) conditions. In Fig. 5.65 graphics of the control moment for arm flexion with a mass of 2.5 kg for gravity fields of different intensity are presented.

The performance of the model motion in a gravity field of increased intensity is

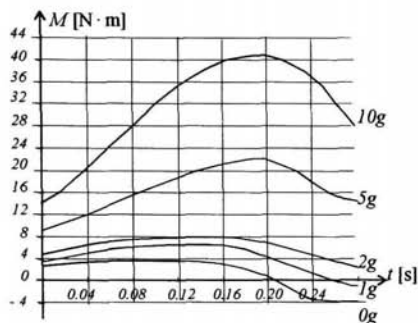


Fig. 5.65. Controlled moments for arm flexion with mass of 2.5 kg.

characterized by increase of the amplitude of the joint moment. This increase value is proportional to the level of overloads. The performance of motions with pre-set kinematics in weightlessness is fulfilled by restructuring of the motion control functions. Thus, in earth conditions deceleration of a moving element is performed by equalising the muscle and gravity forces. In weightlessness for the same purpose a change of the joint moment sign is needed. In other words, analogous work is performed by the muscle-antagonists. Deceleration of a moving body against a fixed support with a following push-off is the space-flight analogue of the second model motion. Ankle and knee interelement moments are less than these for the model motion, but the hip moment value is greater. This is due to the fact that this interelement moment performs additional work for the motion stabilisation (prevention of rotation with respect to the support point). During the push-off phase in weightlessness motion is performed due to the kinetic energy stored in the system, since the values of the ankle and knee moments practically do not change. The hip moment once again performs the stabilizing function. If acceleration and push-off from the support are performed without previous adaptation, the so-called redundancy (in weightlessness) and insufficiency (for overloads) of motion control appear. This is characterized by kinematics and coordination distortion (Fig. 5.66).

As examples of computer synthesis of goal-oriented motions, let us consider two test motions raising up from a semi-squatting position in case when $g=9.8 \text{ m/s}^2$ and $g=0 \text{ m/s}^2$. As it can be seen from results of investigation both methods give practically analogous results.

Kinematic scheme of the synthesised motion is depicted in Fig. 5.67, mass-inertia characteristics are given in Table 4.1.

Centre of mass moved strictly vertically in start-stop regime. In Fig. 5.68 and Fig. 5.69 centre of mass velocity and interelement angular velocities are depicted correspondingly. As it should have been expected one and the same motion performance

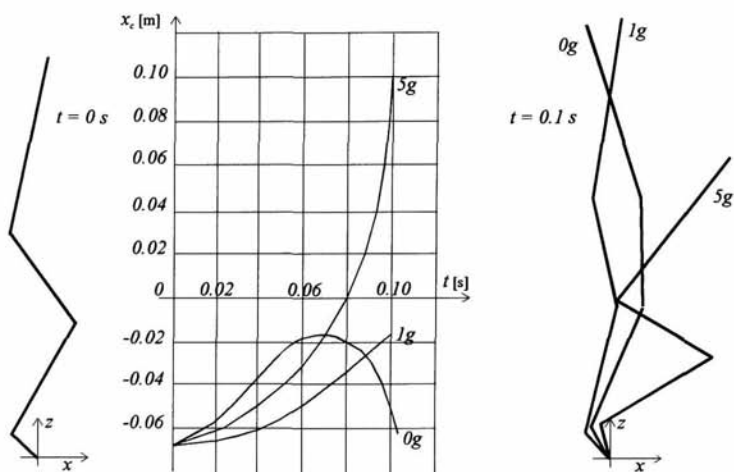


Fig. 5.66. AM centre of mass horizontal displacement in different gravity fields (upward jump).



Fig. 5.67. Kinematic scheme of the 7-element model motion (raising up from a semi-squatting position, pre-set kinematics).

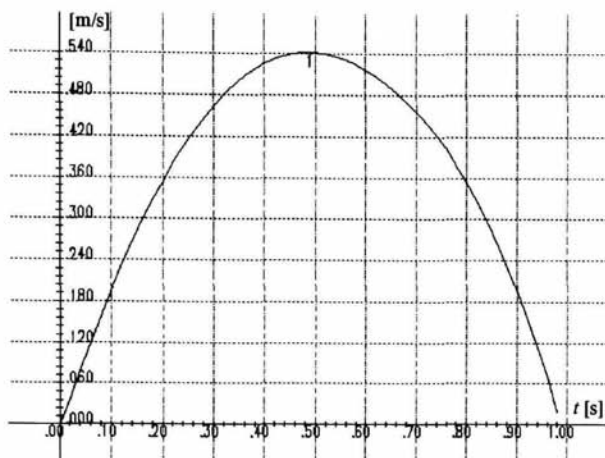


Fig. 5.68. Vertical component of the centre of mass velocity ($g=9.8 \text{ m/s}^2$).

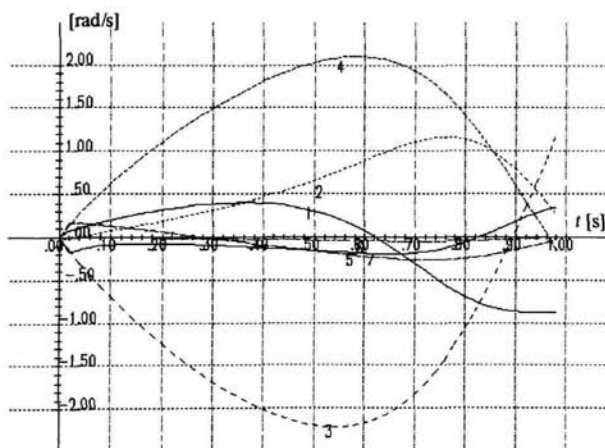


Fig. 5.69. Inter-element angular velocities distribution ($g=9.8 \text{ m/s}^2$).

requires much less energy expenditures under weightlessness.

Let us compare energy-force characteristic for value of $g=9.8 \text{ m/s}^2$ and performance duration $t=1 \text{ s}$ and for the case when $g=0$, $t=0.5 \text{ s}$. In the latter case motion performance velocity is doubled, which leads to increase of power and energy expenditures required for motion performance up to corresponding values of the first case. In order to preserve energy-force picture of motion in weightlessness considered test motion should be performed two times quicker than in the case of normal gravity.

In Fig. 5.70 curves reflecting interelement moments behaviour in earth conditions are shown. Influence of gravity force upon control structure is obvious. As one can see from the figure, the main motion controlling moments do not change sign which is due to decelerating action of gravity force, whereas phases of acceleration and deceleration are connected with change of moments signs in weightlessness (Fig. 5.71). Moments

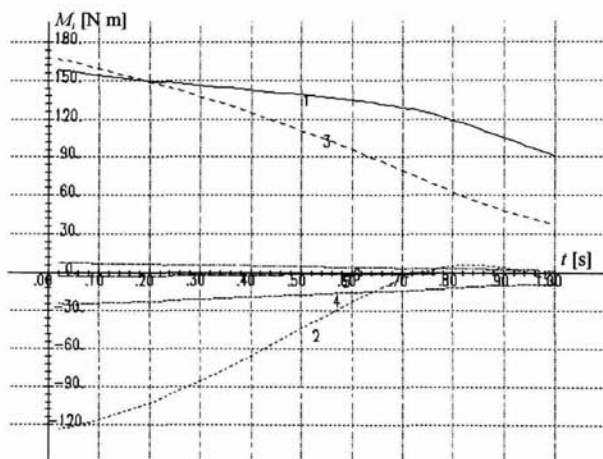


Fig. 5.70. *Inter-element moments ($g=9.8 \text{ m/s}^2$, $t=1 \text{ s}$).*

maximal and minimal values coincide for the two problems. In Fig. 5.72 and Fig. 5.73 curves which reflect interelement moments power behaviour are depicted. It can be seen that under normal gravity no “unproductive” motions in joints (moments powers values do not take negative value) was performed, i.e. minimal required biomechanical work (about 300 J) needed for the centre of mass lifting up to 0.4 m higher was performed.

In weightlessness joint moments power was spent on successive acceleration and deceleration; total biomechanical energy losses proved to be less than in the case of normal gravity: compare Fig. 5.74 and Fig. 5.75. Depicted in the same figures

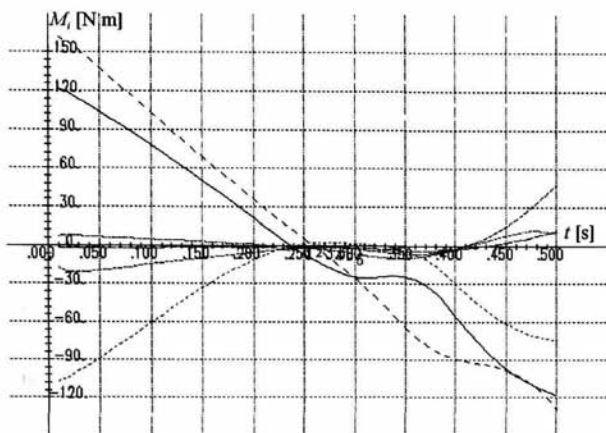


Fig. 5.71. Inter-element moments ($g=0.0 \text{ m/s}^2$, $t=0.5 \text{ s}$).

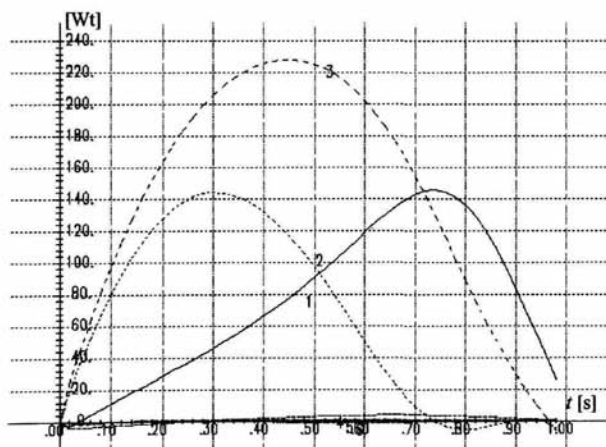


Fig. 5.72. Inter-element moments power ($g=9.8 \text{ m/s}^2$, $t=1 \text{ s}$).

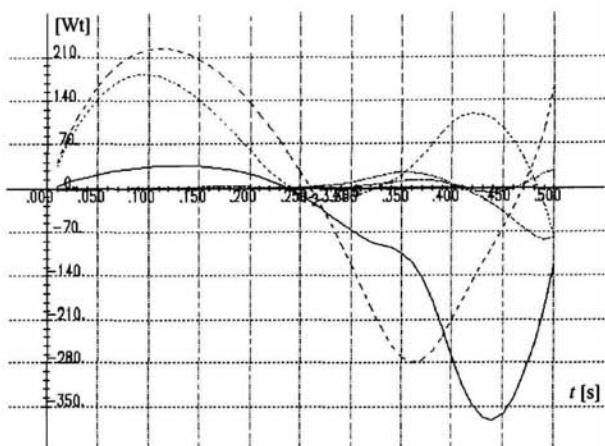


Fig. 5.73. *Inter-element moments power* ($g=0.0 \text{ m/s}^2$, $t=0.5 \text{ s}$).

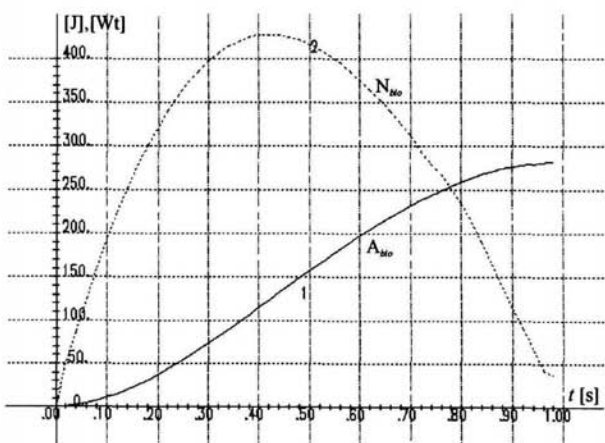


Fig. 5.74. *Biomechanical work and power* ($g=9.8 \text{ m/s}^2$, $t=1 \text{ s}$).

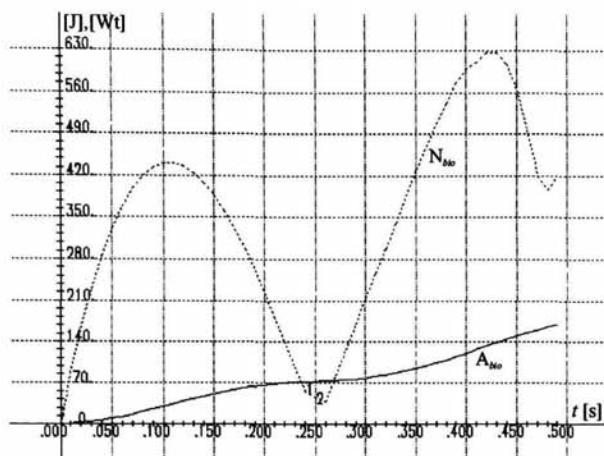


Fig. 5.75. Biomechanical work and power ($g=0.0 \text{ m/s}^2$, $t=0.5 \text{ s}$).

biomechanical power behaviour reflects, in particular, that energy expenditures are approximately the same for both motions.

Let us also give joint forces charts (Fig. 5.76 and Fig. 5.77 — horizontal components, Fig. 5.78 and Fig. 5.79 — vertical components). Vertical components of joint reaction forces are of essentially different character for acceleration and deceleration phases, whereas horizontal components, are qualitatively similar, but differ quantitatively.

Investigation showed that human motions in weightlessness are characterized by the absence of shock-like dynamic loads. This fact shows that such a phenomenon as washing out of calcium salts from the bone tissues of astronauts is in fact a result of not only weightlessness, but is a consequence of absence of adequate mechanical loads on the human SMA. Truly, under earth conditions every step is accompanied by the shock-like interaction of the feet and the support. By shock-like interaction we understand, as it is common in theoretical mechanics, such interaction when the body velocity (and, correspondingly, the momentum of this body) is changed in a very short period of time over a certain finite value. There appears a shock force, acting for a short time, but characterized by a large value. These shock forces apparently serve as a mechanical stimulus providing for a sound morphological and functional state of the bone tissue. Special investigations of bones and joints of sportsmen showed that dynamic and shock loads provide for growth and strengthening of the human skeletal apparatus. During the space flight such loads are almost excluded, except for the time of training on a treadmill (to which the astronaut binds himself by rubber

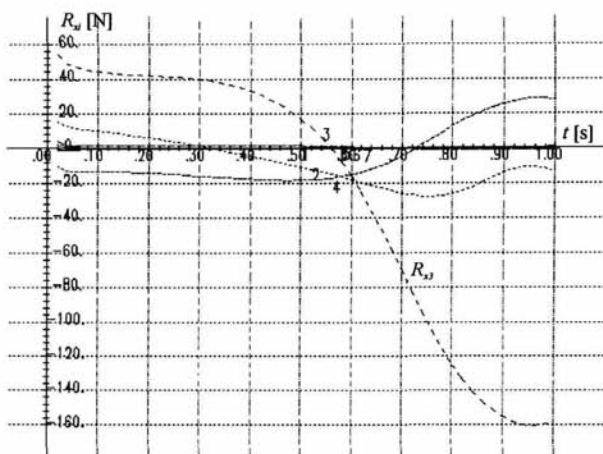


Fig. 5.76. Horizontal components of joint reaction forces ($g=9.8 \text{ m/s}^2$, $t=1 \text{ s}$).

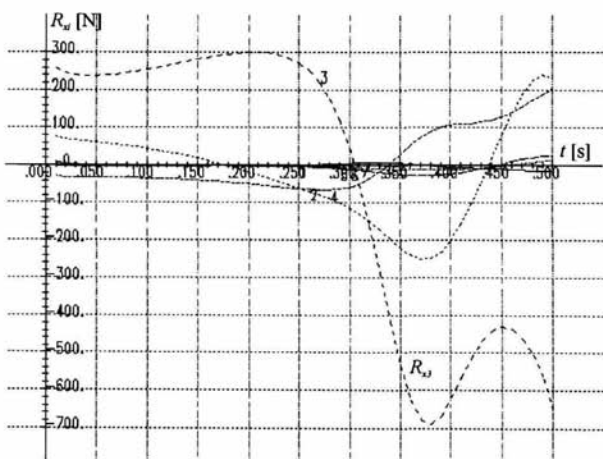


Fig. 5.77. Horizontal components of joint reaction forces ($g=0.0 \text{ m/s}^2$, $t=0.5 \text{ s}$).

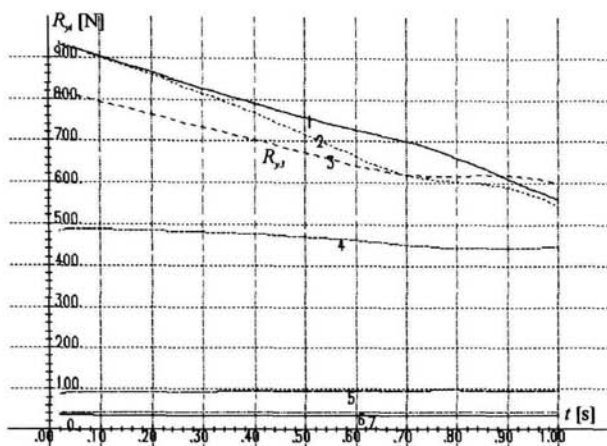


Fig. 5.78. Vertical components of joint reaction forces ($g=9.8 \text{ m/s}^2$, $t=1 \text{ s}$).

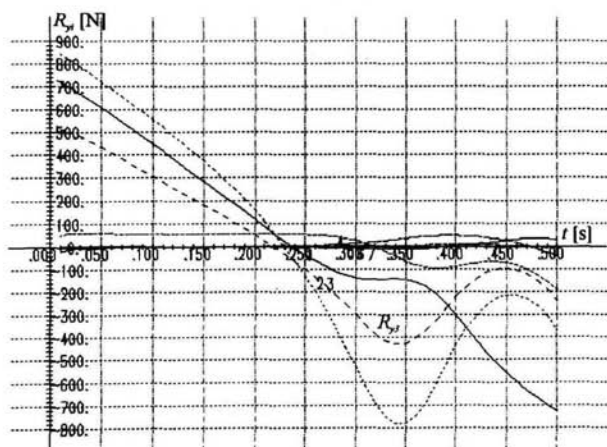


Fig. 5.79. Vertical components of joint reaction forces ($g=0 \text{ m/s}^2$, $t=0.5 \text{ s}$).

strips). In our view the lack of this dynamic and shock loads is the main reason of the deterioration of the skeletal apparatus functional and morphological state of the astronauts. The investigation conducted by means of imitational modelling of astronauts motions provides ground for the conclusion that preservation of the human motion coordination under varying gravity force is given by reconstruction of the control of the muscle forces, which consists in a characteristic change of the joint moments amplitudes (in accordance to the change of the gravity field). The possibility of a quick rehabilitation of the motion coordination [18, 19, 90] once more confirms Bernsteins words that "... motion is possible only in case of subtle and continuous, not beforehand foreseen, coordination of control neural impulses with phenomena, taking place in outlying areas" [9].

5.9 Some Notes and Conclusions

In preceding paragraphs, methodology of synthesis of complex motions of AM consisting of a ramified system of bodies with constraints was considered. Suggested technology of taking into account of constraint equations was illustrated on examples of modelling of human motions performed by the whole AM. When considering separate elements of the AM (or joints), types of constraint equations introduced above can be used for superelements of complex construction, modelling of ramified and/or closed-loop structures (e. g., foot, spine models, etc.). Principles of adequate substitution of elements or joints were discussed in Sec. 5.5.

One of the main results of considered synthesis examples consists in demonstration of possibility of modelling of dynamic behaviour of AM with given kinematics by a system of bodies of variable structure, and, therefore, varied number of elements and freedom degrees.

Possibility of AM structure variation conserving main energy-force characteristics of motion, by means of imposition of corresponding equations of non-stationary dynamic constraints, presents a basis for realization of new principles of adequate modelling of concrete motions of human SMA.

In all considered examples of synthesis as a final result graphics of interelement joint control time functions for ramified kinematic chains are presented. In other words, control laws for all generalized coordinates were received. This can serve as a ground for the next stage of adequate modelling, namely, calculation of actual forces acting at SMA joints due to muscles contraction, elasticity and damping properties of SMA joints and elements. This recalculation is obviously one of the main problems of biomechanical modelling because it is connected with problems of modelling of SMA joints and elements "construction" and motion "drivers" (muscles).

As one of the simplest examples, let us write relations for calculation of one joint interelement moment from its muscles contraction forces. In Fig. 5.80 is given the main nomenclature for kinematic scheme of flexing and extending forces at the joint.

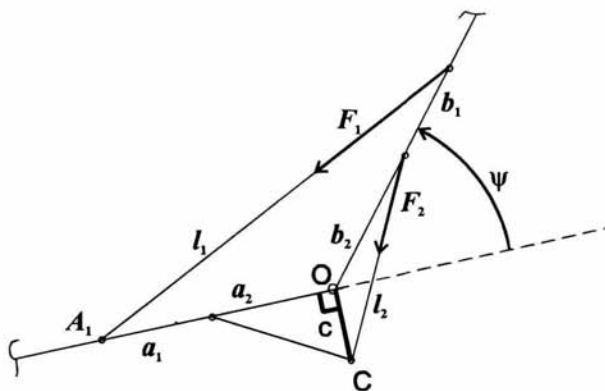


Fig. 5.80. Kinematic scheme of joint flexing and extending forces action.

Here a_1 , a_2 , b_1 , b_2 , c stand for positions of fixation points of joint muscles. Let us take the angle (A_1OC) to be right. Then, taking into account variation of the interelement angle ψ , we can write expressions connecting velocities of muscle contraction V_1 (flexor), V_2 (extender) with the increment of angular velocity $\dot{\psi}$:

$$\dot{\psi} = -V_1 \frac{l_1}{a_1 b_1 \sin \psi} = V_2 \frac{l_2}{c b_2 \cos \psi}, \quad (5.55)$$

where $l_1^2 = a_1^2 + b_1^2 + 2a_1 b_1 \cos \psi$, $l_2^2 = c^2 + b_2^2 + 2c b_2 \sin \psi$ determine behaviour of muscles length depending on contraction forces F_1 , F_2 .

Analogously with relations of Eq. (5.55) expressions connecting forces F_1 , F_2 with M_1 , M_2 ($M = M_1 + M_2$ — interelement moment) can be obtained:

$$M_1 = F_1 \frac{a_1 b_1}{l_1} \sin \psi, \quad M_2 = -F_2 \frac{b_2 c}{l_2} \cos \psi. \quad (5.56)$$

Since F_1 and $F_2 \geq 0$, let us give possible “distribution” of the moment M in supposition that if $M_1 \neq 0$, then $M_2 = 0$ and vice versa (i. e. at any moment of time there is only one group of muscles acting at the joint).

Flexing: $\dot{\psi} > 0$, $V_1 < 0$, $V_2 > 0$, then for $M > 0$, we put $M = M_1$ and for $M < 0$, $M = M_2$.

Extending: $\dot{\psi} < 0$, $V_1 > 0$, $V_2 < 0$, then for $M > 0$, we put $M = M_1$, and for $M < 0$, $M = M_2$.

Finally, for $M > 0$ we put $F_2 = 0$ and $F_1 = M l_1 / (a_1 b_1 \sin \psi)$, for $M < 0$ we put $F_1 = 0$ and $F_2 = -M l_2 / (c b_2 \cos \psi)$. Sign of the momentary power $N_i = F_i V_i$, $i = \overline{1, 2}$

depends on the sign of V_i and, correspondingly, one can assess whether muscle works in "flexing" ($N_i > 0$) or "extending" ($N_i < 0$) regime.

These relations only illustrate one of variants of real joint work realization. Practical recommendations on this subject lie outside of this monograph framework and are reflected quite fully in literature [44, 45].

In conclusion, let us underline that successful solution of complexly coordinated motion synthesis problem should be based on well-working procedure of numerical integration of a system of differential-algebraic motion equations which reflects adopted mechanical and mathematical model of SMA with non-stationary constraints. The idea of multilevel superelement approach allows to make MM step by step closer to adequate description of SMA motion and its characteristics. Correspondingly, a researcher too step by step approaches adequate assessment of general energy-force picture of motion from the biomechanical point of view.

Conclusion

In this monograph we have addressed the main aspects and problems of anthropomorphic biomechanical systems motion analysis and synthesis. The difficulties and obstacles which numerical methods of human motion modelling face include at least all those which can be met in modelling of complex physical systems. The process of biomechanical modelling starts from analysis and is followed by development (in accordance with analysis results) of mathematical models of different complexity. The final stage consists in comparing of characteristics obtained through model calculations with experimental data. Actually a great number of factors determine whether results of physical and computer experiments will agree or disagree. This brings us to understanding that biomechanical computer model must be not only full and adequately complex, but also self-testable and should easily allow for modifications. Authors of this book have endeavoured to satisfy these requirements in developing of computer programs package SIMAM — intended for imitational dynamic modelling of human motions [84, 106].

In the basis of biomechanical model lies a system of differential-algebraic equations of dynamics of ramified kinematic chain under non-stationary constraints. System of constraint equations can be divided into two subsystems, one of which sets restrictions of geometric and kinematic character and includes conditions of joint AM elements motion, constraints which are imposed by external environment and constraints imposed for motion goal realization. The second subsystem of constraint equations includes restrictions on reaction forces and moments. This subsystem can include equations of conservation laws: conservation of momentum vector, moment of momentum and energy of a mechanical system, which can include either all bodies of the model or some of its subsystems. External moments and forces play the role of boundary conditions which can be formulated on the basis of experimental data.

The approach developed by researches to formation of internal control on the basis of data on behaviour of certain system points or bodies coordinates, external active forces and constraint reactions allows one to synthesize a goal-oriented motion of the imitation model. New experimental data and additional measurements can be easily fed into the modelling system. All this allows for creation of a trustable adaptive imitational dynamic model of human skeletal-muscular apparatus.

A peculiar property of imitational dynamic modelling of biomechanical systems consists in possibility of structural and parametric adjustment of the imitational

model to real human motion. Model structure choice is carried out by imposing of constraints (holonomic, non-holonomic constraints of the first order and linear non-holonomic constraints of the second order). Parametric adjustment of the imitational model is necessary due to errors in measurements of kinematic and dynamic motion characteristics of biomechanical systems.

Modelling of human motion on the basis of motion equations of a system of bodies suggests presence of a large number of parameters for description of structure and kinematics of motion. Choice of these parameter values significantly depends on available experimental data. Concrete combination of parameter values allows to conduct calculations and compare values received by computer modelling and corresponding experimental data. In this work a new approach to parametric adjustment of the imitational model is presented. For models describing real human motions the number of parameters can be over one hundred. Therefore it becomes an obvious necessity for formulation of adequacy criteria which would provide for parametric adjustment of the imitational model to concrete human motion. Presence of non-stationary constraint equations allows one to use part of the experimental data as such constraints.

Main feature of the suggested approach consists in possibility of imitation of part of the experimental data and following comparison of corresponding experimental and modelled (received by solution of synthesis problem) parameters. Most significant motion characteristics can be synthesised with necessary error level by their introduction into constraint equations. The computer model allows for motion modelling using *a priori* information of practically arbitrary form. Kinematics of markers, force platform and acceleration measuring units data can serve as a ground for synthesis of a goal-oriented human-like motion.

Investigation results presented in the monograph testify that employment of imitational dynamic modelling for human motion simulation has wide prospects. In all of the considered motion synthesis examples, interelement moments behaviour in time is depicted. That means that imitational modelling allows one to assess required control functions value with respect to all of the generalised coordinates, which provide grounds for the next stage of research at which one can obtain from generalised forces value estimates of actual muscle forces and reactions in model joints. This recalculation of real forces value from generalised ones appears to be one of the important biomechanical modelling problems.

Finally let us name the main promising fields of application of the developed imitational dynamic modelling approach:

- development of imitational models of man-machine systems;
- development of imitational models of human motion under extreme conditions (motion of astronauts, sportsmen, complexly coordinated operators motion);
- development of imitational models of robots control systems;
- development of imitational models intended for investigation of strength properties of human skeletal-muscular apparatus.

BIBLIOGRAPHY

1. Aleshinsky S. Yu., Zatsiorsky V. M., (Алешинский С. Ю., Зациорский В. М.) *Биофизика* т. XX, в. 6 (1975) 1121–1126.
2. Aristotel, (Аристотель) *О частях животных* (М.: 1937) 219.
3. Bae D., Yang S., In E. Haug and R. Deyo, editors, *NATO Advanced Research Workshop on Real-Time Integration Methods for Mechanical System Simulation* (Springer, Heidelberg, 1991) 209–232.
4. Beletskiy V. V., Kirsanova T. S., Chudinov P. S., (Белецкий В. В., Кирсанова Т. С., Чудинов П. С.) в кн.: *Биомеханика* в. 13 (1975) 627–631.
5. Beletskiy V. V., Konikova N. S., (Белецкий В. В., Коникина Н. С.) *Известия АН СССР. Механика твердого тела* N05 (1979) 46–52.
6. Beletsky V. V., (Белецкий В. В.) *Двуногая ходьба: модельные задачи динамики управления* (Наука, М., 1976) 288 с.
7. Bernstein N. A., (Бернштейн Н. А.) *Исследования по биомеханике локомоций* (М.-Л.: Медгиз, 1935) 340 с.
8. Bernstein N. A., (Бернштейн Н. А.) *О построении движений* (М.: Медгиз, 1974) 255 с.
9. Bernstein N. A., (Бернштейн Н. А.) *Очерки физиологии движений и физиологии активности* (М., Медицина, 1966) 349 с.
10. Blauberger I. V., Sadovsky B. N., Yudin E. G., (Блауберг И. В., Садовский В. Н., Юдин Э. Г.) *Проблемы методологии системного исследования* (М., Мысль, 1970) 455 с.
11. Bogdanov V. A., Gurfinkel V. S., Ostapchuk V. G., (Богданов В. А., Гурфинкель В. С., Остапчук В. Г.) *Известия АН СССР. Техническая кибернетика* N04 (1980) 81–89.
12. Borelli A., *De Motu Animalium* / 2 vols Ranae, To be found in *Pathologie de Chirurgie*, vol. 2 of 3 vols (by Jean Baptiste Verdue, Paris, 1727)
13. Boyarintsev Yu. E., (Бояринцев Ю. Е.) *Регулярные и сингулярные системы линейных обыкновенных дифференциальных уравнений* (Новосибирск: Наука, 1980) 220 с.
14. Braune W., Fisher O., *Verh X. Intern. med. Kongress* (Berlin, 1890) 151 s.
15. Braune W., Fisher O., *Der Gang des Menschen* 1– 6 (Leipzig, Teubner, 1895–1904) .
16. Bresler B., Frankel I. P., *Trans. ASME* 72 (1950) 27–32.

17. Chernousko F. L., Bolotnik N. N., Gradetsky V. G., (Черноусько Ф. Л., Болотник Н. Н., Градетский В. В.) *Манипуляционные роботы: динамика, управление и оптимизация* (М., 1988)
18. Chkaidze L. V., (Чхаидзе Л. В.) *Об управлении движениями человека* (Наука, М., 1970) 136 с.
19. Chkaidze L. V., (Чхаидзе Л. В.) *Координация произвольных движений человека в условиях космического полета* (Наука, М., 1965) 134 с.
20. Dennis J. E. and Schnabel R. B., *Numerical Methods for Unconstrained Optimization and Nonlinear Equation* (Prentice-Hall, Englewood Cliffs, 1983)
21. Donskoy D. D., (Донской Д. Д.) *Биомеханика физических упражнений* (ФиС, Москва, 1958) 240 с.
22. Efimov V. A. et al, (Ефимов В. А. и др.) в кн.: *Тезисы докладов II Всесоюзной конференции по проблемам биомеханики* () 183–184.
23. Efimov V. M., Kudriavtsev M. V., Proskuriakov V. V., (Ефимов В. М., Кудрявцев М. В., Проскуряков В. В.) в кн.: *Биомеханика* (РИТО, Рига, 1975) 604–609.
24. Elfman H., *Amer. J. Physiol.* **125** (1939) 357–366.
25. Elfman H., *Acad. Sci., Transaction Ser.* **11** N06 (Acad. Sci., N.-Y., 1943) 1–4.
26. Emelichev B. A., Melnikov O. I., Sarvanob V. I., Tyshkevich R. I., (Емеличев В. А., Мельников О. И., Сарванов В. И., Тышкевич Р. И.) *Лекции по теории графов* (Наука, М., 1990) 384 с.
27. Führer C., In E. Haug and R. Deyo, editors, *NATO Advanced Research Workshop on Real-Time Integration Methods for Mechanical System Simulation* (Springer, Heidelberg, 1991) 143–154.
28. Farber B. S., Vitenzon A. C., Moreinis I. Sh., (Фарбер Б. С., Витензон А. С., Морейнис И. Ш.) *Теоретические основы построения протезов нижних конечностей и коррекции движения т.1–3* (ШНИИПП, М., 1994)
29. Fisher O., *Theoretische Grundlagen für eine Mechanik der lebenden Körper. Mit speziellen Anwendungen auf den Menschen sowie auf feine Bewegungsvorgänge*. (Tuebner, Leipzig–Berlin, 1906) 372 s.
30. Forester J., (Форестер Дж.) *Динамика развития города* перевод с англ. (Прогресс, М., 1974) 285 с.
31. Formalsky, A. M., (Формальский А. М.) *Движение антропоморфных механизмов* (Наука, М., 1982) .
32. Frolov K. V., Vorobyev E. I., (Фролов К. В., Воробьев Е. И.) *Механика индустриальных роботов* (М., 1988) .
33. Gear C. W., Leimkuhler B. and Gupta G. K., *Journal of Computational and Applied Mathematics* **12& 13** (1985) 77–90.
34. Gear C. W., In E. Haug and R. Deyo, editors, *NATO Advanced Research Workshop on Real-Time Integration Methods for Mechanical System Simulation* (Springer, Heidelberg, 1991) 117–126.
35. Granit R., (Гранит Р.) *Основы регуляции движений* перевод с англ.

- (Мир, М., 1973) 368 с.
36. Grishenko G. P., Moreynis I. Sh., (Гриценко Г. П., Морейнис И. Ш.) *Ортопедия. Протезирование и протезостроение* т.12 (1974) 42–55.
 37. Gurfinkel V. S., Safonov V. A., (Гурфинкель В. С., Сафронов В. А.) *А.с. 255483 (СССР). Оpubл. в Б.И. N033 (1978)* .
 38. Hailer E., Norsett S. P., Wanner G., *Solving Ordinary Differential Equations*, (Springer-Verlag, Berlin—Heidelberg, 1987) .
 39. Hatze H., *Mathematical Biosciences* **28** (1976) 99–135.
 40. Hatze H., *Med. Sport, Biomechanics III* **8** (1973) 138–142.
 41. Hill A., V., (Хилл А. В.) *Механика мышечного сокращения. Старые и новые методы*. перевод с англ. (Мир, М., 1972) 183 с.
 42. Himmelblau D., (Химельблау Д.) *Прикладное нелинейное программирование* перевод с англ. (Мир, М., 1975) 536 с.
 43. Huston R. L., Passerello C. E., *J. of Biomechanics* **4** (1971) 209–216.
 44. *International Society of Biomechanics, XIV-th Congress, Paris, July 4–8, Abstracts* (Paris, 1993)
 45. *International Society of Biomechanics, XV-th Congress, Jyväskylä, July 2–6, Book of abstracts* (Finland, 1995) .
 46. Korenev G. V., (Корнев Г. В.) *Введение в механику управляемого тела* (М.:Наука, 1964) 568 с.
 47. Korenev G. V., (Корнев Г. В.) *Цель и приспособляемость движений* (М.:Наука, 1974) 528 с.
 48. Korenev G. V., (Корнев Г. В.) в кн.: *Биомеханика* (РИТО, Рига, 1975) 677–681.
 49. Kostuk P. G., (Костюк П. Г.) *Структура и функции нисходящих систем спинного мозга* (Наука, Москва, 1973) 279.
 50. Kozlovskaya I. V., (Козловская И. В.) *Афферентный контроль произвольных движений* (Наука, Москва, 1976) 296 с.
 51. Kruskal J., *Proc. American Mathematical Soc.* **7** (1956) .
 52. Kudriavtsev M. V. et al, (Кудрявцев М. В. и др.) в кн.: *Биомеханика* (РИТО, Рига, 1975) 591–594.
 53. Kulakov F. M., Looze H., Horizontova N. P., (Кулаков Ф. М., Лоозе Н., Горизонтова Н. П.) *Численное моделирование систем твердых тел и приложения в робототехнике* (Л., 1986) .
 54. Lilov L. K., (Лилов Л. К.) *Моделирование систем связанных тел* (Наука, М., 1993) 272 с.
 55. Loizansky L. G., Lurie A. I., (Лойцянский Л. Г., Лурье А. И.) *Курс теоретической механики* т.1 & т.2 (Наука, М., 1987)
 56. Lurie A. I., (Лурье А. И.) *Аналитическая механика* (М., 1961) 824 с.
 57. Marey F. J., *Le mouvement* (Paris, 1894)
 58. Marey F. J., *Traité de phys. biol.* (Paris, 1901) .
 59. Miller D., *A computer simulation model of the airborne phase of diving*. — *Ph.D.D.*

- (Pennsylvania State University, 1970)
60. Milsum J., (Милсум Дж.) *Анализ биологических систем управления* перевод с англ. (Мир, М., 1968) 501 с.
 61. *Modern Numerical Methods for Ordinary Differential Equations*, ed. G. Hall and J. M. Watt (Clarendon Press, Oxford, 1976) .
 62. Moiseev N. N., Ivanilov Yu. P., Stolyarova E. M., (Моисеев Н. Н., Иванилов Ю. П., Столярова Е. М.) *Методы оптимизации*. (М.:Наука, 1978) 352 с.
 63. Moiseev N. N., (Моисеев Н. Н.) *Математические задачи системного анализа* (М.:Наука, 1981) 488 с.
 64. Moiseev N. N., (Моисеев Н. Н.) *Элементы теории оптимальных систем*. (М.:Наука, 1975) 526 с.
 65. *Multibody System Handbook*, ed. W. O. Schiehlen (Springer- Verlag, Berlin—Heidelberg—New York—Tokyo, 1990) p. 432.
 66. *NATO Advanced Reseach Workshop on Real-Time Integration Methods for Mechanical System Simulation*, E. Haug and R. Deyo, editors, (Springer, Heidelberg, 1991) p. 357.
 67. Nazarov V. G., Назаров В. Г. *Биомеханические основы деятельности при освоении ациклических упражнений (на примере спортивной гимнастики)*. — Дис. ... док. пед. наук. (М., 1973) 196 с.
 68. Newton I., (Ньютон И.) *Оптика или трактат об отражениях, преломлениях, изгибаниях и цветах света*. перевод с англ. (Гостехиздат, М., 1954)
 69. Noldus E. G. L., *Acta Univers Oucuenis, Journal A*, **18** N01 (1974) 18–23.
 70. Nubar Y., Contini R., *Bull. Math. Biophys.* **23** N04 (1961) 377–390.
 71. Okhotcimsky, D. E., Golubev Yu. R., Alekseeva L. A., (Охоцимский Д. Е., Голубев Ю. Р., Алексеева Л. А.) *Управление динамической моделью шагающего аппарата* (ИПМ, АН СССР, 1974) 32–48.
 72. Okhotcimsky, D. E., Golubev Yu. R., Alekseeva L. A., (Охоцимский Д. Е., Голубев Ю. Р., Алексеева Л. А.) в кн.: *Управление в пространстве* (Наука, М., 1976) 240–249.
 73. Okhotcimsky D. E., Platonov A. K., (Охоцимский Д. Е., Платонов А. К.) в кн.: *Биомеханика* (РИТО, Рига, 1975) 594– 598.
 74. Ostermeier G., In E. Haug and R. Deyo, editors, *NATO Advanced Reseach Workshop on Real-Time Integration Methods for Mechanical System Simulation* (Springer, Heidelberg, 1991) 193–208.
 75. Pandy M. G., Anderson F. C., Hull D. G., *ASME J. Biomechanical Engineering* **114** (1992) 450–460.
 76. Petrov V. A., (Петров В. А.) *Теория и практика физической культуры* N012 (1967) с. 57–61.
 77. Petzold L., In E. Haug and R. Deyo, editors, *NATO Advanced Reseach Workshop on Real-Time Integration Methods for Mechanical System Simulation* (Springer,

- Heidelberg, 1991) 127–140.
78. Polyahov N. N., Zegjda S. A., Yushkov M. P., (Поляхов Н., Н., Зегжда С., А., Юшков М., П.) *Теоретическая механика* (Изд-во ЛГУ, Л., 1985) 536 с.
79. Proskuriakov V. B., Kudriavtsev M. V., Titov A. F., (Проскуряков В. Б., Кудрявцев М. В., Титов А. Ф.) *Биомеханика* (РИТО, Рига, 1975) 615–618.
80. Ramey H. R., In *Biomechanics V-B*. (University Park Press, Baltimore, 1976) 167–173.
81. Reinsch C. H., *Numer.Math.* N010 (1967) 177–183.
82. Shahinpur M., (Шахинпур М.) *Курс робототехники* перевод с англ. (Мир, М., 1990).
83. Shennon R., (Шеннон Р.) *Имитационное моделирование систем — искусство и наука* перевод с англ. (Мир, М., 1978) 420 с.
84. Sholuha V. A., Zinkovsky A. V., in *Vth International Symposium on Computer Simulation in Biomechanics, Jyväskylä, June 28–30, 1995, Book of Abstracts* (Finland, 1995) 40–41.
85. Sholuha V. A., Zinkovsky A. V., Ivanov A. A., in *International Society of Biomechanics, XV-th Congress, Jyväskylä, July 2–6, Book of abstracts* (Finland, 1995) 844–845.
86. Sinelnikov R. D., (Синельников Р. Д.) *Атлас анатомии человека. Учение о костях, суставах, связках и мышцах т.1* (Медицина, Москва, 1978) 471 с.
87. Sliede P. B., Auzinsh J. P., (Слиеде П. Б., Аузиньш И. П.) в кн.: *Вопросы динамики и прочности* (Зинатне, Рига, 1980)
88. Sobol I. M., Statnikov R. B., (Соболь И. М., Статников Р. Б.) *Выбор оптимальных параметров в задачах со многими критериями* (Наука, М., 1981) 112 с.
89. Stechkin S. B., Subbotin V. M., (Стечкин С. Б., Субботин В. М.) *Сплайны в вычислительной математике* (Наука, М., 1990)
90. Stepanov V. I., Kremim A. V., (Степанов В. И., Кремим А. В.) *Космические исследования т.VII*, в.6 (1969) 886–895.
91. Tikhonov V. N., (Тихонов В. Н.) *Теория и практика физической культуры* N08 (1973) 17–19.
92. Uicker J. J., *J. Appl. Mech.* 34 (1967)
93. Uicker J. J., *Trans. ASME, Mech.* 68 (1968)
94. Vereshagin A. F., (Верещагин А. Ф.) *Известия АН СССР. Техническая кибернетика т.6* (1974) 89–95.
95. Vereshagin A. F., (Верещагин А. Ф.) *Доклады АН СССР т.220 N01* (1975) 89–95.
96. Vukobratovic M., Hristic D., *Automatika* N01 (1971) 18–25.
97. Vukobratovich M., (Вукобратович М.) *Шагающие роботы и механизмы* (Мир, М., 1976) 541 с.

98. Weber W. E., *Mechanik der menschlichen Gewerkezeuge* (Gottingen, 1836) 116 s.
99. Winters J. M., In J. M. Winters and S. L.-Y. Woo (Eds.) *Multimuscule systems* (Springer-Verlag, New York, 1990) 69-93.
100. Witni D. E., (Уитни Д. Е.) *Труды амер. общ. инж. мех. Динамические системы и управление т.34, NO 4* перевод с англ. (Мир, М., 1972) 19-27.
101. Wittenburg J., *Dynamics of Systems of Rigid Bodies* (Teubner, Stuttgart, 1977) 292 p.
102. Zatsiorsky V. M., Aruin A. S., Seluyanov V. N., (Зациорский В. М., Аруин А. С., Селуянов В. Н.) *Биомеханика двигательного аппарата человека* (ФиС, Москва, 1981) 144 с.
103. Zatsiorsky V. M., Sereda M. G., Sarsania S. K., (Зациорский В. М., Середя М. Г., Сарсания С. К.) *А.с.427698 (СССР). Оpubл. в Б.И. NO19* (1974) .
104. Zinkovsky A. V., (Зинковский А. В.) *Кибернетика и вычислительная техника* в.66 (Киев, 1985) 99-103.
105. Zinkovsky A. V., Chistyakov V. A., Trofimova I. A., (Зинковский А. В., Чистяков В. А., Трофимова И. А.) *Биофизика т. XXVI, NO1* (1981) 113-116.
106. Zinkovsky A. V., Ivanov A. A., Sholuha V. A., in *Vth International Symposium on Computer Simulation in Biomechanics, Jyväskylä, June 28-30, 1995, Book of Abstracts* (Finland, 1995) 54-55.
107. Zinkovsky A. V., Sholuha V. A., *Anthropomorphic mechanisms: modelling, motion analysis and syntesis* (SPSTU, St.-Petersburg, 1994) p. 128.
108. Zinkovsky A. V., Trofimova I. A., Chistyakov V. A., (Зинковский А. В., Трофимова И. А., Чистяков В. А.) *Космическая биология и авиакосмическая медицина т.6* (1981) 31-33.
109. Zinkovsky A. V., (Зинковский А. В.) *Теория и практика физической культуры NO9* (1973) с. 66-70.

Index

- A**
 - accelerometers 52
 - adequacy criteria 77
 - anthropomorphic model reduction 48
- B**
 - basic AM model (BM) 48
 - biomechanical
 - criteria 123
 - work 162
 - BM GMIC 49
- C**
 - center of mass motion theorem 15
 - comparator axes 45
 - compensation of gravity force acceleration 180
 - control structurization 112
- D**
 - differential index 69
 - differential-algebraic equations (DAE) 68
 - direct and inverse dynamics problems 40
 - disintegration 61
 - double-somersault synthesis 162
 - double-support phases 150
- E**
 - energy-force motion characteristics 157
 - error margins 79
 - experimental data analysis 77
 - external obstacles 113
- F**
 - force
 - constraint equation 43
 - platform 95
 - frame
 - axes 45
 - minimization procedure 80
 - freedom degrees 17
 - full energy of the freezed system 130
- G**
 - GMIC 45, 48
 - goal-oriented motion 80
 - grand circles 100, 157, 164
 - graph
 - framework 19
 - weighted 16
 - tree-like 16
 - unidirectional 16
 - ground reaction 93
- H**
 - hip joint moment 101
 - holonomic and non-holonomic constraints
 - of the first and second order 40
 - holonomic constraints 71
 - Huggens-Steiner theorem 26
- I**
 - imitational
 - dynamics model 10
 - methodology 10
 - model 10
 - modelling 10
 - implicit form 68

incompatibility problem 142
 integration method
 explicit 69
 implicit 69
 interelement angles 164
 iteration of correction step 71

J

joint
 cylindrical 31
 spherical 19
 universal 35
 joints non-linear dampers and springs
 124

K

kinetic energy of
 the freezed system 162
 body 14
 point 13
 system 25
 knee moment 93

L

Lagrange multipliers 71, 113
 least squares method (LSM) 52, 76
 limit sensible number 55
 long jump 169
 LP- τ sequences 55

M

macro-motion 145
 mass-inertia characteristics estimation
 4
 matrices-column of generalized
 accelerations 68
 coordinates 68
 inertia forces and external forces 68
 velocities 68
 matrix of incidencey 20
 measurement error 104
 mechanical

 energy 123, 152
 work 136
 MM identification 111
 model
 of human body 1
 moment
 of momentum
 of body 14
 of point 13
 momentary power of the freezed system
 130
 momentum
 of body 14
 of point 13
 motion
 registration frequency 78
 will 114
 muscle-antagonists 183

N

Newton-Euler equations 26
 Newton-Raphson method 70
 noise-damaged phase picture 62
 non-stationary constraint 150, 157
 non-holonomic constraints of the first
 order 73
 nonlinear visco-elastic support 113
 nonsingular matrix 73
 numerators tables 55

O

one-support phase 146
 open kinematic loop 80
 optimal parameters 54
 overloads 180

P

parametric adjustment methodology 77
 polyhedron 56
 polynomial coefficients 116
 problems of analysis and synthesis of
 AM motions 40

pseudo-inverse matrix 73, 74
pseudostochastic search method 55, 61
pushing-off phase 78

R

radioisotopic method of GMIC estimation 4
real experimental 93
redundant number of freedom degrees 78
registration of real motion 77
regularization according to Baumgarte 75, 76
relative angular
 acceleration 39
 velocity 30, 39

S

semi-inverse matrix 71
shin-ankle 82
shock-like dynamic loads 188
single-support phase 156
SMA (skeletal muscular apparatus) 45
smoothing splines 52
solid body 13
speeding-up circles 123
splining parameter 79
start-stop motion 116
structure matrix 17, 19
superelement 112, 146, 155, 157
support phase period 95

T

tensor of inertia 15, 22
theorem of moment of momentum 156
time derivative with respect basis 37
total
 AM moment of momentum 24
 straitening-up 134
two-leg
 push off 158
 walking 143

two-support phase of motion 143
typical constraint equations 115

U

uncontrollable joints 146
unproductive energy expenditures 136

V

visco-elastic
 character of superelement model 113
 properties 100

W

walking motion 159
weightlessness 183

Z

zero-gravity 180